Publishing House ASV

begell house, inc. publishers

PAACH

Scientific coordination is carried out by the Russian Academy of Architecture and Construction Sciences (RAACS)

Volume 19 • Issue 4 • 2023

ISSN 2588-0195 (Online)
ISSN 2587-9618 (Print) Continues ISSN 1524-5845

International Journal for

Computational Civil and Structural Engineering

Международный журнал по расчету гражданских и строительных конструкций

https://ijccse.iasv.ru/

DOI: 10.22337/2587-9618
GICID: 71.0000.1500.2830

EXECUTIVE EDITOR

Vladimir I. Travush,
Full Member of RAACS, Professor, Dr.Sc.,
Vice-President of the Russian Academy
of Architecture and Construction Sciences;
Urban Planning Institute
of Residential and Public Buildings;
24, Ulitsa Bolshaya Dmitrovka, 107031, Moscow, Russia

EDITOR-IN-CHIEF

Vladimir N. Sidorov,
Corresponding Member of RAACS, Professor, Dr.Sc.,
National Research Moscow State University of Civil
Engineering; Russian University of Transport
(RUT – MIIT); Moscow Institute of Architecture
(State Academy); Perm National Research Polytechnic
University; 26, Yaroslavskoe Shosse, 129337,
Moscow, Russia

EDITORIAL DIRECTOR

Valery I. Telichenko,
Full Member of RAACS, Professor, Dr.Sc.,
The First Vice-President of the Russian Academy
of Architecture and Construction Sciences;
Honorary President of National Research
Moscow State University of Civil Engineering;
24, Ulitsa Bolshaya Dmitrovka, 107031, Moscow, Russia

MANAGING EDITOR

Nadezhda S. Nikitina,
Professor, Ph.D.,
Director of ASV Publishing House;
National Research Moscow State University
of Civil Engineering;
26, Yaroslavskoe Shosse, 129337, Moscow, Russia

ASSOCIATE EDITORS

Pavel A. Akimov,
Full Member of RAACS, Professor, Dr.Sc.,
Acting Rector of National Research
Moscow State University of Civil Engineering;
Vice-President of the Russian Academy
of Architecture and Construction Sciences;
Tomsk State University of Architecture and Building;
Russian University of Friendship of Peoples;
26, Yaroslavskoe Shosse, 129337, Moscow, Russia

Alexander M. Belostotsky,
Full Member of RAACS, Professor, Dr.Sc.,
Research & Development Center "STADYO";
National Research Moscow State University of Civil
Engineering; Russian University of Transport (RUT –
MIIT); Russian University of Friendship of Peoples;
Perm National Research Polytechnic University;
Tomsk State University of Architecture and Building;
Irkutsk National Research Technical University;
8th Floor, 18, ul. Tretya Yamskogo Polya,
125040, Moscow, Russia

Mikhail Belyi, Professor, Dr.Sc.,
Dassault Systèmes Simulia;
1301 Atwood Ave Suite 101W
02919 Johnston, RI, United States

Vitaly Bulgakov, Professor, Dr.Sc.,
Micro Focus;
Newbury, United Kingdom

Nikolai P. Osmolovskii, Professor, Dr.Sc.,
Systems Research Institute, Polish Academy of Sciences;
Kazimierz Pulaski University
of Technology and Humanities in Radom;
29, ul. Malczewskiego, 26-600, Radom, Poland

Gregory P. Panasenko, Professor, Dr.Sc.,
Equipe d'Analise Numerique; NMR CNRS 5585
University Gean Mehnet;
23 rue. P.Michelon 42023, St.Etienne, France

Scientific coordination is carried out by the Russian Academy of Architecture and Construction Sciences (RAACS)

PUBLISHER

ASV Publishing House
(ООО «Издательство АСВ»)
19/1,12, Yaroslavskoe Shosse, 120338, Moscow, Russia
Tel. +7(925)084-74-24; E-mail: iasv@iasv.ru; Интернет-сайт: http://iasv.ru/

ADVISORY EDITORIAL BOARD

Mojtaba Aslami, Ph.D,
Fasa University; Daneshjou blvd,
Fasa, Fars Province, Iran

Klaus-Jurgen Bathe, Professor
Massachusetts Institute
of Technology;
Cambridge, MA 02139, USA

Alexander T. Bekker,
Academician of RAACS,
Professor, Dr.Sc.,
Far Eastern Federal University;
Russian Academy of Architecture
and Construction Sciences;
8, Sukhanova Street, Vladivostok,
690950, Russia

Tomas Bock, Professor, Dr.-Ing.,
Technical University of Munich,
Arcisstrasse 21, D-80333
Munich, Germany

Jan Buynak, Professor, Ph.D.,
University of Žilina;
1, Univerzitná, Žilina, 010 26,
Slovakia

Vladimir T. Erofeev,
Full Member of RAACS,
Professor, Dr.Sc.,
Ogarev Mordovia State University;
68, Bolshevistskaya Str., Saransk
430005, Republic of Mordovia,
Russia

Victor S. Fedorov,
Full Member of RAACS,
Professor, Dr.Sc.,
Russian University of Transport
(RUT – MIIT);
9b9 Obrazcova Street, Moscow,
127994, Russia

Sergey V. Fedosov,
Full Member of RAACS,
Professor, Dr.Sc.,
Russian Academy of Architecture
and Construction Sciences;
24, Ul. Bolshaya Dmitrovka, 107031,
Moscow, Russia

Sergiy Yu. Fialko,
Professor, Dr.Sc.,
Cracow University of Technology;
24, Warszawska Street, Kraków,
31-155, Poland

Vladimir G. Gagarin,
Corresponding Member
of RAACS, Professor, Dr.Sc.,
Research Institute of Building
Physics of Russian Academy
of Architecture and Construction
Sciences;
21, Lokomotivny Proezd,
Moscow, 127238, Russia

Vyatcheslav A. Ilyichev,
Full Member of RAACS,
Professor, Dr.Sc.,
Russian Academy of Architecture
and Construction Sciences;
Podzemproekt Ltd.;
24, Ulitsa Bolshaya Dmitrovka,
Moscow, 107031, Russia

Marek Iwański,
Professor, Dr.Sc.,
Kielce University of Technology;
7, al. Tysiąclecia Państwa Polskiego
Kielce, 25 – 314, Poland

Sergey Yu. Kalashnikov,
Advisor of RAACS,
Professor, Dr.Sc.,
Volgograd State Technical
University; 28, Lenin avenue,
Volgograd, 400005, Russia

Semen S. Kaprielov,
Academician of RAACS,
Professor, Dr.Sc.,
Research Center of Construction;
6, 2nd Institutskaya St., Moscow,
109428, Russia

Nikolay I. Karpenko,
Full Member of RAACS,
Professor, Dr.Sc.,
Research Institute of Building
Physics of Russian Academy
of Architecture and Construction
Sciences; Russian Academy of
Architecture and Construction
Sciences; 21, Lokomotivny Proezd,
Moscow, 127238, Russia

Vladimir V. Karpov,
Professor, Dr.Sc., Saint Petersburg
State University of Architecture and
Civil Engineering;
4, 2-nd Krasnoarmeiskaya Steet,
Saint Petersburg, 190005, Russia

Galina G. Kashevarova,
Corresponding Member
of RAACS, Professor, Dr.Sc.,
Perm National Research
Polytechnic University;
29 Komsomolsky pros., Perm,
Perm Krai, 614990, Russia

John T. Katsikadelis,
Professor, Dr.Eng, PhD, Dr.h.c.,
National Technical University of
Athens; Zografou Campus
9, Iroon Polytechniou str
15780 Zografou, Greece

Vitaly I. Kolchunov,
Full Member of RAACS,
Professor, Dr.Sc., Southwest State
University; Russian Academy of
Architecture and Construction
Sciences; 94, 50 let Oktyabrya,
Kursk, 305040, Russia

Dmitry V. Kozlov, Dr. Sc.
Engineering, Professor, Head of
the Department of Hydraulics and
Hydrotechnical Construction, NRU
MGSU,
26, Yaroslavskoe Shosse., 129337,
Moscow, Russia

Markus König, Professor
Ruhr-Universität Bochum;
150, Universitätsstraße, Bochum,
44801, Germany

Sergey B. Kositsin,
Advisor of RAACS,
Professor, Dr.Sc.,
Russian University of Transport
(RUT – MIIT); 9b9 Obrazcova
Street, Moscow, 127994, Russia

Sergey B. Krylov,
Corresponding Member
of RAACS, Professor, Dr.Sc.,
Research Center of Construction;
6, 2nd Institutskaya St., Moscow,
109428, Russia

Sergey V. Kuznetsov,
Professor, Dr.Sc.,
Ishlinsky Institute for Problems
in Mechanics of the Russian
Academy of Sciences;
101-1, Prosp. Vernadskogo,
Moscow, 119526, Russia

Vladimir V. Lalin,
Professor, Dr.Sc.,
Peter the Great Saint-Petersburg Polytechnic University;
29, Ul. Politechnicheskaya,
Saint-Petersburg, 195251, Russia

Leonid S. Lyakhovich,
Full Member of RAACS,
Professor, Dr.Sc., Tomsk State University of Architecture and Building; 2, Solyanaya Sq., Tomsk, 634003, Russia

Rashid A. Mangushev,
Corresponding Member of RAACS, Professor, Dr.Sc.,
Saint Petersburg State University of Architecture and Civil Engineering;
4, 2-nd Krasnoarmeiskaya Steet,
Saint Petersburg, 190005, Russia

Ilizar T. Mirsayapov,
Advisor of RAACS,
Professor, Dr.Sc., Kazan State University of Architecture and Engineering; 1, Zelenaya Street,
Kazan, 420043, Republic of Tatarstan, Russia

Vladimir L. Mondrus,
Corresponding Member of RAACS, Professor, Dr.Sc.,
National Research Moscow State University of Civil Engineering;
Yaroslavskoe Shosse 26,
Moscow, 129337, Russia

Valery I. Morozov,
Corresponding Member of RAACS, Professor, Dr.Sc.,
Saint Petersburg State University of Architecture and Civil Engineering;
4, 2-nd Krasnoarmeiskaya Steet,
Saint Petersburg, 190005, Russia

Anatoly V. Perelmuter,
Foreign Member of RAACS,
Professor, Dr.Sc., SCAD Soft;
Office 1,2, 3a Osvity street,
Kiev, 03037, Ukraine

Alexey N. Petrov,
Advisor of RAACS, Professor, Dr.Sc., Petrozavodsk State University; 33, Lenina Prospect,
Petrozavodsk, 185910,
Republic of Karelia, Russia

Vladilen V. Petrov,
Full Member of RAACS,
Professor, Dr.Sc.,
Yuri Gagarin State Technical University of Saratov;
77 Politechnicheskaya Street,
Saratov, 410054, Russia

Jerzy Z. Piotrowski,
Professor, Dr.Sc.,
Kielce University of Technology;
al. Tysiąclecia Państwa Polskiego 7,
Kielce, 25 – 314, Poland

Chengzhi Qi, Professor, Dr.Sc.,
Beijing University of Civil Engineering and Architecture;
1, Zhanlanlu, Xicheng District,
Beijing, China

Vladimir P. Selyaev,
Full Member of RAACS,
Professor, Dr.Sc., Ogarev Mordovia State University;
68, Bolshevistskaya Str., Saransk 430005, Republic of Mordovia, Russia

Eun Chul Shin,
Professor, Ph.D.,
Incheon National University;
(Songdo-dong)119 Academy-ro,
Yeonsu-gu, Incheon, Korea

D.V. Singh,
Professor, Ph.D,
University of Roorkee;
Roorkee, India, 247667

Wacław Szcześniak,
Foreign Member of RAACS,
Professor, Dr.Sc.,
Lublin University of Technology;
Ul. Nadbystrzycka 40,
20-618 Lublin, Poland

Tadatsugu Tanaka,
Professor, Dr.Sc.,
Tokyo University; 7-3-1 Hongo,
Bunkyo, Tokyo, 113-8654, Japan

Josef Vican,
Professor, Ph.D,
University of Žilina;
1, Univerzitná, Žilina, 010 26,
Slovakia

Zbigniew Wojcicki,
Professor, Dr.Sc.,
Wroclaw University of Technology;
11 Grunwaldzki Sq., 50-377,
Wrocław, Poland

Artur Zbiciak, Professor, Dr.Sc.,
Warsaw University of Technology;
Pl. Politechniki 1, 00-661 Warsaw,
Poland

Segrey I. Zhavoronok, Ph.D.,
Institute of Applied Mechanics of Russian Academy of Sciences;
Moscow Aviation Institute (National Research University);
7, Leningradsky Prt.,
Moscow, 125040, Russia

Askar Zhussupbekov,
Professor, Dr.Sc.,
Eurasian National University;
5, Munaitpassov street, Astana,
010000, Kazakhstan

TECHNICAL EDITOR

Taymuraz B. Kaytukov,
Advisor of RAACS,
Associate Professor, Ph.D.,
Vice-Rector of National Research Moscow State University of Civil Engineering;
Yaroslavskoe Shosse 26,
Moscow, 129337, Russia

EDITORIAL TEAM

Vadim K. Akhmetov, Professor, Dr.Sc., National Research Moscow State University of Civil Engineering; 26, Yaroslavskoe Shosse, 129337 Moscow, Russia

Pavel A. Akimov, Full Member of RAACS, Professor, Dr.Sc., Acting Rector of National Research Moscow State University of Civil Engineering; Vice-President of the Russian Academy of Architecture and Construction Sciences; Tomsk State University of Architecture and Building; Russian University of Friendship of Peoples; 26, Yaroslavskoe Shosse, 129337, Moscow, Russia

Alexander M. Belostotsky, Full Member of RAACS, Professor, Dr.Sc., Research & Development Center "STADYO"; National Research Moscow State University of Civil Engineering; Russian University of Transport (RUT – MIIT); Russian University of Friendship of Peoples; Perm National Research Polytechnic University; Tomsk State University of Architecture and Building; Irkutsk National Research Technical University; 8th Floor, 18, ul. Tretya Yamskogo Polya, 125040, Moscow, Russia

Mikhail Belyi, Professor, Dr.Sc., Dassault Systèmes Simulia; 1301 Atwood Ave Suite 101W 02919 Johnston, RI, United States

Vitaly Bulgakov, Professor, Dr.Sc., Micro Focus; Newbury, United Kingdom

Charles El Nouty, Professor, Dr.Sc., LAGA Paris-13 Sorbonne Paris Cite; 99 avenue J.B. Clément, 93430 Villetaneuse, France

Natalya N. Fedorova, Professor, Dr.Sc., Novosibirsk State University of Architecture and Civil Engineering (SIBSTRIN); 113 Leningradskaya Street, Novosibirsk, 630008, Russia

Darya Filatova, Professor, Dr.Sc., Probability, Assessment, Reasoning and Inference Studies Research Group, EPHE Laboratoire CHART (PARIS) 4-14, rue Ferrus, 75014 Paris

Vladimir Ya. Gecha, Professor, Dr.Sc., Research and Production Enterprise All-Russia Scientific-Research Institute of Electromechanics with Plant Named after A.G. Iosiphyan; 30, Volnaya Street, Moscow, 105187, Russia

Taymuraz B. Kaytukov, Advisor of RAACS, Associate Professor, Ph.D, Vice-Rector of National Research Moscow State University of Civil Engineering; 26, Yaroslavskoe Shosse, 129337, Moscow, Russia

Marina L. Mozgaleva, Professor, Dr.Sc., National Research Moscow State University of Civil Engineering; 26, Yaroslavskoe Shosse, 129337 Moscow, Russia

Nadezhda S. Nikitina, Professor, Ph.D., Director of ASV Publishing House; National Research Moscow State University of Civil Engineering; 26, Yaroslavskoe Shosse, 129337 Moscow, Russia

Nikolai P. Osmolovskii, Professor, Dr.Sc., Systems Research Institute Polish Academy of Sciences; Kazimierz Pulaski University of Technology and Humanities in Radom; 29, ul. Malczewskiego, 26-600, Radom, Poland

Gregory P. Panasenko, Professor, Dr.Sc., Equipe d'Analise Numerique NMR CNRS 5585 University Gean Mehnet; 23 rue. P.Michelon 42023, St.Etienne, France

Andreas Rauh, Prof. Dr.-Ing. habil. Carl von Ossietzky Universität Oldenburg, Germany School II - Department of Computing Science Group Distributed Control in Interconnected Systems D-26111 Oldenburg, Germany

Zhan Shi, Professor LPSM, Université Paris VI 4 place Jussieu, F-75252 Paris Cedex 05, France

Marina V. Shitikova, National Research Moscow State University of Civil Engineering, Advisor of RAACS, Professor, Dr.Sc., Voronezh State Technical University; 14, Moscow Avenue, Voronezh, 394026, Russia

Igor L. Shubin, Corresponding Member of RAACS, Professor, Dr.Sc., Research Institute of Building Physics of Russian Academy of Architecture and Construction Sciences; 21, Lokomotivny Proezd, Moscow, 127238, Russia

Vladimir N. Sidorov, Corresponding Member of RAACS, Professor, Dr.Sc., National Research Moscow State University of Civil Engineering; Russian University of Transport (RUT – MIIT); Moscow Institute of Architecture (State Academy); Perm National Research Polytechnic University; 26, Yaroslavskoe Shosse, 129337, Moscow, Russia

Valery I. Telichenko, Full Member of RAACS, Professor, Dr.Sc., The First Vice-President of the Russian Academy of Architecture and Construction Sciences; National Research Moscow State University of Civil Engineering; 24, Ulitsa Bolshaya Dmitrovka, 107031, Moscow, Russia

Vladimir I. Travush, Full Member of RAACS, Professor, Dr.Sc., Vice-President of the Russian Academy of Architecture and Construction Sciences; Urban Planning Institute of Residential and Public Buildings; 24, Ulitsa Bolshaya Dmitrovka, 107031, Moscow, Russia

INVITED REVIEWERS

Akimbek A. Abdikalikov, Professor, Dr.Sc.,
Kyrgyz State University of Construction, Transport and Architecture n.a. N. Isanov;
34 Maldybayeva Str., Bishkek, 720020, Biskek, Kyrgyzstan

Vladimir N. Alekhin, Advisor of RAACS, Professor, Dr.Sc.,
Ural Federal University named after the first President of Russia B.N. Yeltsin;
19 Mira Street, Ekaterinburg, 620002, Russia

Irina N. Afanasyeva, Ph.D., University of Florida; Gainesville, FL 32611, USA

Ján Čelko, Professor, PhD, Ing., University of Žilina; Univerzitná 1, 010 26, Žilina, Slovakia

Tatyana L. Dmitrieva, Professor, Dr.Sc.,
Irkutsk National Research Technical University; 83, Lermontov street, Irkutsk, 664074, Russia

Petr P. Gaidzhurov, Advisor of RAACS, Professor, Dr.Sc.,
Don State Technical University; 1, Gagarina Square, Rostov-on-Don, 344000, Russia

Jacek Grosel, Associate Professor, Dr inz.
Wroclaw University of Technology; 11 Grunwaldzki Sq., 50-377, Wrocław, Poland

Stanislaw Jemioło, Professor, Dr.Sc.,
Warsaw University of Technology; 1, Pl. Politechniki, 00-661, Warsaw, Poland

Konstantin I. Khenokh, M.Ing., M.Sc.,
General Dynamics C4 Systems; 8201 E McDowell Rd, Scottsdale, AZ 85257, USA

Christian Koch, Dr.-Ing., Ruhr-Universität Bochum;
Lehrstuhl für Informatik im Bauwesen, Gebäude IA, 44780, Bochum, Germany

Gaik A. Manuylov, Professor, Ph.D.,
Moscow State University of Railway Engineering; 9, Obraztsova Street, Moscow, 127994, Russia

Alexander S. Noskov, Professor, Dr.Sc.,
Ural Federal University named after the first President of Russia B.N. Yeltsin;
19 Mira Street, Ekaterinburg, 620002, Russia

Grzegorz Świt, Professor, Dr.hab. Inż.,
Kielce University of Technology; 7, al. Tysiąclecia Państwa Polskiego, Kielce, 25 – 314, Poland

AIMS AND SCOPE

The aim of the Journal is to advance the research and practice in structural engineering through the application of computational methods. The Journal will publish original papers and educational articles of general value to the field that will bridge the gap between high-performance construction materials, large-scale engineering systems and advanced methods of analysis.

The scope of the Journal includes papers on computer methods in the areas of structural engineering, civil engineering materials and problems concerned with multiple physical processes interacting at multiple spatial and temporal scales. The Journal is intended to be of interest and use to researches and practitioners in academic, governmental and industrial communities.

ОБЩАЯ ИНФОРМАЦИЯ О ЖУРНАЛЕ

International Journal for Computational Civil and Structural Engineering

(Международный журнал по расчету гражданских и строительных конструкций)

Международный научный журнал "International Journal for Computational Civil and Structural Engineering (Международный журнал по расчету гражданских и строительных конструкций)" (IJCCSE) является ведущим научным периодическим изданием по направлению «Инженерные и технические науки», издаваемым, начиная с 1999 года (ISSN 2588-0195 (Online); ISSN 2587-9618 (Print) Continues ISSN 1524-5845). В журнале на высоком научно-техническом уровне рассматриваются проблемы численного и компьютерного моделирования в строительстве, актуальные вопросы разработки, исследования, развития, верификации, апробации и приложений численных, численно-аналитических методов, программно-алгоритмического обеспечения и выполнения автоматизированного проектирования, мониторинга и комплексного наукоемкого расчетно-теоретического и экспериментального обоснования напряженно-деформированного (и иного) состояния, прочности, устойчивости, надежности и безопасности ответственных объектов гражданского и промышленного строительства, энергетики, машиностроения, транспорта, биотехнологий и других высокотехнологичных отраслей.

В редакционный совет журнала входят известные российские и зарубежные деятели науки и техники (в том числе академики, члены-корреспонденты, иностранные члены, почетные члены и советники Российской академии архитектуры и строительных наук). Основной критерий отбора статей для публикации в журнале − их высокий научный уровень, соответствие которому определяется в ходе высококвалифицированного рецензирования и объективной экспертизы, поступающих в редакцию материалов.

Журнал входит в Перечень ВАК РФ ведущих рецензируемых научных изданий, в которых должны быть опубликованы основные научные результаты диссертаций на соискание ученой степени кандидата наук, на соискание ученой степени доктора наук по научным специальностям и соответствующим им отраслям науки:

- 1.1.8 – Механика деформируемого твердого тела (технические науки),
- 1.2.2 – Математическое моделирование численные методы и комплексы программ (технические науки),
- 2.1.1 – Строительные конструкции, здания и сооружения (технические науки),
- 2.1.2 – Основания и фундаменты, подземные сооружения (технические науки),
- 2.1.5 – Строительные материалы и изделия (технические науки),
- 05.23.07 – Гидротехническое строительство (технические науки),
- 2.1.9 – Строительная механика (технические науки)

В Российской Федерации журнал индексируется Российским индексом научного цитирования (РИНЦ).

Журнал входит в базу данных Russian Science Citation Index (RSCI), полностью интегрированную с платформой Web of Science. Журнал имеет международный статус и высылается в ведущие библиотеки и научные организации мира.

Издатели журнала – *Издательство Ассоциации строительных высших учебных заведений /АСВ/* (Россия, г. Москва) и до 2017 года *Издательский дом Begell House Inc*. (США, г. Нью-Йорк). Официальными партнерами издания является *Российская академия архитектуры и строительных наук* (РААСН), осуществляющая научное курирование издания, и *Научно-исследовательский центр СтаДиО* (ЗАО НИЦ СтаДиО).

Цели журнала – демонстрировать в публикациях российскому и международному профессиональному сообществу новейшие достижения науки в области вычислительных методов

решения фундаментальных и прикладных технических задач, прежде всего в области строительства.

Задачи журнала:

• предоставление российским и зарубежным ученым и специалистам возможности публиковать результаты своих исследований;

• привлечение внимания к наиболее актуальным, перспективным, прорывным и интересным направлениям развития и приложений численных и численно-аналитических методов решения фундаментальных и прикладных технических задач, совершенствования технологий математического, компьютерного моделирования, разработки и верификации реализующего программно-алгоритмического обеспечения;

• обеспечение обмена мнениями между исследователями из разных регионов и государств.

Тематика журнала. К рассмотрению и публикации в журнале принимаются аналитические материалы, научные статьи, обзоры, рецензии и отзывы на научные публикации по фундаментальным и прикладным вопросам технических наук, прежде всего в области строительства. В журнале также публикуются информационные материалы, освещающие научные мероприятия и передовые достижения Российской академии архитектуры и строительных наук, научно-образовательных и проектно-конструкторских организаций.

Тематика статей, принимаемых к публикации в журнале, соответствует его названию и охватывает направления научных исследований в области разработки, исследования и приложений численных и численно-аналитических методов, программного обеспечения, технологий компьютерного моделирования в решении прикладных задач в области строительства, а также соответствующие профильные специальности, представленные в диссертационных советах профильных образовательных организациях высшего образования.

Редакционная политика. Политика редакционной коллегии журнала базируется на современных юридических требованиях в отношении авторского права, законности, плагиата и клеветы, изложенных в законодательстве Российской Федерации, и этических принципах, поддерживаемых сообществом ведущих издателей научной периодики.

За публикацию статей плата с авторов не взымается. Публикация статей в журнале бесплатная. На платной основе в журнале могут быть опубликованы материалы рекламного характера, имеющие прямое отношение к тематике журнала.

Журнал предоставляет непосредственный открытый доступ к своему контенту, исходя из следующего принципа: свободный открытый доступ к результатам исследований способствует увеличению глобального обмена знаниями.

Индексирование. Публикации в журнале входят в системы расчетов индексов цитирования авторов и журналов. «Индекс цитирования» – числовой показатель, характеризующий значимость данной статьи и вычисляющийся на основе последующих публикаций, ссылающихся на данную работу.

Авторам. Прежде чем направить статью в редакцию журнала, авторам следует ознакомиться со всеми материалами, размещенными в разделах сайта журнала (интернет-сайт Российской академии архитектуры и строительных наук (http://raasn.ru); подраздел «Издания РААСН» или интернет-сайт Издательства АСВ (http://iasv.ru); подраздел «Журнал IJCCSE»): с основной информацией о журнале, его целями и задачами, составом редакционной коллегии и редакционного совета, редакционной политикой, порядком рецензирования направляемых в журнал статей, сведениями о соблюдении редакционной этики, о политике авторского права и лицензирования, о представлении журнала в информационных системах (индексировании), информацией о подписке на журнал, контактными данными и пр. Журнал работает по лицензии Creative Commons типа cc by-nc-sa (Attribution Non-Commercial Share Alike) – Лицензия «С указанием авторства – Некоммерческая – Копилефт».

Рецензирование. Все научные статьи, поступившие в редакцию журнала, проходят обязательное двойное слепое рецензирование (рецензент не знает авторов рукописи, авторы рукописи не знают рецензентов).

Заимствования и плагиат. Редакционная коллегия журнала при рассмотрении статьи проводит проверку материала с помощью системы «Антиплагиат». В случае обнаружения многочисленных заимствований редакция действует в соответствии с правилами COPE.

Подписка. Журнал зарегистрирован в Федеральном агентстве по средствам массовой информации и охраны культурного наследия Российской Федерации. Индекс в общероссийском каталоге РОСПЕЧАТЬ − 18076.

По вопросам подписки на международный научный журнал “International Journal for Computational Civil and Structural Engineering (Международный журнал по расчету гражданских и строительных конструкций)” обращайтесь в Агентство «Роспечать» (Официальный сайт в сети Интернет: http://www.rosp.ru/) или в издательство Ассоциации строительных вузов (АСВ) в соответствии со следующими контактными данными:

ООО «Издательство АСВ»

Юридический адрес: 129337, Россия, г. Москва, Ярославское ш., д. 26, офис 705;

Фактический адрес: 129337, Россия, г. Москва, Ярославское ш., д. 19, корп. 1, 5 этаж, офис 12 (ТЦ Соле Молл);

Телефоны: +7 (925) 084-74-24;

Интернет-сайт: www.iasv.ru. Адрес электронной почты: iasv@iasv.ru.

Контактная информация. По всем вопросам работы редакции, рецензирования, согласования правки текстов и публикации статей следует обращаться к главному редактору журнала члену-корреспонденту РААСН *Сидорову Владимиру Николаевичу* (адреса электронной почты: sidorov.vladimir@gmail.com, sidorov@iasv.ru, iasv@iasv.ru, sidorov@raasn.ru) или к техническому редактору журнала советнику РААСН *Кайтукову Таймуразу Батразовичу* (адреса электронной почты: tkaytukov@gmail.com; kaytukov@raasn.ru). Кроме того, по указанным вопросам, а также по вопросам размещения в журнале рекламных материалов можно обращаться к генеральному директору ООО «Издательство АСВ» *Никитиной Надежде Сергеевне* (адреса электронной почты: iasv@iasv.ru, nsnikitina@mail.ru, ijccse@iasv.ru).

Журнал становится технологичнее. Издательство АСВ с сентября 2016 года является членом Международной ассоциации издателей научной литературы (Publishers International Linking Association (PILA)), осуществляющей свою деятельность на платформе CrossRef. Оригинальным статьям, публикуемым в журнале, будут присваиваться уникальные номера (индексы DOI – Digital Object Identifier), что значительно облегчит поиск метаданных и местонахождение полнотекстового произведения. DOI – это система определения научного контента в сети Интернет.

С октября 2016 года стал возможен прием статей на рассмотрение и рецензирование через онлайн систему приема статей Open Journal Systems на сайте журнала (электронная редакция): https://ijccse.iasv.ru.

Автор имеет возможность следить за продвижением статьи в редакции журнала в личном кабинете Open Journal Systems и получать соответствующие уведомления по электронной почте.

В феврале 2018 года журнал был зарегистрирован в Directory of open access journals (DOAJ) (это один из самых известных поисковых сервисов в мире, который предоставляет открытый доступ к материалам и индексирует не только заголовки журналов, но и научные статьи), в сентябре 2018 года включен в продукты EBSCO Publishing.

В ноябре 2020 года журнал начал индексироваться в международной базе Scopus.

International Journal for
Computational Civil and Structural Engineering
(Международный журнал по расчету гражданских и строительных конструкций)
Volume 19, Issue 4 ***2023***

Scientific coordination is carried out by the Russian Academy of Architecture and Construction Sciences (RAACS)

CONTENTS

Nonlinear Analysis of Solid Reinforced Concrete Structures with Cracks **14**
Vladimir P. Agapov, Alexey S. Markovich

Features of Development of Dynamic Models of Hydro Structures and Their Verification According to Field Measurement Data Using the Example of Sayano-Shushenskaya HPP **27**
Alexander M. Belostotsky, Dmitry S. Dmitriev, Sergey O. Petryashev

Aggregate Risk of a Large Complex Construction Projects of NPP **38**
Petr G. Grabovy, Denis E. Sezemin

Repair of Masonry After Dynamic Impacts. Calculation and Design Methods **48**
Oleg V. Kabantsev, Oleg A. Simakov

Computer Modeling the Stress State of Operating Tanks Using Geometric Interpolators **69**
Evgeniy V. Konopatskiy, Oksana A. Shevchuk, Andrey A. Bezditnyi

Analytical Analysis of Combined Foundation Plates, Subjected to an Action of Antisymmetric Loads **83**
Elena B. Koreneva, Valery R. Grosman

Information Modeling of Concrete: Current Status and Development Prospects **95**
Aleksey I. Makeev

Calculation Model of Deformation of The Soil Foundation of a High-Rise Building, Taking into Account the Loading History **116**
Ilizar T. Mirsayapov, Irina V. Koroleva

Digital Tools in The Design Practice for Reconstruction of Underground Pipelines with Trenchless Methods **124**
Vladimir A. Orlov, Sergey P. Zotkin, Dmitry V. Podolyan

Deposition of Particles from a Turbulent Flow on the Walls of Pipes and Channels **135**
Sergey V. Fedosov , Alexandr V. Markelov

Determination of Concrete Rheological Parameters Using Nonlinear Optimization Methods 147
Anton S. Chepurnenko, Stepan V. Litvinov, Batyr M. Yazyev

Development of Computational Schemes of Generalized Kinematic Devices that Precisely Regulate the Natural Frequency Spectrum of Elastic Systems with a Finite Number of Degrees of Mass Freedom, in Which the Directions of Motion Are Parallel, But Do Not Lie in the Same Plane. Part 2: Samples of Analysis 155
Leonid S. Lyakhovich, Pavel A. Akimov, Zaur R. Galyautdinov, Andrey S. Plyaskin

Static Bearing Capacity of Steel-plate Composite Walls
Vladimir I. Travush, Petr D. Arleninov, Mikhail A. Desyatkin, Andrey N. Ivaschenko, Semen S. Kaprielov, Denis V. Konin, Alexey S. Krylov, Sergey B. Krylov, Igor A. Chilin, Alexey I. Shakhvorostov, Andrey V. Sheinfeld 166

Performance of a Base-Isolated RC Building Supported on Square Un-Bonded Fiber Reinforced Elastomeric Isolator Under Earthquakes 182
Van-Thuyet Ngo

Comparative Study of Axial Bearing Capacity for Pile Foundation Based on Empirical, Numerical Method and Pile Driving Analyzer Test 196
Tsaana Khoirunisaa, Bambang Setiawan, Yusep M. Purwana

Strength Analysis of Formwork Using Falsework Flying System on Slab-On Pile Structure 208
Fendi Hary Yanto

International Journal for
Computational Civil and Structural Engineering
(Международный журнал по расчету гражданских и строительных конструкций)
Volume 19, Issue 4 ***2023***

Scientific coordination is carried out by the Russian Academy of Architecture and Construction Sciences (RAACS)

СОДЕРЖАНИЕ

Нелинейный анализ массивных железобетонных конструкций с учетом трещинообразования **14**
В.П. Агапов, А.С. Маркович

Особенности разработки динамических моделей гидротехнических сооружений и их верификация по данным натурных измерений на примере Саяно-Шушенской ГЭС **27**
А.М. Белостоцкий, Д.С. Дмитриев, С.О. Петряшев

Совокупный риск при реализации крупного комплексного проекта строительства атомной электростанции **38**
П.Г. Грабовый, Д.Е. Сеземин

Восстановление каменной кладки после динамических воздействий. Методы расчета и проектирования **48**
О.В. Кабанцев, О.А. Симаков

Компьютерное моделирование напряженного состояния эксплуатируемых резервуаров с помощью геометрических интерполянтов **69**
Е.В. Конопацкий, О.А. Шевчук, А.А. Бездитный

Аналитический расчет комбинированных фундаментных плит при действии на них антисимметричных нагрузок **83**
Е.Б. Коренева, В.Р. Гросман

Информационное моделирование бетона: обзор современного состояния и перспективы развития **95**
А.И. Макеев

Расчетная модель деформирования грунтового основания высотного здания с учетом предыстории загружения **116**
И.Т. Мирсаяпов, И.В. Королева

Инструменты цифровизации в практике проектирования при реконструкции подземных трубопроводов бестраншейными методами **124**
В.А. Орлов, С.П. Зоткин, Д.В. Подолян

Осаждение частиц из турбулентного потока на стенки труб и каналов **135**
С.В. Федосов, А.В. Маркелов

Определение реологических параметров бетона при помощи методов нелинейной оптимизации **147**
А.С. Чепурненко, С.В. Литвинов, Б.М. Язьев

Формирование расчетных схем обобщенных кинематических устройств, прицельно регулирующих спектр частот собственных колебаний упругих систем с конечным числом степеней свободы масс, у которых направления движения параллельны, но не лежат в одной плоскости. Часть 2: примеры расчета **155**
Л.С. Ляхович, П.А. Акимов, З.Р. Галяутдинов, А.С. Пляскин

Несущая способность сталежелезобетонных стен с листовым армированием на статические нагрузки **166**
В.И. Травуш, П.Д. Арленинов, М.А. Десяткин, А.Н. Иващенко, С.С. Каприелов, Д.В. Конин, А.С. Крылов, С.Б. Крылов, И.А. Чилин, А.И. Шахворостов, А.В. Шейнфельд

Эффективность квадратного армированного волокном эластомерного изолятора для железобетонного здания при землетрясениях **182**
Ван-Тхует Нго

Исследование несущей способности свай на основе эмпирических данных, динамических испытаний и численного моделирования **196**
Тсаана Хойрунисаа, Бамбанг Сетиаван, Юсеп М. Пурвана

Исследование прочности опалубки с применением подвесной системы для плитно-свайной конструкции **208**
Фенди Гарри Янто

DOI:10.22337/2587-9618-2023-19-4-14-26

NONLINEAR ANALYSIS OF SOLID REINFORCED CONCRETE STRUCTURES WITH CRACKS

Vladimir P. Agapov [1], Alexey S. Markovich [1,2]

[1] RUDN University, Moscow, RUSSIA
[2] Moscow State University of Civil Engineering, Moscow, RUSSIA

Abstract: A finite element method, as well as the algorithm and the program for solid reinforced concrete structures analysis have been developed, taking into account plastic deformations of concrete. A modified Willam & Warnke failure criterion was used, supplemented by a flow criterion. Two models of volumetric deformation of concrete have been developed: an elastic model under brittle fracture and an ideal elastic-plastic model. An eight-node solid finite element with linear approximation of displacement functions, which implements the deformation models above mentioned, is constructed. This finite element is adapted to the PRINS computational software, and as part of this program it can be used for physically nonlinear analysis of building structures containing three-dimensional reinforced concrete elements. Modern building codes prescribe to carry out calculations of concrete and reinforced concrete structures in a nonlinear formulation, taking into account the real properties of concrete and reinforcement. To verify the developed finite element, a series of test calculations of a beam in the condition of pure bending was carried out. Comparison of the calculation results with experimental data confirmed the high accuracy and reliability of the results obtained.

Keywords: finite element method, PRINS computational program, building structures, solid reinforced concrete structures, physical nonlinearity, plasticity, flow theory, structural mechanics

НЕЛИНЕЙНЫЙ АНАЛИЗ МАССИВНЫХ ЖЕЛЕЗОБЕТОННЫХ КОНСТРУКЦИЙ С УЧЕТОМ ТРЕЩИНООБРАЗОВАНИЯ

В.П. Агапов [1], А.С. Маркович [1,2]

[1] Российский университет дружбы народов им. Патриса Лумумбы, г. Москва, РОССИЯ
[2] Национальный исследовательский Московский государственный строительный университет, г. Москва, РОССИЯ

Аннотация: Разработан объемный восьмиузловой конечный элемент для расчета массивных железобетонных конструкций с учетом трещинообразования. При построении элемента в области напряженного состояния «сжатие – сжатие – сжатие» использован модифицированный критерий прочности Виллама – Варнке. Напряженное состояние бетона при возникновении трещины в режиме «сжатие – сжатие» рассматривалось как плосконапряженное и использовался модифицированный критерий прочности Мизеса – Губера. Поведение бетона при растяжении принималось линейным вплоть до возникновения трещины. Разработанный конечный элемент адаптирован к вычислительному комплексу ПРИНС и в составе этого комплекса может быть использован инженерами проектных и научных организаций для практических расчетов массивных железобетонных конструкций. Для верификации разработанного конечного элемента проведена серия тестовых расчетов балки, находящейся в условии чистого изгиба. Сравнение результатов расчета с экспериментальными данными подтвердило высокую точность и достоверность полученных результатов.

Ключевые слова: метод конечных элементов, вычислительный комплекс ПРИНС, строительные конструкции, массивные железобетонные сооружения, физическая нелинейность, пластичность, теория течения, механика деформируемых тел

INTRODUCTION

Modern building codes and regulations adopted in our country and abroad prescribe to carry out calculations of reinforced concrete structures in a nonlinear setting, taking into account the real properties of concrete and reinforcement. At the same time, the nonlinear deformation of concrete, taking into account real elastoplastic properties under the conditions of a volumetric stress state, was studied throughout the 20th century by both domestic and foreign scientists.

The prerequisites for the successful implementation of such calculations were created by the development of computer technology, on the one hand, and the development of numerical methods of structural mechanics, primarily the finite element method, on the other [1,2,3,4,5].

Nonlinear methods for calculating structures are implemented in a number of computer programs, such as NASTRAN [6], ANSYS [7], ABAQUS [8], ADINA [9], DIANA [10] and others. Common to all these programs is the use of algorithms based on the execution of step procedures.

However, it should be noted that the calculations of physically nonlinear structures in the above programs are performed using physical relationships based on certain experimental data. In this case, the obtained nonlinear equations for the structure as a whole are solved by approximate methods. To increase the reliability of the results, such calculations should be carried out using several programs. Therefore, engineers should have several available calculation tools in their arsenal. In this regard, the development of alternative computational methods and corresponding programs is still an urgent task.

MATERIALS AND METHODS

As is known, the system of nonlinear algebraic equations is solved by the Newton-Raphson method in full or modified form. The equilibrium equations at the loading step are written as:

$$\mathbf{K}_j^i \Delta \mathbf{u}_j^i = \mathbf{P}_j - \mathbf{F}_j^{i-1}, \quad (1)$$

where $\mathbf{K}_j^i$ is the tangential stiffness matrix, $\Delta \mathbf{u}_j^i$ is the vector of nodal displacements, $\mathbf{P}_j$ is the vector of nodal loads, $\mathbf{F}_j^{i-1}$ is the vector of nodal concentrated forces equivalent to element stresses, j is the step number, i is the iteration number.

A feature of the Newton-Raphson method for solving equation (1) is the calculation and factorization of the tangent stiffness matrix at each iteration. In the case of large-order systems, such calculations can be quite expensive.

When using the modified Newton-Raphson method, the stiffness matrix is calculated and factorized only once at the beginning of the step [4,5]. This simplifies the calculations, but requires more iterations to achieve the specified accuracy. Therefore, to accelerate convergence, different approaches are used based on the correction of the displacement vector at the current iteration [11,12,13].

In the PRINS computer application, the calculation of physically nonlinear structures by the finite element method is carried out in increments according to the equation [1]:

$$\left(\mathbf{K}_0 + \Delta \mathbf{K}\right) \Delta \mathbf{u} = \Delta \mathbf{P}, \quad (2)$$

where $\Delta \mathbf{K} = \frac{1}{2}\left(\mathbf{K}_1 - \mathbf{K}_0\right)$.

Stiffness matrices $\mathbf{K}_0$ and $\mathbf{K}_1$ are calculated at the beginning and at the end of the loading step. Equation (2) is solved by the iterative method:

$$\mathbf{K}_0 \Delta \mathbf{u}_i = \Delta \mathbf{P} - \Delta \mathbf{K}_{i-1} \Delta \mathbf{u}_{i-1}, \quad (3)$$

where i is the iteration number.

Upon reaching the convergence of the iterative process, the full values of displacements and stresses are found using the formulas:

$$\mathbf{u} = \mathbf{u}_0 + \Delta\mathbf{u}\,, \quad \boldsymbol{\sigma} = \boldsymbol{\sigma}_0 + \Delta\boldsymbol{\sigma}\,. \tag{4}$$

In general, stress increments are determined by the formula

$$\Delta\boldsymbol{\sigma} = \mathbf{C}_{ep}\Delta\boldsymbol{\varepsilon}\,, \tag{5}$$

where $\mathbf{C}_{ep}$ is the elastoplastic matrix of material characteristics.

At each loading step, the stress state is analyzed and, in the event of plastic deformations and cracks, the stresses are corrected taking into account the accepted material deformation diagrams. This requires a structural balancing process. Equilibrium iterations are performed according to formula (1), which is modified to the form:

$$\mathbf{K}_j\Delta\mathbf{u}_j^i = \mathbf{P}_j - \mathbf{F}_j^{i-1}\,. \tag{6}$$

The difference between formulas (1) and (6) is that in formula (1) the stiffness matrix changes from iteration to iteration (meaning equilibrium iteration), and in formula (6) it does not change, and is taken equal to the stiffness matrix, found at the end of the step during iterations according to formula (3).

Thus, in formula (3) the stiffness matrix is iterated, and according to formula (6) is iterated the vector of nodal forces, which is equivalent to internal stresses.

The stiffness matrix for a single finite element is found by the formula [2]:

$$\mathbf{K} = \int_V \mathbf{B}^T\mathbf{C}_e\mathbf{B}d\mathbf{V}\,, \tag{7}$$

where $\mathbf{B}$ is the matrix relating the strain components of the element to the nodal displacement components (geometric matrix), $\mathbf{C}_e$ is the matrix relating the stress components to the strain components (physical matrix).

The technique for calculating a geometric matrix is well known (see, for example, [3]).

THE MAIN PREREQUISITES FOR THE ANALYSIS OF THE VOLUMETRIC STRESS STATE

Four types of stress state are considered: compression – compression – compression, compression – compression – tension, compression – tension – tension, tension – tension – tension.

The following types of material behavior are taken into account: loading, unloading and reloading. The deformation paths of the material corresponding to the indicated types of behavior are shown in figs. 1.

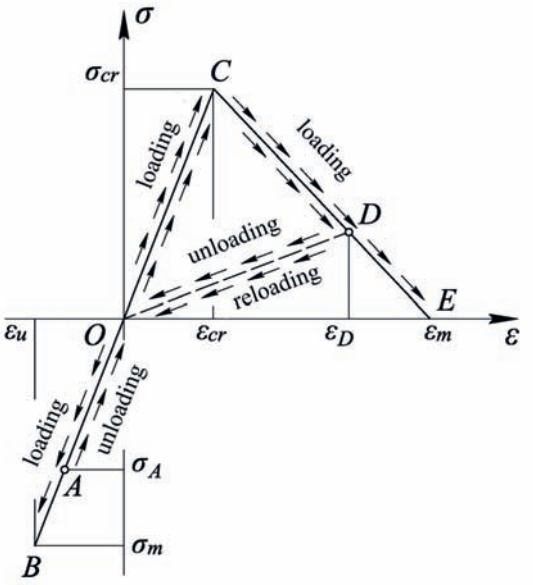


Figure 1. Material Deformation Path

Loading of tensile concrete after the formation of a crack (path $C - D - E$) occurs with the modulus of elasticity

$$E_i = \frac{\sigma_{cr}}{\varepsilon_m - \varepsilon_{cr}}\,, \tag{8}$$

where ε_m is the ultimate strain of concrete with cracks in tension and ε_{cr} is the cracking strain, respectively (Fig. 1).

Unloading and reloading of concrete with cracks (path $D - O$) occur according to a linear law with a fictitious modulus of elasticity

$$E_i' = \frac{1}{\varepsilon_D}\frac{\sigma_{cr}\left(\varepsilon_m - \varepsilon_D\right)}{\varepsilon_m - \varepsilon_{cr}},\ \varepsilon_{cr} < \varepsilon_D < \varepsilon_m \quad (9)$$

The stress in tensile concrete after the occurrence of a crack is found by the formula

$$\sigma = \sigma_{cr}\frac{\varepsilon_m - \varepsilon_D}{\varepsilon_m - \varepsilon_{cr}}, \quad (10)$$

which is easily obtained from the similarity of the triangles in fig. 1.

Deformation of concrete in the «compression – compression – compression» mode

When constructing a physical matrix, an elastic model was adopted for brittle fracture of concrete in the «compression – compression – compression» mode. The behavior of concrete is considered to be linearly elastic until reaching the fracture surface.

The five-parameter model proposed by Willam & Warnke [14] was adopted as the fracture surface. On fig. 2 shows the deviatoric section of this surface, and in fig. 3 shows the main meridians of tension and compression.

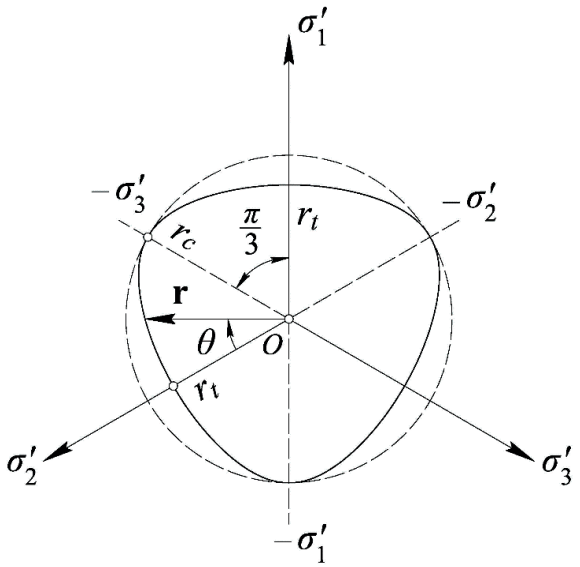


Figure 2. Deviatoric section of the fracture surface (r_t and r_c – the meridians of tension and compression, θ – the angle of the type of the stress state)

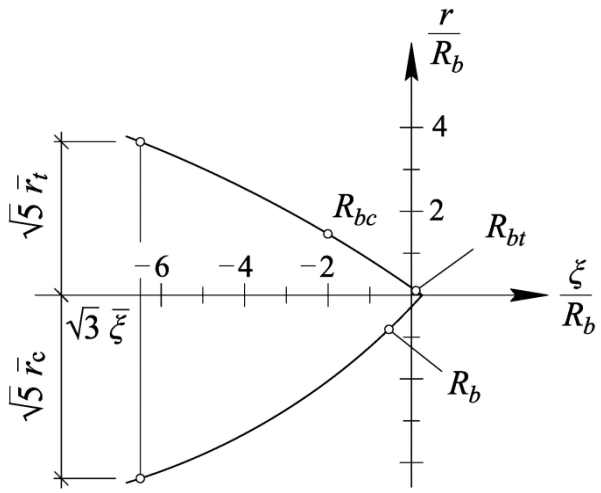


Figure 3. Tension and compression meridians of fracture surface (R_b and R_{bt} – ultimate strength of concrete for axial compression and tension, R_{bc} – ultimate strength of concrete for uniform biaxial compression, $r = \sqrt{5}\tau_m$, $\xi = \sqrt{3}\sigma_m$)

The failure criterion is determined by the formula [14]:

$$f(\boldsymbol{\sigma}) = f\left(\sigma_m, \tau_m, \theta\right) = \frac{1}{\bar{r}\left(\sigma_m, \theta\right)}\frac{\tau_m}{R_b} - 1 = 0\,, \quad (11)$$

where σ_m and τ_m are the average values of normal and shear stresses in the vicinity of the point, θ is the angle of the stress state, and $\bar{r}\left(\sigma_m, \theta\right) = \frac{r}{\sqrt{5}R_b}$ is the radius-vector of the point on the fracture surface in the deviator section (fig. 2).

The radius-vector $\bar{r}\left(\sigma_m, \theta\right)$ is determined by the formula [14]:

$$\bar{r}\left(\sigma_m, \theta\right) = \frac{2r_c\left(r_c^2 - r_t^2\right)\cos\theta + r_c\left(2r_t - r_c\right)\Psi}{4\left(r_c^2 - r_t^2\right)\cos^2\theta + \left(r_c - 2r_t\right)^2}, \quad (12)$$

where $\Psi = \sqrt{4\left(r_c^2 - r_t^2\right)\cos^2\theta + 5r_t^2 - 4r_t r_c}$.

The radius-vectors r_t and r_c (fig. 2) define the meridians of tensile $(\theta = 0)$ and compression $(\theta = \pi/3)$. In the Willam & Warnke model these meridians are square parabolas:

$$\frac{\tau_{m,t}}{R_b} = r_t = a_0 + a_1\frac{\sigma_m}{R_b} + a_2\left(\frac{\sigma_m}{R_b}\right)^2,$$
$$\frac{\tau_{m,c}}{R_b} = r_c = b_0 + b_1\frac{\sigma_m}{R_b} + b_2\left(\frac{\sigma_m}{R_b}\right)^2. \qquad (13)$$

The coefficients a_0, a_1, a_2 and b_0, b_1, b_2 are obtained on the basis of experimental data for specific concrete grades (table 1).

$$a_0 = \frac{2}{3}\overline{R}_{bc}a_1 - \frac{4}{9}\overline{R}_{bc}^2 a_2 + \sqrt{\frac{2}{15}}\overline{R}_{bc},$$
$$a_1 = \frac{1}{3}\left(2\overline{R}_{bc} - \overline{R}_{bt}\right)a_2 + \sqrt{\frac{6}{5}}\frac{\overline{R}_{bt} - \overline{R}_{bc}}{2\overline{R}_{bc} + \overline{R}_{bt}},$$
$$a_2 = \frac{\sqrt{\frac{6}{5}}\overline{\xi}_t\left(\overline{R}_{bt} - \overline{R}_{bc}\right) - \sqrt{\frac{6}{5}}\overline{R}_{bt}\overline{R}_{bc} + \overline{r}_t\left(2\overline{R}_{bc} + \overline{R}_{bt}\right)}{\left(2\overline{R}_{bc} + \overline{R}_{bt}\right)\lambda}$$
$$\lambda = \overline{\xi}_t^2 - \frac{2}{3}\overline{R}_{bc}\overline{\xi}_t + \frac{1}{3}\overline{R}_{bt}\overline{\xi}_t - \frac{2}{9}\overline{R}_{bt}\overline{R}_{bc}, \qquad (14)$$

and

$$b_0 = -\rho b_1 - \rho^2 b_2,\ b_1 = \left(\overline{\xi}_c + \frac{1}{3}\right)b_2 + \frac{\sqrt{\frac{6}{5}} - 3r_c}{3\overline{\xi}_c - 1},$$
$$b_2 = \frac{r_c\left(\rho + \frac{1}{3}\right) - \sqrt{\frac{2}{15}}\left(\overline{\xi}_c + \rho\right)}{\left(\overline{\xi}_c + \rho\right)\left(\overline{\xi}_c - \frac{1}{3}\right)\left(\rho + \frac{1}{3}\right)}. \qquad (15)$$

Table 1. To the determination of the parameters of the Willam & Warnke model

	Type of stress state	Criterion	Stresses	Angle θ
1.	Uniaxial compression	R_b	$\sigma_3 = -R_b,\ \sigma_1 = \sigma_2 = 0$	0
2.	Uniaxial tension	R_{bt}	$\sigma_1 = R_{bt},\ \sigma_2 = \sigma_3 = 0,$ $\overline{R}_{bt} = \frac{R_{bt}}{R_b}$	0
3.	Uniform biaxial compression	R_{bc}	$\sigma_1 = \sigma_2 = -R_{bc},$ $\sigma_3 = 0,$ $\overline{R}_{bc} = \frac{R_{bc}}{Rb} = 1,2$	0
4.	Triaxial compression in high compression mode $(\sigma_3 < \sigma_1 = \sigma_2,\ \theta = 0)$	$\frac{\sigma_m}{R_b} = -\overline{\xi}_t,$ $\overline{\xi}_1 > 0,$ $\frac{\tau_m}{R_b} = \overline{r}_t$	$\sigma_1 \neq 0,\ \sigma_2 \neq 0,\ \sigma_3 \neq 0,$ $\overline{\xi}_1 = 3,67*,\ \overline{r}_t = 1,59*$	0
5.	Triaxial compression in low compression mode $(\sigma_3 > \sigma_1 = \sigma_2,\ \theta = \pi/3)$	$\frac{\sigma_m}{R_b} = -\overline{\xi}_c,$ $\overline{\xi}_2 > 0,$ $\frac{\tau_m}{R_b} = \overline{r}_c$	$\sigma_1 \neq 0,\ \sigma_2 \neq 0,\ \sigma_3 \neq 0,$ $\overline{\xi}_c = 3,67*,\ \overline{r}_c = 1,94*$	$\pi/3$

*According to the results of Lourse & Gachon's experiments

Deformation of concrete in the modes «compression – compression – tension», «compression – tension – tension» and «tension - tension – tension» (taking into account cracking)

The physical matrix for concrete with one, two and three cracks is formed as follows.

When one crack is formed the stress state of concrete in two other directions is considered as plane stressed and, in this case, the modified von Mises – Huber strength criterion is used [29].

Initially, the stresses in the finite element are calculated in the global axes of the structure $x – y – z$. At the moment the first crack occurs the position of the main axes 1 – 2 – 3 is fixed (fig. 4).

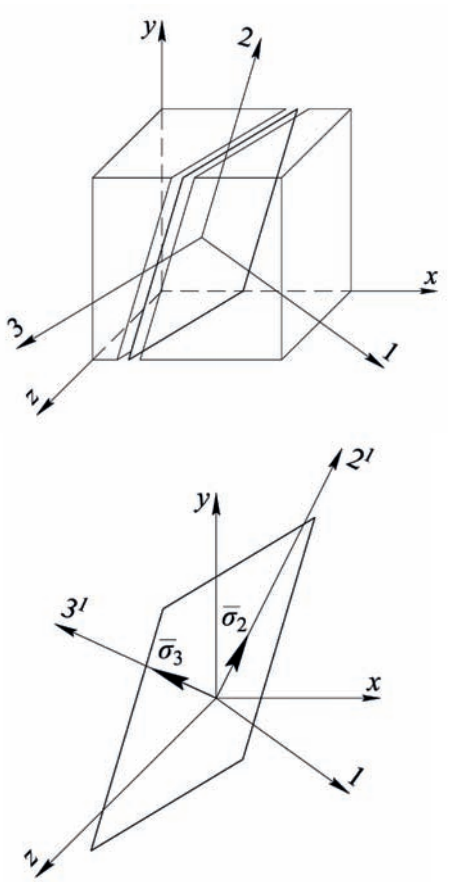


Figure 4. Analysis of the stress state of concrete during the formation of one crack

When the first crack occurs the material in the volume of the element breaks up, according to the accepted hypothesis, into a number of plane stressed plates. In each such plate there are such areas with normals 2^1 and 3^1, on which the normal stresses have extreme values. Further analysis of cracking is carried out according to the principal stresses and acting along axes 2^1 and 3^1 (fig. 4). These stresses, as well as the angle of rotation of axes 2^1 and 3^1 relative to axes 2 and 3 are found according to the general rules for the strength of materials. Further calculation of the structure is performed in axes $1 – 2^1 – 3^1$, for which the matrix of direction cosines of these axes is preliminarily calculated in the global axes $x – y – z$.

In the presence of two cracks the module of elasticity of concrete in the third direction is determined by the «stress-strain» diagram for a uniaxial stress state, and the shear modules are taken according to the recommendations given in [1].

In this case, the physical matrix is calculated as follows:

$$\mathbf{C}_e = \begin{bmatrix} 0 & 0 & 0 & 0 & 0 & 0 \\ 0 & 0 & 0 & 0 & 0 & 0 \\ 0 & 0 & E & 0 & 0 & 0 \\ 0 & 0 & 0 & G_{12}^c & 0 & 0 \\ 0 & 0 & 0 & 0 & G_{23}^c & 0 \\ 0 & 0 & 0 & 0 & 0 & G_{31}^c \end{bmatrix}, \quad (16)$$

In the presence of three cracks the modulus of elasticity is zero.

The modulus E in matrix (16) is taken equal to either the initial modulus if the concrete is tensiled in the third main direction, or the tangent modulus of the stress-strain curve if the concrete is compressed in the third main direction.

Experiments show that cracked concrete with reinforcement transmits significant shear stresses. In this case, the magnitude of shear stiffness is influenced by such factors as the width of the crack opening, the coefficient of reinforcement, the diameter of the reinforcement, the structure of concrete, etc. [28]. Following the recommendations of [28], we take the shear modulus as a function of the current tensile strain.

For concrete with a crack in the first principal direction

$$G_{12}^c = 0,25G\left(1-\frac{\varepsilon_1}{0,004}\right),$$
$$G_{12}^c = 0 \text{ if } \varepsilon_1 > 0,004, \quad (17)$$
$$G_{31}^c = G_{12}^c,$$

where G is the shear modulus of concrete without cracks, ε_1 is the tensile strain in the main direction 1.

For concrete with a crack in two directions:

$$G_{13}^c = 0,25G\left(1-\frac{\varepsilon_1}{0,004}\right),$$
$$G_{13}^c = 0 \text{ if } \varepsilon_1 > 0,004,$$
$$G_{23}^c = 0,25G\left(1-\frac{\varepsilon_2}{0,004}\right), \quad (18)$$
$$G_{23}^c = 0 \text{ if } \varepsilon_2 > 0,004,$$
$$G_{12}^c = \frac{1}{2}\min\left[G_{13}^c, G_{23}^c\right].$$

For concrete with a crack in three directions:

$$G_1 = 0,25G\left(1-\frac{\varepsilon_1}{0,004}\right),$$
$$G_1 = 0 \text{ if } \varepsilon_1 > 0,004,$$
$$G_2 = 0,25G\left(1-\frac{\varepsilon_2}{0,004}\right), \quad (19)$$
$$G_2 = 0 \text{ if } \varepsilon_2 > 0,004,$$
$$G_3 = 0,25G\left(1-\frac{\varepsilon_3}{0,004}\right),$$
$$G_3 = 0 \text{ if } \varepsilon_3 > 0,004,$$
$$G_{12}^c = G_{23}^c = G_{31}^c = \frac{1}{2}\min\left[G_1, G_2, G_3\right].$$

Based on the above algorithm, a program adapted to the PRINS computer application was developed.

RESEARCH RESULTS

To test the developed finite element, the results of experiments by Obernikhin D.V. and Nikulin A.I. were used from the article [26], in which the strength and crack resistance of reinforced concrete beams were studied.

Beam material – class B22.5 concrete. The beam had double longitudinal reinforcement with A500 Ø12 and A240 Ø8 mm rebar, respectively. The transverse reinforcement is reinforcement class Bp500 Ø5 mm (Fig. 5).

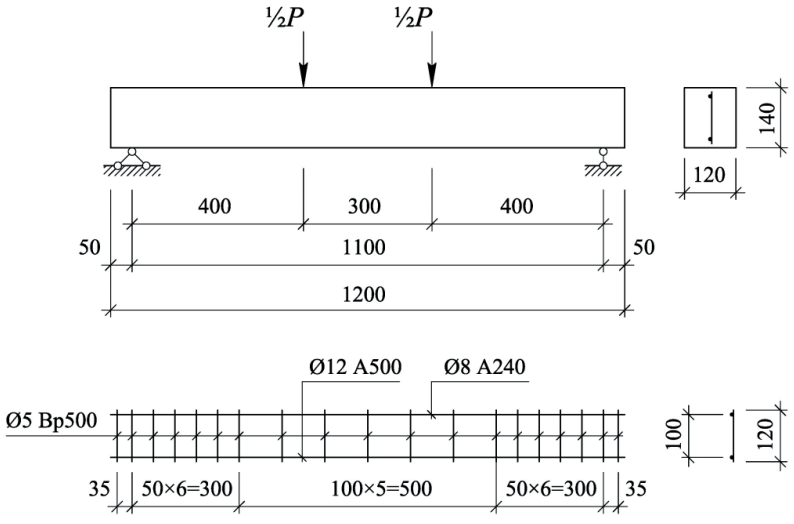
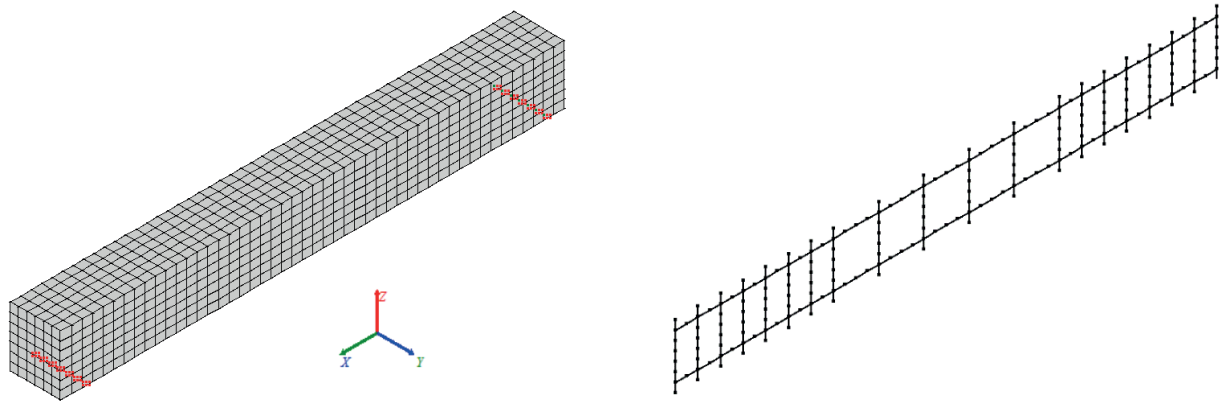


Figure 5. Geometric dimensions and reinforcement scheme of beams

The finite element model of the experimental beam consisted of 2016 three-dimensional eight-node elements (fig. 6). Beam reinforcement was modeled by one-dimensional bar elements with three degrees of freedom at the node. For longitudinal reinforcement the hypothesis of ideal elastoplastic behavior was accepted and the influence of the squares of rotation angles on longitudinal forces was taken into account. The transverse reinforcement rods were under conditions of linear elastic deformation.

The loading and fixing conditions of the beam corresponded to the methodology carried out by Obernikhin D.V. and Nikulin A.I. experiments [26].

It should be noted that earlier similar problems were considered by Rimshin V.I. and Amelin P.A. in [27] using the foreign complex ABAQUS.



a) *b)*

Figure 6. FE scheme of the experimental beam: a – FE model of the «body» of the beam, b – bar FE scheme of reinforcement

The total load on the beam was taken equal to P = 48 kN. The calculations were performed by the step-iterative method. 41 loading steps were set, the coefficient to the load at the first step was taken equal to 0.01, and at the remaining steps – 0.03.

According to the calculation results, the process of crack formation in concrete, beam displacements at fixed load values, as well as the ultimate (failure) load were researched.

The calculation results are presented in table 2.

Table 2. Beam calculation results

Analyzed value	Average displacements of beams (mm) under load, kN			Average cracking load, kN	Average failure load, kN
	16	24	32		
Experimental results [26]	1,76	3,23	4,90	6,41	40,218
Calculation results in the PRINS computer application	1,63	2,98	4,82	6,24	39,36
Divergence, %	7,98	8,39	1,66	2,72	2,18

As can be seen from table. 2, the divergences in the values of the ultimate (failure) load, obtained from the results of calculations in the PRINS computer program, in comparison with the experimental data [26] does not exceed 2.18%, which indicates the high accuracy of the

developed finite element, as well as reliability and stability used nonlinear calculation algorithms.

The process of cracking of the considered beam is shown in Fig. 7.

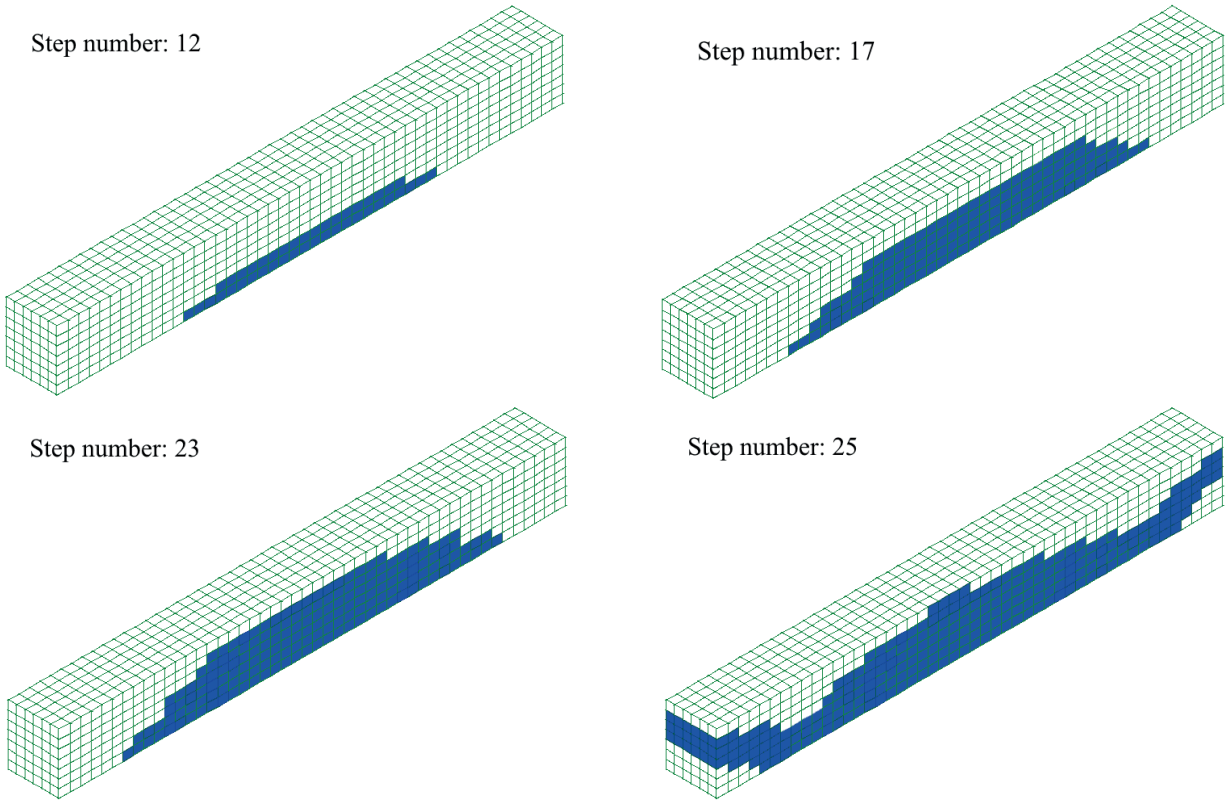
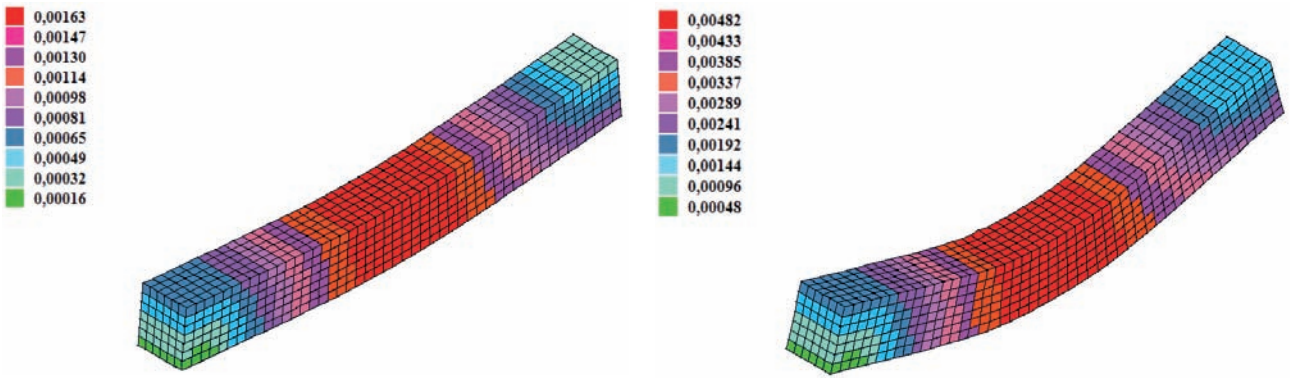


Figure 7. Cracking of the considered beam

The beam displacements corresponding to the total load of 16 kN and 32 kN are shown in fig. 8.



a) *b)*

Figure 8. Beam displacements (m): a – at a load of 16 kN, b – at a load of 32 kN

CONCLUSION

The authors have developed and implemented a physically nonlinear volumetric finite element for calculating massive reinforced concrete structures, which makes it possible to take into account the brittle fracture of concrete in the compression mode and the process of cracking

in tensile concrete. When creating an element to take into account the work of concrete in the «compression – compression – compression» mode, the Willam & Warnke failure criterion was used.

When a crack occurs in concrete in the first main direction, the stress state of concrete in the other two directions (in the «tension – compression – compression» mode) is considered as plane-stressed and the modified von Mises – Huber failure criterion is used.

In the presence of two cracks, the modulus of elasticity of concrete in the third direction is determined by a simple stress-strain diagram, and, at the same time, the influence of shear stresses on the work of concrete with cracks is taken into account.

Since the reinforcement of the structure can be performed arbitrarily, its features can be fully taken into account by including one-dimensional bar elements characterizing the reinforcement in the finite element diagram of the structure. In this case, for reinforcing steel, it is possible to set both elastic and elastic-plastic deformation models.

To verify the created finite element, a series of test calculations of the beam, which is in the condition of a four-point bending (pure bending), was carried out. The subsequent comparison of the calculation results with the experimental data confirmed the high accuracy and reliability of the results obtained.

This finite element is adapted to the PRINS computer application and, as part of this software application, can be used by engineers of design and scientific organizations for practical calculations of reinforced concrete structures.

Thus, the PRINS software application can be successfully used to solve a large class of engineering problems [23,24,25].

REFERENCES

1. **Agapov V.P.** Metod konechnyh elementov v statike, dinamike i ustojchivosti konstrukcij [Finite element method in statics, dynamics and stability of structures]. Izdatel'stvo ASV, 2005. 245 p. (In Russ.)
2. **Zienkiewicz O.C., Taylor R.L.** The Finite Element for Solid and Structural Mechanics. Sixth edition. McGraw-Hill, 2005, 631 p.
3. **Bathe K.J., Wilson E.L.** Numerical methods in finite element analysis. – N.J.: Prentice-Hall, 1976, 528 p.
4. **Crisfield M.A.** Non-linear finite element analysis of solids and structures. John Wiley & Sons Ltd, 1977, 488 p.
5. **Oden J.T.** Finite elements in nonlinear continua. McGraw, Hill Book Company, New York, 1972, 464 p.
6. MSC NASTRAN 2016. Nonlinear User's Guide SOL 400. – MSC Software, 2016, 790 p.
7. ANSYS Theory Reference. Release 5.6. ANSYS Inc. Canonsburg, PA, 1999, 1286 p.
8. ABAQUS 6.11. Theory manual. DS Simulia, 2011
9. ADINA. Theory and Modelling Guide. ADINA R & D, Inc. 71 Elton Avenue Watertown, MA 02472, USA, 705 p.
10. DIANA FEA User's Manual. Release 10. – DIANA FEA BV, 2017
11. **Shanno D.F.** Conditioning of Quasi-Newton methods for function minimization, Math. Comp., 24, 1970, pp. 647-656
12. **Dennis J.E., Jr. and Jorge J. More**. Quasi-Newton Methods, Motivation and Theory. SIAM Review, Vol. 19, No. 1, January 1977. pp. 46-89
13. **H. Matthies and G. Strang.** The Solution of Nonlinear Finite Element Equations. International Journal for Numerical Methods in Engineering, Vol. 14, 1979, p. 1613-1626
14. **Willam K.J., Warnke E.P.** Constitutive Model for the Triaxial Behavior of Concrete. Proceedings of IABSE. Structural Engineering Report 19, Section III, 1975, pp. 1-30

15. SP 63.13330.2018 «SNiP 52-01-2003 Betonnye i zhelezobetonnye konstrukcii. Osnovnye polozheniya» [Concrete and reinforced concrete structures. Key points]. 2018. 148 p.
16. CEB, CEB-FIP Model Code 1990 / CEB Bulletin d'Information № 213/214, Comite Euro-International du Beton, Lausanne, Switzerland, 1993. 437 p.
17. Rekomendacii po opredeleniyu prochnostnyh i deformacionnyh harakteristik betona pri neodnoosnyh napryazhennyh sostoyaniyah [Recommendations for determining the strength and deformation characteristics of concrete in non-uniaxial stress states]. M. NIIZhB Gosstroya USSR, 1985, 72 p.
18. **Kupfer, H., Hilsdorf, H., Rusch, H.** Behavior of Concrete under Biaxial Stresses, ACI Journal, Proceedings Vol. 66, No. 8, August, 1969, pp. 656-666
19. **Launay P., Gachon H.** Strain and Ultimate Strength of Concrete under Triaxial Stress, Am. Concrete Inst. Spec. Publ. 34, pap. 13, 1972
20. **Mills L.L., Zimmerman R.M.** Compressive Strength of Plain Concrete under Multiaxial Loading Conditions, ACI Journal, Vol. 67, No. 10, 1970, October, pp. 802-807
21. **Korsun V.I.** Sopostavitel'nyj analiz kriteriev prochnosti dlya betonov [Comparative analysis of strength criteria for concrete] / V.I. Korsun, A.V. Nedorezov, S.Yu. Makarenko // Sovremennoe promyshlennoe i grazhdanskoe stroitel'stvo [Modern industrial and civil construction]. – 2014. – T. 10. – № 1. – P. 65-78. – EDN THXXCZ (In Russ.)
22. **Hansen T.C.** Triaxial test with concrete and cement paste: Report № 319 / T. C. Hansen. – Lyngby : Technical University of Denmark, 1995. – 54 p
23. **Agapov V.P. and Markovich A.S.** The family of multilayered finite elements for the analysis of plates and shells of variable thickness: La familia de elementos finitos multicapa para el análisis de placas y cascos de espesor variable. South Florida Journal of Development. 2021;2(4):034-5048. https://doi.org/10.46932/sfjdv2n4-007
24. **Agapov V.P., Markovich A.S.** Dynamic method for determining critical loads in the PRINS computer program. Structural Mechanics of Engineering Constructions and Buildings. 2020;16(5):380-389. (In Russ.) DOI: 10.22363/1815-5235-2020-16-5-380-389
25. **Agapov V.P., Markovich A.S.** Investigation of the accuracy and convergence of the results of thin shells analysis using the PRINS program. Structural Mechanics of Engineering Constructions and Buildings. 2021; 17(6):617-627. (In Russ.) DOI: 10.22363/1815-5235-2021-17-6-617-627
26. **Obernikhin D.V., Nikulin A.I.** Experimental studies of strength, crack resistance and deformability of reinforced concrete beams of trapezoidal and rectangular cross sections. Innovative science. 2016; 8(2):73-77.
27. **Rimshin V.I., Amelin P.A.** Numerical calculation of bent reinforced concrete elements of rectangular section in the Abaqus software. Structural Mechanics of Engineering Constructions and Buildings. 2022;18(6):552-563. (In Russ.) http://doi.org/10.22363/1815-5235-2022-18-6-552-563
28. **Cedolin L., S. Deipoli.** Finite element studies of shear-critical R/C beams. ASCE Journal of the Engineering Mechanics Division. June 1977. Vol. 103. No. EM3, Pp. 395-410.
29. **von Mises R.** Mechanik der festen Körper im plastisch-deformablen Zustand. Nachrichten von der Gesellschaft der Wissenschaften zu Göttingen. Mathematisch-Physikalische Klasse. 1913; 1:582-592.

СПИСОК ЛИТЕРАТУРЫ

1. **Агапов В.П.** Метод конечных элементов в статике, динамике и

устойчивости конструкций. Изд-во АСВ, М.: 2005. 245 с.
2. **Zienkiewicz O.C., Taylor R.L.** The Finite Element for Solid and Structural Mechanics. Sixth edition. McGraw-Hill, 2005, 631 p.
3. **Bathe K.J., Wilson E.L.** Numerical methods in finite element analysis. – N.J.: Prentice-Hall, 1976, 528 p.
4. **Crisfield M.A.** Non-linear finite element analysis of solids and structures. John Wiley & Sons Ltd, 1977, 488 p.
5. **Oden J.T.** Finite elements in nonlinear continua. McGraw, Hill Book Company, New York, 1972, 464 p.
6. MSC NASTRAN 2016. Nonlinear User's Guide SOL 400. – MSC Software, 2016, 790 p.
7. ANSYS Theory Reference. Release 5.6. ANSYS Inc. Canonsburg, PA, 1999, 1286 p.
8. ABAQUS 6.11. Theory manual. DS Simulia, 2011
9. ADINA. Theory and Modelling Guide. ADINA R & D, Inc. 71 Elton Avenue Watertown, MA 02472, USA, 705 p.
10. DIANA FEA User's Manual. Release 10. – DIANA FEA BV, 2017
11. **Shanno D.F.** Conditioning of Quasi-Newton methods for function minimization, Math. Comp., 24, 1970, pp. 647-656
12. **Dennis J.E., Jr. and Jorge J. More**. Quasi-Newton Methods, Motivation and Theory. SIAM Review, Vol. 19, No. 1, January 1977. pp. 46-89
13. **H. Matthies and G. Strang.** The Solution of Nonlinear Finite Element Equations. International Journal for Numerical Methods in Engineering, Vol. 14, 1979, p. 1613-1626
14. **Willam K.J., Warnke E.P.** Constitutive Model for the Triaxial Behavior of Concrete. Proceedings of IABSE. Structural Engineering Report 19, Section III, 1975, pp. 1-30
15. СП 63.13330.2018 Бетонные и железобетонные конструкции. Основные положения. Актуализированная редакция СНиП 52-01-2003. М.: Минрегион России, 2018.148 с.
16. CEB, CEB-FIP Model Code 1990 / CEB Bulletin d'Information № 213/214, Comite Euro-International du Beton, Lausanne, Switzerland, 1993. 437 p.
17. Рекомендации по определению прочностных и деформационных характеристик бетона при неодноосных напряженных состояниях. М.: НИИЖБ Госстроя СССР, 1985, 72 с.
18. **Kupfer, H., Hilsdorf, H., Rusch, H.** Behavior of Concrete under Biaxial Stresses, ACI Journal, Proceedings Vol. 66, No. 8, August, 1969, pp. 656-666
19. **Launay P., Gachon H.** Strain and Ultimate Strength of Concrete under Triaxial Stress, Am. Concrete Inst. Spec. Publ. 34, pap. 13, 1972
20. **Mills L.L., Zimmerman R.M.** Compressive Strength of Plain Concrete under Multiaxial Loading Conditions, ACI Journal, Vol. 67, No. 10, 1970, October, pp. 802-807
21. **Корсун В.И.** Сопоставительный анализ критериев прочности для бетонов / В.И. Корсун, А.В. Недорезов, С.Ю. Макаренко // Современное промышленное и гражданское строительство. 2014. Т. 10. № 1. С. 65-78. EDN THXXCZ.
22. **Hansen T.C.** Triaxial test with concrete and cement paste: Report № 319 / T. C. Hansen. – Lyngby : Technical University of Denmark, 1995. – 54 p
23. **Agapov V.P. and Markovich A.S.** The family of multilayered finite elements for the analysis of plates and shells of variable thickness: La familia de elementos finitos multicapa para el análisis de placas y cascos de espesor variable. South Florida Journal of Development. 2021;2(4):034-5048. https://doi.org/10.46932/sfjdv2n4-007
24. **Agapov V.P., Markovich A.S.** Dynamic method for determining critical loads in the PRINS computer program. Structural

Mechanics of Engineering Constructions and Buildings. 2020;16(5):380-389. (In Russ.) DOI: 10.22363/1815-5235-2020-16-5-380-389

25. **Agapov V.P., Markovich A.S.** Investigation of the accuracy and convergence of the results of thin shells analysis using the PRINS program. Structural Mechanics of Engineering Constructions and Buildings. 2021; 17(6):617-627. (In Russ.) DOI: 10.22363/1815-5235-2021-17-6-617-627
26. **Obernikhin D.V., Nikulin A.I.** Experimental studies of strength, crack resistance and deformability of reinforced concrete beams of trapezoidal and rectangular cross sections. Innovative science. 2016; 8(2):73-77.
27. **Rimshin V.I., Amelin P.A.** Numerical calculation of bent reinforced concrete elements of rectangular section in the Abaqus software. Structural Mechanics of Engineering Constructions and Buildings. 2022;18(6):552-563. (In Russ.) http://doi.org/10.22363/1815-5235-2022-18-6-552-563
28. **Cedolin L., S. Deipoli.** Finite element studies of shear-critical R/C beams. ASCE Journal of the Engineering Mechanics Division. June 1977. Vol. 103. No. EM3, Pp. 395-410.
29. **von Mises R.** Mechanik der festen Körper im plastisch-deformablen Zustand. Nachrichten von der Gesellschaft der Wissenschaften zu Göttingen. Mathematisch-Physikalische Klasse. 1913; 1:582-592.

Vladimir P. Agapov, doctor of technical sciences, professor of the Department of Civil Engineering, Engineering Academy; RUDN University, 117198, Russia, Moscow, Miklukho-Maklaya, 6, tel. +7(499)9368787, e-mail: agapovpb@mail.ru.

Alexey S. Markovich, Ph. D., Associate Professor of the Department of Civil Engineering, Engineering Academy; RUDN University, 117198, Russia, Moscow, Miklukho-Maklaya, 6, tel. +7(499)9368787, e-mail: markovich-as@rudn.ru, Associate Professor of the Department of Fundamental Education, Moscow State University of Civil Engineering; 129337, Russia, Moscow, Yaroslavskoe Shosse, 26, tel. +7 (499) 936-87-87, e-mail: markovich-as@rudn.ru

Агапов Владимир Павлович, доктор технических наук, профессор департамента строительства инженерной академии, Российский университет дружбы народов им. Патриса Лумумбы, 117198, Россия, г. Москва, ул. Миклухо-Маклая, д.6, тел. +7(499)9368787, e-mail: agapovpb@mail.ru.

Маркович Алексей Семенович, кандидат технических наук, доцент департамента строительства инженерной академии, Российский университет дружбы народов им. Патриса Лумумбы, 117198, Россия, г. Москва, ул. Миклухо-Маклая, д.6; доцент кафедры фундаментального образования, Национальный исследовательский Московский государственный строительный университет; 129337, Россия, г. Москва, Ярославское шоссе, д. 26, тел. +7 (499) 936-87-87, e-mail: markovich-as@rudn.ru

International Journal for Computational Civil and Structural Engineering, 19(4) 27–37 (2023)

DOI:10.22337/2587-9618-2023-19-4-27-37

FEATURES OF DEVELOPMENT OF DYNAMIC MODELS OF HYDRO STRUCTURES AND THEIR VERIFICATION ACCORDING TO FIELD MEASUREMENT DATA, USING THE EXAMPLE OF SAYANO-SHUSHENSKAYA HPP

Alexander M. Belostotsky, Dmitry S. Dmitriev, Sergey O. Petryashev

National Research Moscow State University of Civil Engineering, Moscow, RUSSIA
Research & Development Centre StaDyO, Moscow, RUSSIA

Abstract: This article presents the results of the development and verification of a dynamic finite element model of a high-pressure concrete hydraulic structure (Sayano-Shushenskaya HPP). A brief analysis of previously developed models of the hydraulic structure was carried out. An algorithm for sequential refinement of the results of dynamic calculations of hydraulic structures, significant factors and approaches to modeling the dynamic stress-strain state of hydraulic structures is presented.

Keywords: Arch-gravity dam, dynamic characteristics, added masses, natural frequencies and mode shapes

ОСОБЕННОСТИ РАЗРАБОТКИ ДИНАМИЧЕСКИХ МОДЕЛЕЙ ГИДРОТЕХНИЧЕСКИХ СООРУЖЕНИЙ И ИХ ВЕРИФИКАЦИЯ ПО ДАННЫМ НАТУРНЫХ ИЗМЕРЕНИЙ, НА ПРИМЕРЕ САЯНО-ШУШЕНСКОЙ ГЭС

А.М. Белостоцкий, Д.С. Дмитриев, С.О. Петряшев

Национальный исследовательский Московский государственный строительный университет,
г. Москва, РОССИЯ
АО «Научно-исследовательский центр СтаДиО», г. Москва, РОССИЯ

Аннотация: В настоящей статье представлены результаты разработки и верификации динамической конечно-элементной модели высоконапорного бетонного гидротехнического сооружения (Саяно-Шушенской ГЭС). Проведен краткий анализ разработанных ранее моделей гидроузла. Представлен алгоритм последовательного уточнения результатов динамических расчетов ГТС, значимые факторы и подходы к моделированию динамического НДС гидротехнических сооружений.

Ключевые слова: Арочно-гравитационная плотина, динамические характеристики, присоединенные массы, собственные частоты и формы колебаний

1. INTRODUCTION

Today, increased attention is being paid to the safety of high-pressure concrete hydraulic structures all over the world. Reliable and trouble-free operation of high-pressure dams is a key issue for researchers and practitioners in the field of construction and operation of such structures. Since a significant part of concrete dams were designed and built in the middle of the last century [1] and have been in operation for several decades, monitoring their condition is fundamental to ensuring an adequate level of safety.

Assessing the dynamic characteristics of concrete water-retaining structures is of great importance in monitoring the safety of such structures. The regulatory legal acts in force in Russia [2] oblige regular dynamic testing of hydraulic structures and the preparation of dynamic

passports of such objects. In addition to the results of dynamic testing, the dynamic passport includes calculated natural frequencies and vibration modes obtained from numerical models.
Having information about changes in the dynamic characteristics of a structure, one can draw conclusions about its condition and changes in the stress-strain state (SSS) of the object, which increases the overall level of reliability and safety of the object [3, 4].
In world practice, there are examples of the use of dynamic monitoring systems of concrete dams as a basis for diagnostic, mathematical models of hydraulic structures that can adapt according to the readings of instrumentation equipment (CAI) and conduct a predictive analysis of changes in the SSS of a structure [5, 6, 7].
Another important aspect of using the dynamic characteristics of a structure is the possibility of verifying the developed numerical models of the structure using natural frequencies and shapes measured in situ (if they are determined experimentally).
Therefore, the issue of calculation and full-scale determination of the dynamic characteristics of concrete pressure dams is an urgent and sought-after task in the hydraulic engineering industry.
In this article, using the example of the Sayano-Shushenskaya HPP (SSHHPP) hydroelectric complex, we consider the important features of creating dynamic computational models of hydraulic structures, the disadvantages of simplified methods for modeling dynamic stress-strain state and the most significant factors that must be taken into account when creating dynamic models of hydraulic structures. The article also presents the results of a comparison of the dynamic characteristics obtained from calculation models developed in 2023 with the results of field studies at the SSHHPP dam.

2. REVIEW OF PREVIOUSLY DEVELOPED SSHHPP MODELS

During the operation of the SSHHPP, a number of calculation models of the "dam-base" system were built, in various software systems, with different formulations and details [8, 9, 10, 11, 12], which were developed in the period from 2024 to 2014. Natural frequencies of dam vibrations obtained from these models differed significantly from field measurements [13, 14]. These significant differences were due to simplified approaches to modeling the dynamic characteristics of a structure and insufficient detail of the calculation models.
To bring the calculated eigenvalues closer to the natural ones, approaches related to adjusting the added mass of water on the pressure face were forced to pressure face [8]. Criticism of the application of the distribution of hydrodynamic pressure on the pressure face of arch dams, obtained from the Westergaard solution [15], is associated with the obvious simplification of this method. This approach considers the motion of an absolutely rigid body in a fluid, but in reality the rigidity of arched dams is not infinite. Thus, the Center for Geodynamic Observations in the Electric Power Industry, when calculating the model in 2014, proposed to significantly change the distribution of hydrodynamic pressure on the pressure face (figure 1) in order to bring the calculated dynamic characteristics closer to those measured in situ [8].

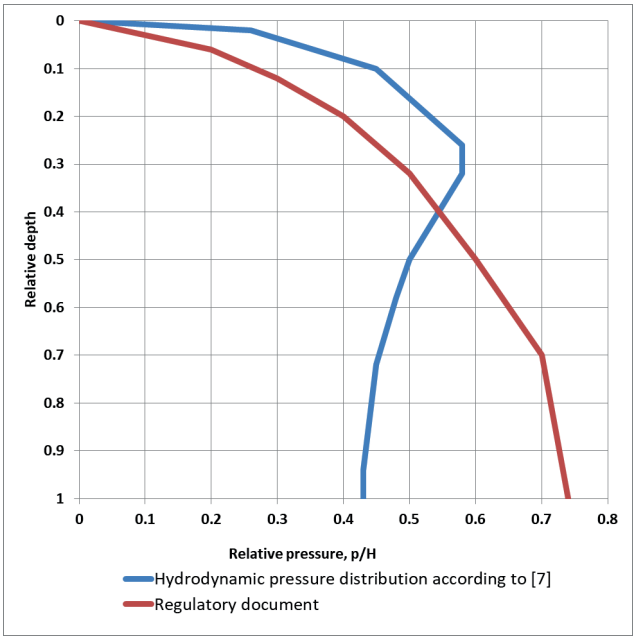


Figure 1. Distribution of hydrodynamic pressure along the height of the dam

The disadvantages of the outdated approach to taking into account fluid and added masses when performing dynamic calculations were demonstrated in a number of works devoted to determining the dynamic characteristics of high-pressure hydraulic structures [16, 17]. In most cases, taking into account the hydrodynamic pressure on the pressure face of the hydraulic structure, calculated according to Westergard, gives overestimated values at higher natural frequencies.

In another case, on a site built by a group of specialists. VNIIG B.E. Vedeneev finite element models of the system "dam-base of the SSHHPP" in the ANSYS software package [9], when performing calculations in the period from 2004 to 2013. *«Attempts were constantly made to calibrate the model in such a way as to bring the calculated data closer to the field measurement data»* [18].

In many cases, to determine the elastic modulus of a structure or foundation, "calibration" of the calculation model is used, during which, by changing the properties of the materials of the foundation and structure, a number of design parameters are achieved to match the field measurement data [19]. Such "calibration" is in some cases unfounded and is a necessary measure in the absence of initial data or deficiencies in the calculation model. Below (Table 1) are the lowest natural frequencies of the SSHHPP dam when varying (significantly increasing) the value of the elastic modulus of concrete, obtained in [9].

Table 1. Values of the first five natural frequencies of the SSHHPP dam, Hz [9]

Excluding water		Headwater level 500 m		Headwater level 540 m	
E_{concr} 50 GPa	E_{concr} 45 GPa	E_{concr} 50 GPa	E_{concr} 45 GPa	E_{concr} 50 GPa	E_{concr} 45 GPa
1.568	1.481	1.384	1.312	1.159	1.099
1.625	1.532	1.481	1.398	1.265	1.196
2.019	1.895	1.862	1.751	1.580	1.490
2.531	2.372	2.351	2.208	1.999	1.882
3.164	2.972	2.999	2.768	2.520	2.374

It must be taken into account that a model "calibrated" in such a free manner, in the absence of justification for this, cannot be considered verified, even if the calculated parameters correspond to field measurements.

3. NEW DYNAMIC MODEL OF SSHHPP

As part of the contract with the Branch of JSC Institute Hydroproject - employees of R&D Centre StaDyO in the period 2020 - 2023, a volumetric finite element model of the system "base - reservoir - dam - station building of the Sayano-Shushenskaya HPP" was developed and verified in ANSYS.

The main goal of the research work was to assess the occurrence of resonance phenomena in the structures of the station building during equipment operation or hydrodynamic phenomena in the flow part. Since the SSS of the station is directly influenced by the SSHHPP dam, which is confirmed by the readings of control and measuring equipment, it was decided to create a general (basic) model of the hydroelectric complex, including all the main structures. And after verification of the basic model, proceed to the analysis of the station building within the framework of a local model, refined in terms of building structures and the foundation mass under the structure.

Two families of basic models were created: dynamic and static models, which have differences related to the features of calculations (for example, properties of materials, loads, the need to take into account the sequence of construction, etc.).

When creating the basic dynamic model, a series of computational studies were carried out with sequential consideration of various factors and assessment of their influence on the natural frequencies and vibration modes of the SSHHPP arch-gravity dam. As a result, more than ten groups of dynamic models were prepared, which reflect the evolution of the basic model in terms of clarifying the criterion dynamic characteristics.

To consistently refine the dynamic model, the following factors were taken into account:

1. Use of volumetric finite elements of the 2nd order. Grid Convergence Analysis
3. Taking into account a number of design features of the dam body.
4. Various methods of accounting for fluid on models with and without a rock base. Assessing the impact of boundary conditions settings for FLUID30 acoustic elements on the results.
5. Taking into account a homogeneous rock base.
6. Taking into account the heterogeneous rock base, the structure and characteristics of the geological elements of which correspond to the current results of geophysical research.
7. Taking into account additional factors: masses of water in water pipelines, gantry cranes on the crest and other loads.

An analysis of the influence of most of the above factors on the dynamic characteristics of the dam has not been previously carried out. It is the consistent "complication" of the calculation model with an assessment of the contribution of each of the factors under consideration that is a mandatory requirement when preparing dynamic models.

Estimation of grid convergence of the basic dynamic model.

When conducting these studies, the reservoir was not taken into account, and the foundation was assumed to be absolutely rigid and massless. After a series of calculations, a comparison was made of the natural vibration frequencies of the dam for variants of the model with a free breakdown (1,578 thousand nodes) and the model with an optimized mesh in part of the dam body (243 thousand nodes). When comparing the models, agreement was noted in the shapes of natural vibrations, and the differences in the first 10 frequencies do not exceed 0.25% (Table 2). For further research, a variant with an optimized mesh and second-order volumetric finite elements was adopted.

Table 2. Estimation of grid convergence

№	Free mesh 1 578 000 nodes	Optimized model 243 000 nodes	Δ,%
1	1.0037	1.0012	0.25
2	1.1241	1.1218	0.21
3	1.4106	1.4108	0.01
4	1.7986	1.8006	0.11
5	2.2581	2.2588	0.03
6	2.4948	2.4888	0.24
7	2.7343	2.7349	0.02
8	2.8931	2.8916	0.05
9	3.2307	3.2327	0.06
10	3.4157	3.4135	0.06

Assessment of the influence of the design features of the body of the SSHHPP dam.

In the previously developed models of the SSHHPP, the arch-gravity dam was assumed to be simplified (with a smooth pressure face), because taking into account the protruding elements of a structural element in the area of water intake holes (figure 2) increases the dimension of the problem, and the influence of these elements on the dynamic characteristics was considered insignificant (although such assessments were not carried out).

When assessing the influence of this factor, three models were considered:

1) Without taking into account these structural elements. The surface of the dam on the upstream side is "smooth".
2) Taking into account the protruding structural element in the area of the water intake openings of the spillway.
3) Taking into account the protruding structural element in the area of the water intake openings of the spillway and pressure water conduits (figure 2).

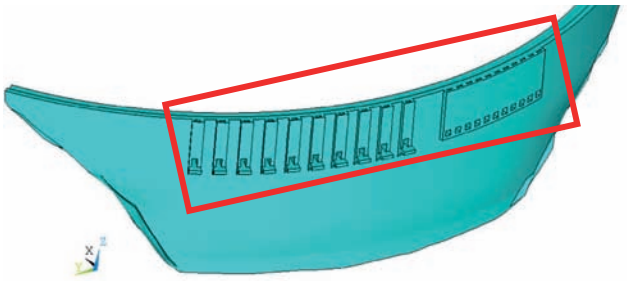


Figure 2. Structural element on the pressure face of the dam

The base was assumed to be absolutely rigid, the reservoir was not taken into account.
With the contribution of these design features to the total mass of the dam at the level of 1.4%, the influence on the lower natural frequencies of the dam turned out to be significantly higher - up to 3.65% (Table 3).

Table 3. Comparison of natural frequencies

№	Model 1	Model 2	Model 3	Model 1 / 3 Δ,%
	Natural frequency, Hz			
1	1.5301	1.5073	1.4791	3.33%
2	1.6122	1.5825	1.5533	3.65%
3	1.9492	1.9402	1.9120	1.91%
4	2.4125	2.4129	2.3942	0.76%
5	2.9750	2.9921	2.9683	0.23%

The studies carried out showed a significant influence of this factor on the lower frequencies of natural vibrations of the arch-gravity dam of the SSHHPP. For further research, a model was adopted that took into account the structural elements in the area of the spillway inlet openings and pressure conduits.

Assessment of the impact of different liquid accounting methods
In assessing this factor, a series of calculations were carried out in which the dimensions of the acoustic reservoir, boundary conditions for the reservoir elements and the properties of the foundation were varied.
Due to the inability to present the results of all calculations performed in the article, the results for the model with a homogeneous elastic foundation, E = 50 GPa, are presented below.
Two methods of accounting for the reservoir were considered:
1. Added masses (with distribution according to Westerhard [15]). This method was used on all previously developed models of the SSHHPP hydroelectric power station.
2. Using acoustic finite elements (FLUID30). Previously, such a method was not used for SSHPP models.
For the acoustic elements of the reservoir that are in contact with the structure and foundation, additional degrees of freedom in the form of displacements are specified [20].
Analysis of natural frequencies showed that when the reservoir is taken into account with added masses, the natural values of the dam are significantly lower than when modeling the fluid with acoustic elements. At lower frequencies the difference reaches 10% (Table 4). The first 3 modes of the dam's natural vibrations coincide; at higher frequencies in model No. 2, forms appear that are not detected in model No. 1. Some natural vibration modes are similar.

Assessment of the influence of additional factors.
A separate series of studies was carried out to assess the influence on the dynamic characteristics of the SSHHPP dam of such factors as the position of gantry cranes on the dam crest and the presence of water in the water conduits.
Based on the results of the studies, it was revealed that the position of the gantry cranes on the crest affects the change in the lower natural frequencies of the dam by no more than 0.38%, and the added mass of water in the water conduits significantly affects the dynamic characteristics of the water conduits themselves, but not on the lower natural frequencies and vibration patterns of the SSHHPP dam.
The final dynamic model of SSHHPP.
The final dynamic model of the system "base – reservoir – dam – station building of the Sayano-Shushenskaya HPP" was made on an elastic heterogeneous foundation. Dynamic properties are based on reasonable grounds based on geophysical research data. The dam material was adopted based on the results of laboratory studies of cores from the dam body with the following characteristics $E=41.5$ GPa, $\nu=0.15$, $\rho=2.45$ t/m^3. The model takes into account 4 reservoir filling levels: 500 m, 520 m and 540 m and 539 m. The volume of the reservoir is taken into account by FLUID30 acoustic finite elements. All significant design features of the dam are taken into account.

Table 4. Comparison of natural frequencies/ Matching shapes are shown in color

№	Model 1 Added mass	Model 2 Acoustic elem.	Model 1/2 Δ,δ %
	Natural frequency, Hz		
1	1.0011	1.1071	9,57
2	1.1217	1.2069	7,06
3	1.4108	1.5297	7,77
4	1.8006	1.6786	8,14
5	2.2588	1.9601	8,39
6	2.4874	2.1063	
7	2.7348	2.2677	8,99
8	2.8911	2.4657	10,03
9	3.2327	2.5349	8,97
10	3.4134	2.8993	8,95
11	3.5415	2.9788	
12	3.8096	3.0051	
13	4.0371	3.2133	
14	4.2018	3.3561	
15	4.4122	3.5331	
16	4.5372	3.5513	
17	4.7068	3.6151	
18	4.9933	3.6864	
19	5.0325	3.7491	
20	5.1021	3.9496	

4. RESULTS

For the final basic dynamic model of the system, a comparison was made between the calculated dynamic characteristics and the available set of results of instrumental studies of the actual dynamic properties of the dam, obtained in different years (table 5, 6) (figure 3, 4). The natural mode shapes were compared with field data obtained in 1999 using the standing wave method and in 2022 using the frequency domain decomposition method (table 7).

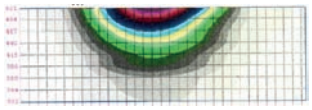
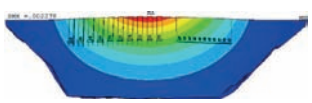
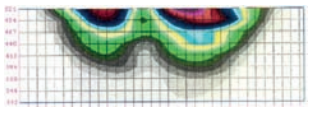
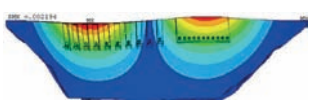
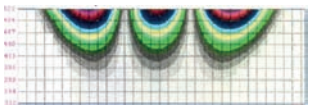
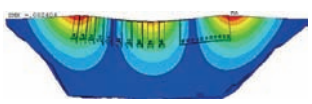
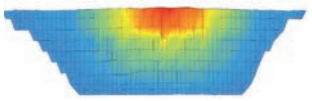
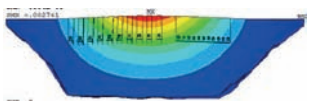
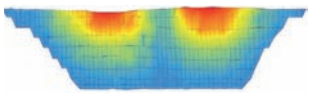
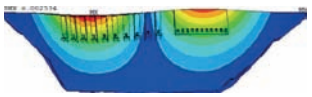
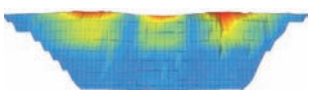
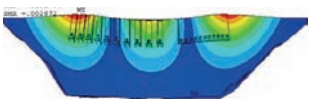
Table 5. Comparison of natural frequencies. Headwater level 539-540

№	Field measurements, 1999 г, Hz	Calculated data, Hz	Δ, Hz	δ, %
1	1.129	1.1181	0.0109	0.97
2	1.217	1.2162	0.0008	0.07
3	1.527	1.5365	0.0095	0.62
4	1.921	1.9651	0.0441	2.24
5	2.448	2.4709	0.0229	0.93
6	2.972	3.0077	0.0357	1.19

Table 6. Comparison of natural frequencies. Headwater level 500

№	Field measurements, 1999 г, Hz	Calculated data, Hz	Δ, Hz	δ, %
1	1.236	1.2861	0.0501	3.90
2	1.325	1.3738	0.0488	3.55
3	1.633	1.7373	0.1043	6.00
4	2.035	2.2044	0.1694	7.68
5	2.531	2.7457	0.2147	7.82
6	3.064	3.3118	0.2478	7.48

Table 7. Comparison of natural mode shapes

Field measurements	Calculated data
Headwater level 539-540 m	
f_1=1.129	f_1=1.118
	
f_2=1.217	f_2=1.216
	
f_3=1.527	f_3=1.537
	
Headwater level 500 m (field measurements carried out by VNIIG in 2022)	
f_1=1.27	f_1=1.286
	
f_2=1.37	f_2=1.374
	
f_3=1.68	f_3=1.738
	

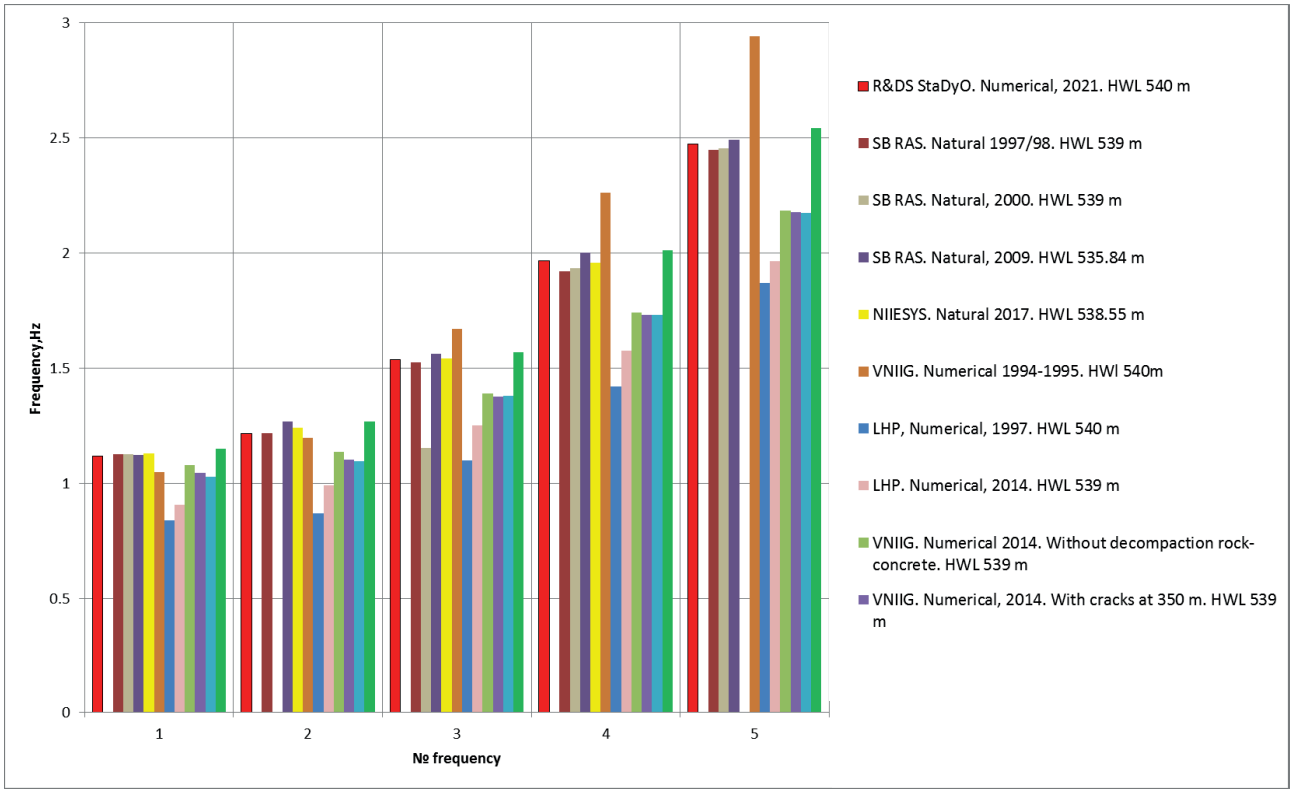


Figure 3. Results of previous studies. Headwater level 539-540 m

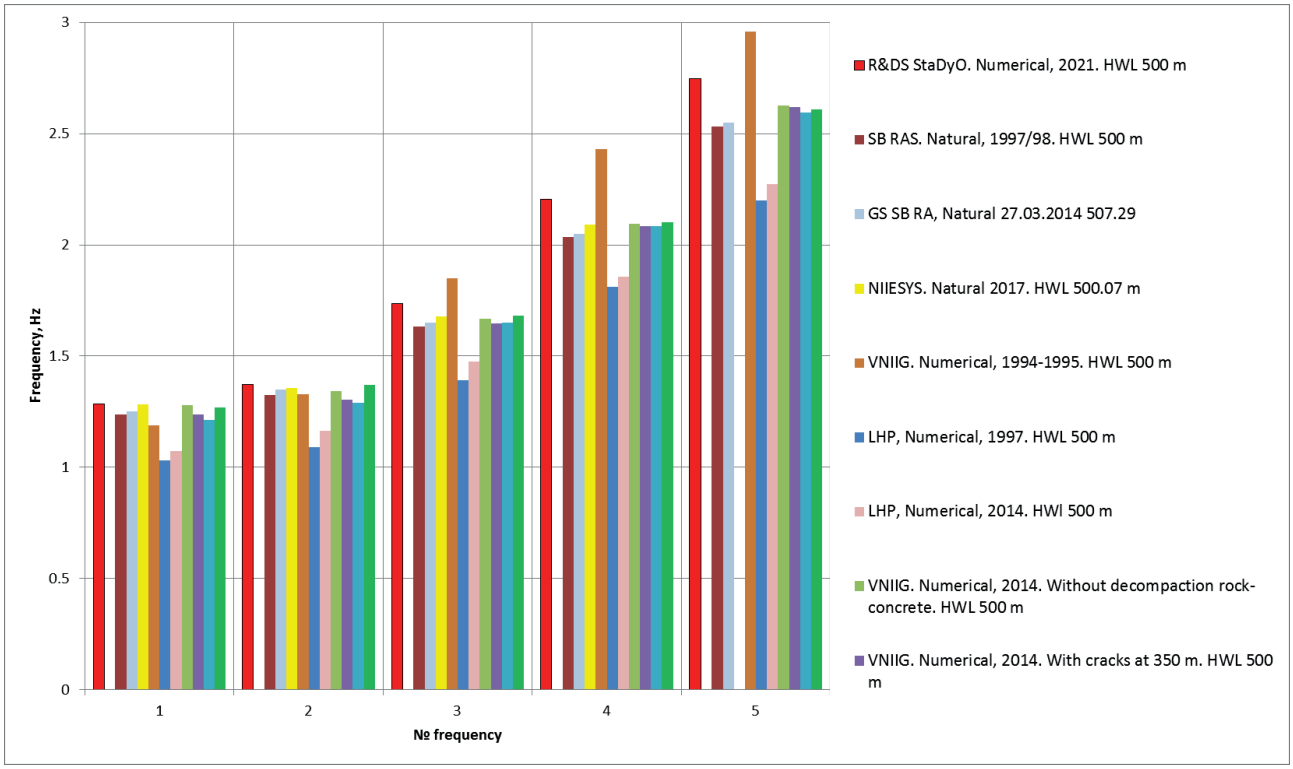


Figure 4. Results of previous studies. Headwater level 500 m

CONCLUSION

A multiparameter and multifactor verification of the spatial finite element base model of the system "foundation – reservoir – dam – station building of the Sayano-Shushenskaya HPP" developed and implemented in the ANSYS Mechanical software package was carried out using field measurement data: significant dynamic characteristics (spectrum of natural frequencies and vibration modes) of the dam.

The accepted and tested verification methodology excludes any "calibration" of model parameters, but represents a systematic movement from the initial basic model to an increasingly more detailed and/or complex one - until an acceptable correspondence of the criterion calculation results to the field data is achieved, or until the source of such discrepancies is identified, associated with the unreliability of the original information.

As a result of the research, the most significant factors were identified that must be taken into account when creating dynamic models of hydraulic structures.

The results obtained for the SSHHPP dam (natural frequencies and vibration modes) exceed in accuracy and correspondence to nature all previously obtained results.

REFERENCES

1. **Perera D. et al.** Ageing water storage infrastructure: An emerging global risk //UNU-INWEH Report Series. – 2021. – T. 11. – C. 25.
2. Code of Practice 358.1325800.2017 "Hydraulic structures. Rules for design and construction in seismic areas.".
3. **Prakash G. et al.** Recent advancement of concrete dam health monitoring technology: A systematic literature review //Structures. – Elsevier, 2022. – T. 44. – C. 766-784.
4. **Dmitriev D. S., Uchevatkin A. A.** Numerical modeling as a basis for monitoring systems for the safety of hydraulic structures and automated stress-strain state control systems // Vestnik MGSU. – 2021. – T. 16. – No. 12. – pp. 1582-1591.
5. **Oliveira, S., & Alegre, A**. Seismic and structural health monitoring of dams in Portugal / S. Oliveira, A. Alegre. / Seismic Structural Health Monitoring. – Springer, 2019. – C. 87-113.
6. **Oliveira S., Alegre A.** Seismic and structural health monitoring of Cabril dam. Software development for informed management // Journal of Civil Structural Health Monitoring. 2020. T. 10. №. 5. C. 913-925.
7. **Alegre, A., Carvalho, E., Matsinhe, B., Mendes, P., Oliveira, S., & Proença, J.** Monitoring vibrations in large dams.
8. **Bronshtein V.I. et al.** Study of the influence of various factors on the stress-strain state and seismic resistance of the Sayano-Shushenskaya HPP dam using the numerical modeling method //Hydrotechnical Construction. – 2014. – No. 12. – pp. 35-43.
9. **Khrapkov A. A. et al.** On the construction of a mathematical model of the arch-gravity dam of the Sayano-Shushenskaya HPP // News of the All-Russian Scientific Research Institute of Hydraulic Engineering named after. BE Vede-neeva. – 2011. – T. 264. – P. 56-69.
10. **Toloshinov A.V. et al.** Construction of a finite element calculation model for assessing the stress-strain state of the Sayano-Shushenskaya HPP dam // News of Higher Educational Institutions. Construction. – 2006. – No. 7. – pp. 38-47.
11. **Yakubson V.M.** Analysis of the stress-strain state of the Sayano-Shushenskaya HPP dam // Engineering and Construction Journal. – 2012. – No. 1. – P. 2-2.7.
12. **Kozinets G.L.** Determination of the dynamic characteristics of structures in con-

tact with water, using the example of the arched concrete dam of the Sayano-Shushenskaya HPP // Magazine of Civil Engineering. – 2011. – No. 5. – pp. 43-48.
13. **Zavalishin S.I., Shablinsky G.E.** Field studies and calculation of the dynamic characteristics of the Sayano-Shushenskaya HPP dam //Hydrotechnical Construction. – 2015. – No. 2. – pp. 52-59.
14. **Liseykin A.V. et al.** Determination of natural vibration frequencies of structures using low-amplitude seismic signals (using the example of the Sayano-Shushenskaya hydroelectric power station dam according to monitoring data from 2001-2021) // Russian Seismological Journal. – 2023. – T. 5. – No. 2. – P. 32-50.9.
15. **Westergaard H.M.** Water pressures on dams during earthquakes / H.M. Westergaard // Proc. Am. Soc. Civ. Engrs. – 1931. – T. 57. – № 9.
16. **Belostotsky A. M. et al.** Comparative analysis of methods for numerical modeling of the dynamics of three-dimensional systems “base-arch dam-reservoir” under seismic impacts // International Journal for Computational Civil and Structural Engineering. – 2016. – T. 12. – No. 2. – pp. 65-74.
17. ICOLD, International Benchmark Workshop on Numerical Analysis of Dams. Theme A – Fluid Structure Interaction Arch Dam – Reservoir at Seismic loading. Graz University of Technology, 2013, pp.15-188.
18. **Kostylev V.S.** Forecast of the stress-strain state of concrete dams using mathematical modeling and natural data: dis. – All-Russian Scientific Research Institute of Hydraulic Engineering named after. BE Vedeneva, 2013.
19. **Ivashintsov D.A. et al.** Parametric identification of calculation models of hydraulic structures // St. Petersburg: Publishing House of OJSC “VNIIG im. B.E. Vedeneeva. – 2001. – P. 432.
20. **Belostotsky A. M., et al.** Verification of the methodology for numerical modeling of the dynamic stress-strain state of three-dimensional “structure-liquid” systems // International Journal for Computational Civil and Structural Engineering. – 2015. – T. 11. – No. 4. – pp. 124-132.

СПИСОК ЛИТЕРАТУРЫ

1. **Perera D. et al.** Ageing water storage infrastructure: An emerging global risk //UNU-INWEH Report Series. – 2021. – T. 11. – C. 25.
2. СП 358.1325800.2017 «Сооружения гидротехнические. Правила проектирования и строительства в сейсмических районах».
3. **Prakash G. et al.** Recent advancement of concrete dam health monitoring technology: A systematic literature review //Structures. – Elsevier, 2022. – T. 44. – C. 766-784.
4. **Дмитриев Д. С., Учеваткин А. А.** Численное моделирование в основе систем мониторинга безопасности гидротехнических сооружений и автоматизированные системы управления напряженно-деформированным состоянием //Вестник МГСУ. – 2021. – Т. 16. – №. 12. – С. 1582-1591.
5. **Oliveira, S., & Alegre, A**. Seismic and structural health monitoring of dams in Portugal / S. Oliveira, A. Alegre. / Seismic Structural Health Monitoring. – Springer, 2019. – C. 87-113.
6. **Oliveira S., Alegre A.** Seismic and structural health monitoring of Cabril dam. Software development for informed management // Journal of Civil Structural Health Monitoring. 2020. Т. 10. №. 5. С. 913-925.

7. **Alegre, A., Carvalho, E., Matsinhe, B., Mendes, P., Oliveira, S., & Proença, J.** Monitoring vibrations in large dams.
8. **Бронштейн В.И. и др.** Исследование влияния различных факторов на напряженно-деформированное состояние и сейсмостойкость плотины Саяно-Шушенской ГЭС методом численного моделирования //Гидротехническое строительство. – 2014. – №. 12. – С. 35-43.
9. **Храпков А. А. и др.** О построении математической модели арочно-гравитационной плотины Саяно-Шушенской ГЭС //Известия Всероссийского научно-исследовательского института гидротехники им. БЕ Веденеева. – 2011. – Т. 264. – С. 56-69.
10. **Толошинов А. В. и др.** Построение конечно-элементной расчетной модели для оценки напряженно-деформированного состояния плотины Саяно-Шушенской ГЭС //Известия высших учебных заведений. Строительство. – 2006. – №. 7. – С. 38-47.
11. **Якубсон В.М.** Анализ напряженно-деформированного состояния плотины Саяно-Шушенской ГЭС //Инженерно-строительный журнал. – 2012. – №. 1. – С. 2-2.
12. **Козинец Г.Л.** Определение динамических характеристик сооружений, контактирующих с водой, на примере арочной бетонной плотины Саяно-Шушенской ГЭС //Magazine of Civil Engineering. – 2011. – №. 5. – С. 43-48.
13. **Завалишин С.И.**, Шаблинский Г. Э. Натурные исследования и расчет динамических характеристик плотины Саяно-Шушенской ГЭС //Гидротехническое строительство. – 2015. – №. 2. – С. 52-59.
14. **Лисейкин А. В. и др.** Определение частот собственных колебаний сооружений по малоамплитудным сейсмическим сигналам (на примере плотины Саяно-Шушенской ГЭС по данным мониторинга 2001-2021 гг.) //Российский сейсмологический журнал. – 2023. – Т. 5. – №. 2. – С. 32-50.
15. **Westergaard H.M.** Water pressures on dams during earthquakes / H.M. Westergaard // Proc. Am. Soc. Civ. Engrs. – 1931. – Т. 57. – № 9.
16. **Белостоцкий А. М. и др.** Сравнительный анализ методик численного моделирования динамики трехмерных систем" основание-арочная плотина-водохранилище" при сейсмических воздействиях //International Journal for Computational Civil and Structural Engineering. – 2016. – Т. 12. – №. 2. – С. 65-74.
17. ICOLD, International Benchmark Workshop on Numerical Analysis of Dams. Theme A – Fluid Structure Interaction Arch Dam – Reservoir at Seismic loading. Graz University of Technology, 2013, pp.15-188.
18. **Костылев В.С.** Прогноз напряжённо-деформированного состояния бетонных плотин с использованием математического моделирования и натурных данных: дис. – Всероссийский научно-исследовательский институт гидротехники им. БЕ Веденеева, 2013.
19. **Ивашинцов Д.А. и др.** Параметрическая идентификация расчетных моделей гидротехнических сооружений //СПб.: Изд-во ОАО “ВНИИГ им. Б.Е. Веденеева. – 2001. – С. 432.
20. **Белостоцкий А. М., и др.** Верификация методики численного моделирования динамического напряженно-деформированного состояния трехмерных систем «сооружение-жидкость» //International Journal for Computational Civil and Structural Engineering. – 2015. – Т. 11. – №. 4. – С. 124-132.

Dmitry S. Dmitriev – CSc, engineer of A.B. Zolotov REC CM of the National Research Moscow State University of Civil Engineering; 129337, Russia, Moscow, Yaroslavskoe shosse, 26.; Deputy General Director for Computational Research of JSC Scientific Research Center StaDyO; 18, 3ya Ulitsa Yamskogo Polya, Moscow, 125040, Russia. E-mail: dmitriev.d.s@yandex.ru

Alexander M. Belostotsky – DSc, Professor, Full Member of the Russian Academy of Architecture and Construction Sciences, Scientific adviser at A.B. Zolotov REC CM of the National Research Moscow State University of Civil Engineering; 129337, Russia, Moscow, Yaroslavskoe shosse, 26. E-mail: amb@stadyo.ru

Sergey O. Petrashev – DSc, Professor, Full Member of the Russian Academy of Architecture and Construction Sciences, Scientific adviser at A.B. Zolotov REC CM of the National Research Moscow State University of Civil Engineering; 129337, Russia, Moscow, Yaroslavskoe shosse, 26. Leading engineer calculation of Scientific Research Center StaDyO; 18, 3ya Ulitsa Yamskogo Polya, Moscow, 125040, Russia. E-mail: petsero@mail.ru

Дмитриев Дмитрий Сергеевич – к.т.н, инженер НОЦ КМ им. А.Б. Золотова Национального исследовательского Московского государственного строительного университета; 129337, Россия, г. Москва, Ярославское шоссе, д. 26. Заместитель генерального директора по расчетным исследованиям АО НИЦ СтаДиО; E-mail: dmitriev.d.s@yandex.ru

Белостоцкий Александр Михайлович – д.т.н., профессор, академик РААСН, научный руководитель НОЦ КМ им. А.Б. Золотова Национального исследовательского Московского государственного строительного университета; 129337, Россия, г. Москва, Ярославское шоссе, д. 26. E-mail: amb@stadyo.ru

Петряшев Сергей Олегович – младший научный сотрудник НОЦ КМ им. А.Б. Золотова Национального исследовательского Московского государственного строительного университета; 129337, Россия, г. Москва, Ярославское шоссе, д. 26. Ведущий инженер-расчетчик АО НИЦ СтаДиО; E-mail: petsero@mail.ru

DOI:10.22337/2587-9618-2023-19-4-38-47

AGGREGATE RISK OF A LARGE COMPLEX CONSTRUCTION PROJECTS OF NPP

Petr G. Grabovy [1], ***Denis E. Sezemin*** [1,2]

[1] National Research Moscow State University of Civil Engineering, Moscow, RUSSIA

[2] JSC Akkuyu Nuclear, Akkuyu, Mersin, Republic of TÜRKIYE

Abstract: The article identifies the problems of the modern international nuclear energy market, analyzes domestic and foreign experience in the construction of technically complex megaprojects, studies and systematizes organizational and technical aspects of the concept of reliability and risks of technically complex industrial facilities on the example of an international project for the construction of a nuclear power plant. The purpose of the research article is to solve one of the most important tasks – to determine the total investment risk and its assessment in an inextricable relationship with the stages of the project life cycle. The article systematizes both the principles of assessing the organizational and technical reliability of the system under study, as well as the methods of types of aggregate investment risk. A proprietary multi-criteria approach to the concept of reliability is being developed using modern theoretical methods in the context of the development of nuclear power plant construction projects abroad, respectively, taking into account country and industry risks.

Keywords: nuclear power plant (NPP) construction, organizational and technical reliability management, aggregate risk, mathematical modelling, computer risk modelling, risk management, industrial construction, membrane method

СОВОКУПНЫЙ РИСК ПРИ РЕАЛИЗАЦИИ КРУПНОГО КОМПЛЕКСНОГО ПРОЕКТА СТРОИТЕЛЬСТВА АТОМНОЙ ЭЛЕКТРОСТАНЦИИ

П.Г. Грабовый [1], ***Д.Е. Сеземин*** [2]

[1] Национальный исследовательский Московский государственный строительный университет (НИУ МГСУ), г. Москва, РОССИЯ

[2] АО «Аккую Нуклеар», Аккую, Мерсин, ТУРЦИЯ

Аннотация: В статье выявлены проблемы современного международного рынка атомной энергетики, проанализирован отечественный и зарубежный опыт строительства технически сложных мегапроектов, исследованы и систематизированы организационно-технические аспекты концепции надежности и рисков технически сложных индустриальных объектов на примере международного проекта строительства атомной электростанции. Целью научной статьи являлось решение одной из важнейших задач - определение совокупного инвестиционного риска и его оценки в неразрывной связи с этапами жизненного цикла проекта. В статье систематизированы как принципы оценки организационно-технической надежности исследуемой системы, так и методы оценки совокупного инвестиционного риска. Разрабатывается проприетарный многокритериальный подход к понятию надежности с использованием современных теоретических методов в контексте развития проектов строительства АЭС за рубежом, соответственно, с учетом международных и отраслевых рисков.

Ключевые слова: строительство атомных электростанций (АЭС), управление организационно-технической надежностью, совокупный риск, математическое моделирование, компьютерное моделирование риска, управление риском, промышленное строительство, мембранный метод

INTRODUCTION

In a broad sense, the developed ACSTP should be based on the feasibility study (feasibility study of the NPP project), where the capacity of the nuclear plant is specified, the number of power units, the number of reactors as part of the justified feasibility study, the region of con-

struction, the assessment of the volume of investment and calculation of return on investment, project profitability and investment yield.
In the ACSTP, the problem of organizational and technical reliability (P^n_t) assessment of NPPs is divided into four levels:

Field level of technological process;

Controller level of process control and management;

Backbone network level;

Upper level of man-machine equipment, and the area of occurrence of cumulative risks (V_{ij}') into three levels (Fig. 1):

Organizational and production subsystem

Financial-investment subsystem

Infrastructure-service subsystem.

As a result of scientific research, the basic principles of cybernetic model of modern Russian ACS for NPP projects have been determined. The stages of development of the method of risk assessment include the following sequence: determination of technical requirements for the control and management system to be designed; development of design and estimate documentation; collection and study of initial data; compilation of a complete list of variables; completion of the ACSTP system (risk assessment); division of the control process into technological sections and subsequent distribution of variables by sections and groups; creation of proprietary databases (project risk map); development of a graphical interface of the screens of operators and management staff alternately in dynamics and statics; drawing up schemes of transitions from static to dynamic images on the screens; drawing up algorithms of scenario control (for all possible modes of operation of the facility, including emergency and post-emergency); creation of a model of the dynamic system of aggregate risk management; verification of databases; development of operational documentation; offline system testing; operational system testing; formal implementation, commissioning, staff training, issuance of relevant orders and instructions.

MODELS AND METHODS

Figure 1 provides a model of cumulative risk management. A system of continuous risk assessment and control is introduced through the development of the ACSTP model at the feasibility study stage as a strategically planned step simultaneously with the risk management model. It allows to achieve the previously presented main four objectives of the project, such as: timing, cost, quality and safety of the project.
The membrane method of risk assessment is based on the algorithm of calculation of the full economic result of the contractor's risk management strategy for each stage (phase) of the NPP project life cycle. For the purposes of this study, the stages, or layers, of the membrane method of risk management and further the software recommended for development on the basis of the membrane method of risk management, are understood as: initiation, planning, development of criteria and strategy of NPP location (interrelated with stages 3, 4, 5, 6, 9), design (interrelated with stages 1,3–9), construction (interrelated with stage 1), commissioning, operation, extension of operation (modernization), termination of operation, shutdown of processes, decommissioning [6].
Each of the eleven project phases represents a layer of the membrane-based risk assessment system. An example of risk assessment is presented in Tables 1–3.
The three-dimensional representation of the membrane model of assessment of organizational and technical reliability Prel(t) looks as follows: risks by groups form the membrane layers, which, in turn, form the so-called "membrane pie" by stacking layers on top of each other The layers are arranged horizontally in the order of the life cycle stages of the project of a technically complex facility – a nuclear power plant.

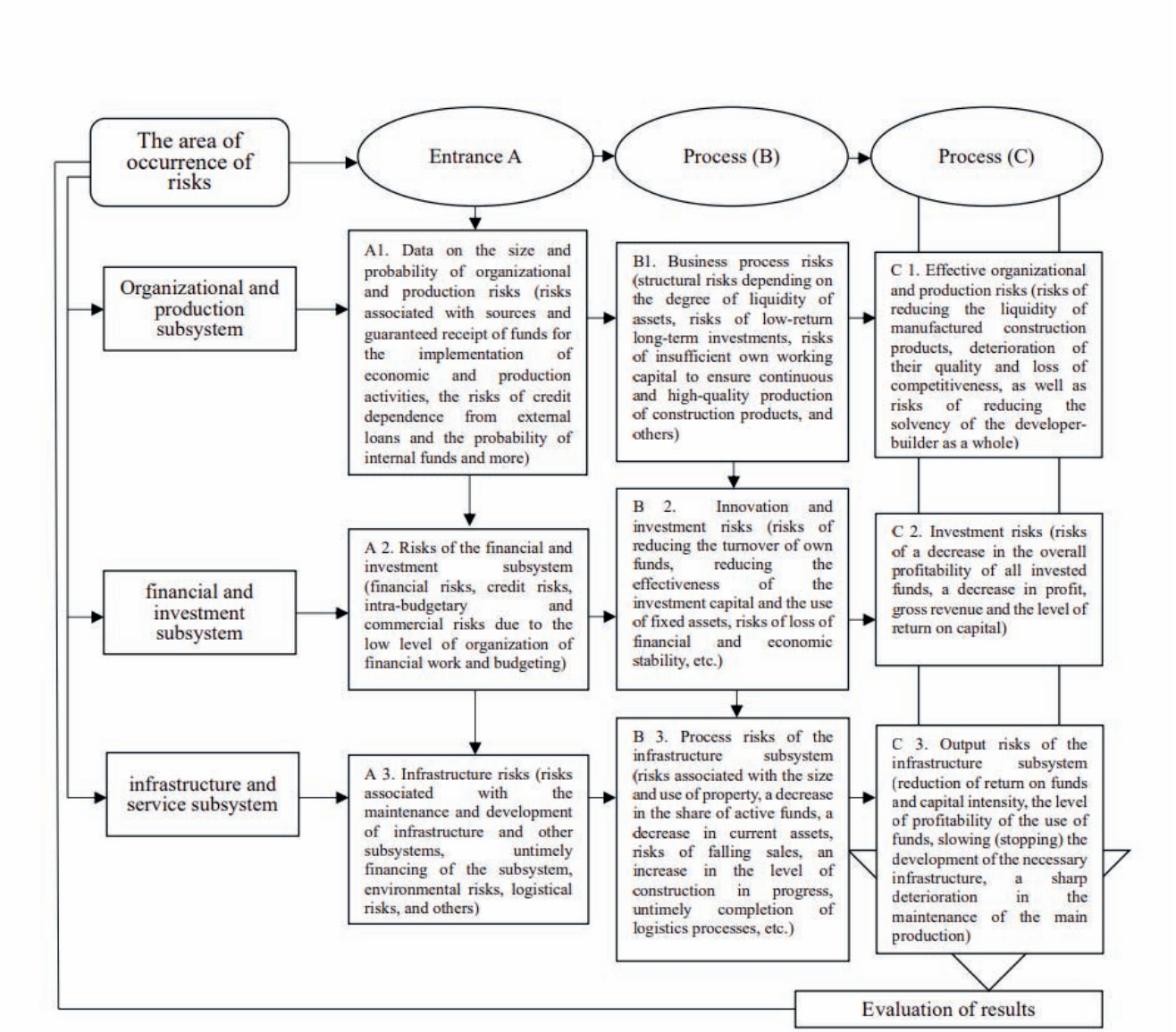


Figure 1. Model of the dynamic system of aggregate risk management at NPPs

The lattice of stacked membranes has several effects: "spring effect," "impermeability effect" (hereinafter impermeability is understood as the optimal degree of overall project reliability), and "layer–problem–balance" effect. It should be noted that the description of the membrane method through the 3D picture gives an idea of the significance and relevance of the task of systematization and digitalization of big data in the field of assessment and reduction of the maximum possible number of risk types during the construction of technically and organizationally complex NPP projects.

Organizational and technical reliability of NPP project implementation by the developer is a state in which its economic activity ensures, under normal conditions, the fulfilment of all obligations to the public procurement authority (Rosatom State Corporation).

Table 1

Example of a summary table of cumulative risks

Risk Category	Name of Risk	Risk Factor	Scenario of Risk	Aftereffect of Risk	Risk Owner	Start and Remanent Risk Level: Value of Risk	Probability	Susceptibility	Chart of Project	Cost of Project	Purpose of Project	Influence of project on quality	Influence of project on quantity	Influence of project on security	Influence of project on reputation	Previouse Index
	Growth	Mistakes at the projecting stage of progect		1. New type of activities. 2. Changes at technical documentatio n. 3. Growth of cost. 4. Delivery delays.												

Changing risk event	Risk influence horizon	Identificator of Risk	Special code of risk	Name of operations under risk	Duration	Start	Completion	Manageabilit y	Level of manageabilit y	Level of risk remanent: Rate of Risk	Probability	Susceptibility	Susceptibility base	Chart of project	Value of project	Purpose of project	Influence of project on quality	Influence of project on quantity	Influence of project on security	Influence of project on reputation	Previouse Index

Table 2

Example of a summary table of risk factor impact assessment

Impact on volume	Impact on safety		Impact assessment
Changes in volumes can be covered by current contractual obligations	The assessment of the impact of risks on safety is carried out in accordance with the requirements of current legislation and local regulations. Methods of risk prioritization, scoring scales and significance criteria for environmental safety, industrial safety, occupational safety, information security and other related risks are set out in special documents issued under the Project.	The level of decrease in public trust at the local level is insignificant.	1
Additional agreements are required within the existing contractual framework		Decrease in the level of public confidence at the local level. Short recovery period	2
Additional agreements with Contractors required		Decline in public confidence at the regional level. Short/moderate recovery period	3
Additional agreements with the Client required		Decline in public confidence at the international/regional level or at the level of important partners. Moderate/long recovery period	4
Revision of substantial terms of EPC contract/contract with Tier 1 Contractor required		Damage to public trust at international or key partner level. Long recovery period	5

Table 3

Assessment of the impact of risks with background colouring

Probability	Impact assessment				
	1 Very low	2 Low	3 Medium	4 High	5 Very high
5 Very high	5	10	15	20	25
4 High	4	8	12	16	20
3 Medium	3	6	9	12	15
2 Low	2	4	6	8	10

Organizational and technical reliability (P_{i-j}^{rel}) affects the production and economic stability, financial and economic performance of the enterprise itself and acts as one of the indicators of risk assessment of the contractor under the state contract (formula 3).

$$P_{i-j}^{rel} = 1 - \frac{\sum_{i=1}^{n}}{n(n-1)} = 1 - \frac{M(PH)}{n(n-1)}, \quad (1)$$

Where P_{i-j}^{rel} is assessment of organizational and technical reliability of the customer;
n is the number of indicators in the dynamic reliability model (normative model);
m_i is the number of inversions in the actual order for the indicator having the 1st rank (occupying the first place) in the dynamic model;
M (P, H) is the sum of inversions in the actual order of indicators (P) relative to the normative order (H) specified in the dynamic model. Inversion (R) in the presented assessment is expressed by the ratio of the value of
M (P, H) relative to n(n-1).
It characterizes the measure of the aggregate risk of deviation of the actual state from the normal state of the customer.
As noted above, the authors' approach proposes to distinguish four main target parameters, which are affected by risks (groups of risks) and the aggregate risk exposure of the enterprise, namely:

1) Project realization timeline;
2) Budget of the project realization;
3) Quality of the project and its products;
4) Project safety.

In this case, we can introduce the following system of registering data on the analysis of risk types, expert assessment of their impact on the target indicator of the project, and the weight of each risk for the indicator "Project Implementation Budget," presented in Tables 4–7.
5) Risk ranking. The assessment is made by evaluating the impact of the relevant risk on the project targets, having previously determined the magnitude of each risk by applying the previously described scoring system – the probability of risk occurrence and the risk exposure of the system.
Table 6 is filled in sequentially from the magnitude of negative consequences of risk types (very low to very high), taking into account their gradient.
6) Identify recommended strategies for the effective impact of risk management activities on project targets.
7) Present the data to the risk expert panel. The results are summarized in a table using the following example (Table 7).

Table 4

Risk scale. Layer 1.

Type of budget risk for project implementation	Budget growth in % up to 1%	Budget growth from 1% to 2%	Budget growth from 2% to 3%	Budget growth from 3% to 4%	Budget growth from 4% to 5%	Budget growth from 5% to 6% and so on
Design delay	*					
Delay in construction works						*
Delay in equipment delivery						*
Level 1 human error resulting in accident and equipment failure (by type of equipment)			*			
Changes in average annual air temperature by 1˚C				*		
Currency exchange rate fluctuations						*
Strike of transport workers for 10 days or more		*				

Table 5

Layer 2

Target indicator		Weight/qualitative indicator				
		Item No	Item No	Item No	Item No	Item No
Budget	Operational costs	Increase by 1%	Increase by 2%	1	2	3
	Capital expenditures					
Schedule		Delayed by 0 month	Delayed by 1–2 months	Delayed by 3–4 months	Delayed by 5–6 months	Delayed by 7–12 months
Quality		No deterioration	Minor impact (on part of project activities), possible adjustment	Requires Client approval	Unacceptable	The project is better not to be implemented in this capacity
Safety	ecological	On the basis of a specially created expert panel, legislative requirements and internal regulations and rules, an appropriate membrane layer of risk impact on project safety is described, taking into account the assessment of costs to ensure the required level of safety. It is included in the terms of reference for the development of software for the risk assessment system using the membrane method.				
	industrial					
	information					
	labour safety					

Table 6

Probability	Impact assessment				
	Very low	Low	Medium	High	Very high
Very high	1/5	2/5	3/5	4/5	5/5
High	1/4	2/4	3/4	4/4	5/4
Medium	1/3	2/3	3/3	4/3	5/3
Low	1/2	2/2	3/2	4/2	5/2
Very low	1/1	2/1	3/1	4/1	5/1

Table 7

Development of strategies and interventions based on the risk score determination

Risk score (determined by experts)	Strategy	Measures
1–4	Acceptance	Control measures
4–15	Control (reduction)	Compensatory measures, continuous monitoring
15–25	Reduction, rejection	Compensatory measures, continuous monitoring

RESULTS

Calculation of acceptable (unmanaged) risk after application of compensating measures is the next stage of the algorithm of work with the risk management system. The calculation is recommended to be carried out in two directions: assessment of the possibility of influence on the probability of occurrence of a risk event and assessment of risk on the possibility of application of compensating measures. Here the derived function formula is applied, similar to the risk analysis, when the value of multipliers is reduced by the value of manageability for each type of multiplier. Manageability can also be determined by expert judgment, when each score (on a selected scale) is assigned a degree from 0 to 100.

The final value of residual risk is calculated as arithmetic mean of the normal Gaussian distribution, where the upper and lower values of the studied parameter are not included into the area of analysis.

Simulation models are used for quantitative assessment of aggregate risks; each of them is assigned a rating in the form of a number. The impact of risk types on the project is assessed both for each separately and aggregate risks. After reducing the degree of risk, a second assessment is done, based on the identified trends, and a decision is made on the further implementation of compensatory measures. The Monte Carlo method is used, based on the use of random number sampling. A special algorithm assigns a random event, with the help of which the probabilistic problem is solved. This method replaces complex algebraic computations in the following three cases:

1. when modelling complex operations with interaction of many random factors;
2. when verifying the applicability of analytical methods of research and clarifying the conditions of their applicability; it should be taken into account that the calculations are carried out repeatedly (e.g., 100 times); and
3. when developing corrections to empirically derived analytical formulas [8].

The essence of the developed risk assessment methodology is in the use of the parametric method as an initial (preliminary) method (for systems that do not have well-defined planned costs and realization terms, including for the assessment of projects at the stage of feasibility study). An example of such a risk assessment is the probability of failure of construction of a nuclear power facility at a given location (territory). This is illustrated by the transfer of the construction site of the Turkish NPP to Akkuyu from Sinop province (in 1980, the planned location of the NPP was Injeburun district of Sinop province, and the site in Akkuyu is Gulnar district of Mersin province). In 2017, the Turkish Atomic Energy Agency approved the design parameters of the Akkuyu NPP site.

Based on the results of identifying all possible types of risks and their assessment using the presented methodological approaches, risk registers are developed, both integrated (for the entire project) and localized (by project subdivisions), and experts on a particular type of risk are involved in the finalization of each of the registers.

It is proposed to organize the activity within a single scale from risk acceptance to risk avoidance (exclusion of action) and then divide the risks into groups depending on the degree of riskiness of action:

1. Acceptable risks are those that can be accepted at a given stage of the project life cycle; it should be noted that risks at different stages of the project life cycle are also distinguished by the degree and the actions that need to be taken to bring the risk to an acceptable level.
2. Risks that should be reduced are those whose management reduces the likelihood of an event. Staff training is a prime example.
3. Risks that should be increased are those leading to positive effects for the project.
4. Planned risks are risks for which it is possible and acceptable to develop and implement an action plan to reduce risk to acceptable levels.
5. Transferable risks, for which the best solution is to transfer them on a contractual basis under certain guarantees and responsibility of the contractor.
6. Avoidable risks are those that result in the avoidance of a given action or such a significant change in the operation of the system that eliminates the risk.

In this regard, the authors identify five main degrees of the customer's risk at the main stages of the NPP construction life cycle: the area of minimal risk; the area of average risk; the area of increased risk; the area of critical risk; the area of unacceptable (catastrophic) risk (Fig. 3).

In order to implement the strategic goals of the Rosatom State Corporation it is proposed to separately identify and analyse the risks that may hinder the implementation of a particular NPP construction project, namely:

1. increasing the share in the international nuclear power markets;
2. reduction of production costs;
3. reduction of production process time;
4. introduction of new products to the market;
5. global leadership in the field of technology [10].

Analysis of risk through the membrane of strategic objectives of Rosatom allows adopting a conceptual economic and mathematical model of risk management of realization of a unique NPP facility by probabilistic-functional dependence:

$$P_{(t)}^{nad} = \cup_{w,i,j=1}, \{V_{ij}\}, \{T_{real(i+1)}\}, \{X_i\}, \{R_{tpn}^{n}, K_{fin}^{n} K_{tr}\}, N_j, E_j, Q(\tau) \rightarrow max, \quad (2)$$

where $P_{(t)}^{nad}$ is effectiveness (organizational and technical reliability) of NPP implementation;
w, i, j is the number of hierarchical levels from 1 to N (macro-, meso- and micro-levels);
$V_{i,j}$ is integral indicator of the aggregate risk;
$T_{real(+1)}$ is time elapsed since the beginning of strategy implementation t_o
X_i is the full life cycle of the NPP;
$(R_{tnp}^{n}, K_{fin}^{n} K_{tr})$ shows total resources (physical, financial, labor) required for decision making;
N_j is a set of alternatives defining the problem situation;
E_j is preference function for choosing a solution option;
$Q_{(\tau)}$ is a set of time parameters on the interval (0,1).

CONCLUSIONS

The analysis of the methodological recommendations for improving the system of preparation and execution of construction works for large and technically complex industrial facilities allowed the authors to suggest ways to improve the organizational and technical reliability of designed solutions in the conditions of aggregate investment risk. Thus, the authors develop and apply their own concepts and methods of reliability and risk assessment. The essence of the membrane method of risk assessment for NPPs developed by engineer Denis Sezemin is that each stage of the project life cycle can be presented as a membrane layer, where one or another type of risk appears, which further contributes to the aggregate investment risk (R_{inv}), supplements it and transfers (grows, "sprouts") to the next layer. Here there is some similarity with physical-technical relation and behaviour of a membrane with its oscillation and attenuation, i.e., the risk has a possibility to pass through all layers of the membrane or, conversely, end on a certain layer, having had its impact. This implies that different types of risks corresponding to the aggregate investment risk can grow, appear or disappear at any stage, starting from the first and ending at the top of the layers. With the help of the necessary and recommended membrane principle of physical-type action throughout the life cycle of the project, the author of the Membrane Method proposes to develop software based on the impact of investment risk on the final target parameters of the whole system. The target parameters of the NPP construction system are: time parameter (duration), cost parameter (economic efficiency), quality parameter, and technical safety parameter, which are associated with the four corners of the square in the form of some volumetric structure. This allows visualizing a graphical representation of the dynamics of risk manifestation in time, displaying the main aspects of the problem under study:
- the fact of risk existence;
- the stage of risk occurrence;
- the stage of risk impact termination;
- impact of each of the risks separately on the system of the organizational and technical reliability of the project at major stages of the project life cycle;
- impact of all types of risks as an aggregate investment risk on the system, assessing it by four "corner" parameters;
- development of risk management methods using the diversification method with mechanisms for taking compensating measures.

REFERENCES

1. https://ru.wikipedia.org/wiki/EPC_(контракт)
2. https://neftegaz.ru/tech-library/menedzhment/141747-epc-podryad-kontrakt/#:~:text=EPC%20-%20контракт%20(Engineering%2C%20Procure-ment%2C,фиксированной%20цене%20к%20фиксированной%20дате
3. The Great Russian Encyclopaedia, 2004–2017. Gavrilov K.A., Krasavina L.N. https://old.bigenc.ru/economics/text/3510546#:~:text=РИСК%20(франц.%20risque%2C%20от%20итал.,в%20обыденном%20и%20политич.%20дискурсе
4. Issues of NPP life cycle management, Mohammed Alshreideh, Igor Yengovatov, 24.01.2023, Energy Policy.
5. Development of risk classifier as a stage of successful risk management, Afrikantov Machine Building Design Bureau, Brykalova S. M., Trifonov V. Yu. Gurieva E. A. Scientific and Practical Journal "Problems of Risk Analysis," vol. 18, 2021, issue 6, p. 44.
6. Methodological guidelines: The Monte Carlo method and instrumental means of its realization. Ministry of Education and Science of the Russian Federation, FGBOU of Higher Education Orenburg State University, Ramenskaya A. V., Pivovarova K. V., Orenburg, 2018.
7. Presentation "Integrated development of undeveloped territories. Experience of NPP Akkuyu construction by Rosatom State Corporation (Türkiye), Sezyomin D.E. National Scientific and Practical Conference, Moscow, October 21–22, 2022, NI MGSU, mgsu.ru
8. Development of risk classifier as a stage of successful risk management, Afrikantov Machine Building Design Bureau, Brykalova S.M., Trifonov V.Yu. Gurieva E.A. Scientific and Practical Journal "Problems of Risk Analysis," vol. 18, 2021, issue 6, p. 44.
9. **Gusakova E.A.** Fundamentals of organization and management in construction: textbook and workshop for universities / E.A. Gusakova, A.S. Pavlov. - 2nd ed., revised and supplemented. Moscow, Yurait Publishing House, 2022. 648 p.
10. Organization of Construction and Real Estate Development. Part I: Organization of construction 4th ed. revised and supplemented. Ed.by Dr. Econ. Sciences, Prof. P. G. Grabovy. Moscow, ASV Publishing House, IIA Prosvetitel, 2018. 648 p.
11. **Ovsyannikova T.Yu.** Economics of the construction complex. Economic substantiation and realization of investment projects: textbook. Tomsk, TGASU, 2004. 239 p.
12. Construction Management. Part I. Organizational models of management and contract constructions of the capital construction project: Textbook in two parts and Practicum (Part 3), 4th ed., revised and suppl. / Prof. P. G. Grabovy, Prof. A. A. Lapidus (eds). Moscow, ASV Publishing House, Prosvetitel, 2022. 484 p.
13. Risk management in real estate: textbook / Ed by P. G. Grabovoy. Moscow, Prospekt, 2012. 424 p.
14. **Mazur I.I., Shapiro V.D.** Project Management: textbook. Moscow, Omega-L, 2010. 960 p.
15. Risks in modern business: a monograph / Ed. by P. G. Grabovy. Moscow, IIA Prosvetitel, 2017. 228 p

СПИСОК ЛИТЕРАТУРЫ

1. https://ru.wikipedia.org/wiki/EPC_(контракт)
2. https://neftegaz.ru/tech-library/menedzhment/141747-epc-podryad-kontrakt/#:~:text=EPC%20-%20контракт%20(Engineering%2C%20Procure-ment%2C,фиксированной%20цене%20к%20фиксированной%20дате
3. The Great Russian Encyclopaedia, 2004–2017. Gavrilov K. A., Krasavina L. N. https://old.bigenc.ru/economics/text/351054

6#:~:text=РИСК%20(франц.%20risque%2C%20от%20итал.,в%20обыденном%20и%20политич.%20дискурсе
4. Вопросы управления жизненным циклом АЭС, Мохаммед Альшрейдех, Игорь Енговатов, 24.01.2023, Энергетическая политика.
5. Разработка классификатора рисков как этап успешного управления рисками, Машиностроительное конструкторское бюро имени Африкантова, Брыкалова С.М., Трифонов В.Ю., Гурьева Е.А. Научно-практический журнал "Проблемы анализа рисков", том 18, 2021, вып. 6, с. 44. Гурьева Е.А. Научно-практический журнал "Проблемы анализа риска", т. 18, 2021, вып. 6, с. 44.
6. Методические указания: Метод Монте-Карло и инструментальные средства его реализации. Министерство образования и науки Российской Федерации, ФГБОУ ВО Оренбургский государственный университет, Раменская А.В., Пивоварова К.В., Оренбург, 2018.
7. Презентация "Комплексное развитие неосвоенных территорий. Опыт строительства АЭС "Аккую" Госкорпорацией "Росатом" (Турция)", Сезёмин Д.Е. Национальная научно-практическая конференция, Москва, 21-22 октября 2022 г., НИ МГСУ, mgsu.ru
8. Разработка классификатора рисков как этап успешного управления рисками, Машиностроительное конструкторское бюро имени Африкантова, Брыкалова С.М., Трифонов В.Ю., Гурьева Е.А. Научно-практический журнал "Проблемы анализа рисков", том 18, 2021, вып. 6, с. 44.
9. **Гусакова Е.А**. Основы организации и управления в строительстве: учебник и практикум для вузов / Е.А. Гусакова, А.С. Павлов. - 2-е изд. переработанное и дополненное. Москва, Издательство "Юрайт", 2022. 648 с.
10. Организация строительства и управление недвижимостью. Часть I: Организация строительства 4-е изд. переработанное и дополненное. Под ред. д-ра экон. наук, проф. наук, профессора П.Г. Грабового. Москва, Издательство АСВ, "Просветитель", 2018. 648 с.
11. **Овсянникова Т.Ю.** Экономика строительного комплекса. Экономическое обоснование и реализация инвестиционных проектов: учебное пособие. Томск, ТГАСУ, 2004. 239 с.
12. Управление строительством. Часть I. Организационные модели управления и контрактные конструкции проекта капитального строительства: Учебник в двух частях и Практикум (часть 3), 4-е изд., переработанное и дополненное. / Проф. П.Г. Грабовый, проф. А.А. Лапидус (ред.). Москва, Издательство АСВ, Просветитель, 2022. 484 с.
13. Управление рисками в недвижимости: учебник / под ред. П.Г. Грабового. Москва, Проспект, 2012. 424 с.
14. **Мазур И.И., Шапиро В.Д**. Управление проектами: учебник. Москва, Омега-Л, 2010. 960 с.
15. Риски в современном бизнесе: монография / Под ред. П.Г. Грабового. Москва, МИС "Просветитель", 2017. 228 с.

Петр Григорьевич Грабовый, кандидат технических наук, доктор экономических наук, профессор, заведующий кафедрой организации строительства и управления недвижимостью МГСУ; заслуженный строитель России; член RICS (Великобритания).

Денис Евгеньевич Сеземин, аспирант кафедры организации строительства и управления недвижимостью МГСУ; директор по строительству и организации производства АО "Аккую Нуклеар" (Республика Турция)

Petr G. Grabovy, PhD in Technical Sciences, Doctor of Economic Sciences, Professor, Head of the Department of Construction Organization and Real Estate Management, Moscow State University of Civil Engineering; Honored Builder of Russia; RICS Fellow (Great Britain).

Denis E. Sezemin, PhD stident of the Department of Construction Organization and Real Estate Management at the Moscow State University of Civil Engineering; Director for Construction and Industrial Organization, JSC Akkuyu Nuclear (Republic of Türkiye)

International Journal for Computational Civil and Structural Engineering, 19(4) 48–68 (2023)

DOI:10.22337/2587-9618-2023-19-4-48-68

REPAIR OF MASONRY AFTER DYNAMIC IMPACTS. CALCULATION AND DESIGN METHODS

Oleg V. Kabantsev, Oleg A. Simakov

Department of Reinforced Concrete and Masonry Structures, Moscow State University of Civil Engineering (National Research University), Moscow, RUSSIA

Abstract: Civil engineers are encouraged to apply novel techniques, to improve and to adapt well-known methods amid the reality of modern life. An impressive number of restoration and strengthening techniques are developed for unreinforced masonry (URM) material well-known for centuries. Masonry may need restoration and strengthening due to errors made in the course of design, construction or long-term operation of buildings and structures. Besides, masonry needs strengthening in seismic areas. Strengthening of masonry structures, subjected to dynamic impacts during military operations, was initiated after the Second World War. Construction technologies advanced considerably over the last seventy years, and today shotcrete, a widely known strengthening technique, can be applied for a good reason. This article addresses shotcrete as a method for restoring masonry damaged by explosion impacts. Results of the laboratory testing of materials and parts of structures are provided together with improved methods of analysis. The methodology for computer-aided analysis of buildings is also presented, taking into account the staged nature of work and the ability of external shotcrete to support loads. Practical restoration of buildings is addressed in the conclusions section, and conclusions are drawn there.

Keywords: masonry restoration; shotcrete; fiber reinforced shotcrete; dynamic impacts; external reinforcement

ВОССТАНОВЛЕНИЕ КАМЕННОЙ КЛАДКИ ПОСЛЕ ДИНАМИЧЕСКИХ ВОЗДЕЙСТВИЙ. МЕТОДЫ РАСЧЕТА И ПРОЕКТИРОВАНИЯ

О.В. Кабанцев, О.А. Симаков

Национальный исследовательский Московский государственный строительный университет, г. Москва, РОССИЯ

Аннотация: Современные реалии требуют от инженеров в области строительства применение как новых техник, так и совершенствование и адаптацию уже известных методик. Для хорошо известного на протяжении столетий материала каменной кладки разработано значительное количество методов восстановления и усиления, необходимость которых обоснована ошибками проектирования, строительства или длительной эксплуатацией, а также усиление кладки в сейсмических районах. В то же время вопросами усиления конструкций из каменной кладки, получивших динамические повреждения в результате боевых действий, полноценно занимались только после второй мировой войны. За последние 70 лет строительные технологии значительно продвинулись, появилась возможность обоснованно применять хорошо известный метод усиления путем устройства аппликаций из торкрет-бетона. В настоящей статье рассмотрены вопросы применения современного торкрет-бетона для восстановления каменной кладки, разрушенной после взрывных воздействий. Приведены результаты лабораторных ипытаний материалов, фрагментов конструкций, а также скорректированные методики расчета. Также представлена методика компьютерного расчета здания с учетом этапности проведения работ и включении в работу внешней аппликации. В заключении приведен практический опыт восстановления зданий, сделаны выводы.

Ключевые слова: восстановление каменной кладки, торкрет-бетон, торкрет-фибробетон, динамические воздействия, внешнее армирование

1. INTRODUCTION

1.1. Review of the literature

Masonry has been widely used to make bearing structures of buildings for over 200 years. Masonry structures have served as frameworks of multi-storey buildings since the 50s of the 20th century. At present, although reinforced concrete structures and modular systems made of wood and metal have leapfrogged in development, masonry is still used to make bearing walls. Studies [1, 2] confirm that frameworks of numerous buildings and structures are made of masonry. Besides, a great number of such buildings and structures have more than two storeys. The analysis of masonry buildings shows their nearly uniform distribution over regions, except for northern areas, where the percent share of buildings with masonry bearing walls is somewhat lower.

Methods of design and analysis of masonry structures are based on a traditional masonry model viewed as a continuous medium with generalized ("effective") characteristics. The validity of this model for regular ("standard") operating conditions is confirmed by numerous studies [1-5]. However, it is extremely difficult, and in some cases impossible, to use this model to project the behavior of masonry structures subjected to inelastic deformations with different areas on the diagram.

The need to analyze the projected ability of masonry structures to support loads beyond the elastic phase of deformation is evident. It is explained by special conditions, such as seismic impacts, beyond-design soil deformations, versatile beyond-design loads and external impacts on bearing masonry structures during the term of operation. To analyze the ability of masonry structures to support loads beyond the elastic phase of deformation, a masonry model was developed. It represents masonry as a piecewise homogeneous composite material featuring discontinuous fields of adhesive interaction between composite material elements and different values of the modulus of elasticity [6-12]. The key element of this model is the mechanism of adhesive interaction between masonry materials (bricks/stone and mortar), which has its own mechanical characteristic R_{adh}. If neither contact zone of the composite material demonstrates adhesive interaction (R_{adh}=0), masonry materials interact in the "dry" friction mode, and masonry loses integrity, its most valuable property [13-15].

In the model [6-8], the most complex state of biaxial stress of masonry is schematically represented as interacting piecewise homogeneous elements of the composite material featuring different mechanisms of interaction (Figure A.1. - Figure A.3), where F is the generalized force parameter of interaction; N_i denotes shear forces.

A model of interaction between elements of a composite material in a vertical mortar joint is presented in Figure A.1. Interaction between bricks and mortar in a vertical mortar joint is determined by the lack of adhesion between these materials, because a microcrack emerges under the action of shrinkage stresses in the zone of contact between bricks and mortar.

Figure A.2 shows a model of interaction between elements of the composite material in a horizontal masonry joint under the action of compression stresses perpendicular to the joint

Figure A.3. shows a model of interaction between elements of a composite material in a horizontal masonry joint under the action of tensile stresses, perpendicular to the joint.

Analysis of the masonry model that represents a piecewise homogeneous composite material featuring discontinuous fields of adhesive interaction between composite material elements and different values of the modulus of elasticity confirms the crucial role of adhesive interaction between masonry materials in ensuring the integrity of masonry.

For a number of reasons, masonry structures need restoration and strengthening [3-5]. The main reasons are:

- errors made in the course of design;
- errors made in the course of construction;
- an increase in design loading;

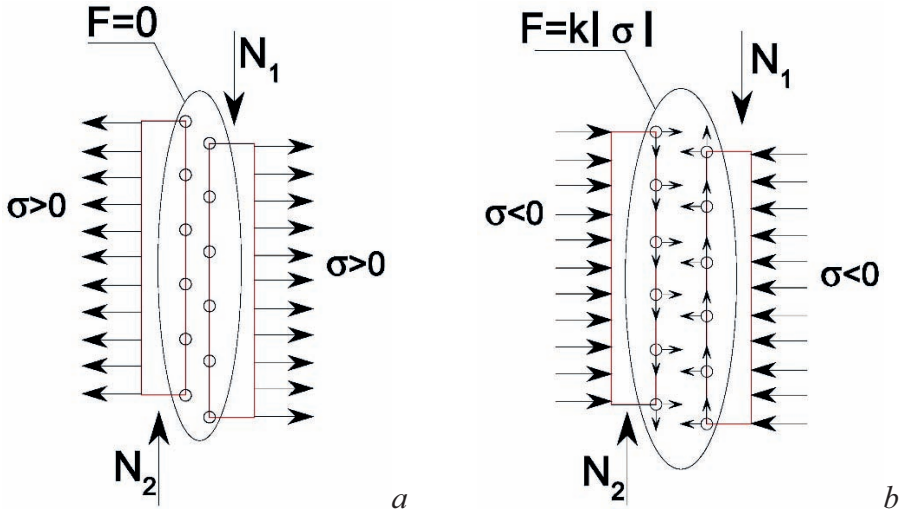


*Figure A.1. Model of interaction between masonry materials (bricks/stone and mortar): a - interaction in the absence of compression stresses perpendicular to the joint, (**σ>0**); b - interaction under compression stresses perpendicular to the joint, (**σ<0**). k - friction factor along the line of contact between bricks and mortar*

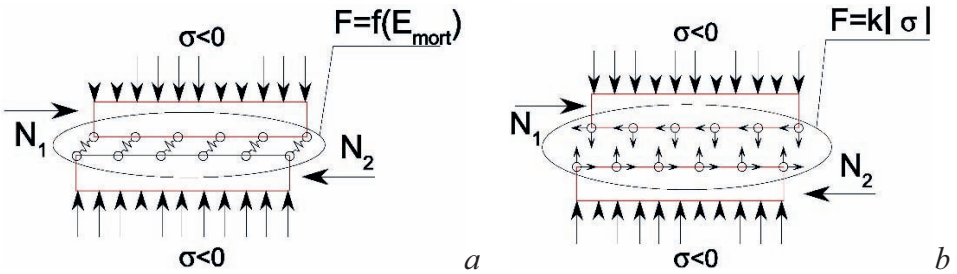


*Figure A.2. Model of interaction between masonry materials (bricks/stone and mortar) in a horizontal masonry joint under the action of compression stresses perpendicular to the joint (**σ<0**): a - when conditions of mortar strength and/or adhesion strength accompanying interaction between masonry materials are met; b - when conditions of the mortar strength and/or adhesion strength accompanying interaction between masonry materials are not met; k - friction factor along the brick and mortar contact line*

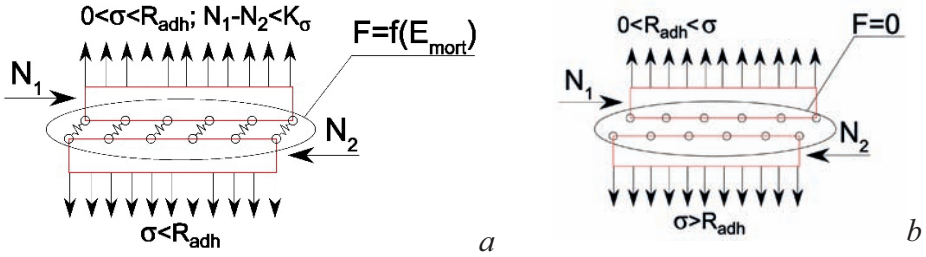


Figure A.3. Model of interaction between masonry materials (bricks/stone and mortar) in a horizontal masonry joint under the action of tensile stresses perpendicular to the joint (σ<0): a - when conditions of the mortar strength and/or adhesion strength accompanying interaction between masonry materials are met; b - when conditions of the mortar strength and/or adhesion strength accompanying interaction between masonry materials are not met; k is the mortar cohesion factor.

- structural collapse as a result of operation (beyond-design impacts; lack of repair work, in particular, lack of repair of insulation);
- other causes (accidents).

Methods of masonry restoration and strengthening are available for masonry structures in operation in traditional conditions triggering most widely spread types of damage and defects [16, 17]. These methods demonstrate good convergence with experimental results and the real behavior of strengthened structures. Besides, masonry failure under static loading and dynamic seismic impacts is also considered.

Masonry structures damaged by explosion impacts are clustered into an independent group. Explosive loading is the cause of damage types characterized by high-intensity local dynamic impacts (energy). Such impacts lead not only to the local damage of masonry, but can also cause disintegration of internal bonds between masonry materials, such as bricks and mortar, as well as disintegration of internal bonds between outer and inner layers of masonry structures. This kind of damage determines the need for a detailed masonry model in the form of a piecewise homogeneous composite material featuring discontinuous fields of adhesive interaction between composite material elements and different values of the modulus of elasticity. This model is used to analyze the behavior of damaged masonry structures.

No detailed scientific studies of masonry damage caused by explosive loading were conducted. There is no systematized information about the features, the structure and the characteristics of such damage in the research literature.

Presently, two main options are used to restore and strengthen masonry structures damaged by explosion impacts:

Option 1. The implementation of recommendations developed for the restoration of structures damaged during combat operations in the years of World War II [18, 19]. These recommendations have a "prescriptive" nature; they have no detailed verification of analysis, but they stem from practical experience and focus on large-scale application in case of limited mechanization, traditional technologies and construction materials. Evidently, the application of this principle of strengthening and restoration of damaged masonry structures is feasible in individual cases. The principle of masonry restoration and strengthening, that has no reliable methods of validation, cannot be recommended for large-scale use.

Option 2. Using techniques developed to increase the seismic stability of masonry by restoring its integrity. Two main principles are employed to improve masonry integrity: (1) the principle of increasing the number of internal bonds in masonry using a method of special elements introduced into masonry, for example [20]; (2) the principle of adding external structures that have the required bearing capacity. Different techniques are used to attach these structures to masonry, for example, composite materials [21] and shotcrete [20-23] serve as the external reinforcement for masonry structures.

Masonry restoration made according to option 2 is backed by research that serves as the basis for analysis of reinforced masonry structures and strengthening elements. In general, these methods of strengthening masonry structures can be considered similar in terms of the principles of restoration of masonry structures damaged by explosion impacts.

This one-sided shotcrete technology is the most technologically advanced method of improving the seismic stability of masonry structures.

The shotcrete method used to apply concrete to the surface of an existing structure is well known; it is based on a sophisticated technology. However, a century-long application of the shotcrete technology improved each principal component of this method. As a result, present-day shotcrete differs greatly from the initial technology. Today the shotcrete technology is optimal (in terms of parameters of shotcrete machines, composition of materials, new types and combinations of admixtures), and its efficiency is close to the maximum.

Considerable research is contributed to the application of shotcrete used to strengthen mason-

ry structures of buildings in earthquake-prone areas [20, 24-26].
Studies of laboratory specimens and full-scale experiments have the following results:
1. An increase in the general stiffness of masonry that equals, at least, 20%. In this case, stiffness parameters depend on conditions of bonding between strengthening elements and existing masonry (bonding in the form of keys and micro-keys; adhesive bonding between shotcrete concrete and existing masonry).
2. A considerable (up to 3 times) increase in the total bearing capacity of shotcrete-strengthened masonry. The key condition for increasing the bearing capacity of a strengthened structure is strong bonding between shotcrete concrete and existing masonry (see point 1). According to the research findings, the most effective method of increasing bonding between shotcrete concrete and existing masonry is either the use of customized shotcrete compositions or mechanical surface preparation by making keys and micro-keys (joint pointing, making keys with pre-set dimensions). The effect of adhesion produced on bonding between shotcrete concrete and strengthened masonry, as well as the value of the bearing capacity varies in the range of 30-75% of the final value of the bearing capacity of a strengthened element.
3. The collapse mechanism typical for masonry strengthened using one-sided shotcrete differs greatly from the collapse mechanism typical for masonry that has no strengthening: masonry without strengthening or reinforcement is prone to brittle failure. Masonry strengthened using one-sided shotcrete is characterized by elasto-plastic deformation that triggers disintegration of bonds between shotcrete and masonry.
4. The recommended shotcrete thickness of 4-6 cm was identified in an experiment conducted before the practical application of shotcrete aimed at improving the seismic stability of existing buildings.
The practical development of methods aimed at increasing the seismic stability of masonry structures shows that problems solved to design earthquake-resistant masonry are totally different from tasks focused on restoration of masonry structures damaged by local high-intensity explosion impacts.
Given that explosion impacts cause complete destruction of masonry in certain parts of bearing structures, new masonry is needed to restore them, and special design solutions should be applied for the new masonry to support loads.
Evidently, there is a need to study interaction between strengthening structures, or one-sided shotcrete, and existing masonry, and to identify mechanisms of their interaction.
Analysis of a detailed masonry model, that represents a piecewise homogeneous composite material with discontinuous fields of adhesive interaction between composite material elements and different values of the modulus of elasticity, demonstrates the need to develop a shotcrete composition featuring high adhesive strength between shotcrete and existing masonry made of different types of bricks. This type of interaction is particularly important because the contact develops over the entire area of shotcrete.

1.2. Purpose, Objective and Summary of the Study Outlined in This Article

The world is being rocked by versatile armed conflicts, resulting in substantial damage to buildings and structures. Masonry buildings are the backbone of built-up areas in any populated locality. Therefore, such buildings are inevitably damaged by explosion impacts. Hence, the development of effective sophisticated methods of restoration and strengthening of masonry structures is highly relevant.
The purpose of this project is to develop an integrated research-based method of strengthening masonry bearing structures damaged as a result of explosion impacts. An integrated method is understood as a method and technology of masonry restoration, development of special compositions of materials, performance of research to check the effectiveness of the proposed method, identification of principal mechanical characteristics, development of a method of

analysis of design solutions for restoration and strengthening of damaged structures.

One-sided shotcrete is chosen as the main strengthening method. It is highly mechanized, easy to implement, and it ensures a sufficient increase in the bearing capacity of masonry.

To achieve this goal, masonry damage, caused by explosion impacts, and earlier experimental studies were analyzed, key characteristics of materials were identified, the composition of the shotcrete material was developed, studies were conducted to identify characteristics of interaction between strengthening structures and masonry materials, and a method of analysis was refined in order to take into account the actual nature of damage to masonry as a result of explosion impacts. The composition, focused on masonry strengthening after dynamic impacts, was developed; its physical and mechanical properties, adhesion to the main types of bricks were studied. Methodological fundamentals of (1) analysis of masonry in multi-story buildings and (2) masonry strengthening techniques are developed.

2. MATERIALS AND METHODS

2.1. Theoretical fundamentals of modeling

2.1.1 Studies of masonry damage from explosion impacts

The following data characterize the explosion damage of one-storey and multi-storey buildings built in 1970-2010:

- materials: 250x120x65 (55) mm ceramic and silicate bricks; strength of bricks: 5-12,5 MPa; strength of cement-sand mortar: 2,5-10 MPa. The percentage of silicate bricks used to make bearing structures is high;
- building frameworks have longitudinal and transverse bearing walls;
- three types of building collapse patterns (figure 1).



a) *b)* *c)*

Figure 1. Collapse patterns typical for bearing structures of masonry buildings. Pattern 1: complete destruction of one floor (a); Pattern 2: Complete destruction of a large part of brickwork encompassing several floors and accompanied by destruction of adjacent parts of floor slabs (b); destruction of a part of a building (c)

Masonry damage from explosion impacts has the following features:

1. Exterior walls of buildings suffer from the greatest damage due to the lower accessibility of interior walls to impact factors.
2. Inclined and vertical cracking of intact brickwork in the areas adjacent to local damage (figure 2.a);
3. Types of hidden damage in intact brickwork:

3.1. Disintegrated bonds between the outer course and the brickwork (figure 2.b);

Disruption of adhesive interaction between basic elements of brickwork (mortar and bricks) in horizontal joints affecting large areas of walls subjected to explosion impacts. Research results show that few structures retain adhesive strength at the interface between masonry materials, and these structures can be neglected.



a) *b)*

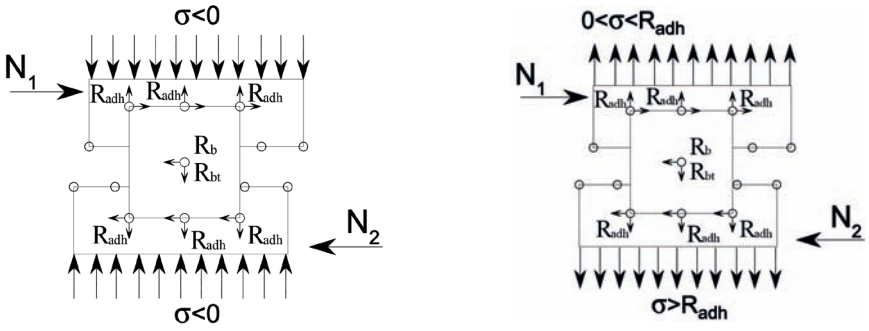
Figure 2. Brickwork destruction patterns characteristic for explosion damage; inclined cracking (a); disintegrated bonding along the outer course (b)

3.3 As a rule, large parts of brickwork feature disintegrated bonding between the outer course and the brickwork throughout the entire wall height. In this regard, the outer course cannot be taken into account during the analysis of further brickwork operation. Accordingly, the proposed strengthening method assumes that the outer course should be dismantled despite the absence of external damage.

2.1.2 Brickwork models

The analysis is made for a masonry model representing a piecewise homogeneous composite material with discontinuous fields of adhesive interaction between composite material elements and different values of the modulus of elasticity. The research of structures subjected to explosion damage proves that in case of disrupted adhesive bonding the model of interaction between masonry materials in horizontal masonry joints follows the patterns presented in Figure A.2.b and Figure A.3.b.

Adhesive interaction missing from existing masonry structures is needed to restore masonry structures damaged by explosion impacts. Towards this end, the shotcrete method is applied to ensure strong contact interaction with existing masonry structures (figure 5). Adhesive strength and other types of contact between shotcrete and existing masonry structures can ensure this type of interaction.



a) *b)*

Figure 5. Model of interaction between damaged masonry and shotcrete elements in compression and shear (a), tension and shear (b)

2.1.3. Methods of taking account of interaction between a shotcrete element and an existing masonry structure

The masonry model strengthened with one-sided shotcrete is implementable in the case of reliable interaction between a shotcrete element and existing masonry structures. This general condition is difficult to implement due to a large difference between stiffness values of masonry and shotcrete. This method ensures high adhesive strength at the interface between shotcrete and masonry without special actions aimed at adhesion improvement (dismantling of existing structures, etc.). In general, the mechanism of interaction between shotcrete elements and existing masonry has the following two components: the adhesion mechanism (the main mechanism) and interaction based on the shear of micro-keys (figure 6). Micro-keys emerge in existing masonry due to natural openings in areas of masonry joints.



a) *b)*

Figure 6. A model of interaction between shotcrete and masonry; adhesion mechanism (a), micro-key mechanism (b)

If adhesion is sufficient and micro-keys are in place (which is less important), the shotcrete method used to restore damaged masonry (1) serves as compensation for disintegrated internal bonds between masonry materials and (2) increases the bearing capacity of a masonry structure as a whole.

In general, the bearing capacity of strengthened masonry can be found using formula (3).

$$Q_f = Q + Q_{ad}. \quad (1)$$

where Q is the bearing capacity of a masonry specimen without strengthening; Qad is the bearing capacity of a strengthening element. Earlier studies [24] describe the general failure mechanism for masonry specimens strengthened with one-sided shotcrete: masonry specimens fail along unbonded joints in the area of contact between shotcrete and masonry, and an increase in the bearing capacity is limited by the value of Qad,max, determined using formula (2).

$$Q_{ad,max} = R'_{sq} 0{,}2 A_{micro-key}, \quad (4)$$

where Rsq' is the design shear strength of masonry along the unbonded joint;

A is the area where force is transferred; it can be approximated as 20% of the area of contact between shotcrete and masonry (taken as 0,2 in formula (2)).

2.4. Studying shotcrete materials

Properties of shotcrete are determined by the composition of shotcrete materials and the shotcrete technology used (coupled with the experience of a nozzleman). As for the shotcrete material composition, a special shotcrete mix is developed using the prior experience. It's focused on brickwork strengthening, and the main emphasis is on its adhesive strength.

Special specimens were prepared for testing purposes. These were (1) slabs designated for strength testing and (2) joint-free masonry specimens used to test shotcrete adhesion to different masonry materials (silicate bricks,

solid and hollow ceramic bricks, figure 7). Specimens were made at a construction site by a standard team of builders (figure 8).
Four prism-shaped specimens (figure 7), having dimensions of 70×70×280 mm, were made of a shotcrete slab to find the modulus of elasticity and the prism strength. Besides, cylinder-shaped specimens, that were 64 mm in diameter, were drilled using a diamond drilling machine to find the compressive strength.



a) *b)*

Figure 7. General view of specimens; specimens used to test properties (a), specimens used to test adhesion (b).



Figure 8. The manufacturing of specimens

The following results were obtained as a result of research (table 1):
- The modulus of elasticity of shotcrete is 25600 - 28000 MPa.
- The compressive strength of shotcrete exceeds 63 MPa.

Table 2. Prism-shaped specimens: testing results

№	Cross-sectional area cm^2	Size, cm^3	Mass, g	Density, g/cm^2	R (compressive strength), MPa	Eb (modulus of elasticity), ×103, MPa
1	50,28	1447,8	3118	2,154	46,68	28,0
2	50,73	1415,3	3052	2,156	43,60	26,2
3	54,87	1536,3	3306	2,152	37,28	25,9
4	51,73	1448,4	3126	2,158	40,48	25,6

Adhesive strength (adhesion) was found via a tearing force whose value was sufficient to detach a specimen, made of a cured composition, from the brickwork, made of different types of bricks. The force was applied to the specimen through a metal disk with an anchor (hereinafter referred to as a stamp) glued to the surface of the specimen.

Before testing five measurement points were prepared on each slab; the number of points was determined by the regulatory documents.

The preparation procedure included:

- grinding needed to smooth the surface;
- using a cutting tool to cut a layer of shotcrete to reach the masonry and to make a specimen with a diameter of 50 mm.

When the specimen was ready, metal stamps were glued to them using a high-strength fast-setting adhesive composition.

Adhesion tester was used to find the value of the tearing force in accordance with the operating instruction.

As a result of testing it was found that the “shotcrete-masonry" contact line did not collapse. Rather, masonry collapsed in the area adjacent to the contact line.

Adhesion testing results demonstrated the brickwork collapse (Figure 9), meaning that the adhesive strength exceeds the tensile strength of brickwork (the tensile strength of the interface between shotcrete and brickwork, identified in an experiment, is 0,9-1,2 MPa).



Figure 9. Testing adhesion between shotcrete and brickwork

The results can be presented as a diagram (figure 10).

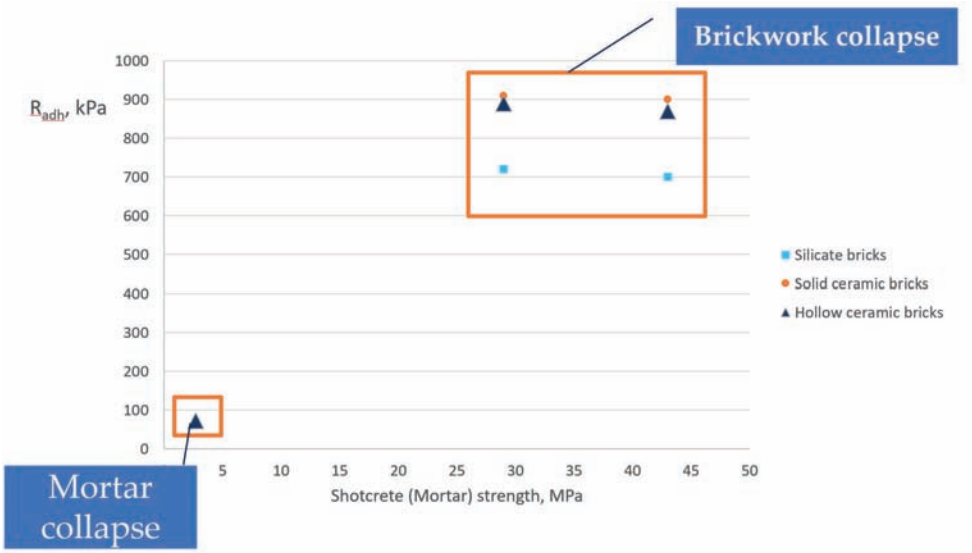


Figure 10. Testing adhesion between shotcrete and masonry.

2.5. Analysis of strengthening

The studies of adhesion between shotcrete and brickwork confirm the general principles of analysis conducted using formulas (1) and (2), namely, a limit on an increase in the bearing capacity of strengthened brickwork based on the strength of masonry materials rather than shotcrete.

Earlier experimental studies and numerical modeling serve as the basis for a masonry strengthening method applied to brickwork damaged by explosion impacts. This method employs a one-sided shotcrete technology that has the following stages (figure 11):

Stage 1. Installing temporary slab supports, starting from lower floors. These supports should take loads throughout the entire height of a building. Their ability to support loads needs to be controlled.

Stage 2. Dismantling the outer course. Dismantling masonry elements in the area of explosion damage. Performing masonry work to restore lost elements of masonry structures.

Stage 3. Installing local elements to strengthen wall intersection nodes.

Stage 4. Installing wall reinforcement elements in shotcrete areas. Shotcrete of exterior surfaces of walls (figures 7, 8).

Stage 5. Removing temporary slab supports, starting from upper floors (after shotcrete curing).

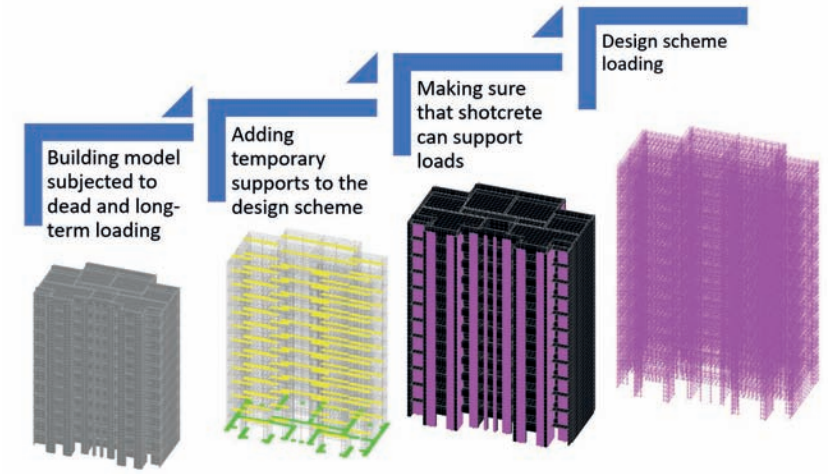


Figure 11. Strengthening of bearing structures in a multi-storey building: stages of computational modeling

Traditional single-stage methods of analysis of strengthening structures for existing buildings (including multi-storey buildings) cannot have accurate results because such methods do not take into account the staged nature of the stress-strain state development, including the ability of strengthening elements to take loads at final stages. In this regard, most reliable modeling results are obtained using MONTAGE software. It is a multi-stage technology of computational analysis implemented by SCad Office software package. The computation technology allows to identify stages of computation corresponding to stages of the stress-strain development in the structures being strengthened.

3. RESULTS

Masonry structures of multi-storey buildings damaged as a result of explosion impacts were investigated.

The following facts were identified in the course of the building examination (figure 12):

Foundations (in the limited serviceable condition):
- local collapse of the perimeter pavement;
- perimeter pavement cracking;
- vegetation growth; perimeter pavement sagging;
- moisture content increase in plinth structures due to damaged sills;
- local collapse of the finishing layer of the plinth;
- damaged finishing layer along the route of utility pipelines.

Exterior walls (in the emergency condition):
- damage and collapse of masonry walls of the engineering floor due to the dynamic impact;
- destruction of masonry and a layer of wall plaster on floors 7-10 due to thermal and dynamic impacts;
- damage and collapse of the main facade brickwork on floors 1-10 resulting from the dynamic impact;
- wall damage; a through hole in the gable facade on the level of the 10th floor;
- exterior walls do not meet the requirements for the thermal conductivity of materials according to the thermal analysis of structures.

Floor slabs (in the emergency condition):
- destruction and collapse of floor slabs from the 5th floor to the engineering floor of entrances 2 and 3, resulting from the dynamic impact;
- destruction of finishing layers resulting from the dynamic impact;
- cracks in joints of floor slabs, resulting from the dynamic impact.

The roof (in the emergency condition):
- destruction and collapse of bearing structures of the roof resulting from the dynamic impact;
- damage to the whole area of roof coating resulting from the dynamic impact;
- local absence of flashing;
- the minimum term of effective operation of building and roofing elements made of roll materials is 10 years for residential buildings.

Stairs (in the emergency condition):
- destruction and collapse of bearing structures of stairs and elevator shafts resulting from the dynamic impact;
- cracks along the joints between staircases and walls;
- spalling concrete steps of staircase structures;
- local destruction of the finishing layer.

Balcony slabs (in the emergency condition):
- destruction of balconies and extended enclosed balconies on floors 6-10 of entrance 2, resulting from the thermal impact;
- local destruction and collapse of structures of balconies and extended enclosed balconies resulting from the dynamic impact;
- concrete deterioration; spalling of facing panels of balconies and extended enclosed balconies due to the dynamic impact;
- damaged protective concrete layer of slabs of balconies and extended enclosed balconies;
- destruction of glazing of balconies and extended enclosed balconies as a result of the dynamic impact.

Entrance halls (in the limited serviceable condition):
- local destruction of the brickwork of entrance halls;
- locally damaged finishing layer of pit walls;
- concrete spalling; cracking steps of entrance lobbies and pits.



Figure 12. General view of the building described in this paragraph

The following actions are recommended in respect of the building's bearing structures judging from the defects and damages identified during the examination:

1. Restoration of damaged parts of bearing walls

The recommendation is to use materials similar to those that existing structures are made of, including silicate bricks M150 or better, and mortar M75 or better. It is recommended to reinforce the parts of masonry to be restored using 100x100 mm steel mesh B500, 4 mm diameter, to be installed every three rows.

Restored parts of walls are to be attached to existing walls by steel anchor rods embedded in the existing masonry using special chemical compositions or mounted in smaller diameter holes.

2. Strengthening bearing walls damaged by dynamic impacts

Exterior bearing walls should be strengthened using one-sided shotcrete with the thickness of 75-85 mm. B500 d5 mm mesh, 100x100 mm, is to be used as the reinforcement. The shotcrete material (whose tensile strength should not be below the tensile strength of brickwork) will stick to brickwork by means of adhesion. An additional layer of mesh should be applied to reinforce the outside corners. A cast-in-place belt should reinforce the upper part of the parapet.

The masonry is additionally reinforced with cast-in-place reinforced concrete pylons not less than 160 mm thick (the size of their section is to be determined in the course of the analysis).

Shotcrete can be applied through 350x50 mm holes in solid balcony slabs; holes should be spaced 700 mm apart. Reinforcement rods should be inserted into these holes.

One-sided shotcrete should be applied to masonry after the outer facing layer is dismantled.

It is recommended to use carbon fiber composite materials to reinforce internal bearing stairwell walls with diagonal cracks. In this case carbon mesh and special polymer cement mortars is the best option. The total reinforcement thickness is up to 25 mm.

3. Restoration of damaged parts of floor slabs and stair landings

Floor slabs and stair landings are to be restored by concreting damaged areas and applying new reinforcement selected according to the analysis.

Floor slabs should be restored by concreting destroyed parts that are 220 mm thick. Concreted parts should have cavities to prevent excessive loading. Both a floor slab and steel beams, such as channels or I-beams, can serve as bearing elements.

It is recommended to restore stair landings (if the integrity of their edges is preserved) using

B20-25 concrete and reinforcement bars; the thickness of a concrete layer should be, at least, 100 mm, and the reinforcement should be selected on the basis of analysis.

4. Restoration of partitions

Partitions should be made of hollow ceramic bricks 120 mm thick. Partitions should be perpendicularly attached to the bearing structures (bearing walls and floor slabs).

Given that the process of strengthening building frameworks is staged, analysis made for the transitory period should also be staged, and each stage should correspond to a certain part of structures being restored. In this case, staged analysis ensures the continuity of the stress-strain state (SSS) of model elements in the course of transition from one stage to another (MONTAGE software module implements the technology ensuring the stage-by-stage incorporation of elements into the model).

Analysis made for the principal term of building operation (standard analysis made for a building subjected to long-term operating loads) corresponds to an independent stage of comprehensive staged analysis taking into account the continuity of SSS that emerges at earlier stages.

Wind loads, acting on building frameworks, are analyzed at an independent stage, and the analysis thus performed should take into account the state of strain that emerges at earlier stages.

In total, five stages of analysis of building frameworks are identified (Table 2).

Principal solutions designed to strengthen the following building structures were developed as a result of modeling made according to the proposed method of analysis:

- strengthening of external bearing walls of a building using one-sided shotcrete;
- installation of monolithic reinforced concrete pylons along the building façade;
- wall restoration on floors 9 – 10,
- reinforcement of internal walls of stairwells by external carbon bonding (figure 13).

Table 2. Description of characteristic stages of analysis

Stage №	Stage analysis
1	Building framework generation mode. An existing building with restored masonry
2	Prevention of vertical displacements of elements simulating floor slabs
3	Mode of transitory analysis Dismantling of the outer facing layer; applying shotcrete for strengthening purposes
4	Mode of transitory analysis Removal of temporary supports from under the floor slabs
5	Mode of standard operation encompassing long-term operating loads and reduced values of long-term operating loads. Loads include the deadweight of structures, floors, partitions, enclosing structures, full values of operating loads, snow and wind loads.

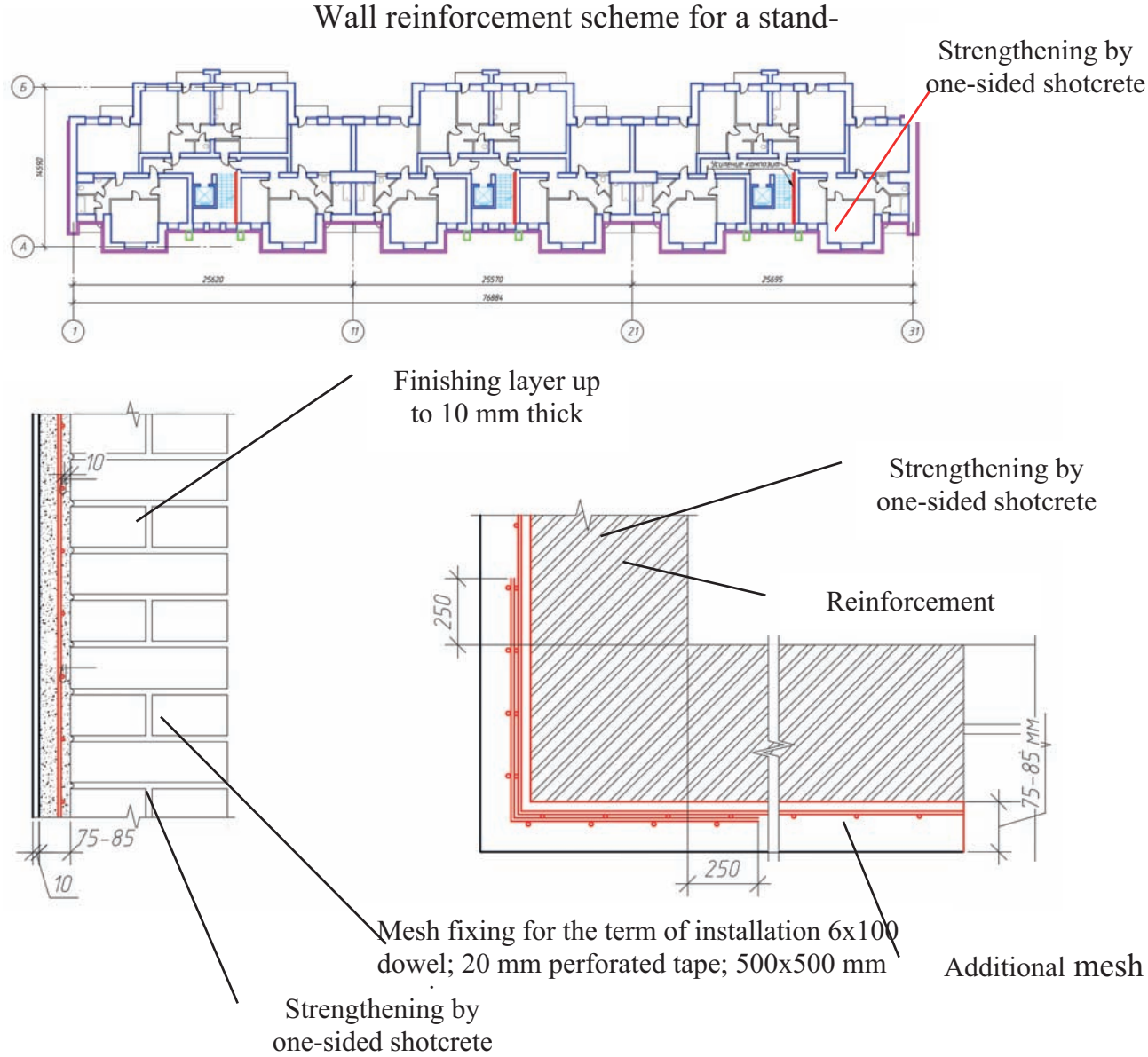


Figure 13. Key structural solutions aimed at strengthening bearing masonry walls

The shotcrete technology applied to strengthen bearing walls requires the following sequence of work performance:

1. Before shotcrete is initiated, spots to be shotcreted should be visually examined; inventory, scaffolding, machines and devices needed for safe work performance should be ready in the work performance area.
2. Defective spots should be cut out so that only strong and dense brickwork is left. Towards this end, boundaries of the spots to be repaired should be chalk marked and spots to be repaired should be cut out in straight lines along the contour by an angle grinder or a diamond saw to a depth of, at least, 10 mm.
3. A jackhammer should be used to remove loose spots to the depth of damage perpendicularly to the repaired surface. The quality of work should be checked by hammer testing.
4. To ensure the best adhesion, the surface should be treated using a high-pressure spray gun, at least, 500 bar, or a sandblaster.
5. The surface to be shotcreted should be cleaned of dirt and moistened.

6. The surface of the spots to be restored to the design dimensions should be shotcreted layer by layer; the thickness of one shotcrete layer is up to 100 mm. Shotcrete concrete rundown should be prevented, as this can lead to cavitation, and it is extremely difficult to detect and eliminate cavities. The thickness of one shotcrete layer should be checked by probing fresh layers in several spots using a thin metal rod.
7. The main layer of shotcrete with a thickness of 30 mm can be applied forty minutes after the restoration of damaged spots.
8. Accumulation of rundown deposits is not allowed in particular areas. They should be removed immediately after formation.
9. The surface to be repaired is to be smoothed.
10. The surfaces to be repaired should be moistened, or film-forming compositions should be applied.

The technology of the final stage of work (shotcrete) is shown in figure 14.
The result of the work is shown in figure 15.



Figure 14. Strengthening masonry walls of a multi-storey building



Figure 15. The strengthening of masonry walls of a multi-storey building

4. DISCUSSION

The explosion damage of bearing masonry walls greatly differs from the damage caused by design, construction or operational errors, for which a large number of solutions, methods of restoration and reinforcement are available. The greatest difficulty is the disintegration of bonding between brickwork materials, namely, mortar and bricks, including the destruction occurring at a considerable distance from the spot of impact. The most effective method is external shotcrete, which ensures compensation for internal bonds in masonry lost due to intensive dynamic impacts. To implement the concept of restoration of damaged masonry structures, a model simulating the behavior of masonry and reinforcement structures is developed together with a method of analysis of bearing structures of a building, which takes into account staged analysis corresponding to stages of strengthening and development by strengthening elements of the ability to support loads.

A composition was designed to strengthen the masonry. It adhesive interaction with all types of brickwork does not require supplementary structural solutions to increase adhesion. The composition was subjected to a exhaustive testing procedures, including those aimed at finding the adhesive strength accompanying interaction with different types of bricks.

The strengthening method, including the composition, the technology, as well as the algorithm of analysis, were pilot tested at a specific construction facility - a multi-storey residential building damaged as a result of explosion impacts.

5. CONCLUSIONS

The method of restoration of masonry structures damaged by dynamic explosion impacts is developed and justified. According to the novel method, damaged internal masonry bonds are compensated by exterior strengthening structures accompanied by a simultaneous increase in the bearing capacity of a masonry structure as a whole. Studies have proven that the most successful and technologically efficient solution to the problem of restoration is the shotcrete technology coupled with the necessary reinforcement.

The shotcrete technology ensures reliable interaction between the strengthening structure and damaged masonry via two mechanisms: interaction via adhesion and interaction via the shear of micro-keys. The value of the adhesive strength at the interface between shotcrete and masonry materials exceeds the tensile strength of both bricks and masonry mortar. The proposed technology ensures fast shotcrete and the required standard of quality.

This work was financially supported by the Ministry of Science and Higher Education of Russian Federation (grant # 075-15-2021-686). Tests were carried out using the research equipment of the Head Regional Shared Research Facilities of the Moscow State University of Civil Engineering

Author Contributions: Conceptualization, O.V.K.; methodology, O.V.K.; software, O.V.K. and O.A.S.; validation, O.A.S.; formal analysis, O.V.K. and O.A.S.; investigation, O.V.K. and O.A.S.; resources, O.V.K. and O.A.S.; data curation O.A.S.; writing—original draft preparation, O.V.K. and O.A.S.; writing—review and editing, O.V.K.; visualization, O.V.K. and O.A.S.; supervision, O.V.K.; project administration, O.V.K.; funding acquisition, O.V.K. All authors have read and agreed to the published version of the manuscript.

FUNDING

This research is funded from the grant issued by the National Research Moscow State University of Civil Engineering as a result of a competition among the lecturers for implementation of fundamental and applied scientific research (R&D) by the teams of NRU MGSU researchers.

Institutional Review Board Statement: Not applicable.
Informed Consent Statement: Not applicable.
Data Availability Statement: The data presented in this study are available on request from the corresponding author.
Conflicts of Interest: The authors declare no conflict of interest.

REFERENCES

1. **Page, A.W.** The biaxial compressive strength of brick masonry, *Proc. Inst. Civ. Eng.* 1981, *71*, pp. 893–906.
2. **Lourenço, P.B.** Computational strategies for masonry structures, Doctoral Thesis. Delft University, 1996.
3. **López, J.; Oller, S.; Oñate, E.** Cálculo del Comportamiento de la Mampostería Mediante Elementos Finitos. Barcelona, 1998.
4. **Geniev, G.A.** About the criterion of strength of masonry under flat stressed state. *Structural Mechanics and Analysis of Structures* 1979, *2*, pp. 7-11.
5. **Tyupin, G.A.** Deformation theory of plasticity of masonry. *Structural Mechanics and Analysis of Structures* 1980, *6*, pp. 28-30.
6. **Kabantsev, O.V.** Modeling nonlinear deformation and destruction of masonry under biaxial stresses. Part 1. *Applied Mechanics and Materials* 2015, 725-726, pp. 681-696.
7. **Kabantsev, O.V.** Modeling nonlinear deformation and destruction of masonry under biaxial stresses. Part 2. *Applied Mechanics and Materials* 2015, 725-726, pp. 808-819.
8. **Kabantsev, O.V.** Research fundamentals of the structural theory of masonry for the assessment of limit states of masonry structures in earthquake resistant buildings, Post-Doctoral Thesis. Moscow State University of Civil Engineering, Moscow, 2016.
9. **Vildeman, V.E.; Sokolkin, Y.V.; Tashkinov, A.A.** *Mechanics of inelastic deformation and fracture of composite materials,* Nauka: Moscow, Russia, 1997, 228 p.
10. **Kashevarova, G.G.; Zobacheva, A.Yu.; Dubinsky, S.I.** Modeling of the process of destruction of a brick masonry of buildings in full-scale and numerical experiments. *Structural Mechanics and Analysis of Structures* 2011, *1*, pp. 69-73.
11. **Kabantsev, O.V.** Discrete model of masonry under the biaxial stressed state. *Proceedings of TSASU* 2015, *4*, pp. 113-134.
12. **Kabantsev, O.V.; Tamrazyan, A.G.** Modeling of elastic-plastic deformation of a masonry under the biaxial stressed state. *International Journal for Computational Civil and Structural Engineering* 2015, *11*, pp. 87-100.
13. **Polyakov, S.V.; Safargaliev, S.M.** *Seismic stability of buildings with bearing brick walls*, Alma-Ata: 1988, 188 p.
14. **Polyakov, S.V.** *Studies on earthquake resistance of large-panel and stone buildings*, Moscow: 1962, 289 p.
15. **Polyakov, S.V.; Konovodchenko, V.I**. *Strength and deformations of vibrating brick panels at skew. Seismic stability of prefabricated large element buildings*, Moscow: 1963, pp. 131-148.
16. **Likhnenko, E.V.; Zhadanov, V.I.; Arkaev, M.A.; Adigamova, Z.S.** Modern methods of reinforcement of masonry structures with the use of composite materials when performing the capital repair of civil buildings. *Expert: theory and practice* 2021, *6 (15)*, pp. 37-44.
17. **Orlovic, R.; Mantegazza, D.; Naichuk, A.; Derkach, V.** Modern methods of repair and strengthening of stone structures. *Architecture, design and construction* 2010, *1 (44)*, pp. 86-87
18. **Shvedova, V.I.; Tumolskiy, A.P.; Molchanova, A.V.** *Application of Stakhanov's methods to rehabilitation works. General construction works*, Moscow, Leningrad: 1945, 88 p.
19. **Basov, M.A.** *Restoration of buildings destroyed by bombardment*, Moscow, Leningrad: People's Commissariat of the RSFSR, 1943, 88 p.

20. **Kabantsev, O.V.; Tonkikh, G.P.; Koshayev, V.V.** Experimental investigations of the bearing capacity of the masonry with cracks during cement mortar injection using the discharge-pulse technology. *Vestnik MGSU* 2011, *1*, pp. 127-135
21. **Tonkikh, G.P.; Kabantsev, O.V.; Granovsky, A.V.; Simakov, O.A.** Experimental studies of seismic reinforcement of masonry with the system of external reinforcement on the basis of carbon fiber. *Vestnik of TGSU* 2014, *6*, pp. 57-69.
22. **Tonkikh, G.P.; Kabantsev, O.V.; Koshayev, V.V.** Methodology of experimental studies on reinforcement of masonry buildings with reinforced concrete applications. *Earthquake-resistant construction. Safety of constructions* 2005, *6*.
23. **Tonkikh, G.P.; Kabantsev, O.V.; Koshayev, V.V.** Experimental studies of bearing capacity of masonry under main loads. *Earthquake-resistant construction. Safety of constructions* 2007, *6*.
24. **Tonkikh, G.P.; Kabantsev, O.V.; Simakov, O.A.; Simakov, A.B., Baev, S.M.; Panfilov, P.S.** Experimental study of seismic strengthening of masonry exterior concrete applications. *Earthquake-resistant construction. Safety of constructions* 2011, *2*.
25. **Tonkikh, G.H.; Simakov, O.A.; Kabantsev, O.V.; Bayev, S.M.** Experimental studies of masonry aseismic reinforcement using external concrete applications. *Earthquake-resistant construction. Safety of constructions* 2011, *2*.
26. **Kabantsev, O.V.; Simakov, O.A.; Neshchadimov, V.A.; Shtyrlov, D.A.** Strengthening bearing masonry walls of damaged multi-storey buildings. *Industrial and Civil Engineering* 2023, *7*, 29-35.

СПИСОК ЛИТЕРАТУРЫ

1. **Page, A.W.** The biaxial compressive strength of brick masonry, *Proc. Inst. Civ. Eng.* **1981**, *71*, pp. 893–906.
2. **Lourenço, P.B.** Computational strategies for masonry structures, Doctoral Thesis. Delft University, 1996.
3. **López, J.; Oller, S.; Oñate, E.** Cálculo del Comportamiento de la Mampostería Mediante Elementos Finitos. Barcelona, 1998.
4. **Гениев Г.А.** О критерии прочности каменной кладки при плоском напряженном состоянии // Строительная механика и расчет сооружений. 1979. №2. С. 7-11.
5. **Тюпин Г.А.** Деформационная теория пластичности каменной кладки // Строительная механика и расчет сооружений. 1980. №6. С. 28-30.
6. **Kabantsev, O.V.** Modeling nonlinear deformation and destruction of masonry under biaxial stresses. Part 1. *Applied Mechanics and Materials* **2015**, 725-726, pp. 681-696.
7. **Kabantsev, O.V.** Modeling nonlinear deformation and destruction of masonry under biaxial stresses. Part 2. *Applied Mechanics and Materials* **2015**, 725-726, pp. 808-819.
8. **Kabantsev, O.V.** Research fundamentals of the structural theory of masonry for the assessment of limit states of masonry structures in earthquake resistant buildings, Post-Doctoral Thesis. Moscow State University of Civil Engineering, Moscow, 2016.
9. **Вильдеман В.Э. Соколкин Ю.В., Ташкинов А.А.** Механика неупругого деформирования и разрушения композиционных материалов. М. : Наука, 1997. 228 с.
10. **Кашеварова Г.Г., Зобачева А.Ю., Дубинский С.И.** Моделирование процесса разрушения кирпичной кладки зданий в натурных и численных экспериментах // Строительная механика и расчет сооружений. 2011. – №1. – С. 69-73.
11. **Кабанцев О.В.** Дискретная модель каменной кладки в условиях двухосного напряженного состояния // Вестник ТГАСУ. 2015. № 4. С. 113-134.
12. **Кабанцев О.В., Тамразян А.Г.** Моделирование упругопластического деформирования каменной кладки в условиях двухосного наряженного состояния // International Journal for Computational Civil

and Structural Engineering. 2015. Iss. 3. Vol. 11. Pp. 87–100.
13. **Поляков С.В., Сафаргалиев С.М.** Сейсмостойкость зданий с несущими кирпичными стенами. – Алма-Ата: 1988. – 188 с
14. **Поляков С.В.** Исследования по сейсмостойкости крупнопанельных и каменных зданий. - М.: 1962. – 289 с.
15. **Поляков С.В., Коноводченко В.И.** Прочность и деформации виброкирпичных панелей при перекосе. // Сейсмостойкость сборных крупноэлементных зданий. - М.: 1963. - С. 131-148.
16. **Лихненко Е.В, Жаданов В.И., Аркаев М.А., Адигамова З.С.** Современные методы усиления каменных конструкций с применением композитных материалов при выполнении капитального ремонта гражданских зданий // Эксперт: теория и практика. 2021. № 6 (15). С. 37-44. doi:10.51608/26867818_2021_6_37
17. **Орлович Р., Мантегацца Д., Найчук А., Деркач В.** Современные способы ремонта и усиления каменных конструкций // Архитектура, дизайн и строительство. 2010. №1 (44). С. 86-87
18. **Шведова В.И., Тумольский А.П., Молчанова А.В.** Применение стахановских методов на восстановительных работах. Общестроительные работы. Москва, Ленинград, 1945 - 88 с.
19. **Басов М.А.** Восстановление зданий, разрушенных бомбардировкой. Москва ; Ленинград : Наркомзем РСФСР, 1943. - 88 с.
20. **Кабанцев, О.В.** Экспериментальные исследования несущей способности каменной кладки с трещинами при их инъецировании цементным раствором по разрядно-импульсной технологии [Текст] / О.В. Кабанцев, Г.П. Тонких, В.В. Кошаев, В.Я. Еремин, М.В. Тихонов // Научно-технический вестник МГСУ. – 2011. – №2 (т.1) . – С. 127-135
21. **Тонких Г.П., Кабанцев О.В., Грановский А.В., Симаков О.А.** Экспериментальные исследования сейсмоусиления каменной кладки системой внешнего армирования на основе углеволокна/ Вестник ТГАСУ 2014 г. № 6. С. 57-69. EDN: REJYWB
20. **Тонких Г.П., Кабанцев О.В., Кошаев В.В.** Методика экспериментальных исследований по усилению зданий из каменной кладки железобетонными аппликациями. Журнал «Сейсмостойкое строительство. Безопасность сооружений» №6, 2005 г.
22. **Тонких Г.П., Кабанцев О.В., Кошаев В.В.** Методика экспериментальных исследований по усилению зданий из каменной кладки железобетонными аппликациями. Журнал «Сейсмостойкое строительство. Безопасность сооружений» №6, 2005 г.
23. **Тонких Г.П., Кабанцев О.В., Кошаев В.В.** Экспериментальные исследования несущей способности каменной кладки при главных нагрузках. Журнал «Сейсмостойкое строительство. Безопасность сооружений» №6, 2007 г.
24. **Кабанцев О.В., Тонких Г.П., Тонких Г.П., Кабанцев О.В., Симаков О.А., Симаков А.Б., Баев С.М., Панфилов П.С.** Экспериментальные исследования сейсмоусиления каменной кладки наружными бетонными аппликациями. // Сейсмостойкое строительство. Безопасность сооружений. 2011. № 2.
25. **Кабанцев О.В., Тонких Г.П., Симаков О.А., Симаков А.Б., Баев С.М.** Повышение сейсмостойкости каменных конструкций односторонними аппликациями из торкрет-бетона//Аэропорты. Прогрессивные технологии. 2011. №2. С. 26-32.
26. **Кабанцев О.В., Симаков О.А., Нещадимов В.А., Штырлов Д.А.** Усиление несущих стен из каменной кладки поврежденных многоэтажных зданий // Промышленное и гражданское строительство. 2023. № 7. С. 29-35. doi: 10.33622/0869-7019.2023.07.29-35

Kabantsev Oleg — Doctor of Technical Sciences, Associate Professor, Professor of Departments of Reinforced Concrete and Stone Structures, National Research Moscow State University of Civil Engineering (NRU MGSU); 129337, Moscow, Yaroslavskoe Highway, 26; E-mail: ovk531@gmail.com

Simakov Oleg – Candidate of Technical Sciences, Associate Professor Departments of Reinforced Concrete and Stone Structures, National Research Moscow State University of Civil Engineering (NRU MGSU); 129337, Moscow, Yaroslavskoe Highway, 26; E-mail: simakov-ne@mail.ru

Олег Васильевич Кабанцев — доктор технических наук, доцент, профессор кафедры железобетонных и каменных конструкций, Национальный исследовательский Московский государственный строительный университет (НИУ МГСУ); 129337, г. Москва, Ярославское шоссе, д. 26; эл. почта: ovk531@gmail.com

Симаков Олег Александрович - кандидат технических наук, доцент кафедры железобетонных и каменных конструкций, Национальный исследовательский Московский государственный строительный университет (НИУ МГСУ); 129337, г. Москва, Ярославское шоссе, д. 26, эл. почта: simakov-ne@mail.ru;

International Journal for Computational Civil and Structural Engineering, 19(4) 69–82 (2023)

DOI:10.22337/2587-9618-2023-19-4-69-82

COMPUTER MODELING THE STRESS STATE OF OPERATING TANKS USING GEOMETRIC INTERPOLATORS

Evgeniy V. Konopatskiy [1], Oksana A. Shevchuk [2], Andrey A. Bezditnyi [3]

[1] Nizhny Novgorod State University of Architecture and Civil Engineering, Nizhny Novgorod, RUSSIA
[2] Donbas National Academy of Civil Engineering and Architecture, Makeyevka, RUSSIA
[3] Sevastopol branch of «Plekhanov Russian University of Economics», Sevastopol, RUSSIA

Abstract. On the example of modeling the stress state of cylindrical tanks for the storage of petroleum products with geometrical imperfections, a method for the numerical study of thin-walled shells of engineering structures is implemented. It includes the compilation and numerical solution of differential equations array, followed by interpolation of the results and determination of the displacements extreme values (or stresses) that occur in the reservoir from the action of a hydrostatic load, taking into account geometric and structural non-linearity. To implement the proposed method, the geometric theory of multidimensional interpolation and approximation is used, including a new way of processing the initial conditions of the differential equation. It consists in the parallel transfer of the numerical solution to the desired point, the coordinates of which correspond to the initial conditions. As a result, it was possible to achieve a significant increase in the speed of the numerical solution while maintaining an accuracy sufficient for engineering calculations.

Keywords: computer modeling, differential equation, geometric interpolant, parallel transfer, response surface, stress state, operating tank

КОМПЬЮТЕРНОЕ МОДЕЛИРОВАНИЕ НАПРЯЖЕННОГО СОСТОЯНИЯ ЭКСПЛУАТИРУЕМЫХ РЕЗЕРВУАРОВ С ПОМОЩЬЮ ГЕОМЕТРИЧЕСКИХ ИНТЕРПОЛЯНТОВ

Е.В. Конопацкий [1], О.А. Шевчук [2], А.А. Бездитный [3]

[1] Нижегородский государственный архитектурно-строительный университет, г. Нижний Новгород, РОССИЯ
[2] Донбасская национальная академия строительства и архитектуры, г. Макеевка, РОССИЯ
[3] Севастопольский филиал РЭУ им. Г.В. Плеханова, г. Севастополь, РОССИЯ

Аннотация. На примере моделирования напряжённого состояния эксплуатируемых цилиндрических резервуаров для хранения нефтепродуктов с несовершенствами геометрической формы реализован метод численного исследования тонкостенных оболочек инженерных сооружений, который включает составление и численное решение массива дифференциальных уравнений с последующей интерполяцией результатов и определением экстремальных значений перемещений (или напряжений), возникающих в резервуаре от действия гидростатической нагрузки с учётом геометрической и конструктивной нелинейности. Для реализации предложенного метода используется геометрическая теория многомерной интерполяции и аппроксимации, включая новый способ учёта начальных условий дифференциального уравнения. Последний заключается в параллельном переносе численного решения в нужную точку, координаты которой соответствуют начальным условиям. В результате удалось достичь значительного повышения быстродействия численного решения при сохранении достаточной для инженерных расчётов точности.

Ключевые слова: компьютерное моделирование, напряжённое состояние, эксплуатируемый резервуар, дифференциальное уравнение, геометрический интерполянт, поверхность отклика

INTRODUCTION

In engineering practice, steel thin-walled shells of revolution are widely used. Such structures also include steel vertical cylindrical tanks for storing petroleum products. The existing cases of destruction of the above engineering structures have led to the need for periodic

monitoring of their technical condition throughout the entire period of operation.

Among the methods for diagnosing the technical condition of cylindrical tanks, taking into account the imperfections of the geometric shape, the most widespread methods are based on modeling both general and local imperfections of the geometric shape [1-4]. In [5-7], a technique is proposed according to which the interpolation of the tank surface is performed using closed and open contours of the first order of smoothness, followed by the calculation of the stressed state (SS) of the shell in the system of finite element analysis. This approach has a number of advantages and opens up new opportunities for analyzing the technical condition of thin-walled shells of engineering structures, taking into account geometric and structural nonlinearity, and for predicting the impact of the geometric shape imperfections development on the strength and stability of the shell under study. On the other hand, the method proposed in [5-7] contains a number of features. Firstly, the calculation of the SS of a storage tank for petroleum products, containing 65854 finite elements in the form of rectangular plates, in a nonlinear formulation (taking into account geometric and structural nonlinearity) took more than 25 hours on a computer running an Intel Core i5-2400 processor (4-core processor with a maximum clock speed of 3.40 GHz), which is long enough for engineering tasks. Secondly, the complexity of considering constructive nonlinearity, leading to the need to implement a special staged loading scheme proposed in the work [6].

All this leads to the need to improve numerical modeling methods to assess the technical condition of the exploited steel thin-walled shells of engineering structures and develop effective measures to increase their safe operation life.

1. METHODS

In the domestic literature, the model for determining the SS of an elastic cylindrical shell under axisymmetric loading has become widespread [8, 9]. In this case, a differential equation is obtained, which has an exact mathematical solution, taking into account the initial and boundary conditions [9]:

$$D\frac{d^4w}{dx^4}+\frac{Ehw}{r^2\left(1-\alpha\mu\right)}=p,$$

where w is the desired displacements due to hydrostatic load;

x is the height coordinate of the wall, counting from the rim weld of the tank;

r is the radius of a cylindrical tank;

h is the wall thickness of a cylindrical tank;

p is the evenly distributed load;

$E=2.1\cdot10^{11}$ is the Young's modulus for steel;

$\mu=0.3$ is the Poisson's ratio;

α is the parameter, which, in accordance with [8], in a uniaxial stress state is taken equal to 0 (hydrostatic pressure in an open cylindrical vessel), and at internal gas pressure in a closed cylindrical vessel is taken to be 0.5;

$D=\frac{Eh^3}{12\left(1-\mu^2\right)}$ is the cylindrical stiffness.

At the same time, the presence of even minor imperfections in the geometric shape, which are expressed in the form of tank wall deviations from the vertical, lead to the fact that the loading of the shell becomes non-axisymmetric. In addition, the presence of geometric nonlinearity in this case leads to the need to take into account also the constructive nonlinearity that occurs in the process of filling the reservoir with liquid [6]. Therefore, it becomes necessary to refine the original differential equation, taking into account the initial deviations of the surface of the cylindrical shell from the vertical.

We compose the initial equilibrium equation in accordance with Figure 1, which shows an infinitesimal element of a cylindrical tank with all the acting loads and forces in the sections:

$$2N_2\sin\frac{\alpha}{2}+\frac{dQ_1}{dx}-pdxdy=0.$$

In accordance with [8], we take the size of a square element $dx = dy = \alpha r = 1$. For small values of the angle, the value $\sin\frac{\alpha}{2} = \frac{\alpha}{2} = \frac{1}{2r}$. Then the original differential equation takes the following form:

$$\frac{N_2}{r} + \frac{dQ_1}{dx} - p = 0.$$

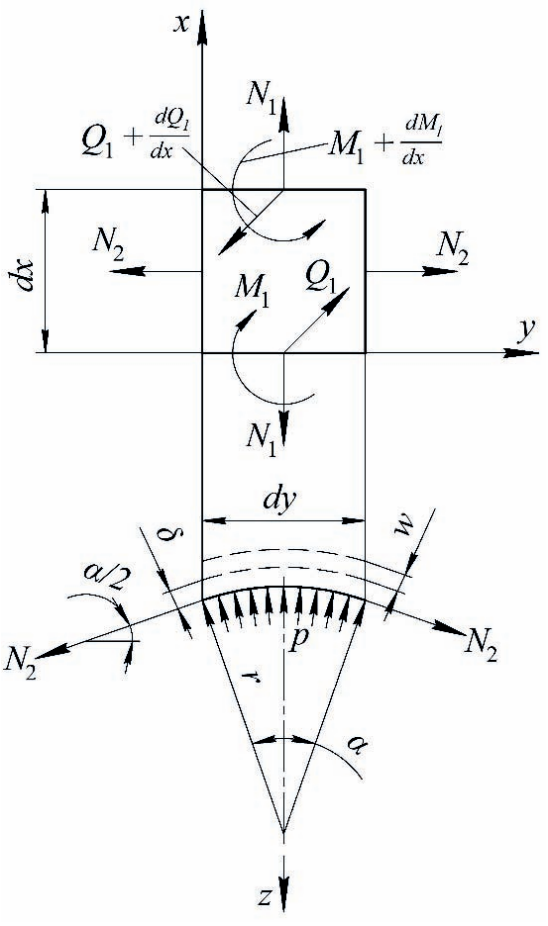


Figure 1. Scheme for compiling a differential equation for the equilibrium of a cylindrical tank with geometric imperfections element

Let us express the force N_2 in terms of the corresponding deformation ε_2. Taking into account the initial deviations from the vertical δ, we obtain:

$$\varepsilon_2 = \frac{\alpha(r + \delta + w) - \alpha r}{\alpha r} = \frac{w + \delta}{r} = \frac{1}{kE}\left(\frac{N_2}{h} - \mu\frac{N_1}{h}\right),$$

where $\delta = \delta(x)$ is the function of initial deviations of a cylindrical tank from the vertical;

k is the correction factor that takes into account the geometric and structural non-linearity [5-7] and the stresses that arise in the upper chord of the shell due to its interaction with the tank roof.

Based on the similarity of right triangles (Fig. 1), we have $N_1 = N_2 \sin\frac{\alpha}{2} = \frac{\alpha}{2}N_2$. Then we get:

$$\varepsilon_2 = \frac{w + \delta}{r} = \frac{N_2}{kEh}\left(1 - \alpha\mu/2\right) \Rightarrow N_2 = \frac{kEh(w + \delta)}{r\left(1 - \alpha\mu/2\right)}.$$

Taking into account that $Q_1 = \frac{dM_1}{dx}$ and, therefore, $\frac{dQ_1}{dx} = \frac{d^2M_1}{dx^2}$, we get:

$$\frac{d^2M_1}{dx^2} + \frac{kEh(w + \delta)}{r^2\left(1 - \alpha\mu/2\right)} = p.$$

The last equation contains two unknowns: M_1 and w. Eliminating one of them, we express the effort in terms of displacements. According to Bernoulli's law, we have:

$$\frac{1}{\rho} = \frac{M_1}{D},$$

where ρ is the radius of curvature when the shell is bent in the meridional direction.

On the other hand, geometrically, the curvature is given by the following expression:

$$K = \frac{1}{\rho} = \frac{d^2w/dx^2}{\left[1+\left(dw/dx\right)^2\right]^{3/2}}.$$

Small displacements cause small curvatures K. Then the quantity $\left(dw/dx\right)^2$ is so small compared to unity that it can be neglected. As a result, we get: $1/\rho \approx d^2w/dx^2$.

Differentiating the twice approximate value of the curvature, we have:

$$\frac{d^2M_1}{dx^2} = D\frac{d^4w}{dx^4}.$$

As a result, we obtain a differential equation with an unknown displacement function $w = w(x)$:

$$D\frac{d^4w}{dx^4} + \frac{kEh(w+\delta)}{r^2\left(1-\alpha\mu/2\right)} = p.$$

Let us define the uniformly distributed hydrostatic load p by the linear relation: $p = -\gamma g(d-x)$, where γ is the density of stored liquid; g is the free fall acceleration (we take 9.81 m/s^2); d is the height of the liquid level in the tank.

Then the final differential equation takes the following form:

$$D\frac{d^4w}{dx^4} + \frac{kEh(w+\delta)}{r^2\left(1-\frac{\alpha\mu}{2}\right)} = \gamma g(x-d). \quad (1)$$

Given that the initial deviations δ and the desired displacements w are functions of the variable x, the mathematically exact solution proposed in [9] gives significant errors (Fig. 2), which leads to the need to solve it numerically.

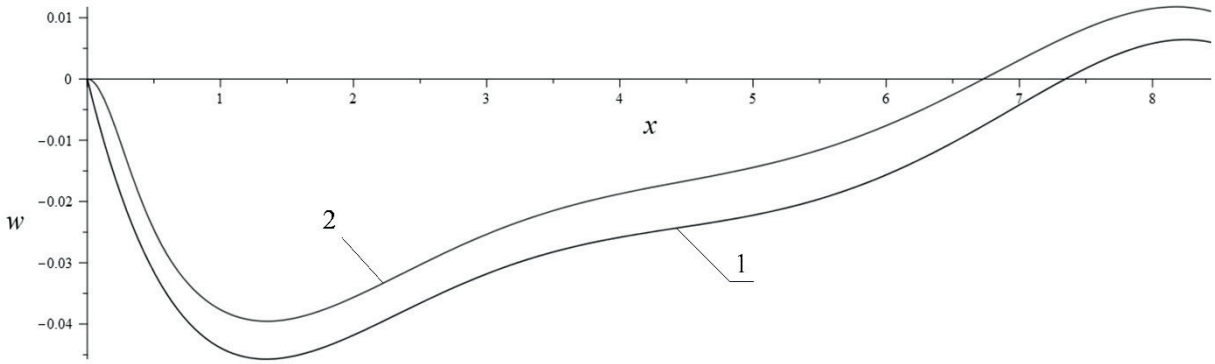


Figure 2. Comparison of the results of solving the differential equation (1): 1 – reference solution; 2 – mathematically exact solution proposed in [9]

The reference solution was obtained by approximating the values of displacements from the action of a hydrostatic load, taking into account the geometric and structural nonlinearity [5-7] when modeling the SS in the SCAD finite element analysis software package. The calculations were carried out in accordance with the strength theory of octahedral shear stresses or the specific energy of deformation (the energy theory of Huber-Henki-Mize).

A method for the numerical solution of differential equations using geometric interpolants was proposed in the works [1010,11]. It can be attributed to the category of superelement methods [12-14] used to solve a wide range of engineering and applied problems. A feature of the method proposed in

[10, 11] is that a geometric interpolant is used as an approximating function - a geometric object passing through predetermined points (interpolation nodes). Thus, a multidimensional geometric interpolant is a superelement that includes information about both geometric and physical parameters of its state. Only in this case, the interpolation nodes are not known in advance. They are calculated from the condition of compliance with the original differential equation. Correspondence of intermediate points to the original differential equation is provided automatically due to interpolation. Thus, the more interpolation nodes, the closer the geometric interpolant is to the desired numerical solution of the differential equation. This approach, by analogy with the isogeometric method [15-18] proposed by Tom Hughes, eliminates the need to coordinate geometric information in the process of interaction between CAD and FEA systems.

In this case, the solution to the differential equation (1) is the displacement function $w = w(x)$, which is a one-parameter set of points – a curved line. We define the displacement function using an algebraic curve passing through predetermined points as a one-parameter geometric interpolant [19, 20]. Based on the conditions for differentiating the displacement function in equation (1), the curve must be at least 5th order.

As a test of the simulation results, each of the reference curves should pass through 7 points. Therefore, a 6th order curve is needed to describe them. Based on these considerations, we take as an approximating function a polynomial of the 6th degree, which describes an algebraic curve of the 6th order. In accordance with the geometric theory of multidimensional interpolation [19], such a curve is determined by the following point equation:

$$M = M_1 p_1 + M_2 p_2 + M_3 p_3 + \\ + M_4 p_4 + M_5 p_5 + M_6 p_6 + M_7 p_7, \quad (2)$$

where M is the current point of the arc of the 6th order algebraic curve;

M_i are the interpolation nodes;

$$p_1 = \bar{t}^6 - 8.7\bar{t}^5 t + 22.7\bar{t}^4 t^2 - 22.7\bar{t}^3 t^3 + \\ + 8.7\bar{t}^2 t^4 - \bar{t}t^5;$$

$$p_2 = 36\bar{t}^5 t - 133.2\bar{t}^4 t^2 + 151.2\bar{t}^3 t^3 - \\ - 61.2\bar{t}^2 t^4 + 7.2\bar{t}t^5;$$

$$p_3 = -45\bar{t}^5 t + 301.5\bar{t}^4 t^2 - 418.5\bar{t}^3 t^3 + \\ + 184.5\bar{t}^2 t^4 - 22.5\bar{t}t^5;$$

$$p_4 = 40\bar{t}^5 t - 308\bar{t}^4 t^2 + 600\bar{t}^3 t^3 - \\ - 308\bar{t}^2 t^4 + 40\bar{t}t^5;$$

$$p_5 = -22.5\bar{t}^5 t + 184.5\bar{t}^4 t^2 - 418.5\bar{t}^3 t^3 + \\ + 301.5\bar{t}^2 t^4 - 45\bar{t}t^5;$$

$$p_6 = 7.2\bar{t}^5 t - 61.2\bar{t}^4 t^2 + 151.2\bar{t}^3 t^3 - \\ - 133.2\bar{t}^2 t^4 + 36\bar{t}t^5;$$

$$p_7 = -\bar{t}^5 t + 8.7\bar{t}^4 t^2 - 22.7\bar{t}^3 t^3 + \\ + 22.7\bar{t}^2 t^4 - 8.7\bar{t}t^5 + t^6;$$

t is the current parameter, which changes from 0 to 1;

$\bar{t} = 1 - t$ is the addition of parameter t to 1.

Next, we need to move from a point equation, which is a symbolic notation, to a system of parametric equations through a coordinate-wise calculation:

$$\begin{cases} x = x_1 p_1 + x_2 p_2 + x_3 p_3 + x_4 p_4 + \\ + x_5 p_5 + x_6 p_6 + x_7 p_7 \\ w = w_1 p_1 + w_2 p_2 + w_3 p_3 + w_4 p_4 + \\ + w_5 p_5 + w_6 p_6 + w_7 p_7 \end{cases}. \quad (3)$$

Taking into account the special properties of algebraic curves passing through predetermined points, obtained on the basis of Bernstein polynomials [19], the first equation of the system takes a linear dependence in the case of a uniform distribution of the interpolation nodes coordinates along the axis Ox: $x = td$. Then, to

determine the geometric interpolant explicitly, it suffices to perform a change of variables in the second equation of the system: $t = \frac{x}{d}$, where d is the height of the liquid level in the tank.

Next, it is necessary to divide the curve into 7 equal parts along the Ox axis and alternately substitute the obtained values x_j into the original differential equation (1), where j varies from 0 to 7. Thus, a system of linear algebraic equations (SLAE) with 7 unknowns is formed w_j. After solving the, the obtained values w_j must be substituted into the second equation of the system (3), which is the numerical solution of the differential equation (1) in the range of the variable from 0 to d.

A separate issue is the use of initial and boundary conditions to refine the numerical solution of differential equation (1). Traditionally, these conditions are used to determine the constants of integration [9]. But in this case, this is precisely the source of errors in the solution (Fig. 2). In the proposed method, a numerical solution is obtained, which corresponds to the initial differential equation (1) at the nodal points of interpolation. It should be noted that this solution does not take into account the initial conditions and therefore the resulting curve is arbitrarily in the plane xOy. To satisfy the initial condition $w(0) = 0$, it is necessary to transfer the resulting curved line to the origin of coordinates. For this, it is necessary to subtract the free term of the approximating polynomial function from the obtained solution $w = w(x)$.

2. RESULTS AND DISCUSSION

As an example, consider a vertical cylindrical steel tank No. 1 for storing gasoline with a volume of 1000 m^3 of the integrated collection point «Beshensky».

The initial data for modeling are the geometric dimensions of the tank (tank radius $r = 6.165$ m; shell thickness $h = 0.005$ m), the height of the liquid level in the tank ($d = 8.44$ m), the physical properties of the stored liquid (usually tanks are tested with water, so we take the water density $\gamma = 1000$ kg/m^3) and the initial deviations of the tank wall from the vertical δ.

To determine the functions of the initial deviations of a cylindrical tank from the vertical at reference points along the circumference of the tank $\delta_i = \delta_i(x)$, where $i = 0,\ 30,\ 60,\ ...,\ 330$, the approximation tool Fit from the Statistics package of the Maple computer algebra system was used.

The initial data entry was organized using the MS Excel software package. Thus, 12 equations were obtained that characterize the functions of the initial deviations of the cylindrical tank from the vertical at 12 reference points along the circumference of the tank. As an example, we give one of the equations (at the point 0°), taking into account the rounding of polynomial coefficients:

$$\delta_0 = 4.188 \cdot 10^{-6} x^6 - 0.00017 x^5 + \\ +0.0025 x^4 - 0.018 x^3 + 0.061 x^2 - 0.089 x.$$

Considering that in the process of approximation the amount of initial data corresponded to the degree of the polynomial, the coefficients of determination for all 12 lines were obtained $R^2 = 1$. That is, in fact, using the Fit function, the initial deviations were interpolated δ.

Similarly, 12 equations were obtained that characterize the functions of displacements of a cylindrical tank from the vertical at 12 reference points along the circumference of the tank, which were then used as reference curves to verify the simulation results. As an example, we give the reference equation at the point 0°, taking into account the rounding of polynomial coefficients:

$$\omega_0 = 3.71 \cdot 10^{-6} x^6 - 0.00016 x^5 + \\ +0.0024 x^4 - 0.017 x^3 + 0.06 x^2 - 0.089 x.$$

As a result of computational experiments, taking into account the initial data, 12 equations were obtained that characterize the functions of displacements of a cylindrical reservoir from the vertical at 12 reference points along the circumference of the reservoir. For comparison, we present the numerical solution of the differential equation (1) at the point 0°, taking into account the rounding of polynomial coefficients:

$$w_0 = 4.19 \cdot 10^{-6} x^6 - 0.00017 x^5 + 0.0025 x^4 - \\ -0.018 x^3 + 0.061 x^2 - 0.09 x - 0.007.$$

Comparison of graphical interpretations of the obtained numerical solution with the reference one (Fig. 3) shows that the curves are very similar, but are at some distance from each other. Based on this, we can conclude that the solution was obtained correctly, but is in the wrong place. To agree on them, it is necessary to fulfill the initial conditions. In our case, this condition is – $w(0) = 0$, which says that it is necessary to perform a parallel transfer of the resulting curve to the origin. To do this, it suffices to subtract the free term from the obtained numerical solution.

As an example, we present the numerical solution of the differential equation (1) at the point 0° after applying the initial condition $w(0) = 0$:

$$w_0 = 4.19 \cdot 10^{-6} x^6 - 0.00017 x^5 + \\ +0.0025 x^4 - 0.018 x^3 + 0.061 x^2 - 0.09 x. \quad (4)$$

As can be seen when comparing the equations w_0 and ω_0, almost all polynomial coefficients in pairs have very close values. Graphical visualization of the comparison results also shows a high level of similarity of algebraic curves (Fig. 4).

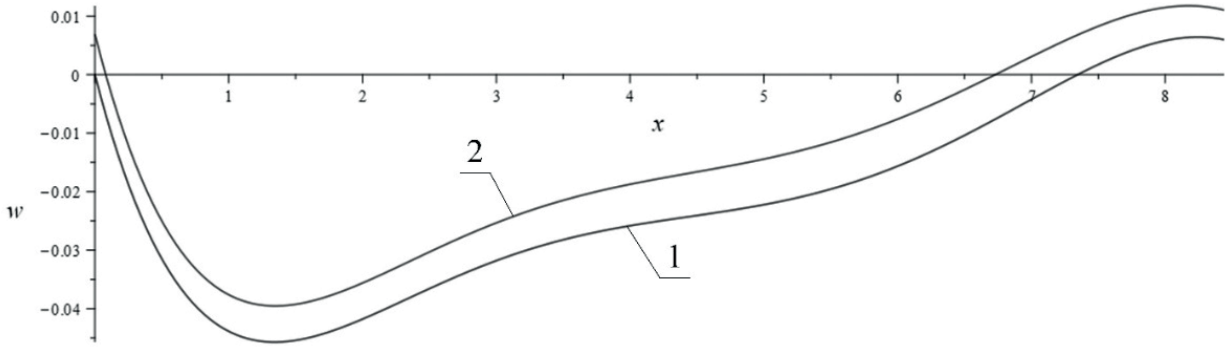


Figure 3. Comparison of the results of solving the differential equation (1): 1 – reference solution; 2 – numerical solution

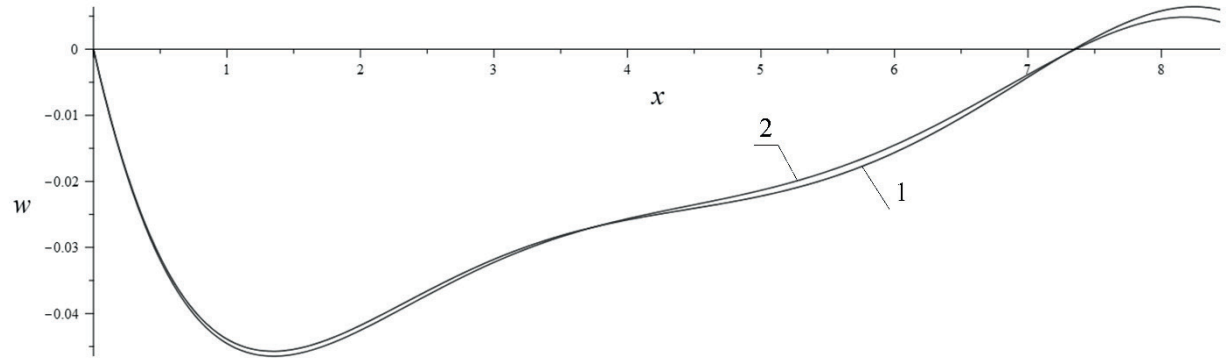


Figure 4. Comparison of the results of solving the differential equation (1) after applying the initial condition $w(0) = 0$: reference solution; 2 – numerical solution

To numerically determine the degree of similarity of the reference and numerical solutions, we use the method of comparing multidimensional geometric objects using the determination coefficient R^2, proposed in the work [5]. We discretize the curves with subsequent comparison of two-point sets using the coefficient of determination. As a result, when comparing algebraic curves, the coefficient of determination was achieved $R^2 = 0.998$. A similar comparison was made for all 12 lines around the circumference of the tank and high values of the coefficient of determination were obtained, confirming the reliability of the results.

In the process of examining the technical condition of steel cylindrical tanks, an important task is to determine the places of maximum displacements and, accordingly, maximum stresses in the tank wall. To solve this problem, one can use the methods of two-dimensional interpolation with the subsequent determination of the extreme points of the response surface. Given the distortion of the geometric shape of the actual surface of a cylindrical tank, it is convenient to build a response surface by presenting the tank in an unfolded form. Only along the abscissa axis we will plot not the length of the arc, which will constantly change due to distortions of the cylindrical surface, but the angle φ, which also determines the position of each point on the tank surface. On the y-axis we will plot the height of the tank d, on the applicate axis - the required displacements of the tank wall w.

The guide lines of the required response surface are defined as functions of the displacements $w_i = w_i(x)$, where $i = 0°, 30°, 60°, ..., 360°$, which are obtained as a result of the numerical solution of the differential equation (1). An example of such a function is equation (4) at the point 0°. For convenience, let's move from the variable x to the parameter v, which changes from 0 to 1. This transition is provided by the change of variables: $x = v \cdot d$. For example, for displacements at the point 0°, taking into account the rounding of polynomial coefficients, we get:

$$w_0 = 1.514v^6 - 7.314v^5 + 12.847v^4 - \\ -10.628v^3 + 4.347v^2 - 0.762v.$$

In this case, 12 such equations were found in a similar way along the circumference of the tank. Since the reservoir with imperfections is a closed shell, the last displacement function corresponds to the first one. $w_0 = w_{360}$. At the same time, the required number of guide lines can be increased to achieve the required calculation accuracy.

Taking into account a large number of guide lines, in order to avoid unplanned oscillations, we will interpolate them using one-dimensional open contours of the 1st order of smoothness. Their geometric construction algorithms are presented in [5]. Based on this, we obtain the following computational algorithm for constructing the generatrix of the response surface:

1. Determine the coordinates of the initial points A_j along the x-axis:

$$\varphi_{A_{j+1}} = 360 \, {}^{j}\!/_{n}, \quad j = 0,1,...,n,$$

where n is the number of response surface guide lines.

2. Determine the length of the segment $A_j A_{j+1}$:

$$\left|A_j A_{j+1}\right| = \sqrt{\left(\varphi_{A_j} - \varphi_{A_{j+1}}\right)^2 + \left(w_{A_j} - w_{A_{j+1}}\right)^2}, \\ j = 1,2,...,n-1,$$

where w_{A_j} is the response surface guide line equations;

$\left|A_{j+1} A_{j+2}\right|$ determined from the same point by a shift by one.

3. Determine the length of the segment $A_j A_{j+2}$:

$$\left|A_j A_{j+2}\right| = \sqrt{\left(\varphi_{A_j} - \varphi_{A_{j+2}}\right)^2 + \left(w_{A_j} - w_{A_{j+2}}\right)^2},$$

where $j = 1, 2, ..., n-2$

4. Determine the coordinates of the points B_{j+1}, C_{j+1}, forming tangents at the points of the curve arc tracing:

$$\begin{cases} \varphi_{B_j} = \left(\varphi_{A_{j+2}} - \varphi_{A_j}\right)\dfrac{\left|A_{j+1}A_{j+2}\right|}{\pi\left|A_jA_{j+2}\right|} + \varphi_{A_{j+1}} \\ w_{B_j} = \left(w_{A_{j+2}} - w_{A_j}\right)\dfrac{\left|A_{j+1}A_{j+2}\right|}{\pi\left|A_jA_{j+2}\right|} + w_{A_{j+1}} \end{cases},$$

$$\begin{cases} \varphi_{C_j} = \left(\varphi_{A_j} - \varphi_{A_{j+2}}\right)\dfrac{\left|A_jA_{j+1}\right|}{\pi\left|A_jA_{j+2}\right|} + \varphi_{A_{j+1}} \\ w_{C_j} = \left(w_{A_j} - w_{A_{j+2}}\right)\dfrac{\left|A_jA_{j+1}\right|}{\pi\left|A_jA_{j+2}\right|} + w_{A_{j+1}} \end{cases},$$

where $j = 1, 2, ..., n-1$.

5. Define the curve contour arcs for the first and last sections:

$$\begin{cases} \varphi_1 = \varphi_{A_1}\overline{u}^2 + 2\varphi_{C_1}u\overline{u} + \varphi_{A_2}u^2 \\ d_1 = d \cdot v \\ w_1 = w_{A_1}\overline{u}^2 + 2w_{C_1}u\overline{u} + w_{A_2}u^2 \end{cases},$$

$$\begin{cases} \varphi_n = \varphi_{A_n}\overline{u}^2 + 2\varphi_{B_{n-1}}u\overline{u} + \varphi_{A_{n+1}}u^2 \\ d_n = d \cdot v \\ w_n = w_{A_n}\overline{u}^2 + 2w_{B_{n-1}}u\overline{u} + w_{A_{n+1}}u^2 \end{cases},$$

where $\overline{u} = 1 - u$ is the addition of parameter u to 1.

6. Define the curve contour arcs for intermediate sections:

$$\begin{cases} \varphi_j = \varphi_{A_j}\overline{u}^3 + 3\varphi_{B_{j-1}}\overline{u}^2u + 3\varphi_{C_j}\overline{u}u^2 + \varphi_{A_{j+1}}u^3 \\ d_j = d \cdot v \\ w_j = w_{A_j}\overline{u}^3 + 3w_{B_{j-1}}\overline{u}^2u + 3w_{C_j}\overline{u}u^2 + w_{A_{j+1}}u^3 \end{cases},$$

where $j = 2, 3, ..., n-1$.

As a result of the execution of the above computational algorithm, we obtain a response surface that characterizes displacements in the wall of a steel cylindrical tank with imperfections (Fig. 5).

As can be seen from Figure 5, the maximum displacements occur in the lower part of the tank in the range from 150° to 300° around the circumference of the tank. Let us determine the values of the maximum displacements and their exact position by the methods of mathematical analysis. To do this, it is necessary to solve a system of two equations with partial derivatives with respect to the parameters u and v, on the interval of their change from 0 to 1. Thus, the maximum displacements of 92.2 mm occur at a height of 2.298 m and 258.6° around the circumference of the tank.

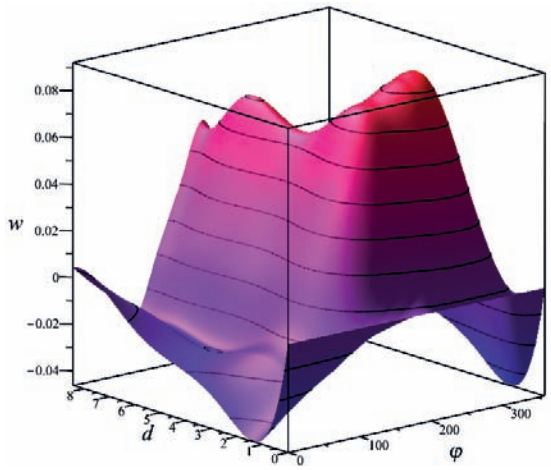


Figure 5. Visualization of the response surface of the tank wall movements with imperfections from the hydraulic load

It is also possible to determine the maximum displacements of the tank wall from the action of hydrostatic load for each belt along its height. To do this, it suffices to cut the resulting response surface with vertical planes parallel to the axis φ. Analytically, this is determined by step-by-step fixing the height values of each tank belt with the determination of the maximum displacements at each stage.

The paper proposes a method for determining the SS of an oil storage tank with imperfections

based on displacements. If necessary, it is quite easy to switch to stresses. In accordance with [22], for this it is sufficient to multiply the resulting displacements by the quotient from dividing the Young's modulus by the tank radius. But since the radius varies along the height of the tank due to imperfections in the geometric shape, when moving from displacements to stresses, it is necessary to take into account the functions of the initial deviations $\delta_j = \delta_j(x)$. Thus, Young's modulus must be divided by $r + \delta_j$.

CONCLUSIONS

Improvement of the differential equation and numerical solution, including a new way of taking into account the initial conditions, which are described in the paper, are not the only possible ones. In a similar way, other designs of thin-walled shells of engineering structures can be studied, taking into account the imperfections of the geometric shape or without them, except for vertical cylindrical tanks. It is also possible to model other types of loads (for example, wind load, snow load, structural self-weight load, etc.) using interpolation and approximation methods. This makes it possible to avoid the need for expensive full-scale experiments, which in some cases are not only not profitable, but even impossible.

A feature of the proposed method is that the model is quite simply described by a 4th order differential equation using interpolation and approximation methods. This equation has a simple numerical solution in the form of a 6th degree polynomial. At the same time, there is no need to perform long and complex calculations for modeling thin-walled shells, taking into account both geometric and structural non-linearity.

Due to the use of interpolation and approximation methods for solving the problem, it was possible to achieve sufficient numerical simulation accuracy for engineering calculations, increasing their speed. The calculation of an array consisting of 12 numerical solutions of differential equations that define 12 guide lines of the response surface (as well as the construction of its generatrix using one-dimensional contours of the first order of smoothness, taking into account visualization) takes about 20 seconds even without parallelization of computational threads. If necessary, the number of guide lines of the response surface can be significantly increased to achieve greater accuracy of engineering calculations. At the same time, the proposed method is easily amenable to parallelization of computational operations. This became possible due to the fact that it combines the potential of constructive methods of geometric modeling, which are able to provide parallelization of geometric constructions by tasks (message passing), and the mathematical apparatus "Point calculus", capable of implementing parallelization according to data due to coordinate-wise calculation (data parallel). In the future, this makes it possible to realize the entire available computing potential of modern multi-core processors.

Based on the results of the research, a new engineering technique for examining the technical condition of an oil storage tank with geometric imperfections is proposed based on the numerical solution of differential equations using geometric interpolants [23].

REFERENCE

1. **Aleshina O.O., Ivanov V.N., Cajamarca-Zuniga D.** Stress state analysis of an equal slope shell under uniformly distributed tangential load by different methods // Structural Mechanics of Engineering Constructions and Buildings. 2021. Vol. 17. No. 1. pp. 51-62. DOI: 10.22363/1815-5235-2021-17-1-51-62.
2. **Maraveas C., Balokas G.A., Tsavdaridis K.D.** Numerical evaluation on shell buckling of empty thin-walled steel tanks

under wind load according to current american and european design codes // Thin-Walled Structures. 2015. Vol. 95. pp.152-160. DOI: 10.1016/j.tws.2015.07.007.
3. Behaviour of vertical cylindrical tank with local wall imperfections / A. Šapalas, G. Šaučiuvėnas, K. Rasiulis [et al.] // Journal of Civil Engineering and Management. 2019. 25(3). pp. 287-296. DOI: 10.3846/jcem.2019.9629.
4. **Gorban N.N., Vasiliev G.G., Salnikov A.P.** Accounting actual geometric shape of the tank shell when evaluating its fatigue life // Oil Industry. 2018. No. 8. pp. 75-79. DOI: 10.24887/0028-2448-2018-8-75-79.
5. **Krysko A.A.** Geometricheskoe i komp'yuternoe modelirovanie ekspluatiruemyh konstrukcij tonkostennyh obolochek inzhenernyh sooruzhenij s uchyotom nesovershenstv geometricheskoj formy [Geometric and computer modeling of operating structures of thin-walled shells of engineering structures with regard to geometric form imperfections] // Makeyevka: DONNACEA, 2016. 191 p. (In Russian).
6. **Krysko A.A.** Analiz napryazhenno-deformirovannogo sostoyaniya stenki rezervuara s geometricheskimi nesovershenstvami pri dejstvii gidrostaticheskoj nagruzki [Calculation of the intense deformed state of tank'swall under the action of the hydrostatic load in anonlinear setting with geometric imperfections] // Metallicheskie konstrukcii. 2017. Vol. 23. No. 3. pp. 97-106. (In Russian).
7. **Krysko A.A.** Chislennye issledovaniya mestnyh nesovershenstv geometricheskoj formy vertikal'nogo cilindricheskogo [Numerical studies of local defects in the geometric shape of a vertical cylindrical tank] // Stroitel' Donbassa. 2020. No. 1(10). pp. 13-17. (In Russian).
8. **Lessig E.N., Lileev A.F., Sokolov A.G.** Listovye metallicheskie konstrukcii [Sheet metal structures] // Moscow: Strojizdat, 1970. 488 p. (In Russian).
9. **Timoshenko S.P., Vojnovskij-Kriger S.** Plastinki i obolochki [Plates and shells] // Moscow: Nauka, 1966. 636 p. (In Russian).
10. **Konopatskiy E.V., Voronova O.S., Shevchuk O.A., Bezditnyi A.A.** About one method of numeral decision of differential equalizations in partials using geometric interpolants // CEUR Workshop Proceedings. 2020. Vol. 2763. pp. 213-219. DOI: 10.30987/conferencearticle_5fce27708eb353.92843700.
11. **Konopatskiy E.V., Bezditnyi A.A., Shevchuk O.A.** Modeling geometric varieties with given differential characteristics and its application // CEUR Workshop Proceedings. 2020. Vol. 2744. DOI: 10.51130/graphicon-2020-2-4-31.
12. **Shamloofard M., Hosseinzadeh A., Movahhedy M.R.** Development of a shell superelement for large deformation and free vibration analysis of composite spherical shells // Engineering with Computers. 2021. Vol. 37. No. 4. pp. 3551-3567. DOI: 10.1007/s00366-020-01015-w.
13. **Hughes P.J., Kuether R.J.** Nonlinear interface reduction for time-domain analysis of Hurty/Craig-Bampton superelements with frictional contact // Journal of Sound and Vibration. 2021. Vol. 507. DOI: 10.1016/j.jsv.2021.116154.
14. **Nielsen M.B., Sahin E.** A simple procedure for embedding seismic loads in foundation superelements for combined wind, wave and seismic analysis of offshore wind turbine structures // Paper presented at the COMPDYN Proceedings. 2019. Vol. 3. pp. 4628-4640. DOI: 10.7712/120119.7255.19324.
15. Isogeometric analysis of large-deformation thin shells using RHT-splines for multiple-patch coupling / N. Nguyen-Thanh, K. Zhou, X. Zhuang [et al.] // Computer Methods in Applied Mechanics and

Engineering. 2017. Vol. 316. pp. 1157-1178. DOI: 10.1016/j.cma.2016.12.002.
16. A NURBS-based inverse analysis for reconstruction of nonlinear deformations of thin shell structures / N. Vu-Bac, T.X. Duong, T. Lahmer [et al.] // Computer Methods in Applied Mechanics and Engineering. 2018. Vol. 331. pp. 427-455. DOI: 10.1016/j.cma.2017.09.034.
17. **Leonetti L., Liguori F., Magisano D., Garcea G.** An efficient isogeometric solid-shell formulation for geometrically nonlinear analysis of elastic shells // Computer Methods in Applied Mechanics and Engineering. 2018. Vol. 331. pp. 159-183. DOI: 10.1016/j.cma.2017.11.025.
18. **Li W., Nguyen-Thanh N., Zhou K.** Geometrically nonlinear analysis of thin-shell structures based on an isogeometric-meshfree coupling approach // Computer Methods in Applied Mechanics and Engineering. 2018. Vol. 336. pp. 111-134. DOI: 10.1016/j.cma.2018.02.018.
19. **Konopatskiy E.V., Bezditnyi A.A.** Geometric modeling of multifactor processes and phenomena by the multidimensional parabolic interpolation method // Journal of Physics: Conf. Series 1441 (2020) 012063. DOI: 10.1088/1742-6596/1441/1/012063.
20. **Konopatskiy E.V., Bezditnyi A.A.** Application of mixed geometric interpolants for modeling the strength characteristics of steel fiber concrete // Journal of Physics: Conf. Series 1546 (2020) 012037. DOI: 10.1088/1742-6596/1546/1/012037.
21. An approach to comparing multidimensional geometric objects / I.V. Seleznev, E.V. Konopatskiy, O.S. Voronova [et al.] // Proc. of the 31st Int. Conf. on Computer Graphics and Vision (GraphiCon 2021), Nizhny Novgorod, September 27-30, 2021. Vol. 3027. pp. 682-688. DOI: 10.20948/graphicon-2021-3027-682-688.
22. **Chepur P.V.** Napryazhenno-deformirovannoe sostoyanie rezervuara pri razvitii neravnomernyh osadok ego osnovaniya [Stress-strain state of the tank during the development of non-uniform settlements of its base] // Moscow: RGU nefti i gaza (NIU) imeni I.M. Gubkina, 2015. 181 p. (In Russian).
23. **Konopatskiy E.V., Shevchuk O.A., Krysko A.A.** Modeling of the Stress-Strain State of Steel Tank with Geometric Imperfections // Construction of Unique Buildings and Structures. 2022. No. 2(100). P. 10001. DOI: 10.4123/CUBS.100.1. (In Russian).

СПИСОК ЛИТЕРАТУРЫ

1. **Aleshina O.O., Ivanov V.N., Cajamarca-Zuniga D.** Stress state analysis of an equal slope shell under uniformly distributed tangential load by different methods // Structural Mechanics of Engineering Constructions and Buildings. 2021. Vol. 17. No. 1. pp. 51-62. DOI: 10.22363/1815-5235-2021-17-1-51-62.
2. **Maraveas C., Balokas G.A., Tsavdaridis K.D.** Numerical evaluation on shell buckling of empty thin-walled steel tanks under wind load according to current american and european design codes // Thin-Walled Structures. 2015. Vol. 95. pp.152-160. DOI: 10.1016/j.tws.2015.07.007.
3. Behaviour of vertical cylindrical tank with local wall imperfections / A. Šapalas, G. Šaučiuvėnas, K. Rasiulis [et al.] // Journal of Civil Engineering and Management. 2019. 25(3). pp. 287-296. DOI: 10.3846/jcem.2019.9629.
4. **Gorban N.N., Vasiliev G.G., Salnikov A.P.** Accounting actual geometric shape of the tank shell when evaluating its fatigue life // Oil Industry. 2018. No. 8. pp. 75-79. DOI: 10.24887/0028-2448-2018-8-75-79.

5. **Крысько А.А.** Геометрическое и компьютерное моделирование эксплуатируемых конструкций тонкостенных оболочек инженерных сооружений с учётом несовершенств геометрической формы. – Макеевка: ДОННАСА, 2016. – 191 с.
6. **Крысько А.А.** Анализ напряженно-деформированного состояния стенки резервуара с геометрическими несовершенствами при действии гидростатической нагрузки // Металлические конструкции, 2017. – Т. 23. – № 3. – С. 97-106.
7. **Крысько А.А.** Численные исследования местных несовершенств геометрической формы вертикального цилиндрического // Строитель Донбасса, 2020. – № 1(10). – С. 13-17.
8. **Лессиг Е.Н., Лилеев А.Ф., Соколов А.Г.** Листовые металлические конструкции. – М.: Стройиздат, 1970. – 488 с.
9. **Тимошенко С.П., Войновский-Кригер С.** Пластинки и оболочки. – М.: Наука, 1966. – 636 с.
10. **Konopatskiy E.V., Voronova O.S., Shevchuk O.A., Bezditnyi A.A.** About one method of numeral decision of differential equalizations in partials using geometric interpolants // CEUR Workshop Proceedings. 2020. Vol. 2763. pp. 213-219. DOI: 10.30987/conferencearticle_5fce27708eb353.92843700.
11. **Konopatskiy E.V., Bezditnyi A.A., Shevchuk O.A.** Modeling geometric varieties with given differential characteristics and its application // CEUR Workshop Proceedings. 2020. Vol. 2744. DOI: 10.51130/graphicon-2020-2-4-31.
12. **Shamloofard M., Hosseinzadeh A., Movahhedy M.R.** Development of a shell superelement for large deformation and free vibration analysis of composite spherical shells // Engineering with Computers. 2021. Vol. 37. No. 4. pp. 3551-3567. DOI: 10.1007/s00366-020-01015-w.
13. **Hughes P.J., Kuether R.J.** Nonlinear interface reduction for time-domain analysis of Hurty/Craig-Bampton superelements with frictional contact // Journal of Sound and Vibration. 2021. Vol. 507. DOI: 10.1016/j.jsv.2021.116154.
14. **Nielsen M.B., Sahin E.** A simple procedure for embedding seismic loads in foundation superelements for combined wind, wave and seismic analysis of offshore wind turbine structures // Paper presented at the COMPDYN Proceedings. 2019. Vol. 3. pp. 4628-4640. DOI: 10.7712/120119.7255.19324.
15. Isogeometric analysis of large-deformation thin shells using RHT-splines for multiple-patch coupling / N. Nguyen-Thanh, K. Zhou, X. Zhuang [et al.] // Computer Methods in Applied Mechanics and Engineering. 2017. Vol. 316. pp. 1157-1178. DOI: 10.1016/j.cma.2016.12.002.
16. A NURBS-based inverse analysis for reconstruction of nonlinear deformations of thin shell structures / N. Vu-Bac, T.X. Duong, T. Lahmer [et al.] // Computer Methods in Applied Mechanics and Engineering. 2018. Vol. 331. pp. 427-455. DOI: 10.1016/j.cma.2017.09.034.
17. **Leonetti L., Liguori F., Magisano D., Garcea G.** An efficient isogeometric solid-shell formulation for geometrically nonlinear analysis of elastic shells // Computer Methods in Applied Mechanics and Engineering. 2018. Vol. 331. pp. 159-183. DOI: 10.1016/j.cma.2017.11.025.
18. **Li W., Nguyen-Thanh N., Zhou K.** Geometrically nonlinear analysis of thin-shell structures based on an isogeometric-meshfree coupling approach // Computer Methods in Applied Mechanics and Engineering. 2018. Vol. 336. pp. 111-134. DOI: 10.1016/j.cma.2018.02.018.
19. **Konopatskiy E.V., Bezditnyi A.A.** Geometric modeling of multifactor processes and phenomena by the

multidimensional parabolic interpolation method // Journal of Physics: Conf. Series 1441 (2020) 012063. DOI: 10.1088/1742-6596/1441/1/012063.

20. **Konopatskiy E.V., Bezditnyi A.A.** Application of mixed geometric interpolants for modeling the strength characteristics of steel fiber concrete // Journal of Physics: Conf. Series 1546 (2020) 012037. DOI: 10.1088/1742-6596/1546/1/012037.
21. An approach to comparing multidimensional geometric objects / I.V. Seleznev, E.V. Konopatskiy, O.S. Voronova [et al.] // Proc. of the 31st Int. Conf. on Computer Graphics and Vision (GraphiCon 2021), Nizhny Novgorod, September 27-30, 2021. Vol. 3027. pp. 682-688. DOI: 10.20948/graphicon-2021-3027-682-688.
22. **Чепур П.В.** Напряженно-деформированное состояние резервуара при развитии неравномерных осадок его основания. – М.: РГУ нефти и газа (НИУ) имени И.М. Губкина, 2015. – 181 с.
23. **Konopatskiy E.V., Shevchuk O.A., Krysko A.A.** Modeling of the Stress-Strain State of Steel Tank with Geometric Imperfections // Construction of Unique Buildings and Structures, 2022. – No. 2(100). – P. 10001. – DOI: 10.4123/CUBS.100.1.

Evgeniy Viktorovich Konopatskiy – Doctor of Engineering, Docent, Head of the Department of Engineering Graphics and Information Modelling, Federal State Budgetary Educational Institution of Higher Education "Nizhny Novgorod State University of Architecture and Civil Engineering" (NNSAGU), 603000, Nizhny Novgorod, Ilyinskaya str., 65, e-mail: e.v.konopatskiy@mail.ru, +7(831)434-02-91.

Oksana Aleksandrovna Shevchuk – Senior Lecturer, Department of Specialized Information Technologies and Systems, Federal State Budget Educational Institution of Higher Education «Donbas National Academy of Civil Engineering and Architecture» (DONNACEA), 286123, Makeyevka, Derzhavina str., 2, e-mail: o.a.shevchuk@donnasa.ru, +7(856)343-70-33.

Andrey Aleksandrovich Bezditnyi – Candidate of Engineering, Docent of the Department of Economics, Finance and Accounting, Sevastopol branch of «Plekhanov Russian University of Economics» (Sevastopol branch of PRUE), 299053, Sevastopol, Vakulenchuka str., 29, e-mail: bezdytniy@gmail.com, +7(8692)59-00-72.

Евгений Викторович Конопацкий – д-р техн. наук, доцент, заведующий кафедрой инженерной графики и информационного моделирования, Федеральное государственное бюджетное образовательное учреждение высшего образования «Нижегородский государственный архитектурно-строительный университет» (ННГАСУ), 603000, г. Нижний Новгород, ул. Ильинская, д. 65, e-mail: e.v.konopatskiy@mail.ru, +7(831)434-02-91.

Оксана Александровна Шевчук – старший преподаватель кафедры специализированных информационных технологий и систем, Федеральное государственное бюджетное образовательное учреждение высшего образования «Донбасская национальная академия строительства и архитектуры» (ФГБОУ ВО «ДОННАСА»), 286123, г. Макеевка, ул. Державина, д. 2, e-mail: o.a.shevchuk@donnasa.ru, +7(856)343-70-33.

Андрей Александрович Бездитный – канд. техн. наук, доцент кафедры экономики, финансов и учёта, Севастопольский филиал федерального государственного бюджетного образовательного учреждения высшего образования «Российский экономический университет имени Г.В. Плеханова» (Севастопольский филиал РЭУ им. Г.В. Плеханова), 299053, г. Севастополь, ул. Вакуленчука, д. 29, e-mail: bezdytniy@gmail.com, +7(8692)59-00-72.

International Journal for Computational Civil and Structural Engineering, 19(4) 83–94 (2023)

DOI:10.22337/2587-9618-2023-19-4-83-94

ANALYTICAL ANALYSIS OF COMBINED FOUNDATION PLATES, SUBJECTED TO AN ACTION OF ANTISYMMETRIC LOADS

Elena B. Koreneva [1], Valery R. Grosman [2]

[1] Moscow Higher Combined-Arms Command Academy, Moscow, RUSSIA

[2] Academy of Water Transport, the branch of Russian University of Transport (MIIT), Moscow, RUSSIA

Abstract: The combined foundation plates, having circular form and consisting of several parts which have different laws of thickness variation, are under study. The constructions under examination are subjected to an action of antisymmetric load distributed along circumferences according to the laws $cos\theta$ or $sin\theta$. Similar problems occur in the cases of seismic and wind loads. The interaction with elastic foundation is taking into account. The conditions of the construction's different parts conjugation are fulfilled. In this work for solution of such problems the analytical approach is used for the first time. The method of compensating loads (MCL) is applied. The solutions are obtained in closed form in terms of Bessel functions. As an example the foundation plate, consisting of two parts, is considered in detail. The inner part of the slab under study has the variable thickness, the outer one has the constant thickness.

Keywords: combined plates, antisymmetric loads, Bessel functions

АНАЛИТИЧЕСКИЙ РАСЧЕТ КОМБИНИРОВАННЫХ ФУНДАМЕНТНЫХ ПЛИТ ПРИ ДЕЙСТВИИ НА НИХ АНТИСИММЕТРИЧНЫХ НАГРУЗОК

Е.Б. Коренева [1], В.Р. Гросман [2]

[1] Московское высшее общевойсковое орденов Жукова, Ленина и Октябрьской Революции Краснознаменное училище, г. Москва, РОССИЯ

[2] Академия водного транспорта, филиал Российского университета транспорта (МИИТ), г. Москва, РОССИЯ

Аннотация: Рассматриваются комбинированные фундаментные плиты, представляющие собой конструкции, имеющие в плане круговую форму и состоящие из нескольких участков с различными законами изменения толщины. Изучается действие на подобные конструкции антисимметричных нагрузок, распределенных по окружностям по законам $cos\theta$ или $sin\theta$. Подобные задачи возникают при расчетах на действие ветровых и сейсмических нагрузок. Учитывается взаимодействие плиты с упругим основанием. Выполняются условия сопряжения отдельных участков. Впервые для решения подобных задач используется аналитическая методика. Используется метод компенсирующих нагрузок. Получены решения в замкнутом виде, выраженные в функциях Бесселя. В качестве примера изучается комбинированная плита, состоящая из двух участков. Внутренняя часть этой конструкции имеет переменную толщину, внешняя часть – постоянную толщину.

Ключевые слова: комбинированные плиты, антисимметричные нагрузки, функции Бесселя

1. INTRODUCTION

The constructions with piecewise thickness occur among modern structures and buildings. Among them foundation slabs of circular form and bottoms of cylindrical reservoirs are to be mentioned. The combined foundation plates subjected to an action of symmetric loads were studied in the works [1] and [2]. The inner parts of these plates had the variable thickness, the outer ones – the constant thickness. The influence of upper parts of structures and interaction with the elastic subgrade were examined. For the first time for analysis

of similar constructions in [1] and [2] analytical method was applied. The solutions were obtained in closed forms in terms of Bessel functions.

Analytical methods for plates and shells analysis, in particular, connected with the use of special functions, occur in literature. The monographies [3] and [4] can be named. The book [5] is devoted to calculation problems of orthotropic and isotropic plates of variable thickness of different forms; the plates under study are subjected to an action of complicated loads.

In the present time the modern software allows to investigate various structures and building in detail. The numerical methods, in particular, the finite elements method, are widely utilized.

The buckling problems of orthotropic plates with various boundary conditions were considered in [6]. In the work [7] 3D free vibration problems of cross-ply laminated plates were under study. Vibrations of rectangular orthotropic and isotropic plates of linear thickness were investigated in [8].

Numerical analysis on experimental research on buckling of closed shallow conical shells under external pressure was given in [9]. The work [10] concerns free vibration analysis of a blade of variable thickness with arbitrary boundary conditions. The optimization problems of rectangular plates subjected to thermo-mechanical loads we examined in [11]. Comparative assessment of finite element modelling techniques for wind turbine rotors blades was given in [12]. Nonlinear primary resonance analysis of nanoshells was stated in [13]. Vibration problems of layered plates were considered in [14].

Statics, vibration and stability problems of rectangular plates with various boundary conditions were studied in the work [15]; the approximate analytical equation decomposition method was used.

The publications [16], [17], [18], [19] concerns the computation problems of combined plates with piecewise variable thickness, the exact analytical solutions in terms of special functions were obtained.

The present work considers the combined circular foundation plate, consisting of two parts. The plate's inner part has the variable thickness, the outer one has the constant thickness. The plate is subjected to an action of wind and seismic loads, which are considered as antisymmetric ones which vary according to the laws $cos\,\theta$ or $sin\,\theta$. The action of the construction's upper part on the foundation slab is analyzed. The properties of the elastic subgrade are described by Winkler's model.

2. THE ANALISYS OF THE INNER PART OF THE COMBINED PLATE

The inner part of the combined plate subjected to an action of antisymmetric loads is under study. The flexural rigidity of this part when $x_0 \le x \le x_1$ is varying according to the law

$$D = D_0 x^4 . \tag{1}$$

The corresponding law of thickness variation is:

$$h = h_0 x^{4/3} . \tag{2}$$

The antisymmetric distortion of the construction under study is caused by contour or lateral loads, varying according to the laws:

$$\begin{aligned} Q(\theta) &= Q_1 \cos\theta, \\ M(\theta) &= M_1 \cos\theta, \\ q(r,\theta) &= q(r)\cos\theta, \end{aligned} \tag{3}$$

where $Q(\theta)$ and $M(\theta)$ are accordingly intensities of a contour transverse force and a contour bending moment.

It is assumed that the properties of the elastic subgrade are described by Winkler's model.

The differential equation, describing the antisymmetric bending of the circular plate of variable thickness, resting on an elastic Winkler's basis, is:

$$D\nabla^2\nabla^2 w+\frac{dD}{dx}\left\{2\frac{d^3w}{dx^3}+\frac{2+\sigma}{x}\frac{d^2w}{dx^2}-\right.$$
$$-\frac{3}{x^2}\frac{dw}{dx}+\frac{3}{x^3}w\Big\}+\frac{d^2D}{dx^2}\left\{\frac{d^2w}{dx^2}+\right. \quad (4)$$
$$\left.+\sigma\left(\frac{1}{x}\frac{dw}{dx}-\frac{1}{x^2}w\right)\right\}=(q(x)-cw)r_0^4,$$

where D is the cylindrical rigidity, c - modulus of subgrade, $x=\frac{r}{r_0}$, r_0 is the constant.

In our case the cylindrical rigidity varies according to the law (1). Then the equation (4) comes to the following form:

$$\frac{d^4w}{dx^4}+\frac{10}{x}\frac{d^3w}{dx^3}+\frac{(17+4\sigma)}{x^2}\frac{d^2w}{dx^2}-$$
$$-\frac{3(3-4\sigma)}{x^3}\frac{dw}{dx}+\frac{3(3-4\sigma)}{x^4}w+\frac{\beta^4}{x^4}w=\frac{qr_0^4}{D_0}, \quad (5)$$

where $\beta^4=\frac{cr_0^4}{D_0}$.

Homogeneous differential equation, corresponding to (5), is the equation of the Euler class [20]. By means of substitutions $z=e^z$ and $w=ue^{-z}$ the equation (5) can be reduced to the equation with constant coefficients.

As a result we get the following expression for the deflections of the plate:

$$w=x^{-1}\left[A_1x^{\alpha_1}+A_2x^{\alpha_2}+A_3x^{\alpha_3}+A_4x^{\alpha_4}\right]cos\theta, \quad (6)$$

where $\alpha_{1,2,3,4}=\pm\sqrt{2(2-\sigma)\pm\sqrt{2\sigma^2-\beta^4}}$.

It should be marked that $\alpha_1=-\alpha_2$, $\alpha_3=-\alpha_4$.

In the case when the value of β^4 is sufficiently large, the roots of the characteristic equation are mutually complex conjugate.

First the interaction of the inner part of the foundation slab and the upper part of the construction under study will be considered. For this aim the fundamental functions $w_i(x_1)$ for the solutions (6) are to be determined. Their properties are described in [5].

For determination of the fundamental functions the Cauchy functions $Z_i(x_0;x)(i=1,2,3,4)$ are at first to be obtained.

For calculation the properties of Wandermond's determinant are used. As a result we get:

$$Z_1(x_0;x)=\frac{x_0}{2\left(\alpha_3^2-\alpha_1^2\right)}\left\{\frac{\alpha_3^2}{\alpha_1}\left[(\alpha_1+1)x_0^{-\alpha_1}x^{\alpha_1-1}+\right.\right.$$
$$+(\alpha_1-1)x_0^{\alpha_1}x^{-\alpha_1-1}\Big]-\frac{\alpha_1^2}{\alpha_3}\Big[(\alpha_3+1)x_0^{-\alpha_3}x^{\alpha_3-1}+$$
$$\left.+(\alpha_3-1)x_0^{\alpha_3}x^{-\alpha_3-1}\right]\Big\};$$
$$Z_2(x_0;x)=\frac{x_0^2}{2\left(\alpha_3^2-\alpha_1^2\right)}\left\{\frac{\left(\alpha_3^2-3\alpha_1\right)}{\alpha_1}x_0^{-\alpha_1}x^{\alpha_1-1}-\right.$$
$$-\frac{\left(\alpha_3^2-3\alpha_1\right)}{\alpha_1}x_0^{-\alpha_1}x^{-\alpha_1-1}-\frac{\left(\alpha_1^2-3\alpha_3\right)}{\alpha_3}\times$$
$$\left.\times x_0^{-\alpha_3}x^{\alpha_1-1}+\frac{\left(\alpha_1^2-3\alpha_3\right)}{\alpha_3}x_0^{-\alpha_3}x^{-\alpha_3-1}\right\}; \quad (7)$$
$$Z_3(x_0;x)=\frac{x_0^3}{2\left(\alpha_3^2-\alpha_1^2\right)}\left\{-\frac{x_0^{-\alpha_1}(6+\alpha_1)}{\alpha_1}x^{-\alpha_1-1}+\right.$$
$$+\frac{x_0^{-\alpha_1}(6-\alpha_1)}{\alpha_1}x^{-\alpha_1-1}+\frac{x_0^{-\alpha_3}(6+\alpha_3)}{\alpha_3}x^{\alpha_3-1}-$$
$$\left.-\frac{x_0^{-\alpha_3}(6-\alpha_3)}{\alpha_3}x^{-\alpha_3-1}\right\};$$
$$Z_4(x_0;x)=\frac{x_0^4}{2\left(\alpha_3^2-\alpha_1^2\right)}\left\{\frac{x_0^{-\alpha_1}x^{\alpha_1-1}}{\alpha_1}+\right.$$
$$\left.+\frac{x_0^{\alpha_1}x^{-\alpha_1-1}}{\alpha_1}+\frac{x_0^{-\alpha_1}x^{\alpha_3-1}}{\alpha_3}-\frac{x_0^{\alpha_3}x^{-\alpha_3-1}}{\alpha_3}\right\}.$$

As it was mentioned above for the case of sufficiently large β^4 the roots $\alpha_{1,2,3,4}$ are mutually complex conjugate. Then introducing the notations

$$\alpha_{1,2}=\varepsilon\pm\delta i,\ \alpha_{3,4}=-\varepsilon\pm\delta i$$

we write the general solution of the homogeneous differential equation, corresponding to (5), in the following form:

$$w(x) = x^{\varepsilon}\left[B_1\, sin(\delta\, ln\, x) + B_2 cos(\delta\, ln\, x)\right] + \\ + x^{-\varepsilon}\left[B_3\, sin(\delta\, ln\, x) + B_4 cos(\delta\, ln\, x)\right]. \quad (8)$$

Introducing the notation

$$sin(\delta\, ln\, x) = \alpha(x),\ cos(\delta ln\, x) = \gamma(x).$$

We cite below one of Cauchy functions as an example:

$$Z_4(x_0;x) = \frac{x_0^4}{4\varepsilon\delta\left(\varepsilon^2+\delta^2\right)}\left\{x_0^{-\varepsilon}x^{\varepsilon}\times\right. \\ \times\{-[\gamma(x_0)\delta+\varepsilon\alpha(x_0)]\gamma(x)+[\gamma(x_0)\varepsilon-\delta\alpha(x_0)]\times \quad (9) \\ \times\alpha(x)\}-x_0^{\varepsilon}x^{-\varepsilon}\{[-\gamma(x_0)\delta+\varepsilon\alpha(x_0)]\gamma(x)- \\ \left.-[\varepsilon\gamma(x_0)+\delta\alpha(x_0)]\alpha(x)\}\right\}.$$

Further, using (7) and taking into account the properties of fundamental functions, we get the following expressions:

$$w_1(x_0;x) = Z_1(x_0;x)+\frac{\sigma}{x_0^2}Z_3(x_0;x)- \\ -\frac{(\sigma+2)}{x_0^3}Z_4(x_0;x);$$

$$w_2(x_0;x) = Z_2(x_0;x)-\frac{\sigma}{x_0}Z_3(x_0;x)+ \\ +\frac{(\sigma+2)}{x_0^2}Z_4(x_0;x); \quad (10)$$

$$w_3(x_0;x) = -\frac{1}{D(x_0)}\left\{Z_2(x_0;x)-\left[\frac{1}{x_0}+\right.\right. \\ \left.\left.+\frac{1}{D(x_0)}\frac{dD(x_0)}{dx}\right]Z_4(x_0;x)\right\};$$

$$w_4(x_0;x) = -\frac{1}{D(x_0)}Z_4(x_0;x).$$

It is assumed that the influence of the construction's upper part is transmitted on the foundation slab inner part as moments $M_A cos\,\theta$ and forces $Q_A cos\,\theta$, distributed along circumference with the radius x_A, where $x_0 < x_A < x_1$. As a result we can write the following expression for the deflection:

$$w_{inner} = \left[w_0 w_1(x_0;x)+\vartheta_0 r_0 w_2(x_0;x)-\right. \\ -M_0 r_0^2 w_3(x_0;x)-Q_0 r_0^3 w_4(x_0;x)+ \\ \left.+M_A r_0^2 w_3(x_A;x)+Q_A r_0^3 w_4(x_A;x)\right]cos\,\theta = \\ =\left[w_1(x_0;x)+M_A r_0^2 w_3(x_A;x)+\right. \quad (11) \\ \left.+Q_A r_0^3 w_4(x_A;x)\right]cos\,\theta = \left[w_1(x_0;x)+\right. \\ \left.+w_{II}(x_A;x)\right]cos\,\theta,$$

where w_0, ϑ_0, M_0, Q_0 are accordingly the deflection, the angle, the moment, the force when $x = x_0$.

When for computation we assume that the influence of the upper part is transmitted on the foundation inner part as the load $q(x)cos\,\theta$, distributed over surface of the ring $x_A \le x \le x_B$. The result can be obtained by integrating in (11) the term containing Q_A.

3. THE COMPUTATION OF THE OUTER PART OF THE PLATE. THE BASIC SOLUTION

We go to the consideration of the outer part of the ring plate, subjected to an action of antisymmetric load. The thickness of the foundation slab part under study is constant. The general solution of the differential equation describing the antisymmetric bending of a circular plate resting on an elastic Winkler's subgrade is:

$$w = \left(A_1 u_1(x)+A_2 v_1(x)+A_3 f_1(x)+\right. \\ \left.+A_4 g_1(x)\right)cos\,\theta, \quad (12)$$

where u_1, v_1, f_1, g_1 are Bessel functions [4], [21]; A_1, A_2, A_3, A_4 - coefficients; $x=\frac{r}{l}$, $l=\sqrt[4]{\frac{D}{c}}$.

Method of compensating loads (MCL) [1], [2], [4] is used for the receiving of the solution. The basic and the compensating solutions are to be determined.

First the basic solution will be obtained.

When the circular plate is loaded by a concentrated force applied at the centre, the solution has the following form:

$$w=\frac{Pl^2}{4D}f_0(x). \tag{13}$$

The solution (13) mentioned above is the fundamental influence function when $P=1$. Integrating this solution, we can obtain the basic solutions for consideration of several problems.

Let us assume that this part of the plate is subjected to the action of the load $q\cos\theta$, distributed along the circumference with the reduced radius α.

Further, the principle of addition of the effects will be used.

For the determination of the deflection of the point with the coordinates x and φ the following expression will be used:

$$w=\frac{q\alpha l^2}{4D}\times \\ \times\int_0^{2\pi} f_0\left(\sqrt{\alpha^2+x^2-2\alpha x\cos(\theta-\varphi)}\right)\cos\theta d\theta. \tag{14}$$

For this integral calculation the formula of the cylindrical functions addition is used:

$$Z_0\left(\sqrt{\alpha^2+x^2-2\alpha x\cos(\theta-\varphi)}\right)= \\ =2\sum_{n=0}^{1}{}'J_n(\alpha)Z_m(x)\cos n(\theta-\varphi). \tag{15}$$

Here the symbol $'$ denotes that when $n=0$ the coefficient $\frac{1}{2}$ should be introduced. The expression (15) is valid when $\alpha<x$. When $\alpha>x$ in the right part of the expression (15) the terms α and x must be replaced.

Assuming

$$Z_0=H_0^{(1)}\left(\sqrt{i}\sqrt{\alpha^2+x^2-2\alpha x\cos(\theta-\varphi)}\right)$$

we get the following expressions fulfilling the integration and separating the real and the imaginary parts:

when $x\le\alpha$

$$w=w_{\mathrm{I}}^{(0)}=\frac{\pi\alpha q l^3}{2D}[u_1(x)f_1(\alpha)-v_1(x)g_1(\alpha)]\times \\ \times\cos\theta, \tag{16}$$

when $x\ge\alpha$

$$w=w_{\mathrm{II}}^{(0)}=\frac{\pi\alpha q l^3}{2D}[u_1(\alpha)f_1(x)-v_1(\alpha)g_1(x)]\times \\ \times\cos\varphi. \tag{17}$$

Using the Wronskian of the Bessel equation it can be shown that the received solutions satisfy to the conjugation conditions when $x=\alpha$.

The problem of infinite plate subjected to an action of the load $\psi(x)\cos\theta$, where $\psi(x)$ is the given function, is considered for the obtaining of the basic solution.

When the construction under study is subjected to an action of the load $q(\varphi)$ distributed along the circumference with the reduced radius α, we will present the load in the following form:

$$q=a_1\cos\theta+b_1\sin\theta$$

and using the formulae (16) and (17) we get the solutions:

when $\alpha\le x$

$$w = \frac{\pi\alpha l^3}{2D} \times$$
$$\times \{a_1[u_1(\alpha)f_1(x) - v_1(\alpha)g_1(x)]sin\varphi + \quad (18)$$
$$+ b_1[u_1(\alpha)f_1(x) - v_1(\alpha)g_1(x)]cos\varphi\},$$

when $\alpha \geq x$

$$w = \frac{\pi\alpha l^3}{2D} \times$$
$$\times \{a_1[u_1(x)f_1(\alpha) - v_1(x)g_1(\alpha)]sin\varphi + \quad (19)$$
$$+ b_1[u_1(x)f_1(\alpha) - v_1(x)g_1(\alpha)]cos\varphi\}.$$

For the basic solution receiving for the load $q = F(x,\theta)$ the formulae (18) and (19) should be used. The load can be represented in the form:

$$q = x(a_1 cos\theta + b_1 sin\theta) \quad (20)$$

or

$$q = x^{-1}(a_1 cos\theta + b_1 sin\theta). \quad (21)$$

The integrating for these cases is highly simple. The formulae for Bessel functions derivation are:

$$\left.\begin{aligned} \frac{d}{dz}\left[z^n J_n(z)\right] &= z^n J_{n-1}(z), \\ \frac{d}{dz}\left[z^n H_n^{(1)}(z)\right] &= z^n H_{n-1}^{(1)}(z). \end{aligned}\right\} \quad (22)$$

Let us assume $z = x\sqrt{i}$. Fulfilling integration and separating real and imaginary parts, we get the following expression:

$$\left.\begin{aligned} \int x u_0(x)dx &= \frac{x}{\sqrt{2}}[u_1(x) + v_1(x)], \\ \int x v_0(x)dx &= -\frac{x}{\sqrt{2}}[u_1(x) - v_1(x)], \end{aligned}\right\} \quad (23)$$

$$\left.\begin{aligned} \int x f_0(x)dx &= \frac{x}{\sqrt{2}}[f_1(x) + g_1(x)], \\ \int x g_0(x)dx &= -\frac{x}{\sqrt{2}}[f_1(x) - g_1(x)]. \end{aligned}\right\} \quad (24)$$

The solution for the case of the load varying according to the law (20) and distributed over a surface of the ring $\alpha_1 \leq x \leq \alpha_2$ is to be received. For this aim the expressions (16) and (17) are to be integrated. In the mentioned expressions the load q must be replaced by the elementary load $q_0\alpha dz = q_0\alpha d\alpha$. It should be marked that the multiplier $\frac{l^4}{D}$, which is equal to $\frac{1}{c}$, appears.

Further we integrate the received solutions within the limits $\alpha = \alpha_1$ and $\alpha = \alpha_2$.

When $x \leq \alpha_1 < \alpha_2$ the solution has the following form:

$$w = \frac{\pi q}{2c\sqrt{2}}\Big(\{\alpha_2^2[f_2(\alpha_2) + g_2(\alpha_2)] -$$
$$- \alpha_1^2[f_2(\alpha_1) + g_2(\alpha_1)]\}u_1(x) + \quad (25)$$
$$+ \{\alpha_2^2[f_2(\alpha_2) - g_2(\alpha_2)] - \alpha_1^2 \times$$
$$\times [f_2(\alpha_1) - g_2(\alpha_1)]\}v_2(x))cos\varphi;$$

when $x \geq \alpha_2 > \alpha_1$

$$w = \frac{\pi q}{2c\sqrt{2}}\Big(\{\alpha_2^2[u_2(\alpha_2) + v_2(\alpha_2)] -$$
$$- \alpha_1^2[u_2(\alpha_1) + v_2(\alpha_1)]\}f_1(x) + \quad (26)$$
$$+ \{\alpha_2^2[u_2(\alpha_2) - v_2(\alpha_2)] - \alpha_1^2 \times$$
$$\times [u_2(\alpha_1) - v_2(\alpha_1)]\}g_1(x))cos\varphi;$$

when $\alpha_1 \leq x \leq \alpha_2$

$$w = \frac{\pi q}{2\sqrt{2}c}\Big\{\alpha_2^2[f_2(\alpha_2)+g_2(\alpha_2)]\times \\ \times u_1(x)+\alpha_2^2[f_2(\alpha_2)-g_2(\alpha_2)]\times \\ \times v_1(x)-\alpha_1^2[u_2(\alpha_1)+v_2(\alpha_1)]f_1(x)- \\ -\alpha_1^2[u_2(\alpha_1)-v_2(\alpha_1)]g_1(x)-2x\frac{\sqrt{2}}{\pi}\Big\}cos\,\varphi. \quad (27)$$

These formulae give the expressions for the deflections of the foundation plate.

4. THE OUTER PART OF THE PLATE. THE COMPENSATING SOLUTION

The compensating solution should be determined for the plate's outer part investigation. This solution satisfies to boundary conditions and with the basic solutions satisfies to the resolving differential equation of the problem. For the foundation slab under study, which is subjected to an action of antisymmetric loads, the case of free edges is more actual. Below, however, another cases of boundary conditions will be considered.

The sought solution can be represented as the result of an action of two compensating loads q_1 and q_2, which are applied along the concentric circumferences with the reduced radius α_1 and α_2. Let us note the reduced radius of the outer contour as β.

a) First it is assumed that the outer boundary of the plate, subjected to an action of antisymmetric load, is clamped. For example it is possible for the plate when $x=\beta$ connected with the upper part of the construction which is represented by the shell of the rotation and subjected to an action of seismic or wind loads.

Let us present the deflection w_0 and the angle $\frac{\partial w_0}{\partial x}$ from the basic solution in the following form:

$$w_0 = A_1\,sin\,\varphi + B_1\,cos\,\varphi, \quad (28)$$

$$\frac{\partial w_0}{\partial x} = C_1\,sin\,\varphi + D_1\,cos\,\varphi. \quad (29)$$

The compensating loads q_1 and q_2, which with the sum of the basic solution are satisfying to the case of the clamped boundary, are to be determined.

As a result we get the following system of equations:

$$\alpha_1\int_0^{2\pi} q_1(\theta)\,f_0\left(\sqrt{\alpha_1^2+\beta^2-2\alpha_1\beta\,cos(\theta-\varphi)}\right)d\theta + \\ +\alpha_2\int_0^{2\pi} q_2(\theta)\,f_0\left(\sqrt{\alpha_2^2+\beta^2-2\alpha_2\beta\,cos(\theta-\varphi)}\right)d\theta + \\ +\frac{4D}{l^2}w_0 = 0, \quad (30)$$

$$\alpha_1\int_0^{2\pi} q_1(\theta)\frac{\partial}{\partial x}f_0\left(\sqrt{\alpha_1^2+\beta^2-2\alpha_1\beta\,cos(\theta-\varphi)}\right)d\theta + \\ +\alpha_2\int_0^{2\pi} q_2(\theta)\frac{\partial}{\partial x}f_0\left(\sqrt{\alpha_2^2+\beta^2-2\alpha_2\beta\,cos(\theta-\varphi)}\right)d\theta + \\ +\frac{4D}{l^2}\frac{\partial w_0}{\partial x} = 0. \quad (31)$$

The given above integral equations (30) and (31) express the conditions of equality of the values of deflections and angles to zero at the contour.

Further using the formulae of Bessel functions addition the integration is fulfilled [21]. The functions q_1 and q_2 are to be expanded into trigonometrical series. As a result we get a system of algebraic equations with respect to the coefficients of these series. Here this system is not cited.

The compensating solution can be written in the following form when $x \le \alpha$:

$$w_k = (a_1\,sin\,\varphi + b_1\,cos\,\varphi)u_1(x) + \\ +(c_1\,sin\,\varphi + d_1\,cos\,\varphi)v_1(x). \quad (32)$$

The coefficients of the expression (32) can be determined from the following equations, using (30) and (31):

$$\left.\begin{aligned} a_1 u_1(\beta) + c_1 v_1(\beta) + A_1 = 0, \\ a_1 u_1'(\beta) + c_1 v_1'(\beta) + C_1 l = 0; \end{aligned}\right\} \quad (33)$$

$$\left.\begin{aligned} b_1 u_1(\beta) + d_1 v_1(\beta) + B_1 = 0, \\ b_1 u_1'(\beta) + d_1 v_1'(\beta) + D_1 l = 0. \end{aligned}\right\} \quad (34)$$

Solving these systems, we obtain:

$$a_1 = -\frac{C_1 l v_1(\beta) - A_1 v_1'(\beta)}{v_1(\beta)u_1'(\beta) - u_1(\beta)v_1'(\beta)}, \quad (35)$$

$$b_1 = -\frac{D_1 l v_1(\beta) - B_1 v_1'(\beta)}{v_1(\beta)u_1'(\beta) - u_1(\beta)v_1'(\beta)}, \quad (36)$$

$$c_1 = \frac{C_1 l u_1(\beta) - A_1 u_1'(\beta)}{v_1(\beta)u_1'(\beta) - u_1(\beta)v_1'(\beta)}, \quad (37)$$

$$d_1 = \frac{D_1 l u_1(\beta) - B_1 u_1'(\beta)}{v_1(\beta)u_1'(\beta) - u_1(\beta)v_1'(\beta)}. \quad (38)$$

We receive introducing (35)-(38) into expression (32):

$$\begin{aligned} w_k = \frac{1}{v_1(\beta)u_1'(\beta) - u_1(\beta)v_1'(\beta)} \times \\ \times (\{[C_1 l v_1(\beta) - A_1 v_1'(\beta)]sin\varphi + \\ + [D_1 l v_1(\beta) - B_1 v_1'(\beta)]cos\varphi\} u_1(x) - \\ - \{[C_1 l u_1(\beta) - A_1 u_1'(\beta)]sin\varphi + \\ + [D_1 l u_1(\beta) - B_1 u_1'(\beta)]cos\varphi\} v_1(x)). \end{aligned} \quad (39)$$

b) The case when the outer boundary is simply supported is under study. The deflections are represented in the form (28). The radial bending moments on the contour are represented in the form:

$$M_r = M_1 sin\varphi + L_1 cos\varphi. \quad (40)$$

The following notations are introduced:

$$u_1^{(M)}(\beta) = -u_1(\beta) - \frac{1-\sigma}{\beta}\left[v_1'(\beta) - \frac{1}{\beta}v_1(\beta)\right], \quad (41)$$

$$v_1^{(M)}(\beta) = v_1(\beta) - \frac{1-\sigma}{\beta}\left[u_1'(\beta) - \frac{1}{\beta}u_1(\beta)\right], \quad (42)$$

$$f_1^{(M)}(\beta) = -f_1(\beta) - \frac{1-\sigma}{\beta}\left[g_1'(\beta) - \frac{1}{\beta}g_1(\beta)\right], \quad (43)$$

$$g_1^{(M)}(\beta) = g_1(\beta) - \frac{1-\sigma}{\beta}\left[f_1'(\beta) - \frac{1}{\beta}f_1(\beta)\right]. \quad (44)$$

The following compensating solution is obtained:

$$\begin{aligned} w_k = -\frac{1}{u_1(\beta)u_1^{(M)}(\beta) - v_1(\beta)v_1^{(M)}(\beta)} \times \\ \times \left(\left\{\left[M_1 \frac{l^2}{D} v_1(\beta) + A_1 u_1^{(M)}(\beta)\right]sin\varphi + \right.\right. \\ \left. + \left[L_1 \frac{l^2}{D} v_1(\beta) + B_1 u_1^{(M)}(\beta)\right]cos\varphi\right\} u_1(x) - \\ - \left\{\left[M_1 \frac{l^2}{D} u_1(\beta) + A_1 v_1^{(M)}(\beta)\right]sin\varphi + \right. \\ \left.\left. + \left[L_1 \frac{l^2}{D} u_1(\beta) + B_1 v_1^{(M)}(\beta)\right]cos\varphi\right\} v_1(x)\right). \end{aligned} \quad (45)$$

c) The case of free contour of the fundament plate is under consideration. It is known that the bending moment and the reduced transverse force are equal to zero at the contour.
The boundary bending moment is defined by the expression (40). The boundary reduced transverse force will be written in the form:

$$Q - \frac{dH}{dS} = N_1 sin\varphi + O_1 cos\varphi. \quad (46)$$

The following notation, taking into account (40), and (46) are introduced:

$$u_1^{[Q]}(\beta) = -u_1'(\beta) - (1-\sigma)\frac{1}{\beta^2}\left[v_1'(\beta) - \frac{v_1(\beta)}{\beta}\right], \quad (47)$$

$$v_1^{[Q]}(\beta) = v_1'(\beta) - (1-\sigma)\frac{1}{\beta^2}\left[u_1'(\beta) - \frac{u_1(\beta)}{\beta}\right], \quad (48)$$

$$f_1^{[Q]}(\beta) = -f_1'(\beta) - (1-\sigma)\frac{1}{\beta^2}\left[g_1'(\beta) - \frac{g_1(\beta)}{\beta}\right], \quad (49)$$

$$g_1^{[Q]}(\beta) = g_1'(\beta) - (1-\sigma)\frac{1}{\beta^2}\left[f_1'(\beta) - \frac{f_1(\beta)}{\beta}\right]. \quad (50)$$

As a result we get the compensating load:

$$w_k = -\frac{l^2}{D}\frac{1}{u_1^{[Q]}(\beta)v_1^{[M]}(\beta) - u_1^{[M]}(\beta)v_1^{[Q]}(\beta)} \times$$
$$\times \left\{ \left(\left[lN_1 u_1^{[M]}(\beta) - M_1 u_1^{[Q]}(\beta) \right] sin\,\varphi + \right.\right.$$
$$+ \left. \left[lO_1 u_1^{[M]}(\beta) - L_1 v_1^{[Q]}(\beta) \right] cos\,\varphi \right) u_1(x) - \qquad (51)$$
$$- \left(\left[lN_1 u_1^{[M]}(\beta) - M_1 v_1^{[Q]}(\beta) \right] sin\,\varphi + \right.$$
$$+ \left. \left. \left[lO_1 v_1^{[M]}(\beta) - L_1 v_1^{[Q]}(\beta) \right] cos\,\varphi \right) v_1(x) \right\}.$$

The solution for the outer part, according to the MCL, is represented by the sum of the basic and the compensating solutions [22], [23]:

$$w = w_0 + w_k. \qquad (52)$$

The solution of the problem under study can be presented as the sum of the expressions (11) and (52) for the study of bend of the whole combined plate.

5. THE CONCLUSIONS

The work receives the exact solution of the antisymmetric deformation of the combined plate which inner part has variable thickness and the outer one – the constant thickness. The solution is obtained in closed form in terms of Bessel functions. Method of compensating loads (MCL) is used. An influence of the construction's upper part is taken into account. The received results can be used for the analysis of the combined plates subjected to an action of seismic and wind loads.

REFERENCES

1. **Koreneva E.B.** Analysis of Combined Plates with Allowance for Contact with Elastic Foundation. // International Journal for Computational Civil and Structural Engineering. 2019. 15(4). Pp. 83-87.
2. **Koreneva E.B.** Usovershenstvovannyi Raschet Kombinirovannoj Fundamentnoj Plity Spetsialnogo Sooruzhenija [The Refined Computation of the Combined Foundation Plate of the Special Structure]. Sb. Trudov Natsionalnoj Nauchno-Tehnicheskoj Konferentsii s Inostrannym Uchastiem "Mehanika Gruntov v Geotehnike i Fundamentostroenii", g. Novocherkassk, Rostovskaja obl., 29-31 maja, 2018. Pp. 193-197 (in Russian).
3. **Kovalenko A.D.** Izbrannyie Trudyi [Selected Memoirs]. Kiev, Naukova Dumka, 1976, 703 pages (in Russian).
4. **Korenev B.G.** Nekotoryye Zadachi Teorii Uprugosti i Teploprovodnosti, Reshaemyye v Besselevych Funktsiyakh [Some Problems of the Theory of Elasticity and Heat Conductivity, Solved in Terms of Bessel Functions]. Moscow, Fizmatgiz, 1960, 458 pages (in Russian).
5. **Koreneva E.B.** Analiticheskie Metody Rascheta Plastin Peremennoj Tolschiny i ih Practicheskije Prilozhenija [Analytical Methods for Calculation of Plates with Varying Thickness and Their Practical Application]. Moscow, ASV, 2009, 240 pages (in Russian).
6. **Bank L.C. and Yin J.** Buckling of Orthotropic Plates with Free and Rotationally Restrained Unloaded Edges. // Thin-Walled Structures. 1996. 24. Pp. 83-96.
7. **Chen W.Q., Lüe C.F.** 3D Free Vibration Analysis of Cross-Ply Laminated Plates with One Pair of Opposite Edges Simply Supported. // Composite Structures. 2005. 69. Pp. 77-87.
8. **Civalek Öm.** Fundamental Frequency of Isotropic and Orthotropic Rectangular Plates with Linearly Varying Thickness by Discrete Singular Convolution Method. // Applied Mathematical Modelling. 2009. 33. Pp. 3825-3835.
9. **Karasev Al., Varianychko M., Bessmertnyi Ya., Krasovsky V., Karasev G.** Numerical Analysis on Experimental Research on Buckling of Closed Shallow Conical Shells under External Pressure. // Journal of Theoretical and Applied Mechanics. Warsaw. 2020. 58(1). Pp. 117-126.

10. **Li C., Cheng H.** Free Vibration Analysis of a Rotating Varying-Thickness-Twisted Blade with Arbitrary Boundary Conditions. // Journal of Sound and Vibration. https://doi.org/10.1016/j.jsv.2020.11579/
11. **Khakpour Komarsofla M. et al.** Optimization of Three-Dimensional up to Yield Bending Behaviour Using the Full Layer-Wise Theory for FGM Rectangular Plate Subjected to Thermo-Mechanical Loads. // Compos. Struct. https://doi.org/10.1016/j.compstruct.2020.113172.
12. **VanSkike W.P., Hale R.D.** Comparative Assessment of Finite Element Modelling Techniques for Wind Turbine Rotors Blades. American Institute of Aeronautics and Astronautics. // Downloaded by University of Texas at Austin on January 8. 2020 // http://arc.aiaa.org. Pp. 1-18.
13. **Sarafraz A., Sahmani S. and Aghdam M.M.** Nonlinear Primary Resonance Analysis of Nanoshells Including Vibrational Mode Interaction Based on the Surface Elasticity Theory. // Applied Mathematics and Mechanics (English Edition). 2020. https://doi.org/10.1007/10483-020-2564-5.
14. **Saira Javed, F.H.H. Al Mukahal and S.B.A. El Sayed.** Geometrical Influence on the Vibration of Layered Plates. Hindawi. // Shock and Vibration. V. 2021. Article ID 8843358. Pp. 1-17. https://doi.org/10.1155/2021/8843358.
15. **Koreneva E.B., Grosman V.R.** Equation Decomposition Method for Solving of Problems of Statics, Vibration and Stability of Thin-Walled Constructions. // International Journal for Computational Civil and Structural Engineering. 2020. 16(2). Pp. 63-70.
16. **Koreneva E.B., Grosman V.R.** Analiticheskij Raschet Kombinirovannyh Konstruktsij [Analytical Computation of Combined Constructions]. // Stroitelnaya Mehanika i Raschet Sooruzhenij. 2020. 2. Pp. 28-32 (in Russian).
17. **Koreneva E.B., Grosman V.R.** The Problems of Computation of Combined Plates with Piece-Wise Variable Thickness. Solution in Orthogonal Polynomials. // International Journal for Computational Civil and Structural Engineering. 2020. 16(2). Pp. 30-34.
18. **Koreneva E.B.** Analysis of Combined Disks with Piecewise Thickness. // International Journal for Computational Civil and Structural Engineering. 2021. 17(2). Pp. 12-21.
19. **Koreneva E.B.** Izgib Kombinirovannyh Plastin Kysochno-Peremennoj Tolschiny [The Flexure of Combined Plates with Piece-Wise Thickness]. // Stroitelnaya Mehanika i Raschet Sooruzhenij. 2021. 2. Pp. 10-18 (in Russian).
20. **Kamke E.** Spravochnik po Obyknovennym Differentsialnym Uravneniyam [The Handbook for Ordinary Differential Equations]. Moscow, Nauka, 1965, 703 pages (in Russian).
21. **Abramovitz M., Stigan I.A.** Handbook of Mathematical Functions. National Bureau of Standards. 10th Edition. 1972. 820 pages (in Russian).
22. **Koreneva E.B.** Metod Kompensirujuschih Nagruzok dlya Reshenija Zadach ob Anizotropnyh Sredah [Method of Compensating Loads for Solving of the Problems of Anisotropic Medium]. // International Journal for Computational Civil and Structural Engineering. 2018. 14(1). Pp. (in Russian).
23. **Koreneva E.B.** Metod Kompensirujuschih Nagruzok dlya Reshenija Zadach o Tsiklicheski-Simmetrichnom Izgibe Anizotropnyh Plastin, Kontaktirujuschih s Uprugim Osnovanijem [The Method of Compensating Loads for Solving of Problems of Cyclic Symmetrical Flexure of Anisotropic Plates, Resting on an Elastic Subgrade]. // Stroitelnaya Mehanika Inzhenernyh Konstruktsij i Sooruzhenij. 2021. 2. Pp. 99-111 (in Russian).

СПИСОК ЛИТЕРАТУРЫ

1. **Koreneva E.B.** Analysis of combined plates with allowance for contact with elastic foundation. // International Journal for Computational Civil and Structural Engineering. - 2019. – Vol. 15. – Issue 4. - Pp. 83-87.
2. **Коренева Е.Б.** Усовершенствованный расчет комбинированной фундаментной плиты специального сооружения. // Сб. трудов Национальной научно-технической Конференции с иностранным участием «Механика грунтов в геотехнике и фундаментостроении». - Новочеркасск, Ростовская обл., 29-31 мая, 2018. - С. 193-197.
3. **Коваленко А.Д.** Избранные труды. - Киев: Наукова думка, 1976. - 703 с.
4. **Коренев Б.Г.** Некоторые задачи теории упругости и теплопроводности, решаемые в бесселевых функциях. - М.: Физматгиз, 1960. - 458 с.
5. **Коренева Е.Б.** Аналитические методы расчета пластин переменной толщины и их практические приложения. - М.: АСВ, 2009. - 240 с.
6. **Bank L.C. and Yin J.** Buckling of orthotropic plates with free and rotationally restrained unloaded edges. // Thin-Walled Structures. - 1996. - 24. - Pp. 83-96.
7. **Chen W.Q., Lüe C.F.** 3D free vibration analysis of cross-ply laminated plates with one pair of opposite edges simply supported. // Composite Structures. - 2005. - 69. - Pp. 77-87.
8. **Civalek Öm.** Fundamental frequency of isotropic and orthotropic rectangular plates with linearly varying thickness by discrete singular convolution method. // Applied Mathematical Modelling. - 2009. - 33. - Pp. 3825-3835.
9. **Karasev Al., Varianychko M., Bessmertnyi Ya., Krasovsky V., Karasev G.** Numerical analysis on experimental research on buckling of closed shallow conical shells under external pressure. // Journal of Theoretical and Applied Mechanics. - Warsaw. - 2020. - 58. - 1. - Pp. 117-126.
10. **Li C., Cheng H.** Free vibration analysis of a rotating varying-thickness-twisted blade with arbitrary boundary conditions. // Journal of Sound and Vibration. - https://doi.org/10.1016/j. - jsv. - 2020. - 11579/
11. **Khakpour Komarsofla M. et al.** Optimization of three-dimensional up to yield bending behaviour using the full layer-wise theory for FGM rectangular plate subjected to thermo-mechanical loads. // Compos. Struct. - 2020. - https://doi.org/10.1016/j.compstruct. - 2020. - 113172.
12. **VanSkike W.P., Hale R.D.** Comparative assessment of finite element modelling techniques for wind turbine rotors blades. // American Institute of Aeronautics and Astronautics. - Downloaded by University of Texas at Austin on January 8. - 2020 // http://arc.aiaa.org. - Pp. 1-18.
13. **Sarafraz A., Sahmani S. and Aghdam M.M.** Nonlinear primary resonance analysis of nanoshells including vibrational mode interaction based on the surface elasticity theory. // Applied Mathematics and Mechanics (English Edition). - 2020. - https://doi.org/10.1007/10483-020-2564-5.
14. **Saira Javed, F.H.H. Al Mukahal and S.B.A. El Sayed.** Geometrical influence on the vibration of layered plates. // Hindawi. - Shock and Vibration. - V. 2021. - Article ID - 8843358. - Pp. 1-17. https://doi.org/10.1155/2021/8843358.
15. **Koreneva E.B., Grosman V.R.** Equation decomposition method for solving of problems of statics, vibration and stability of thin-walled constructions. // International Journal for Computational Civil and Structural Engineering. - 2020. - Vol. 16. – Issue 2. - Pp. 63-70.
16. **Коренева Е.Б., Гросман В.Р.** Аналитический расчет комбинированных конструкций. // Строительная механика и расчет сооружений. - 2020. - № 2. - С. 28-32.

17. **Koreneva E.B., Grosman V.R.** The problems of computation of combined plates with piece-wise variable thickness. Solution in orthogonal polynomials. // International Journal for Computational Civil and Structural Engineering. - 2020. – Vol. 16. – Issue 2. - Pp. 30-34.
18. **Koreneva E.B.** Analysis of combined disks with piecewise thickness. // International Journal for Computational Civil and Structural Engineering. - 2021. – Vol. 17. – Issue 2. - Pp. 12-21.
19. **Коренева Е.Б.** Изгиб комбинированных пластин кусочно-переменной толщины. Решения в функциях Лежандра. // Строительная механика и расчет сооружений. - 2021. - № 2. - С. 10-18.
20. **Камке Э.** Справочник по обыкновенным дифференциальным уравнениям. - М.: Наука, 1965. - 703 с.
21. **Abramovitz M., Stigan I.A.** Handbook of mathematical functions. - National bureau of Standards. - 10th Edition. - 1972. - 820 p.
22. **Коренева Е.Б.** Метод компенсирующих нагрузок для решения задач об анизотропных средах. // International Journal for Computational Civil and Structural Engineering. - 2018. – Vol. 14. – Issue 1. - Pp.
23. **Коренева Е.Б.** Метод компенсирующих нагрузок для решения задач о циклически-симметричном изгибе анизотропных пластин, контактирующих с упругим основанием. // Строительная механика инженерных конструкций и сооружений. - 2021. - № 2. - С. 99-111.

Elena B. Koreneva, Professor, Dr.Sc., Moscow Higher Combined-Arms Command Academy, 2, Golovacheva str., Moscow, 109380, Russia. Phone: +7(499)175-82-45, E-mail: elena.koreneva2010@yandex.ru

Valery R. Grosman, Engineer, Academy of Water Transport, 2, Novodanilovskaya nab., corp.1, Moscow, 117105, Russia. Phone: +7(499)618-52-56, E-mail: elena.koreneva2010@yandex.ru

Коренева Елена Борисовна, профессор, доктор технических наук, Московское высшее общевойсковое орденов Жукова, Ленина и Октябрьской Революции Краснознаменное училище, 109380, Россия, г. Москва, ул. Головачева, д.2, тел.: +7(499)175-82-45, E-mail: elena.koreneva2010@yandex.ru.

Гросман Валерий Романович, инженер, Академия водного транспорта, 117105, Россия, г. Москва, Новоданиловская наб., д.2, корп.1, тел.: +7(499)618-52-56, E-mail: elena.koreneva2010@yandex.ru.

International Journal for Computational Civil and Structural Engineering, 19(4) 95–115 (2023)

DOI:10.22337/2587-9618-2023-19-4-95-115

INFORMATION MODELING OF CONCRETE: CURRENT STATUS AND DEVELOPMENT PROSPECTS

Aleksey I. Makeev

Voronezh State Technical University, Voronezh, RUSSIA

Abstract: The paper addresses the challenges posed by the digitization of building materials science. It highlights the importance of developing a digital model of concrete for optimizing the design and synthesis of its structure and improving the technology used in its production. It is demonstrated how this model will enable building experts to better calculate and clarify methods for creating sturdy and efficient structures. The paper also examines the evolution of information modeling of concrete within the context of the various stages of development in system-building materials science and technology.

A review is presented of the primary contemporary techniques used in computer modeling of concrete structures in both domestic and foreign scientific research. It is worth noting that these methods fail to consider the intricate composition of concrete. The article explains that concrete can be characterized as a conglomerate composite that boasts a hierarchically organized structure with dimensions ranging from 10-10 to 10-1 meters. It is comprised of no fewer than 5-6 distinct scale levels and three distinct types of substructure design. Substructures vary in scale, origin, and manifestation of properties. The first type of substructure is observed at macro, meso, and micro scales. It is composed of a two-component structure consisting of a spatially continuous matrix and deterministically and stochastically distributed discrete inclusions. The second type of substructure pertains to the sub-micro, ultra-micro, and nanoscale levels. It is believed that the cementing substance takes the form of a microscale spatial structure resulting from the consolidation of individual crystalline differences. The third type corresponds to the atomic-molecular structure of newly formed cementing substance.

The characteristics of each substructure type are presented based on the component scale, formation features, mechanics of property manifestation, design criteria, and means of synthesis. A default assumption is made regarding the unique modeling of the three concrete substructure types and their consolidation into a unified digital model. The objective is to create an information platform for this purpose. The platform should consist of a knowledge base rooted in theory, an empirical database, a database consisting of analytical, numerical, and statistical models, algorithms for the purpose of designing and synthesizing structures, optimization criteria and boundary conditions, and specific terms of reference for computer modeling of concrete.

Keywords: design of structures, synthesis of materials with specified properties, digitalization of building materials science, digital model of concrete, information platform

ИНФОРМАЦИОННОЕ МОДЕЛИРОВАНИЕ БЕТОНА: ОБЗОР СОВРЕМЕННОГО СОСТОЯНИЯ И ПЕРСПЕКТИВЫ РАЗВИТИЯ*

А.И. Макеев

Воронежский государственный технический университет, г. Воронеж, РОССИЯ

Аннотация: Публикация относится к проблемам цифровизации строительного материаловедения. Показана актуальность разработки цифровой модели бетона для решения оптимизационных задач конструирования и синтеза его структуры, уточнения методик расчета строительных конструкций, совершенствования технологии их изготовления. Анализируется эволюция информационного моделирования бетона в контексте этапов развития системно-строительного материаловедения и технологии.

* Содержание статьи было частично доложено на VIII международном симпозиуме «Актуальные проблемы компьютерного моделирования конструкций и сооружений», 17-21 мая 2023 г., Тамбов

Приводится обзор основных современных методов компьютерного моделирования структуры бетона в отечественных и зарубежных научных исследованиях. Отмечается, что эти методы не учитывают всю сложность строения бетона. В статье бетон представлен как конгломератный композит с иерархически организованной структурой размерностью от 10^{-10} до 10^{-1} м. Он обладает минимум 5-6 масштабными уровнями и тремя типами конструкции подструктур. Подструктуры отличаются по своему масштабу, генезису и механике проявления свойств. Первый тип подструктуры характерен для макро-, мезо- и микромасштабного уровней. Принимается в виде двухкомпонентной «конструкции» из пространственно непрерывной матрицы и детерминировано-стохастически распределённых в ней дискретных включений. Второй тип относится к субмикро-, ультрамикро- и наномасштабным уровням. Полагается в виде «микромасштабной пространственной конструкции» новообразований цементирующего вещества из консолидированных индивидуальных кристаллических разностей. Третий тип соответствует атомно-молекулярному строению новообразований цементирующего вещества.
Дается характеристика каждого типа подструктуры по: масштабу компонентов; особенностям формирования; механике проявления свойств; критериям конструирования; средствам синтеза. Формулируется предположение о специфичности моделирования каждого из трех типов подструктур бетона и их интегрирования в единую цифровую модель. Ставится задача разработки информационной платформы такой модели. Платформа должна включать: базу теоретических знаний; базу эмпирических данных; базу аналитических, численных и статистических моделей; алгоритмы конструирования и синтеза структур; критерии оптимизации и граничные условия; техническое задание на компьютерное моделирование бетона.

Ключевые слова: конструирование структур, синтез материалов с заданными свойствами, цифровизация строительного материаловедения, цифровая модель бетона, информационная платформа

INTRODUCTION

Currently, the methods of design and calculation of structures, buildings and facilities rely on computer modeling of their stress-strain state, loads and impacts. Information technologies are used in experimental and field studies [1, 2].
The transition to computer modeling of construction objects, in our opinion, forms a favorable situation for the involvement of material scientists in this process. Their task is to design optimal structures of concretes with specified properties. Structure construction is a speculative, virtual procedure of "filling" the volume of the designed building structure that takes into account its configuration, peculiarities of reinforcement, etc., with structural elements forming the material. The outcome is the creation of a spatial and geometric "structure design" capable of maximizing the use of force structural bonds under the conditions of destructive impact of the operating environment on the building structure. Based on the results of the design, a set of control actions is assigned during the synthesis of the structure. This is a chemical-technological procedure for the implementation of the compiled project of spatial-geometric "structure design" in the production process of a building product [3].
However, the opportunities for interaction and mutual understanding between specialists in the calculation of building structures ("mechanics") and material scientists have been limited so far. They were confronted with the "watershed" between the used concepts, methods, passing through the scale boundary of 10^{-1} m in the "space and world" of construction science. Objectively, it turned out that "mechanics" deal with bodies on the scale of 10^{-1} m and larger. The material structure of such a body (structure) is modeled as a continuous homogeneous iso-tropic medium with some averaged "effective" characteristics [4]. The degree of compliance of these characteristics with the real values predetermines the predictive value of the calculation results. The potential deviations are compensated by the assignment of overestimated material reserve coefficients. Material scientists "work" with structured solids, which are a complex construction of elements with dimensions from 10^{-1} to 10^{-10} meters. In most cases, such a structure is perceived as a "black box" - an

experimental-statistical model relevant in a strictly limited factor space [5].

The lack of adequate models limits the possibilities of designing and subsequent synthesis of concrete structure with a given level of quality. It is known that the method of designing concrete mixture composition for concrete of a given strength was developed in the late 19th century. Nevertheless, the efficiency of concrete property management is still much lower than that of metals or polymers. This is clearly demonstrated by the difference in the values of the reserve coefficients of the compared materials.

In our opinion, a digital model of concrete can overcome the "barrier" between mechanics and material scientists. It should, first, describe identification universals and qualitative-quantitative attributes of concrete structure at all its scale levels. Secondly, it should reveal cause-and-effect links and relations in the system "technology" - "composition, structure, state" - "properties at the moment of production and unfolded in time in the operational environment".

The usage of a digital model of concrete in the design and calculation of building structures is aimed at clarifying the real pattern of their stress-strain state [6]. In system-structural materials science, the numerical model is intended for the development of fundamental principles of design and formation of an arsenal of means for synthesizing optimal concrete structures with predetermined characteristics. This model is most relevant for obtaining variable structures of new generation concretes (construction composites): super dense, especially high-strength, ultra-lightweight, ultra-resistant to the action of the operating environment, etc.

Applied goal of the digital model of concrete is to solve the problems of optimization design of concrete composition and structure depending on the operating conditions in building structures. The result of this is the assignment of rational modes and parameters of manufacturing of structures. In the future, the digital twin of concrete (reinforced concrete) structures should be integrated into BIM-technologies. Here it will manage the automated manufacturing process of the product, and then monitor its condition during operation with the forecast of residual resource.

Let us consider the evolution of system-structural concrete science in the context of digital approach.

EVOLUTION OF CONCRETE INFORMATION MODELING

Optimization of the structure and technology of concrete lies in the context of the system-wide task of creating a methodology and a comprehensive quality management system for industrial products. The development of solutions for quality management is based on a quantitative description of the phenomena of substance and energy transformations in the procedures of production. The highest form of such description is an information model of phenomena, for the creation of which it is necessary to formalize the transition from the real sides and relations of the object to their symbolic designation. In turn, formalization is feasible only after appropriate identification (recognition for display in human consciousness [7, 8]).

Academician of RAACS E.M. Chernyshov carried out a retrospective analysis of the "parallel" chronology of the development of basic scientific knowledge in the field of concrete science [9] and the stages of development of the methodology of the quantitative approach [10]. Table 1 presents the results of the analysis.

Table 1. Stages of development of information modeling of concrete and basic scientific knowledge of concrete science

Stage	Period	Content of the stage	Personalities, schools
I	the first third of the nineteenth century - first third of the 20th century	The formation of the paradigm of quantitative approach, the emergence and development of the science of processes and devices of engineering technologies as a field of scientific and applied knowledge [11-13]. Introduction of physical and mathematical analogies; physical analog modeling; modeling based on the theory of similarity [14-16].	F.A. Denisov, V. Badger, N.D. Zelinsky, A.A. Kirov, V.L. Kirpichov, A.K. Krupsky, V. Luis, W. McAdams, W. McCabe, D.I. Mendeleev, I.A. Tishchenko, W. Walker, etc.
		Obtaining the first scientific data on the influence of technology on concrete properties and processes of its structural formation [17-20].	D. Abrams, I.P. Alexandrin, A.A. Baikov, N.A. Belelyubsky, N.M. Belyaev, I. Bolome, O. Graf, N.A. Zhitkevich, V.A. Kind, I.G. Malyuga, E. Freysine, R. Fere, E.G. Cheliyev, A.R. Shulyachenko, V.V. Ewald and etc.
II	first third of the XX century - middle of the XX century.	Establishment of fundamental principles of the general theory of systems [21-23]. Formation of the methodology of system analysis of engineering and technology objects. Application of mathematical modeling for solving engineering problems [24].	N.A. Belov, A.A. Bogdanov, L. Bertalanffy, W. Ross-Eshby, T. Kotarbiński, M. Petrovic, A. Espinas, et al.
		Identification of regular relations in the system "formulation-technological factors" - "composition, structure, state, properties" of concrete. The beginning of the formation of the structural approach in concrete science [25-28].	V.V. Mikhailov, N.A. Popov, B.G. Skramtaev, A.E. Sheikin, V.N. Jung et al.
III	second half of the 20th century	Implementation of the cybernetic approach to systems as an object of control according to the "black box" principle [29-31]. Development of probabilistic-statistical methods of active planning and design of experiments [32-34]. Application of experimental-statistical models in construction materials science and technology [35-37].	Y.P. Adler, P. Ahnazarova, N. Wiener, V.A. Voznesensky, V.V. Kafarov, R. Fischer, et al. Kafarov, R. Fischer, etc.
		Development of the foundations of system-structural building materials science with active use of the provisions of natural science disciplines [38-42]. Qualification of concrete as a composite material, experimental study of its composition and struc-	I.N. Akhverdov, Y.M. Bazhenov, J. Bernal, I.I. Bernay, P.I. Bozhenov, S.S. Gordon, I.M. Grushko, A.E. Desov, G.I. Gorchakov, A. Grudemo, I.A. Ivanov, F.M.

		ture on the basis of new quantitative physical and chemical methods [43-47]. Development of the foundations of the mechanics of manifestation of structural and functional properties of concrete [48-51].	Ivanov, J.L. Kalousek, P.G. Komokhov, D. Conrad, R. Lermit, F.M. Lee, P.A. Melnichenko, O.P. Mchedlov-Petrosyan, T.P. Pauers, T. Pauers, R. Lermit, F.M. Lee, P.A. Melnichenko. Komokhov, D. Conrad, R. Lermit, F.M. Lee, P.A. Melnichenko, O.P. Mchedlov-Petrosyan, T. Powers, V. Reichel, P.A. Rebinder, A.I. Rybiev, V.I. Solomatov, M.M. Sychev, H.F.W. Tay-lor, V.V. Timashev, A.V. Usherov-Marshak, M.M. Kholmyansky et al.
IV	Since the end of the 20th century	Mathematical and computational optimization problem solving in construction materials science and technology. Development of "computer material science" of concrete on the scientific basis of classical concrete science [5, 52-54]. Attraction of mathematical physics models and simulation modeling. Validation of neuro-computing application in construction materials science [55-58].	A.A. Askadsky, V.V. Belov, V.A. Voznesensky, V.A. Vorobyov, B.V. Gusev, V.I. Kondrashchenko, E.V. Korolev, T.V. Lyashenko, A.S. Ovchinsky, V.P. Selyaev, S.V. Fedosov et al.
		Development of a scientific platform for the development of breakthrough innovative solutions in system-structural materials science and high technologies of concrete with a new level of quality. Staging and realization of special researches of cause-effect relations according to the formula "4C" [7, 59-62]. Development and generalization of provisions of mechanics of concrete properties manifestation as composites [4, 63-66]. Development of methodology and theory of design and synthesis of optimal structures of conglomerate building composites [3, 8, 67, 68].	T.K. Akchurin, O.V. Artamonova, V.N. Vyrovoy, A.M. Danilov, V.T. Erofeev, S.S. Kaprielov, N.I. Karpenko, D.N. Korotkikh, V.S. P. Lesovik, N.I. Makridin, V.I. Morozov, A.P. Proshin, Y.V. Pukharenko, G.S. Slavcheva, E.M. Chernyshov, V.I. Shevchenko, V.P. Yartsev et al.

The stages presented in Table 1 reflect the vector of movement on the way from phenomenological (factual, empirical) knowledge to essential (system-structural, conceptual) knowledge in materials science of construction composites. This movement is accompanied by the evolution of concepts and methodology of information modeling of concrete in the form of deepening and detailing of aspects of identification and formalization of its structure.

It follows from Table 1 that the current state of basic scientific knowledge and information modeling of concrete can be evaluated as an exit to digitalization of construction materials science and technology. Setting and solving problems of designing and synthesis of optimal structures today should be carried out on the basis of formalization and computer modeling of cause-and-effect relations in the system "technology - material - construction - building (structure) - operating environment". Digitalization here should be understood as a transition from physical, in-situ models (concrete samples) to work with its mathematical image. Digitalization makes it possible to perform control actions with a virtual object (a digital twin of a building structure) with the help of a computer. In this case, the computer is used not so much as a means of processing information and calculations, but as a direct "productive force" in obtaining the final result.

REVIEW OF CURRENT METHODS FOR COMPUTER MODELING OF CONCRETE

The goals of digitalization have become achievable due to the emergence of universal shells and increasingly powerful algorithmic programming languages, computational and information resources for applied mathematical modeling. Supercomputer technologies and hybrid architecture computing systems using traditional and advanced algorithms have become commonplace.

The method of neurocomputing ("machine learning" in foreign terminology) has received a particularly rapid development in this respect. Neurocomputing provides the creation of systems and algorithms for information processing capable of autonomously generating adaptive responses of the "cause-effect" type for a specific information environment. Neurocomputing is considered as an alternative to programmed computing due to its ability to "learn" to process information while acting in an informational environment [55, 69]. Since the 90s of the last century, neural networks have been used in the development of concrete composition selection and property prediction [70-77]. Unfortunately, and this is noted by the researchers themselves [78], such developments are reduced to neural network programming of cause-effect links and relations in the system "formulation-technological factors" - "properties" of concrete. Machine learning is carried out on the basis of empirical data according to the "black box" principle, without taking into account structural factors. That is, in their methodological bases and statements such works lie in the context of the III stage of evolution of construction material science and concrete technology (see Table 1). Moreover, according to Lyashenko [79], machine learning models are "more passive" than experimental-statistical models. She argues that the initial data for them are not generated according to a special plan, but in an arbitrary way.

A review of foreign sources shows that the most common method of computer modeling of concrete structure today is mesoscale modeling. According to this method, concrete is considered as a composite material made of aggregates of different shapes and sizes included in the cement matrix. It should be noted that in the domestic materials science terminology, the macroscale level of concrete structure corresponds to this interpretation.

In most cases, mesoscale modeling is based on the formation of pseudo-random 3D packing of particles according to their computer-generated locations and radii [80, 81]. The nonlinear behavior of the simulated structure is investigated by numerical methods using its finite element discretization [82], including the use of general-purpose software such as ANSYS [83].

It is noted that "classical" mesoscale modeling often shows significant discrepancy with the results of physical experiments, as it does not consider microstructural levels of concrete. To refine the mesoscale models, for example, matrix-inclusion contact zone modeling is used [84], microstructure visualization using X-ray computed tomography [85], machine learning [86], including for image analyzer data processing [87].

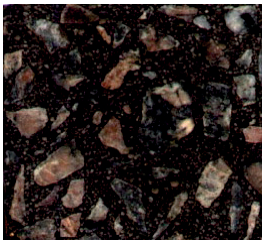
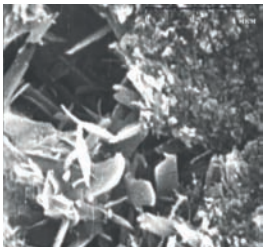
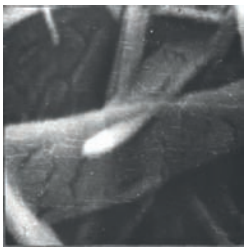
Computer modeling of atomic and molecular structure of cement stone neoplasms by molecu-

lar dynamics methods has become a separate independent direction of digitalization of building materials science. These methods combine quantum-mechanical description of objects and models of "classical forces" [88-90].
In Russian science, Vorobyov should be considered as the founder of the calculation of the composition and prediction of concrete properties using computer modeling of their structure. His methods combine the probabilistic-geometric concept with the theory of percolation and the theory of effective media [91]. Modeling of the structure of building composites today is carried out on a large scale by the leading Russian scientific schools [53, 58, 61, 63, 67, 67, 92, 93].

DISCUSSION OF THE CURRENT STATE OF COMPUTER MODELING OF CONCRETE AND FUTURE PROPOSALS

Despite significant successes, the methods of computer modeling of concrete listed in the previous section do not take into account the complexity of the structure of this material. The applied approaches are differentiated by scale structural levels and do not provide a holistic adequate digital model of concrete. In our opinion, these methods require integration on the basis of modern concepts and data on identification and formalization of concrete structure.
Let us characterize concrete as an object of mathematical modeling. "Concretes are composites of conglomerate type, which are structured solids endowed with the features of substance, multiphase, polystructure, scale multiscale, deterministic, stochastic and dialectic" [94]. E.M. Chernyshov identified these features as universals of structure [95]. The universals of polystructure and scale multilevelness show that, despite the diversity of concrete varieties, their structure is a spatial-geometric construction of characteristic dimensionality from 10^{-10} to 10^{-1} meters. The structure has at least 5-6 structural levels and three types of substructures in the integral structure of concrete. Substructures are distinguished by their scale, genesis and mechanics of properties manifestation (Table 2).

Table 2. Characterization of substructures in the polystructure of concrete

Characteristic feature	Substructure type		
	I (conglomerate composite)	II (microconstruction)	III (continuous medium)
Visualization			
"Occupied" levels of the holistic structure	macro-, meso- and microscales	sub-micro-, ultra-micro- and nanoscale	nanoscale and atomic molecular
Dimensional range of structural elements, m	10^{-1} - $10^{-(4\div5)}$	$10^{-(4\div5)}$ - $10^{-(8\div9)}$	10^{-8} - 10^{-10}

Description of the structure	two-component "construction" of a spatially continuous matrix and deterministically stochastically distributed discrete inclusions; a continuous heterogeneous body	"Microscale spatial construction" of cementitious matter neoplasms from consolidated individual crystalline and hidden crystalline differences	solid-phase substance of individual hidden crystalline or crystalline neoplasms; solid monophasic body endowed with imperfections (defects) in the form of vacancies, substitutions, dislocations.
Genesis	a product of the formation of the "addition system"	a product of the interaction between the "addition system" and the "growth system"	a product of the evolution of the "growth system"
Regularities of property mechanics	mechanics of composites	construction "micromechanics"	thermofluctuation theory, crack mechanics
Design criteria	control of the stress field by parameters of their concentration and localization	Load bearing capacity	kinetic strength, fracture toughness
Scientific basis for synthesis tools	Mechanics and mechanochemistry of granular media, physicochemistry of dispersed systems	physicochemistry of dispersed systems, theory of structure of matter, solid state chemistry, crystal chemistry, nanochemistry	
Volume in the composite space, %	100	15-20	6-10

Each of the identified types of substructures has its own specific formalizations and mathematical model. The first type is a probabilistic-geometric model of granular particle packing, the second type is a finite element model of stochastic structure, the third type is a discrete model of crystal lattice. To obtain an adequate numerical model of concrete, the disclosure and integration of these models is necessary.

In this case, it is most difficult to formalize the substructure of the second type. It has a pronounced stochasticity and variability. It is a structure of morphologically crystalline (or hidden crystalline) lamellar, fibrous-needle, etc. differences of neoplasms. The mathematical model of the second type of substructure can be correlated with the corresponding models of spatial systems of building macroscale structures (rod, rack-and-beam, shell structures, etc.) [96]. However, with this approach we will have to face the problem of determinization of stochastic systems.

CONCLUSION

In our opinion, the proposed approach to the development of a digital model of concrete as a polystructural material requires preliminary creation of an information platform. Such a platform will include:
1) theoretical knowledge base,
2) empirical data base,
3) base of mathematical and computer models of concretes and processes occurring in them during production and operation,
4) algorithms for construction and synthesis of structures,
5) optimization criteria and boundary conditions,
6) terms of reference for computer simulation.
Generation of the knowledge base in the information platform implies a system identification and formalization of concrete polystructure. This should result in a system of quantitative parameters of the structures of each of the three types of substructures.
These parameters with their estimates and characteristics will be a function (output) in mathematical models of the type "formulation-technological factors - composition, structure, state" and "operational factors - composition, structure, state", and then serve as arguments (input) in models of the type "composition, structure, state - properties".
Numerical solution of inverse problems on the basis of these models is the essence of optimization design and technological synthesis of concretes with characteristics specified depending on the conditions of their operation in building structures.

REFERENCES

1. **Travush V.I.** Tsifrovyye tekhnologii v stroitel'stve [Digital technologies in construction] // Academia. Arkhitektura i stroitel'stvo, 2018, Issue 3, pp. 107-117 (in Russian).
2. Informatika v stroitel'stve (s osnovami matematicheskogo i komp'yuternogo modelirovaniya) [Computer science in construction (with the basics of mathematical and computer modeling)] / team of authors; under. ed.P.A. Akimov. Moscow, KNORUS, 2017, 420 pages (in Russian).
3. **Makeyev A.I.** Metodologicheskiye osnovaniya teorii konstruirovaniya i sinteza optimal'nykh struktur konglomeratnykh stroitel'nykh kompozitov [Methodological foundations of the theory of design and synthesis of optimal structures of conglomerate building composites] // Nauchnyy vestnik VGASU. Seriya: Fiziko-khimicheskiye problemy i vysokiye tekhnologii stroitel'nogo materialovedeniya, 2015, Issue 1, pp. 29-37 (in Russian).
4. **Karpenko N.I.** Obshchiye modeli mekhaniki betona [General models of concrete mechanics]. Moscow, Stroyizdat, 1996, 416 pages (in Russian).
5. **Kondrashchenko V.I.** Nekotoryye aspekty komp'yuternogo materialovedeniya [Some aspects of computer materials science] // Modelirovaniye i optimizatsiya kompozitov : Mat. k mezhdunar. seminaru, posvyashch. 80-letiyu V.A. Voznesenskogo. Odessa, Astroprint, 2014, pp. 64-68 (in Russian).
6. **Chernyshov Ye.M., Makeyev A.I.** K modelirovaniyu napryazhennogo sostoyaniya strukturno-neodnorodnykh konglomeratnykh kompozitov v stroitel'nykh konstruktsiyakh [Towards modeling the stress state of structurally inhomogeneous conglomerate composites in building structures] // International Journal of Calculation of Civil and Construction Structures, 2015, Vol. 11, Issue 2, pp. 160-170 (in Russian).
7. **Bazhenov Yu.M., Gar'kina I.A., Danilov A.M., Korolev Ye.V.** Sistemnyy analiz v stroitel'nom materialovedenii [System analysis in construction materials science]. Moscow, MGSU, 2012, 432 pages (in Russian).

8. **Budylina Ye.A., Gar'kina I.A., Danilov A.M.** Obshchaya skhema identifikatsii i sinteza stroitel'nykh materialov [General scheme for identification and synthesis of building materials] // Regional'naya arkhitektura i stroitel'stvo, 2022, Issue 4, pp. 26-30 (in Russian).
9. **Chernyshov Ye.M.** Materialovedeniye i tekhnologiya stroitel'nykh kompozitov kak sistema nauchnogo znaniya i predmet razvitiya issledovaniy. Chast' 2. Razvitiye i evolyutsiya nauchnogo znaniya o konglomeratnykh stroitel'nykh kompozitakh kak strukturirovannykh sistemakh [Materials science and technology of building composites as a system of scientific knowledge and a subject for the development of research. Part 2. Development and evolution of scientific knowledge about conglomerate building composites as structured systems] // Izvestiya vysshikh uchebnykh zavedeniy. Stroitel'stvo, 2020, Issue 1, pp. 57-77 (in Russian).
10. **Chernyshov Ye.M., Makeyev A.I.** O probleme razvitiya, evolyutsii «tsifrovogo podkhoda» v materialovedenii i tekhnologii stroitel'nykh kompozitov [On the problem of development, evolution of the "digital approach" in materials science and technology of building composites] // Sovremennaya nauka: teoriya, metodologiya, praktika: Mat-ly III vserossiyskoy (natsional'noy) nauchno-prakticheskoy konferentsii. Tambov, Izd-vo IP Chesnokova A.V., 2021, pp. 9-21 (in Russian).
11. **Denisov F.A.** Prostrannoye rukovodstvo k obshchey tekhnologii ili k poznaniyu vsekh rabot, sredstv, orudiy i mashin, upotreblyayemykh v raznykh khimicheskikh iskusstvakh [A lengthy guide to general technology or to the knowledge of all works, means, tools and machines used in various chemical arts]. Moscow, 1828, 548 pages (in Russian).
12. **Mendeleyev D.I.** Osnovy fabrichno-zavodskoy promyshlennosti [Fundamentals of the factory industry]. St. Petersburg, Type. V. Demakova, 1897, 201 pages (in Russian).
13. **Tishchenko I.A.** Osnovnyye protsessy i apparaty khimicheskoy tekhnologii. Vyp. I : Obshcheye vvedeniye. Izmel'cheniye i izmel'chayushchiye apparaty [Basic processes and devices of chemical technology. Vol. I: General introduction. Grinding and grinding apparatus]. Moscow, Tipo-Lit. I. Kh. Kavykina, 1913, 161 pages (in Russian).
14. **Walker W.H., Lewis W.K., McAdams W.H.** Principles of chemical engineering. London, McGraw-Hill Publising Co., ltd, 1923. 631 pages.
15. **Badger V., McCab V.** Osnovnyye protsessy i apparaty khimicheskikh proizvodstv [Basic processes and apparatus of chemical production]. Moscow, Leningrad, Goskhimtekhizdat, 1933, 476 pages (in Russian).
16. **Kasatkin A.G.** Osnovnyye protsessy i apparaty khimicheskoy tekhnologii. [Basic processes and apparatuses of chemical technology]. Moscow, Khimiya, 1973. 752 pages (in Russian).
17. **Malyuga I.G.** Sostav i sposob prigotovleniya tsementnogo rastvora (betona) dlya polucheniya naibol'shey kreposti [Composition and method of preparing cement mortar (concrete) to obtain the greatest strength]. St. Petersburg, type. or T. V.A. Tikhanova, 1895, 201 pages (in Russian).
18. **Zhitkevich N.A.** Beton i betonnyye raboty [Concrete and concrete work]. St. Petersburg, 1912, 524 pages (in Russian).
19. **Evald V.V.** Stroitel'nyye materialy. Ikh prigotovleniye, svoystva i ispytaniya [Construction Materials. Their preparation, properties and tests]. Moscow, Gos. nauchtekhn. izd-vo, 1931, 510 pages (in Russian).
20. **Znachko-Yavorsky I.L.** Ocherki istorii vyazhushchikh veshchestv ot drevneyshikh vremen do serediny XIX veka [Essays on the history of binders from ancient times to the mid-19th century]. Leningrad, Izd-vo AN SSSR, 1963, 496 510 pages (in Russian).

21. **Bogdanov A.A.** Vseobshchaya organizatsion-naya nauka (tektologiya) [General organizational science (tectology)] / 3-ye izd. Ch. 1–3, Moscow, Leningrad, 1929, 220 pages (in Russian).
22. **Bertalanffy L.** Obshchaya teoriya sistem - obzor problem i rezul'tatov [General theory of systems - a review of problems and results] // Sistemnyye issledovaniya. Yezhegodnik. Moscow, «Nauka», 1969, pp. 34-35 (in Russian).
23. Issledovaniya po obshchey teorii sistem [Research on general systems theory] // Sb. perevodov pod red. V. N. Sadovskogo i E. G. Yudina. Moscow, Progress, 1969, 519 pages (in Russian).
24. **Karman T., Bio M.** Matematicheskiye meto-dy v inzhenernom dele [Mathematical methods in engineering] / Per s angl., 2-ye izd. Moscow, Leningrad, Gos. izd-vo tekhniko-teoretich. lit-ry, 1948, 424 pages (in Russian).
25. **Skramtaev B.G.** Teoriya prochnosti betona. Novyye vidy betonov [Theory of concrete strength. New types of concrete] / Doklady, prochitannyye na Vseukr. konferentsii po betonu i zhelezobetonu 17-19 iyunya 1933 g. Kharkov, Gos.-nauch. tekhn. izd-vo Ukrainy, 1933, 55 pages (in Russian).
26. **Jung V.N.** Vvedeniye v tekhnologiyu tsementa [Introduction to cement technology]. Moscow, Leningrad, Gosstroyizdat, 1938, 404 pages (in Russian).
27. **Mikhailov V.V.** Elementy teorii struktury betonov [Elements of the theory of concrete structure]. Moscow, Leningrad, Gosstroyizdat, 1941, 227 pages (in Russian).
28. **Sheykin A.E.** Teoriya uprugosti, prochnosti, plastichnosti betona [Theory of elasticity, strength, plasticity of concrete]. Moscow, NIIZhB, 1944, 250 pages (in Russian).
29. **Wiener N.** Kibernetika, ili Upravleniye i svyaz' v zhivotnom i mashine [Cybernetics, or Control and Communication in Animals and Machines]. Moscow, Nauka, 1983, 344 pages (in Russian).
30. **Optner S.L.** Sistemnyy analiz dlya resheniya delovykh i promyshlennykh problem [System analysis for solving business and industrial problems]. Moscow, Sovetskoye radio, 1968, 216 pages (in Russian).
31. **Kafarov V.V.** Metody kibernetiki v khimii i khimicheskoy tekhnologii [Methods of cybernetics in chemistry and chemical technology]. Moscow, Khimiya, 1968, 379 pages (in Russian).
32. **Fisher R.** Statisticheskiye metody dlya issledovateley [Statistical methods for researchers]. Moscow, Gosstatizdat, 1958, 267 pages (in Russian).
33. **Adler Yu.P., Markova E.V., Granovsky Yu.V.** Planirovaniye eksperimenta pri poiske optimal'nykh usloviy [Planning an experiment when searching for optimal conditions]. Moscow, Nauka, 1976, 280 pages (in Russian).
34. **Akhnazarova S.L., Kafarov V.V.** Metody optimizatsii eksperimenta v khimicheskoy tekhnologii. [Methods for optimizing experiments in chemical technology]. Moscow, Vyssh. shk., 1985, 327 pages (in Russian).
35. **Voznesensky V.A., Vyrovoy V.N., Kersh V.Ya. et al.** Sovremennyye metody optimizatsii kompozitsionnykh materialov [Modern methods of optimization of composite materials] / Ed. V. A. Voznesensky. Kyiv: Budivelnik, 1983, 144 pages (in Russian).
36. **Lyashenko T.V.** Optimizatsiya napolniteley poliefirnykh svyazuyushchikh na osnove modeley novogo klassa [Optimization of polyester binder fillers based on new class models]: dis.... cand. tech. Sci. Odessa, 1984, 236 pages (in Russian).
37. **Shinkevich E.S.** [Optimization of the structure of cellular silicate concrete according to a set of quality criteria based on isoparametric analysis]: dis. ...cand. tech. Sci. Kraskovo, 1985, 249 pages (in Russian).
38. **Bazhenov Yu.M.** [Concrete under dynamic loading]. Moscow, Stroyizdat, 1970, 272 pages (in Russian).

39. **Ratinov V.B., Rosenberg T.I.** Dobavki v beton [Additives to concrete]. Moscow, Stroyizdat, 1973, 207 pages (in Russian).
40. **Melnichenko P.A.** Strukturno-statisticheskiy podkhod k resheniyu zadachi upravlyayemogo strukturoobrazovaniya kompozitov [Structural-statistical approach to solving the problem of controlled structure formation of composites] // Snizheniye materialoyemkosti i povysheniye dolgovechnosti stroitel'nykh izdeliy. Kyiv, Budivelnik, 1974, pp. 66-76 (in Russian).
41. **Rebinder P.A.** Poverkhnostnyye yavleniya v dispersnykh sistemakh. Fiziko-khimicheskaya mekhanika. Izbrannyye trudy [Surface phenomena in disperse systems. Physico-chemical mechanics. Selected works]. Moscow, Nauka, 1979, 384 pages (in Russian).
42. **Akhverdov I.N.** Osnovy fiziki betona [Fundamentals of concrete physics]. Moscow, Stroyizdat, 1981, 464 pages (in Russian).
43. **Podvalny A.M.** Opredeleniye velichiny sobstvennykh deformatsiy v betonnom konglomerate na razlichnykh strukturnykh urovnyakh [Determination of the magnitude of intrinsic deformations in concrete conglomerate at various structural levels] // Zavodskaya laboratoriya, 1973, Issue10, pp. 1204 – 1206 (in Russian).
44. **Sheikin A.E., Chekhovsky Yu.V., Brusser M.I.** Struktura i svoystva tsementnykh betonov [Structure and properties of cement concrete]. Moscow, Stroyizdat, 1979, 344 pages (in Russian).
45. **Rybyev I.A., Nekhoroshev A.V.** Iskhodnyye metodicheskiye pozitsii pri issledovanii iskusstvennykh stroitel'nykh konglomeratov [Initial methodological positions in the study of artificial building conglomerates] // Stroitel'nyye materialy, 1980, Issue 2, pp. 24 – 26 (in Russian).
46. **Solomatov V.I.** Elementy obshchey teorii kompozitsionnykh stroitel'nykh materialov [Elements of the general theory of composite building materials] // Izvestiye vuzov. Stroitel'stvo i arkhitektura, 1980, Issue 8, pp. 61 – 70 (in Russian).
47. **Chernyshov E.M.** Upravleniye protsessami strukturoobrazovaniya i kachestvom silikatnykh avtoklavnykh materialov (voprosy metodologii, strukturnoye materialovedeniye, inzhenerno-tekhnologicheskiye zadachi) [Control of structure formation processes and quality of silicate autoclave materials (issues of methodology, structural materials science, engineering and technological problems)]: dis. ... Dr. Tech. Sci. Voronezh, 1988, 600 pages (in Russian).
48. **Bolotin V.V., Goldenblat I.I., Smirnov A.F.** Stroitel'naya mekhanika. Sovremennoye sostoyaniye i perspektivy razvitiya [Structural mechanics. Current state and development prospects]. Moscow, Stroyizdat, 1972, 191 pages (in Russian).
49. **Budeshtsky R.I.** Elementy teorii prochnosti zernistykh kompozitsionnykh materialov [Elements of the theory of strength of granular composite materials]. Tbilisi, Metsniereba, 1972, 82 pages (in Russian).
50. **Zaitsev Yu.V.** Uchet makro- i mikrostruktury materiala i yego fizicheskoy nelineynosti v zadachakh o razvitii treshchin v betone [Taking into account the macro- and microstructure of the material and its physical nonlinearity in problems of the development of cracks in concrete] // Izvestiye vuzov. Stroitel'stvo i arkhitektura, 1975, Issue10 11, pp.15 – 20 (in Russian).
51. **Komokhov P.G.** Fiziko-mekhanicheskiye aspekty razrusheniya betona i printsipy snizheniya yego treshchinoobrazovaniya [Physico-mechanical aspects of concrete destruction and principles of reducing its cracking] // Sovershenstvovaniye tekhnologii stroitel'nogo proizvodstva: Mezhvuz. tematich. sb. Tomsk, 1981, pp. 145 – 151 (in Russian).
52. **Voznesensky V.A., Krovyakov S.A., Lyashenko T.V.** Elementy komp'yuternogo materialovedeniya pri issledovanii betonov [Elements of computer materials science in the study of concrete] // Budivelni kon-

struktsii: Mizhvidomchiy naukovo-tekhnichniy zb., vip. 50. Kyiv, NDIBK, 1999, pp. 310 – 318 (in Russian).
53. **Askadsky A.A., Kondrashenko V.I.** Komp'yuternoye materialovedeniye polimerov. Tom 1. Atomno-molekulyarnyy uroven'. [Computer materials science of polymers. Volume 1. Atomic-molecular level]. Moscow, Nauchnyy mir, 1999, 544 pages (in Russian).
54. **Bazhenov Yu.M., Vorobyov V.A., Ilyukhin A.V.** Osnovnyye podkhody k komp'yuternomu materialovedeniyu stroitel'nykh kompozitnykh materialov [Basic approaches to computer materials science of building composite materials] // Stroitel'nyye materialy, 2006, Issue 3,. P. 71 (in Russian).
55. **Chernyshov E.M., Dyachenko E.I., Dyachenko D.E.** O neyrosetevom modelirovanii v zadachakh sistemno-strukturnogo stroitel'nogo materialovedeniya [On neural network modeling in problems of system-structural construction materials science] // Sovremennyye problemy stroitel'nogo materialovedeniya. Ivanovo, 2000, pp. 175-181 (in Russian).
56. **Danilov A.M., Korolev E.V., Smirnov V.A., Proshin A.P.** Neyrosetevyye metody issledovaniya v stroitel'nom materialovedenii [Neural network research methods in construction materials science] // Izvestiya vysshikh uchebnykh zavedeniy. Stroitel'stvo, 2003, Issue 10, pp. 28-34 (in Russian).
57. **Gusev B.V., Korolev E.V., Grishina A.N.** Modeli polidispersnykh sistem: kriterii otsenki i analiz pokazateley effektivnosti [Models of polydisperse systems: evaluation criteria and analysis of performance indicators] // Promyshlennoye i grazhdanskoye stroitel'stvo, 2018, Issue 8, pp. 31-39 (in Russian).
58. **Smirnov V.A., Korolev E.V.** Iyerarkhicheskoye modelirovaniye stroitel'nykh materialov kak dispersnykh sistem: spetsializirovannaya programmnaya realizatsiya [Hierarchical modeling of building materials as dispersed systems: specialized software implementation] // Stroitel'nyye materialy, 2019, Issue 1-2, pp. 43-53 (in Russian).
59. **Vyrovoy V.N., Dorofeev V.S., Sukhanov V.G.** Kompozitsionnyye stroitel'nyye materialy i konstruktsii: struktura, samoorganizatsiya, svoystva [Composite building materials and structures: structure, self-organization, properties]. Odessa, State. Academy of Construction and Architecture, 2010, 169 pages (in Russian).
60. **Kaprielov S.S., Sheinfeld A.V., Kardumyan G.S., Chilin I.A.** O podbore sostavov vysokokachestvennykh betonov s organomineral'nymi modifikatorami [On the selection of compositions of high-quality concrete with organomineral modifiers] // Stroitel'nyye materialy, 2017, Issue 12, pp. 58-63 (in Russian).
61. **Selyaev V.P., Selyaev P.V.** Fiziko-khimicheskiye osnovy mekhaniki razrusheniya tsementnykh kompozitov [Physicochemical foundations of fracture mechanics of cement composites]. Saransk, Mordov Publishing House. University, 2018, 220 pages (in Russian).
62. **Belov V.V., Obraztsov I.V., Smirnov M.A.** Proyektirovaniye zernovykh sostavov mineral'nykh vyazhushchikh sistem [Design of grain compositions of mineral binder systems] // Vestnik Tverskogo gosudarstvennogo tekhnicheskogo universiteta. Seriya: Stroitel'stvo. Elektrotekhnika i khimicheskiye tekhnologii, 2020, Issue 2, pp. 7-15 (in Russian).
63. **Artamonova O.V., Chernyshov E.M.** Nanomodifitsirovannyye struktury neorganicheskikh sistem tverdeniya stroitel'nykh kompozitov. [Nanomodified structures of inorganic hardening systems for building composites]. Voronezh, Nauchnaya kniga, 2022, 248 pages (in Russian).
64. **Korotkikh D.N.** Treshchinostoykost' sovremennykh tsementnykh betonov (prob-

lemy materialovedeniya i tekhnologii) [Crack resistance of modern cement concrete (problems of materials science and technology)]. Voronezh, Voronezhskiy GASU, 2014, 141 pages (in Russian).

65. **Maksimova I.N., Makridin N.I., Erofeev V.T., Skachkov Yu.P.** Struktura i prochnost' konstruktsionnykh tsementnykh kompozitov [Structure and strength of structural cement composites]. Saransk, 2015, 360 pages (in Russian).
66. **Chernyshov E.M., Makeev A.I., Korotkikh D.N.** Bazovyye polozheniya mekhaniki proyavleniya konstruktsionnykh svoystv konglomeratnykh stroitel'nykh kompozitov. Chast' 1. Obzor rezul'tatov teoreticheskikh issledovaniy problemy konstruirovaniya i sinteza struktur sovremennykh vysokotekhnologichnykh betonov [Basic principles of the mechanics of manifestation of the structural properties of conglomerate building composites. Part 1. Review of the results of theoretical studies of the problem of design and synthesis of structures of modern high-tech concrete] // Izvestiya vuzov. Stroitel'stvo, 2020, Issue 8, pp. 43-51 (in Russian).
67. **Slavcheva G.S., Chernyshov E.M.** Algoritm konstruirovaniya struktury tsementnykh penobetonov po kompleksu zadavayemykh svoystv [Algorithm for designing the structure of cement foam concrete based on a set of specified properties] // Stroitel'nyye materialy, 2016, Issue 9, pp. 58-64 (in Russian).
68. **Chernyshov E.M., Makeev A.I.** K razvitiyu teorii konstruirovaniya i sinteza struktur konglomeratnykh stroitel'nykh kompozitov [Towards the development of the theory of design and synthesis of structures of conglomerate building composites] // Fundamental'nyye, poiskovyye i prikladnyye issledovaniya Rossiyskoy akademii arkhitektury i stroitel'nykh nauk po nauchnomu obespecheniyu razvitiya arkhitektury, gradostroitel'stva i stroitel'noy otrasli Rossiyskoy Federatsii v 2019 godu : Sb. nauch. tr. RAASN, Vol. 2, Moscow, Izdatel'stvo ASV, 2020, pp. 482 - 502 (in Russian).
69. **Anitescu C, Atroshchenko E, Alajlan N, Rabczuk T.** Artificial neural network methods for the solution of second order boundary value problems // Computers, Materials & Continua, 2019, Vol. 59(1), pp. 345-359.
70. **Wittmann F.H., Martinola G.** Optimisation of concrete properties by neural networks // Concrete 2000 - economic and durable construction through exellence: Proc. Int. Conf., London, E & FN Spon, 1993, pp. 1889-1898.
71. **Shishcgaran A, Varaee H, Rabczuk T, Shishcgaran G.** High correlated variables creator machine: Prediction of the compressive strength of concrete // Computers & Structures, 2021, Vol. 247, p. 106479.
72. **Asteris P G, Ashrafian A, Rezaic-Balf M.** Prediction of the compressive strength of self-compacting concrete using surrogate models // Computers and Concrete, 2019, Vol. 24, pp. 137-150.
73. **Nguyen T., Pham Duy H., Pham Thanh T., Vu H.** Compressive strength evaluation of fiber-reinforced high-strength selfcompacting concrete with artificial intelligence // Advances in Civil Engineering, 2020, e30l2139.
74. **Saha P, Prasad M L V, Kuraar P.R.** Predicting strength of SCC using artificial neural network and multivariable regression analysis // Computers and Concrete, 2017, Vol 20(I), pp. 31-38.
75. **Mashhadban H, Kutanaei S., Sayarincjad M.** Prediction and modeling of mechanical properties in fiber reinforced selfcompacting concrete using particle swarm optimization algorithm and artificial neural network // Construction & Building Materials, 2016, Vol. 119, pp. 277-287.
76. **Mai H.-V.T., Nguyen M.H., Trinh S.H., Ly H.-B.** Optimization of machine learning models for predicting the compressive strength of fiber-reinforced self-compacting concrete // Frontiers of Structural and Civil

Engineering, 2023, doi.org/10.1007/s11709-022-0901-6

77. **Balykov A.S., Kaledina E.A., Volodin S.V.** Prognozirovaniye prochnosti pri szhatii i proyektirovaniye sostavov konstruktsionnykh legkikh betonov s primeneniyem metodov mashinnogo obucheniya [Prediction of compressive strength and design of compositions of structural lightweight concrete using machine learning methods] // Nanotekhnologii v stroitel'stve, 2023, Vol. 15, Issue 2, pp. 171–186 (in Russian).
78. **Naser M.Z.** Digital twin for next gen concretes: On-demand tuning of vulnerable mixtures through Explainable and Anomalous Machine Learning // Cement and Concrete Composites, 2022, Vol. 132, art. no. 104640.
79. **Lyashenko T.V.** O neyronnykh setyakh i eksperimental'no-statisticheskom modelirovanii [About neural networks and experimental-statistical modeling] // Modeling and Optimization of Building Composites. - Odessa, 2016. - pp. 86-90 (in Russian).
80. **Eliaš J., Vorechovsky´ M., Skocek J., Bazant Z.P.** Stochastic discrete meso-scale simulations of concrete fracture: Comparison to experimental data // Engineering Fracture Mechanics, 2015, Vol. 135, pp. 1–16.
81. **Xiong Q.A., Wang X., Jivkov A.P.** 3D multi-phase meso-scale model for modelling coupling of damage and transport properties in concrete // Cement and Concrete Composites, 2020, Vol. 109, P. 103545.
82. **Contrafatto L., Cuomo M., Gazzo S.** A concrete homogenisation technique at meso-scale level accounting for damaging behaviour of cement paste and aggregates // Computers & Structures, 2016, Vol. 173, pp. 1-18.
83. **Shams M.Z.** Multi-Scale Modeling of Particle Reinforced Concrete Through Finite Element Analysis: Theses and Dissertations, 2016, Paper 1202, https://dc.uwm.edu/etd/1202
84. **Stroeven P., Stroeven M.** Dynamic Computer Simulation of Concrete on different Levels of the Microstructure – Part 1 // Image Analysis and Stereology, 2003, Issue 22, pp. 91-95.
85. **Homel M.A., Iyer J., Herbold E.B., Semnani S.J.** Mesoscale model and X-ray computed micro-tomographic imaging of damage progression in ultra-high-performance concrete // Cement and Concrete Research, 2022, Vol. 157, P. 106799.
86. **Zhang J., Zhang M., Dong B., Ma H.** Quantitative evaluation of steel corrosion induced deterioration in rubber concrete by integrating ultrasonic testing, machine learning and mesoscale simulation // Cement and Concrete Composites, 2022, Vol. 128, P. 104426.
87. **Imran Waris M., Ahmad A., Plevris V. [et al.]** An alternative approach for measuring the mechanical properties of hybrid concrete through image processing and machine learning // Construction and Building Materials, 2022, Vol. 328, P. 126899.
88. **Li K., Shui Z. H., Dai W.** Molecular dynamic simulation of structural and mechanical properties of cement hydrates: from natural minerals to amorphous phases // Materials Research Innovations, 2012, Vol. 16, Issue 5, pp. 338-344.
89. **Kulik D.A., Miron G.D., Lothenbach B.** A structurally-consistent CASH+ sublattice solid solution model for fully hydrated C-S-H phases: Thermodynamic basis, methods, and Ca-Si-H2O core sub-model // Cement and Concrete Research, 2022, Vol. 151, P. 106585.
90. **Valavi M., Casar Z., Bowen P. [et al.]** Molecular dynamic simulations of cementitious systems using a newly developed force field suite ERICA FF // Cement and Concrete Research, 2022, Vol. 154, P. 106712.
91. **Bazhenov Yu.M., Vorobyov V.A., Ilyukhin A.V. [et al.]** Komp'yuternoye materialovedeniye stroitel'nykh kompozitnykh materialov. [Computer materials science of

building composite materials]. Moscow, Izd-vo Rossiyskoy inzhenernoy akademii, 2006, 256 pages (In Russia).

92. **Magdeev U.Kh., Morozov V.I., Pukharenko Yu.V.** K matematicheskoy postanovke zadachi ob opredelenii osesimmetrichnykh deformatsiy konstruktsiy iz neodnorodno ortotropnykh materialov [Towards a mathematical formulation of the problem of determining axisymmetric deformations of structures made of inhomogeneous orthotropic materials] // Fundamental, search and applied research of the RAASN on scientific support for the development of architecture, urban planning and the construction industry of the Russian Federation in 2016: Collection of scientific papers of the RAASN. Moscow, ASV Publishing House, 2017. pp. 227-230 (in Russian).
93 **Selyaev V.P., Selyaev P.V., Lazarev A.L. [et al.]** Fraktal'naya kvantovo-mekhanicheskaya model' deformirovaniya i razrusheniya betona [Fractal quantum mechanical model of deformation and destruction of concrete] // Regional'naya arkhitektura i stroitel'stvo, 2022, Issue 4, pp. 31-40 (in Russian).
94. **Chernyshov E.M. Makeev A.I.** Materialovedeniye i tekhnologiya stroitel'nykh kompozitov kak sistema nauchnogo znaniya i predmet razvitiya issledovaniy. Chast' 3. Sistemnaya identifikatsiya "konstruktsii struktury" konglomeratnykh stroitel'nykh kompozitov (v kachestvennoy postanovke problemy) [Materials science and technology of building composites as a system of scientific knowledge and a subject of research development. Part 3. System identification of the “structure design” of conglomerate building composites (in a qualitative formulation of the problem)] // Izvestiya vysshikh uchebnykh zavedeniy. Stroitel'stvo, 2021, Issue 3, pp. 5-26 (in Russian).
95. **Chernyshov E.M., Makeev A.I.** Universalii stroitel'nykh kompozitov kak strukturirovannykh tverdykh tel [Universals of building composites as structured solids] // Izvestiya vuzov. Stroitel'stvo, 2021, Issue 11, pp. 37-54 (in Russian).
96. Current problems of numerical modeling of buildings, structures and complexes. Vol. 2. To the 25th anniversary of the StaDiO Research Center / Under the general direction. ed. A.M. Belostotsky and P.A. Akimova. Moscow, Publishing house ASV, 2016, 596 pages (in Russian).

СПИСОК ЛИТЕРАТУРЫ

1. **Травуш В.И.** Цифровые технологии в строительстве // Academia. Архитектура и строительство, 2018. № 3. С. 107-117
2. Информатика в строительстве (с основами математического и компьютерного моделирования) / коллектив авторов ; под. ред. П.А. Акимова. - М.: КНОРУС, 2017. 420 с.
3. **Макеев А.И.** Методологические основания теории конструирования и синтеза оптимальных структур конгломератных строительных композитов // Научный вестник ВГАСУ. Серия: Физико-химические проблемы и высокие технологии строительного материаловедения, 2015. - №1. С. 29-37
4. **Карпенко Н.И.** Общие модели механики бетона. М.: Стройиздат, 1996. 416 с.
5. **Кондращенко В.И.** Некоторые аспекты компьютерного материаловедения // Моделирование и оптимизация композитов : Мат. к междунар. семинару, посвящ. 80-летию В.А. Вознесенского. Одесса: Астропринт, 2014. С. 64-68
6. **Чернышов Е.М., Макеев А.И.** К моделированию напряженного состояния структурно-неоднородных конгломератных композитов в строительных конструкциях // Международный журнал по расчету гражданских и строительных конструкций. 2015. Т. 11, № 2. С. 160-170
7. **Баженов Ю.М., Гарькина И.А., Данилов А.М., Королев Е.В.** Системный

анализ в строительном материаловедении. - М: МГСУ, 2012. 432 с.
8. **Будылина Е.А., Гарькина И. А., Данилов А. М.** Общая схема идентификации и синтеза строительных материалов // Региональная архитектура и строительство, 2022. № 4(53). С. 26-30.
9. **Чернышов Е.М.** Материаловедение и технология строительных композитов как система научного знания и предмет развития исследований. Часть 2. Развитие и эволюция научного знания о конгломератных строительных композитах как структурированных системах // Известия высших учебных заведений. Строительство. 2020. № 1. С. 57-77.
10. **Чернышов Е.М., Макеев А.И.** О проблеме развития, эволюции «цифрового подхода» в материаловедении и технологии строительных композитов // Современная наука: теория, методология, практика: Мат-лы III всероссийской (национальной) научно-практической конференции. Тамбов: Изд-во ИП Чесноков А.В., 2021. С. 9-21.
11. **Денисов Ф.А.** Пространное руководство к общей технологии или к познанию всех работ, средств, орудий и машин, употребляемых в разных химических искусствах. - М., 1828. 548 с.
12. **Менделеев Д.И.** Основы фабрично-заводской промышленности. - С-Пб: Тип. В. Демакова, 1897. 201 с.
13. **Тищенко И.А.** Основные процессы и аппараты химической технологии. Вып. I : Общее введение. Измельчение и измельчающие аппараты. - М. : Типо-Лит. И. Х. Кавыкина, 1913. 161 с.
14. **Walker W.H., Lewis W.K., McAdams W.H.** Principles of chemical engineering. - London: McGraw-Hill Publising Co., ltd, 1923. 631 p.
15. **Бэджер В., Мак-Кэб В.** Основные процессы и аппараты химических производств. - Москва ; Ленинград : Госхимтехиздат, 1933. 476 с.
16. **Касаткин А.Г.** Основные процессы и аппараты химической технологии. - М.: «Химия», 1973. 752 с.
17. **Малюга И.Г.** Состав и способ приготовления цементного раствора (бетона) для получения наибольшей крепости. - С-Пб : тип. и лит. В.А. Тиханова, 1895. 201 с.
18. **Житкевич Н.А.** Бетон и бетонные работы. - СПб, 1912. 524 с.
19. **Эвальд В.В.** Строительные материалы. Их приготовление, свойства и испытания. - М.: Гос. науч-техн. изд-во, 1931. 510 с.
20. **Значко-Яворский И.Л** Очерки истории вяжущих веществ от древнейших времен до середины XIX века. – Л.: Изд-во АН СССР, 1963. 496 с.
21. **Богданов А.А.** Всеобщая организационная наука (тектология) / 3-е изд. Ч. 1–3. - М.; Л.: 1929. 220 с.
22. **Берталанфи Л.** Общая теория систем - обзор проблем и результатов // Системные исследования. Ежегодник. - М.: «Наука», 1969. С. 34-35.
23. Исследования по общей теории систем // Сб. переводов под ред. В.Н. Садовского и Э.Г. Юдина. - М.: Прогресс, 1969. - 519 с.
24. **Карман Т., Био М.** Математические методы в инженерном деле / Пер с англ., 2-е изд. - М.-Л.: Гос. изд-во технико-теоретич. лит-ры, 1948. 424 с.
25. **Скрамтаев Б.Г.** Теория прочности бетона. Новые виды бетонов / Доклады, прочитанные на Всеукр. конференции по бетону и железобетону 17-19 июня 1933 г. - Харьков : Гос.-науч. техн. изд-во Украины, 1933. 55 с.
26. **Юнг В.Н.** Введение в технологию цемента. – М. ; Л. : Госстройиздат, 1938. 404 с.
27. **Михайлов В.В.** Элементы теории структуры бетонов. – М.; Л. : Гос. изд. строит. лит., 1941. 227 с.
28. **Шейкин А.Е.** Теория упругости, прочности, пластичности бетона. -М.: НИИЖБ, 1944. 250 с.
29. **Винер Н.** Кибернетика, или Управление и связь в животном и машине. – М.: Наука, 1983. 344 с.

30. **Оптнер С.Л.** Системный анализ для решения деловых и промышленных проблем / Пер. с англ. - М.: Советское радио, 1968. 216 с.
31. **Кафаров В.В.** Методы кибернетики в химии и химической технологии. - М.: Химия, 1968. 379 с.
32. **Фишер Р.** Статистические методы для исследователей. - М.: Госстатиздат, 1958. 267 с.
33. **Адлер Ю.П., Маркова Е.В., Грановский Ю.В.** Планирование эксперимента при поиске оптимальных условий. - М.: Наука, 1976. 280 с.
34. **Ахназарова С.Л., Кафаров В.В.** Методы оптимизации эксперимента в химической технологии. - М.: Высш. шк., 1985. 327 с.
35. **Вознесенский В. А., Выровой В. Н., Керш В. Я. и др**. Современные методы оптимизации композиционных материалов / Под ред. В. А. Вознесенского. - Киев : Будівельник, 1983. 144 с.
36. **Ляшенко Т.В.** Оптимизация наполнителей полиэфирных связующих на основе моделей нового класса: дис.... канд. техн. наук. - Одесса, 1984. 236 с.
37. **Шинкевич Е.С.** Оптимизация структуры ячеистого силикатного бетона по комплексу критериев качества на основе изопараметрического анализа: дис. ... канд. техн. наук. – Красково, 1985. 249 с.
38. **Баженов Ю.М.** Бетон при динамическом нагружении. – М.: Стройиздат, 1970. 272 с.
39. **Ратинов В.Б., Розенберг Т.И.** Добавки в бетон. М.: Стройиздат, 1973. 207 с.
40. **Мельниченко П.А.** Структурно-статистический подход к решению задачи управляемого структурообразования композитов // Снижение материалоемкости и повышение долговечности строительных изделий. - Киев: Будивельник, 1974. С. 66-76.
41. **Ребиндер П.А.** Поверхностные явления в дисперсных системах. Физико-химическая механика. Избранные труды. – М.: Наука, 1979. 384 с.
42. **Ахвердов И.Н.** Основы физики бетона. – М.: Стройиздат, 1981. 464 с.
43. **Подвальный А.М.** Определение величины собственных деформаций в бетонном конгломерате на различных структурных уровнях // Заводская лаборатория, 1973. №10. С. 1204 – 1206.
44. **Шейкин А.Е., Чеховский Ю.В., Бруссер М.И.** Структура и свойства цементных бетонов. М.: Стройиздат, 1979. 344 с.
45. **Рыбьев И.А., Нехорошев А.В.** Исходные методические позиции при исследовании искусственных строительных конгломератов // Строительные материалы, 1980. №2. С. 24 – 26.
46. **Соломатов В.И.** Элементы общей теории композиционных строительных материалов // Известие вузов. Строительство и архитектура, 1980. №8. С. 61 – 70.
47. **Чернышов Е.М.** Управление процессами структурообразования и качеством силикатных автоклавных материалов (вопросы методологии, структурное материаловедение, инженерно-технологические задачи) : дис. … д-ра техн. наук. - Воронеж, 1988. 600 с.
48. **Болотин В.В., Гольденблат И.И., Смирнов А.Ф.** Строительная механика. Современное состояние и перспективы развития. М.: Стройиздат, 1972. 191 с.
49. **Будештский Р.И.** Элементы теории прочности зернистых композиционных материалов. Тбилиси: Мецниереба, 1972. 82 с.
50. **Зайцев Ю.В.** Учет макро- и микроструктуры материала и его физической нелинейности в задачах о развитии трещин в бетоне // Известие вузов. Строительство и архитектура, 1975. № 11. С.15 – 20.
51. **Комохов П.Г.** Физико-механические аспекты разрушения бетона и принципы снижения его трещинообразования // Совершенствование технологии строительного производства: Межвуз. тематич. сб. – Томск, 1981. С. 145 – 151.
52. **Вознесенский В.А., Кровяков С.А., Ляшенко Т.В.** Элементы компьютерного материаловедения при исследовании бе-

тонов // Будівелні конструкції: Міжвідомчий науково-технічний зб., вип. 50. – Київ: НДІБК, 1999. С. 310 – 318
53. **Аскадский А.А., Кондрашенко В.И.** Компьютерное материаловедение полимеров. Том 1. Атомно-молекулярный уровень. - М.: Научный мир, 1999. 544 с.
54. **Баженов Ю.М., Воробьев В.А., Илюхин А.В.** Основные подходы к компьютерному материаловедению строительных композитных материалов // Строительные материалы, 2006. № 3. С. 71
55. **Чернышов Е.М., Дьяченко Е.И., Дьяченко Д.Е.** О нейросетевом моделировании в задачах системно-структурного строительного материаловедения // Современные проблемы строительного материаловедения. - Иваново, 2000. С. 175-181
56. **Данилов А.М., Королев Е.В., Смирнов В.А., Прошин А.П.** Нейросетевые методы исследования в строительном материаловедении // Известия высших учебных заведений. Строительство, 2003. № 10. С. 28-34.
57. **Гусев Б.В., Королев Е. ., Гришина А.Н.** Модели полидисперсных систем: критерии оценки и анализ показателей эффективности // Промышленное и гражданское строительство, 2018. № 8. С. 31-39.
58. **Смирнов В.А., Королев Е.В.** Иерархическое моделирование строительных материалов как дисперсных систем: специализированная программная реализация // Строительные материалы, 2019. № 1-2. С. 43-53.
59. **Выровой В.Н., Дорофеев В.С., Суханов В.Г.** Композиционные строительные материалы и конструкции: структура, самоорганизация, свойства. – Одесса: Одесская гос. академия стр-ва и архитектуры, 2010. 169 с.
60. **Каприелов С.С., Шейнфельд А.В., Кардумян Г.С., Чилин И.А.** О подборе составов высококачественных бетонов с органоминеральными модификаторами // Строительные материалы, 2017. № 12. С. 58-63.
61. **Селяев В.П., Селяев П.В.** Физико- химические основы механики разрушения цементных композитов. – Саранск: Изд-во Мордов. ун-та, 2018. 220 с.
62. **Белов В.В., Образцов И.В., Смирнов М.А.** Проектирование зерновых составов минеральных вяжущих систем // Вестник Тверского государственного технического университета. Серия: Строительство. Электротехника и химические технологии, 2020. № 2. С. 7-15.
63. **Артамонова О.В., Чернышов Е.М.** Наномодифицированные структуры неорганических систем твердения строительных композитов. - Воронеж: Научная книга, 2022. 248 с.
64. **Коротких Д.Н.** Трещиностойкость современных цементных бетонов (проблемы материаловедения и технологии). Воронеж, Воронежский ГАСУ, 2014. 141 с.
65. **Максимова И.Н., Макридин Н.И., Ерофеев В.Т., Скачков Ю.П.** Структура и прочность конструкционных цементных композитов. - Саранск, 2015. 360 с.
66. **Чернышов Е.М., Макеев А.И., Коротких Д.Н.** Базовые положения механики проявления конструкционных свойств конгломератных строительных композитов. Часть 1. Обзор результатов теоретических исследований проблемы конструирования и синтеза структур современных высокотехнологичных бетонов // Известия вузов. Строительство, 2020. № 8. С. 43-51
67. **Славчева Г.С., Чернышов Е.М.** Алгоритм конструирования структуры цементных пенобетонов по комплексу задаваемых свойств // Строительные материалы, 2016. № 9. С. 58-64.
68. **Чернышов Е.М., Макеев А.И.** К развитию теории конструирования и синтеза структур конгломератных строительных композитов // Фундаментальные, поисковые и прикладные исследования Российской академии архитектуры и строительных наук по научному обеспечению развития архитектуры, градостроительства и строительной отрасли Российской

Федерации в 2019 году : Сб. науч. тр. РААСН. Т. 2. – М.: Издательство АСВ, 2020. С. 482 - 502 с.

69. **Anitescu C, Atroshchenko E, Alajlan N, Rabczuk T.** Artificial neural network methods for the solution of second order boundary value problems // Computers, Materials & Continua, 2019. V. 59(1). pp. 345-359
70. **Wittmann F.H., Martinola G.** Optimisation of concrete properties by neural networks // Concrete 2000 - economic and durable construction through exellence: Proc. Int. Conf. - London: E & FN Spon, 1993. - P. 1889-1898.
71. **Shishcgaran A, Varaee H, Rabczuk T, Shishcgaran G.** High correlated variables creator machine: Prediction of the compressive strength of concrete // Computers & Structures, 2021. V. 247. p. 106479
72. **Asteris P G, Ashrafian A, Rezaic-Balf M.** Prediction of the compressive strength of self-compacting concrete using surrogate models // Computers and Concrete, 2019. V.24. pp. 137-150
73. **Nguyen T., Pham Duy H., Pham Thanh T., Vu H.** Compressive strength evaluation of fiber-reinforced high-strength selfcompacting concrete with artificial intelligence // Advances in Civil Engineering, 2020. e30l2139
74. **Saha P, Prasad M L V, Kuraar P.R.** Predicting strength of SCC using artificial neural network and multivariable regression analysis // Computers and Concrete, 2017. V.20(I). pp. 31-38
75. **Mashhadban H, Kutanaei S., Sayarincjad M.** Prediction and modeling of mechanical properties in fiber reinforced selfcompacting concrete using particle swarm optimization algorithm and artificial neural network // Construction & Building Materials, 2016. V.119. pp. 277-287
76. **Mai H.-V.T., Nguyen M.H., Trinh S.H., Ly H.-B.** Optimization of machine learning models for predicting the compressive strength of fiber-reinforced self-compacting concrete // Frontiers of Structural and Civil Engineering, 2023. doi.org/10.1007/s11709-022-0901-6
77. **Балыков А.С., Каледина Е.А., Володин С.В.** Прогнозирование прочности при сжатии и проектирование составов конструкционных легких бетонов с применением методов машинного обучения // Нанотехнологии в строительстве. 2023. Т. 15, № 2. С. 171–186.
78. **Naser M.Z.** Digital twin for next gen concretes: On-demand tuning of vulnerable mixtures through Explainable and Anomalous Machine Learning // Cement and Concrete Composites, 2022. Vol. 132, art. no. 104640. DOI: 10.1016/j.cemconcomp.2022.104640
79. **Ляшенко Т.В.** О нейронных сетях и экспериментально-статистическом моделировании // Modelling and Optimization of Building Composites. - Одесса, 2016. С. 86-90.
80. **Eliaš J., Vorechovsky´ M., Skocek J., Bazant Z.P.** Stochastic discrete meso-scale simulations of concrete fracture: Comparison to experimental data // Engineering Fracture Mechanics, 2015. V.135. Pp. 1–16
81. **Xiong Q.A., Wang X., Jivkov A.P.** 3D multi-phase meso-scale model for modelling coupling of damage and transport properties in concrete // Cement and Concrete Composites, 2020. Vol. 109. P. 103545.
82. **Contrafatto L., Cuomo M., Gazzo S.** A concrete homogenisation technique at meso-scale level accounting for damaging behaviour of cement paste and aggregates // Computers & Structures, 2016. V. 173. P. 1-18.
83. **Shams M.Z.** Multi-Scale Modeling of Particle Reinforced Concrete Through Finite Element Analysis: Theses and Dissertations, 2016. Paper 1202. https://dc.uwm.edu/etd/1202
84. **Stroeven P., Stroeven M.** Dynamic Computer Simulation of Concrete on different Levels of the Microstructure – Part 1 // Image Analysis and Stereology, 2003. №22. pp. 91-95. DOI: 10.5566/ias.v22.p91-95
85. **Homel M.A., Iyer J., Herbold E.B., Semnani S.J.** Mesoscale model and X-ray computed micro-tomographic imaging of dam-

age progression in ultra-high-performance concrete // Cement and Concrete Research, 2022. Vol. 157. P. 106799.
86. **Zhang J., Zhang M., Dong B., Ma H.** Quantitative evaluation of steel corrosion induced deterioration in rubber concrete by integrating ultrasonic testing, machine learning and mesoscale simulation // Cement and Concrete Composites, 2022. Vol. 128. P. 104426.
87. **Imran Waris M., Ahmad A., Plevris V. [et al.]** An alternative approach for measuring the mechanical properties of hybrid concrete through image processing and machine learning // Construction and Building Materials, 2022. Vol. 328. P. 126899.
88. **Li K., Shui Z. H., Dai W.** Molecular dynamic simulation of structural and mechanical properties of cement hydrates: from natural minerals to amorphous phases // Materials Research Innovations, 2012 . Vol 16. № 5. pp. 338-344
89. **Kulik D.A., Miron G.D., Lothenbach B.** A structurally-consistent CASH+ sublattice solid solution model for fully hydrated C-S-H phases: Thermodynamic basis, methods, and Ca-Si-H2O core sub-model // Cement and Concrete Research, 2022. Vol. 151. P. 106585.
90. **Valavi M., Casar Z., Bowen P. [et al.]** Molecular dynamic simulations of cementitious systems using a newly developed force field suite ERICA FF // Cement and Concrete Research, 2022. Vol. 154. P. 106712.
91. **Баженов Ю.М., Воробьев В.А., Илюхин А.В. [и др.]** Компьютерное материаловедение строительных композитных материалов. - М.: Изд-во Российской инженерной академии, 2006. 256 с.
92. **Магдеев У.Х., Морозов В.И., Пухаренко Ю.В.** К математической постановке задачи об определении осесимметричных деформаций конструкций из неоднородно ортотропных материалов // Фундаментальные, поисковые и прикладные исследования РААСН по научному обеспечению развития архитектуры, градостроительства и строительной отрасли Российской Федерации в 2016 году : Сборник научных трудов РААСН / Российская академия архитектуры и строительных наук. – Москва : Издательство АСВ, 2017. С. 227-230.
93 **Селяев В.П., Селяев П.В., Лазарев А.Л. [и др.]** Фрактальная квантово-механическая модель деформирования и разрушения бетона // Региональная архитектура и строительство, 2022. № 4(53). С. 31-40.
94. **Чернышов Е.М. Макеев А.И.** Материаловедение и технология строительных композитов как система научного знания и предмет развития исследований. Часть 3. Системная идентификация "конструкции структуры" конгломератных строительных композитов (в качественной постановке проблемы) // Известия вузов. Строительство, 2021. № 3(747). С. 5-26.
95. **Чернышов Е.М., Макеев А.И.** Универсалии строительных композитов как структурированных твердых тел // Известия вузов. Строительство, 2021. № 11. С. 37-54.
96. Актуальные проблемы численного моделирования зданий, сооружений и комплексов. Том 2. К 25-летию Научно-исследовательского центра СтаДиО: Монография / Под общ. ред. А.М. Белостоцкого и П.А. Акимова. – М.: Изд-во АСВ, 2016. 596 с.

Aleksey I. Makeev, Ph.D. tech. sciences, Associate Professor, Associate Professor of the Department of Technology of Building Materials, Products and Structures, Voronezh State Technical University, 84, st. 20th Anniversary of October, Voronezh, 394006, Russia; E-mail: makeev@vgasu.vrn.ru

Макеев Алексей Иванович, канд. техн. наук, доцент, доцент кафедры технологии строительных материалов, изделий и конструкций ФГБОУ ВО "Воронежский государственный технический университет", 84, ул. 20-летия Октября, Воронеж, 394006, Россия; E-mail: makeev@vgasu.vrn.ru

International Journal for Computational Civil and Structural Engineering, 19(4) 116–123 (2023)

DOI:10.22337/2587-9618-2023-19-4-116-123

CALCULATION MODEL OF DEFORMATION OF THE SOIL FOUNDATION OF A HIGH-RISE BUILDING, TAKING INTO ACCOUNT THE LOADING HISTORY

Ilizar T. Mirsayapov, Irina V. Korolev

Kazan State University of Architecture and Engineering, Kazan, RUSSIA

Abstract: While designing high-rise buildings, it is necessary to take into account the influence of stages of their erection, this is the sequence of loading, on the change in physical-mechanical properties of soils. The calculation of deformations of subgrade is made with due regard for the change in soils properties comparing with the initial (natural) state. On the basis of the results of experimental studies, the authors substantiate the necessity for introducing the new parameter which makes it possible to characterize the mechanical condition of the soil at any stage of loading and can be used for creating calculation models. An analytical diagram of soil deformation in coordinates «σ_1–ε_1» for triaxial compression (where σ_1 – vertical stresses (deviator), ε_1 – linear deformations under the triaxial compression) is adopted as this parameter. The procedure for constructing transformed diagrams of the soil state under the long performance triaxial loading is described. The procedure obtained was approbated when calculating deformations of the foundation base of the high-rise building with due regard for the influence of staging of construction and rheological properties of soils on the change in the base rigidity and, as a result, on the redistribution of stresses among separate elements of the system "subgrade –foundation – upper part of the building.

Keywords: long regime triaxial loading, analytical diagram of soil deformation, coefficient of subgrade resistance, settlement calculation, high-rise building

РАСЧЕТНАЯ МОДЕЛЬ ДЕФОРМИРОВАНИЯ ГРУНТОВОГО ОСНОВАНИЯ ВЫСОТНОГО ЗДАНИЯ С УЧЕТОМ ПРЕДЫСТОРИИ ЗАГРУЖЕНИЯ

И.Т. Мирсаяпов, И.В. Королева

Казанский государственный архитектурно-строительный университет, г. Казань, РОССИЯ

Аннотация: при проектировании высотных зданий необходимо учитывать влияние этапов их возведения, т. е. последовательности загружения основания, на изменение физико-механических свойств грунтов оснований. Расчет деформаций оснований фундаментов следует выполнять с учетом изменения свойств грунтов по сравнению с первоначальным (природным) состоянием. По результатам экспериментальных исследований авторами обоснована необходимость введения нового параметра, который позволил бы охарактеризовать механическое состояние грунта на любом этапе нагружения и мог использоваться при создании расчетных моделей. В качестве такого параметра принимается аналитическая диаграмма деформирования грунта в координатах σ_1–ε_1 для трехосного сжатия (где σ_1 – вертикальные напряжения (девиатор), ε_1 – линейные деформации при трехосном сжатии). Описана методика построения трансформированных диаграмм состояния грунта при длительном режимном трехосном нагружении. Полученная методика была апробирована при расчете деформаций основания фундамента высотного здания с учетом влияния этапности строительства и реологических свойств грунтов на изменение жесткости основания и, как следствие, на перераспределение усилий между отдельными элементами системы «грунтовое основание – фундамент – надземная часть здания».

Ключевые слова: длительное режимное трехосное нагружение, аналитическая диаграмма деформирования грунта, коэффициент постели, расчет осадки, высотное здание.

INTRODUCTION

Soil bases of foundations of buildings and structures are exposed to various static and dynamic loads under various combinations of these loads. The existing methods of deformation calculation of foundations are developed for a single short-term static loading with constant parameters for the entire period of operation. In real conditions of construction and operation, the loads on the soil foundation are applied in stages as the building or structure is erected [1-5]. In this case, the stages of active loading during the construction period pass into the stages of long-term holding under loading.

Experimental studies (Fig. 1, 2) carried out by the authors [6-7] show that the nature of changes in soil deformations under long-term regime loading differs significantly from the results obtained under short-term static loading, which are the basis for the existing methods of settlement calculation. In this regard, there is a need to improve the methodology for calculating settlement of foundations of buildings with a developed underground part. This task is especially relevant for the foundations of high-rise buildings composed of clayey soils, the stress-strain state of which changes in time and depends on the history of previous loading [1-5].

In addition, in accordance with modern requirements, the calculation of the bases of high-rise buildings should be performed taking into account the joint deformation of the system "subgrade – building", i. e. deformations (settlement) of the subgrade of such a building should be calculated taking into account the influence of the stiffness of the elevated part of the building.

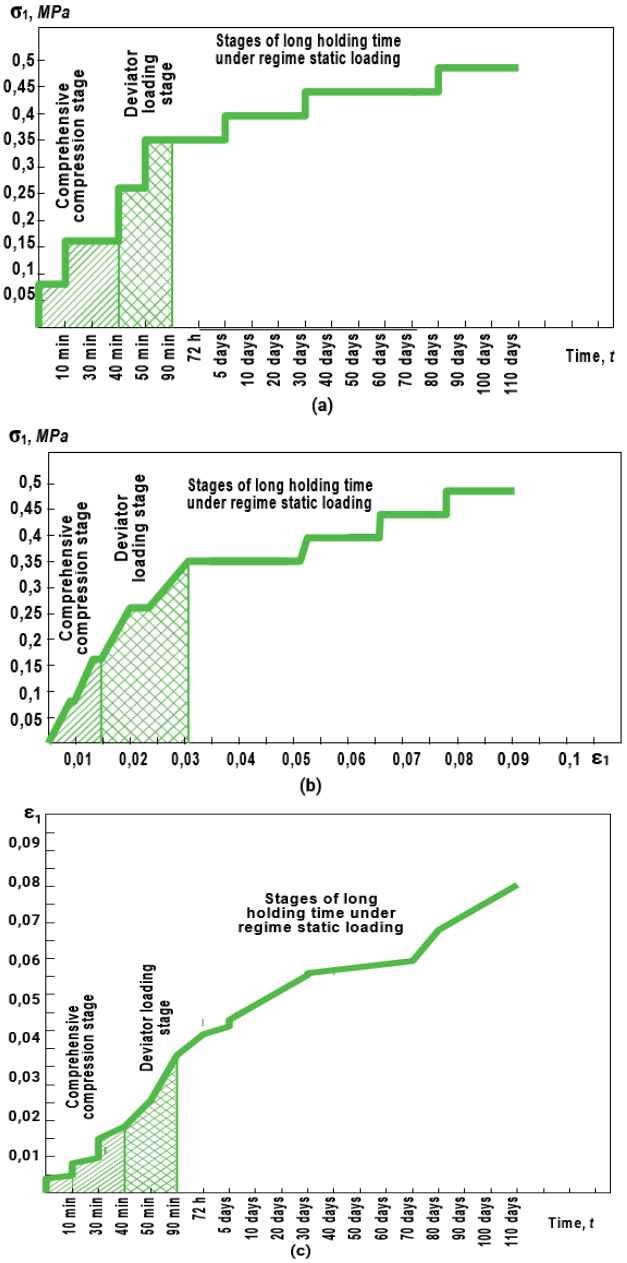


Figure 1. Results of experimental studies: a - regime of loading; b - dependence between average stresses σ_1 and relative linear strains ε_1; c - development of relative linear strains in time

MATERIALS AND METHODS

To calculate the settlement of a high-rise building taking into account the joint deformation of the above-mentioned system, the modified Pasternak method [8] was used as a basis, taking into account the spatial stress-strain state of the

base soils and changes in the rheological properties of soils under long-term regime loading.

As it is known, Pasternak's method [9] describes the performance of the soil by means of compression coefficient C_1, which relates the intensity of vertical soil pushback to its settlement, and shear coefficient C_2, which characterizes the vertical shear forces arising in loose and loosely cohesive soils due to entanglement and internal friction between its particles. These coefficients were determined according to the equation:

$$C_1 = \frac{E_{gr}}{H_c(1-2\mu_{gr})}; C_2 = \frac{C_1 \cdot H_c(1-2\mu_{gr})}{6(1+\mu_{gr})}. \quad (1)$$

Where is the Poisson's coefficient within the compressed layer:

$$\mu_{gr} = \frac{\sum_{i=1}^{n} \mu_{i \cdot h_i}}{H_c}. \quad (2)$$

When using the modified Pasternak method [6], the coefficients of subgrade resistance C_1 and C_2 were also determined according to equation (1), but to determine the average strain modulus, a correction factor u was introduced to the value of the strain modulus of the i-th sublayer. This coefficient varied according to the law of a square parabola from u = 1 at the level of the foundation footing to u = 12 at the level of the already calculated boundary of the compressible strata and was determined by the equation:

$$u = \frac{11Z^2}{H_c^2} + 1. \quad (3)$$

At the same time, the modulus of deformation of the base was calculated:

$$E_{gr} = \frac{H_c}{\sum_{i=1}^{n} \frac{h_i}{u_i \cdot E_i}}. \quad (4)$$

The authors propose to modify the modified Pasternak model. In this case, the pliable properties of base soils under such regimes are taken into account in the model by means of coefficients of subgrade resistance C_1 and C_2 variable in time, depth and in plan:

$$C_1 = \frac{E_1(t,\tau)}{H_c(1-2\mu_{gr})}; C_2 = \frac{C_1 \cdot H_c(1-2\mu_{gr})}{6(1+\mu_{gr})} \quad (5)$$

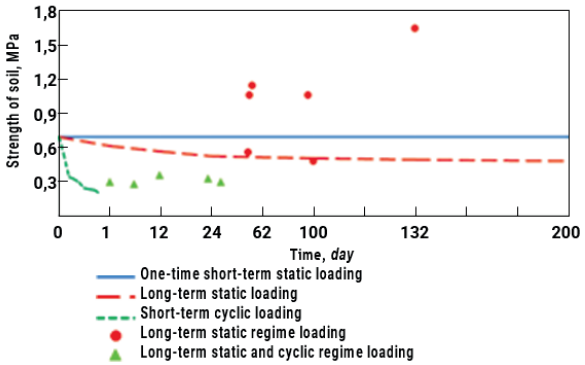


Figure 2. Variation of soil strength under different loading regimes

It is proposed to determine the deformation modulus at each point of the compressible layer on the basis of transformed deformation diagrams by the expression:

$$E_1(t,\tau) = \frac{\Delta\sigma_{1i}(t,\tau)}{\varepsilon_{1i}(t,\tau)}. \quad (6)$$

Then the soil deformation modulus for determining the variable bedding coefficient should be calculated by the equation:

$$E_1(t,\tau) = \frac{H_c}{\sum_{i=1}^{n} \frac{h_i}{E_{1i}(t,\tau)}}. \quad (7)$$

Variability coefficients of subgrade resistance is substantiated by the results of experimental studies (Figs. 1, 2) and the calculation model developed by the authors [6-7]; it was found that under step-by-step loading, all the bases of parameters characterizing the stressed and deformed state of soils change in time, which allows us to conclude that it is necessary to develop a new parameter that would characterize the mechanical state of the soil at any stage of load-

ing and could be used to create calculation models. The analytical diagram of soil deformation in coordinates σ -ε for triaxial compression is taken as such a parameter (where σ_1, ε_1 are vertical stresses (deviator) and linear strains in triaxial compression).

Based on the obtained graphs (Fig. 1), the initial diagrams (state diagrams) of soil deformation under short-term triaxial static loading are constructed. The value of temporary resistance $\sigma_1 = R_{gr,u}$ (deviator) of the soil is taken as the limit point in coordinates (σ). Under triaxial short-term static compression.

The limit point on the ordinate axis (ε) is taken as the value of linear strain ε_{u1}=0,0869. Types of diagrams are presented in Fig. 3.

When considering the state diagrams of clayey soil under triaxial long-term static loading, the deformation diagrams σ_1-ε_1 for the case of triaxial short-term static loading are used as initial ones. By transforming the initial state diagram under triaxial short-term static loading, we obtain analytical dependences to describe the deformation diagrams of clayey soil under triaxial long-term static loading. In form, the transformed diagrams are assumed to be similar to the original state diagram on the basis of the following provisions (Fig. 3).

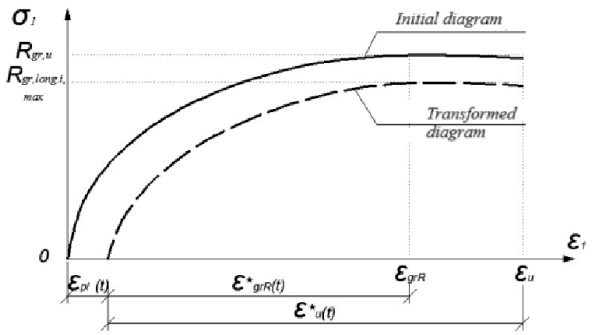


Figure 3. Initial (short-term static) and transformed (long-term static) analytical diagrams

The limiting point of vertical pressure at the top of the diagram is taken to be the stress in the soil, which is equal to the limit of long-term resistance under triaxial load action $R_{gr,long}=(t,\tau)$ and deformations corresponding to the deformations at the top of the state diagram under triaxial short-term static loading $\varepsilon_{gru,red}=\varepsilon_{gru}$;

For the limiting point defining the boundaries of the state diagrams along the ordinate axis, the deformations are equal to the limiting deformations under triaxial short-term static loading $\varepsilon_{gr,red}=\varepsilon_{gr,R}$, and the basic dependencies are used to calculate the stresses in the soil;

The start of the diagram coordinates is assumed to be shifted by the value equal to the creep deformation at the considered time ε_{pl} (t) - at long static loading;

The obtained slope angles of deformation diagrams are taken into account the change in the deformation modulus of clayey soil under triaxial long-term static loading.

In the next step, the diagram is transformed for each block long-term loading block (Fig. 4).

When describing soil deformation modes under triaxial loading, it is necessary to take into account the effect of vertical pressure (σ_1) of the previous block on the strength, strain modulus and relative strains at the top of the diagram during subsequent loading after the regime change.

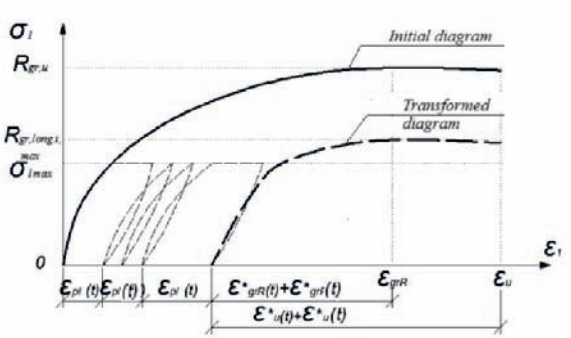


Figure 4. Initial (short-term static) and transformed (regime long-term static) analytical diagrams

On the basis of the obtained transformed analytical deformation diagrams, a method of calculating settlements of foundations of high-rise buildings has been developed, which is based on the method of layer-by-layer summation taking into account changes in the spatial stress-strain state of soils in the process of triaxial regime long-term static loading.

Based on the values obtained from the diagrams, the modulus of total soil deformations at each point of the foundation is determined (Fig. 5), and then the value of coefficient of subgrade resistance for each point is specified.

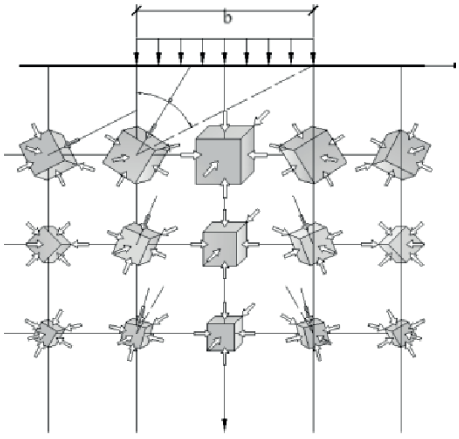


Figure 5. Spatial stress-strain state of the soil

The proposed methodology was used in the calculation of the foundation settlement of a high-rise building, which has a frame-wall system, made of monolithic reinforced concrete and has the following parameters: total height 144.9 m (39 floors); number of underground floors 4; foundation depth 15.15 m; area of foundation 1377 m^2; columns, internal and external walls of the underground part are made with concrete class B40, floor slabs B30, staircases and flights - B25; the building has a distributing technical floor with a 2100 mm thick floor slab, providing load transfer from the above-ground part to the underground part; the thickness of the foundation slab is 2000 mm (Fig. 6). Physical and mechanical characteristics of engineering and geological elements of the base are given in Table 1.

Table1. Characteristics of foundation soils

№ layer	Type of soil	ρ, kg/m3	*E*, MPa	φ, grad	*C*, kPa
Layer-6	Dense dusty sands	2030	32	36	4
Layer-7	Semi-solid clay	1960	23	23	67
Layer-8	Tightly plastic clay	1940	22	26	43
Layer-9	Solid clay	1720	25	19	86

Taking into account that after 35 and 45 months from the beginning of construction the load from the building was 75% of the full load, the following loads were taken into account in the calculation: standard load on the typical upper floor taking into account the weight of load-bearing structures 13.65 kPa; standard load on the underground floor taking into account the weight of load-bearing structures 14.35 kPa; total weight of the building without taking into account the weight of the foundation 82620 t; average pressure at the bottom of the foundation without taking into account its weight 60 t/m2; average pressure under the bottom of the foundation taking into account the weight of the foundation and the floor 64.59 t/m2. Wind pressure was not taken into account.

The settlement was calculated using the LIRA-SAP 2014 software program, which implements the finite element method [7]. At the same time, a spatial model of the whole building was created in the program structure to automatically transfer the load "base".

In the vicinity of the investigated building there is an enclosing structure in the form of a monolithic reinforced concrete "wall in the soil" 0.8 m thick and 35 m deep, providing stability of the excavation walls during the zero cycle works (Fig. 6). Taking into account that the soils below the foundation footing in the wall-in-soil zone are in constricted conditions and are subjected to greater lateral pressure during the application of vertical loads from the building, it can be assumed that the compressibility parameters of the soils will be variable. In the calculation, this was taken into account by introducing different bedding coefficients under the main area of the foundation and the zone of influence of the wall.

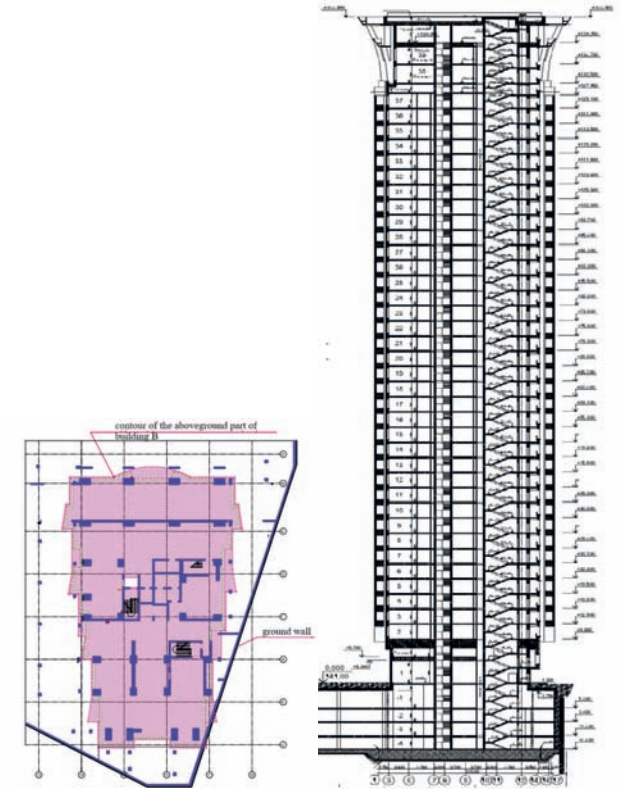


Figure 6. High-rise building of a residential (plan and section)

RESULTS AND DISCUSSIONS

The above-mentioned soil model under triaxial loading was used, taking into account the change of horizontal stresses σ_x and σ_y due to the influence of the excavation enclosing wall. The obtained calculation results are shown in Table 2 and Fig. 7.

Table2. Settlements and inclinations of foundation

N	S_{av}, mm	S_{max}, mm	S_{min}, mm	i
1	137	145	129,7	0,00026
2	135,96	147,29	124,63	0,00038
3	215	226	205	0,00035
4	214	235	193	0,00073
5	242,3	254,7	231,04	0,00035
6	241,18	264,85	217,5	0,00073

Where S_{av}, S_{max}, S_{min}, i – average, maximal, minimal settlement and inclination of foundation; 1 – in 45 month without taking into account the slurry wall and 75% of load; 2 – in 45 month with taking into account the slurry wall and 75% of load; 3 - in 45 month without taking into account the slurry wall and 100% of load; 4 – in 45 month with taking into account the slurry wall and 100% of load, 5 – in 100 years without taking into account the slurry wall and 100% of load; 6 – in 100 years with taking into account the slurry wall and 100% of load.

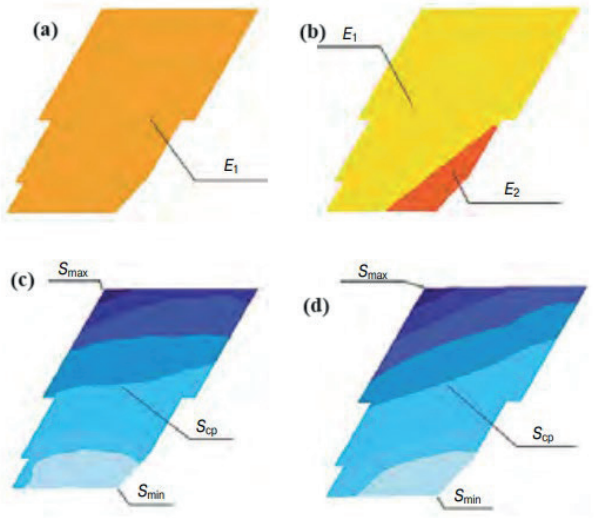


Figure. 7. Calculation results: a - calculated distribution of coefficients of subgrade resistance without taking into account the "slurry wall"; b - the same with taking into account the "slurry wall"; c, d - characteristic picture of vertical displacements of the foundation slab and the base without and with taking into account the influence of the "slurry wall"

The analysis of the results showed that the picture of foundation deformation changes qualitatively when the "slurry wall" operation is taken into account. At the same time, there is a good convergence of the calculated results with the data of geotechnical monitoring. In 45 months since construction, the deviation of the calculated values from the monitoring data on the average settlement was no more than 13%.

CONCLUSIONS

1. The methodology of calculation of deformations of high-rise buildings foundations taking into account the stage of building erection with the use of analytical diagrams of soil deformation under long-term triaxial regime loading has been developed.
2. The testing of the proposed methodology for calculating foundation settlement of a high-rise building on the basis of analytical diagrams of soil deformation allowed us to obtain calculation results with good convergence with the monitoring data. The deviation of the calculated average settlement from the real one was no more than 1% and no more than 13% with the data obtained for 35 and 45 months of monitoring, respectively.

REFERENCES

1. **Mirsayapov I.T., Koroleva I.V**. (2021) Geotekhnicheskii` prognoz vliianiia ustroi`stva svai`nogo fundamenta v ovrage na sushchestvuiushchuiu zastroi`ku [Geotechnical forecast of the influence of the installation of a pile foundation in a ravine on existing buildings], *Zhilishchnoe Stroitel'stvo [Housing Construction],* no 8, pp. 3-11. doi:10.31659/0044-4472-2021-8-3-11.
2. **Ter-Martirosyan A., Sidorov V.** Studying the influence of taking into account the elastic-plastic behavior of strut elements on the retaining system equilibrium. *IOP Conference Series: Materials Science and Engineering:* 7, Tashkent, 11–14 November 2020. Tashkent, 2021, p. 012030. doi:10.1088/1757-899X/1030/1/012030.
3. **Mangusev R.A., Penkov D.V.** (2021) Sravnenie rezul`tatov chislenny`kh raschetov s ispol`zovaniem sovremenny`kh modelei` grunta (Hardening Soil, Hardening Soil Small i Generalized Hardening Soil) s rezul`tatami monitoring [Comparison of the results of numerical calculations using modern soil models (Hardening Soil, Hardening Soil Small and Generalized Hardening Soil) with monitoring results]. *Vestnik Grazhdanskikh Inzhenerov [Bulletin of Civil Engineers],* no 2(85), pp. 85-93. doi:10.23968/1999-5571-2021-18-2-85-93.
4. **I.T. Mirsayapov, N.N. Aysin** (2022) Ocenka vliyaniya ustroystva glubokogo kotlovana na dopolnitelniye osadki zdaniy okruzhaiushchey zastroyki [Assessing the impact of constructing a deep pit on additional settlements of surrounding buildings], *News KSUAE*, no 3(61), pp. 6-13. doi:10.52409/20731523_2022_3_6.
5. **Mirsayapov I.T., Koroleva I.V.** (2020) Seismic and wind impacts on subgrade deformations of high-rise buildings. Proceedings of *the 12th International Conference on Contemporary Problems of Architecture and Construction*, *ICCPAC 2020 (Saint Petersburg , Russia, November 25–26, 2020*), pp. 221-224.
6. **Mirsayapov I.T., Koroleva I.V.** Strength and deformability of clay soil under different triaxial load regimes that consider crack formation. *Soil mechanics and foundation engineering.* 2016. No. 1, pp. 5–10.
7. **Mirsayapov I.T., Koroleva I.V.** (2014) Bearing capacity and deformation of the base of deep foundations' ground bases. *Geotechnical Aspects of Underground Construction in Soft Ground: Proc. intern. symp., Seoul, Korea, 25–27 August 201*4. Lieden: Balkema, pp. 401–404.
8. **Pasternak P.L.** Osnovy novogo metoda rascheta na uprugom osnovanii pri pomoshchi dvukh koeffitsientov posteli. [Bases of a new method of calculation on the elastic basis by means of two coefficients of a bed]. Moscow: Gosstoyizdat, 1954. 56 p.

9. **Gorodetsky A.S., Evzerov I.D.** Komp'yuternye modeli konstruktsii [Computer models of designs]. Moscow: ASV, 2009. 360 p.

СПИСОК ЛИТЕРАТУРЫ

1. **И.Т. Мирсаяпов, И.В. Королева** (2021) Геотехнический прогноз влияния устройства свайного фундамента в овраге на существующую застройку, *Жилищное строительство,* № 8, С. 3-11. doi:10.31659/0044-4472-2021-8-3-11.
2. **Ter-Martirosyan A., Sidorov V**. (2021) Studying the influence of taking into account the elastic-plastic behavior of strut elements on the retaining system equilibrium. *IOP Conference Series: Materials Science and Engineering:* 7, Tashkent, 11–14 November 2020. Tashkent, p. 012030. doi:10.1088/1757-899X/1030/1/012030.
3. **Мангушев Р.А., Пеньков Д.В**. (2021) Сравнение результатов численных расчетов с использованием современных моделей грунта (Hardening Soil, Hardening Soil Small и Generalized Hardening Soil) с результатами мониторинга. *Вестник гражданских инженеров*, № 2(85), с. 85-93. doi:10.23968/1999-5571-2021-18-2-85-93.
4. **И.Т. Мирсаяпов, Н.Н. Айсин** (2022) Оценка влияния устройства глубокого котлована на дополнительные осадки зданий окружающей застройки. *Известия Казанского государственного архитектурно-строительного университета,* № 3(61), С. 6-13. doi:10.52409/20731523_2022_3_6.
5. **Mirsayapov I.T., Koroleva I.V.** (2020) Seismic and wind impacts on subgrade deformations of high-rise buildings. Proceedings of *the 12th International Conference on Contemporary Problems of Architecture and Construction*, *ICCPAC 2020 (Санкт-Петербург, Россия, 25–26 Ноября, 2020 г*), С. 221-224.
6. **Mirsayapov I.T., Koroleva I.V.** (2016) Strength and deformability of clay soil under different triaxial load regimes that consider crack formation. *Soil mechanics and foundation engineering.* 2016. No. 1, pp. 5–10.
7. **Mirsayapov I.T., Koroleva I.V.** (2014) Bearing capacity and deformation of the base of deep foundations' ground bases, *Geotechnical Aspects of Underground Construction in Soft Ground: Proc. intern. symp., Seoul, Korea, 25–27 August 2014.* Lieden: Balkema, Pp. 401–404.
8. **Пастернак П.Л.** Основы нового метода расчета на упругом основании при помощи двух коэффициентов постели. М.: Госстройиздат, 1954. 56 с.
9. **Городецкий А.С., Евзеров И.Д.** Компьютерные модели конструкций. М.: АСВ, 2009. 360 с.

Ilizar Talgatovich Mirsayapov — doctor of technical science, professor, head of department "Bases, Subgrades, Structure Dynamics and Geology", Kazan State University of Architecture and Engineering, 1, Zelenaya st, Kazan, 420043, Russia, mirsayapov1@mail.ru, +7 917 852-14-59

Irina Vladimirovna Koroleva — Candidate of technical science, professor, Associate Professor of department "Bases, Subgrades, Structure Dynamics and Geology", Kazan State University of Architecture and Engineering, 1, Zelenaya st, Kazan, 420043, Russia, prepod-irina@yandex.ru, +7 917 871-12-18

Мирсаяпов Илизар Талгатович — доктор технических наук, профессор, заведующий кафедрой «Основания, фундаменты, динамика сооружений и инженерная геология», Казанский государственный архитектурно-строительный университет», Казанский государственный архитектурно-строительный университет, Россия, 420043, г. Казань, ул. Зеленая, 1, mirsayapov1@mail.ru

Королева Ирина Владимировна — кандидат технических наук, профессор, доцент кафедры «Основания, фундаменты, динамика сооружений и инженерная геология», Казанский государственный архитектурно-строительный университет, Россия, 420043, г. Казань, ул. Зеленая, 1, prepod-irina@yandex.ru

International Journal for Computational Civil and Structural Engineering, 19(4) 124–134 (2023)

DOI:10.22337/2587-9618-2023-19-4-124-134

DIGITAL TOOLS IN THE DESIGN PRACTICE FOR RECONSTRUCTION OF UNDERGROUND PIPELINES WITH TRENCHLESS METHODS

Vladimir A. Orlov, Sergey P. Zotkin, Dmitry V. Podolyan

National Research Moscow State University of Civil Engineering, Moscow, RUSSIA

Abstract. The article focuses on the possibilities of multi-optional design of repair and rehabilitation works on dilapidated pressure pipeline networks with the use of automated complexes in order to achieve minimum energy costs in water transportation with regard to the temperature factor. Two automated programs based on hydraulic and energy calculation operations are presented as digital tools. As a basic variant of reconstruction of dilapidated pipelines, the trenchless Swagelining technology was accepted. It is realized by pulling pre-compressed polymer pipes into old pipelines with their subsequent straightening. The paper presents information on regulatory and technical documentation and the application of advanced technology, installation and operation conditions, as well as comparative assessment of energy consumption after reconstruction of dilapidated sections of pipelines with polymer pipes with the possibility of minimizing energy consumption during water transportation under non-isothermal conditions of pipeline operation.

Keywords: automated programs, pipelines, temperature conditions, hydraulic characteristics, trenchless technologies, energy consumption

ИНСТРУМЕНТЫ ЦИФРОВИЗАЦИИ В ПРАКТИКЕ ПРОЕКТИРОВАНИЯ ПРИ РЕКОНСТРУКЦИИ ПОДЗЕМНЫХ ТРУБОПРОВОДОВ БЕСТРАНШЕЙНЫМИ МЕТОДАМИ

В.А. Орлов, С.П. Зоткин, Д.В. Подолян

Национальный исследовательский Московский государственный строительный университет, г. Москва, РОССИЯ

Аннотация. В статье рассматриваются возможности многовариантного проектирования ремонтно-восстановительных работ на ветхих напорных трубопроводных сетях с помощью автоматизированных комплексов в целях достижения минимальных энергетических затрат при транспортировке воды с учетом температурного фактора. В качестве инструментов цифровизации представлены две автоматизированные программы, в основу которых заложены операции по гидравлическим и энергетическим расчетам. За базовый вариант реконструкции ветхих трубопроводов принята бестраншейная технологии Swagelining, реализуемая путем протаскивания в старые трубопроводы предварительно сжатых полимерных труб с последующим их распрямление. Представлены сведения по нормативной и технической документации и области применения передовой технологии, условиям монтажа и эксплуатации, а также сравнительной оценки энергопотребления после реконструкции ветхих участков трубопроводов полимерными трубами с возможностью минимизации энергозатрат при транспортировке воды в условиях неизотермического режима работы трубопровода.

Ключевые слова: автоматизированные программы, трубопроводы, температурные условия, гидравлические характеристики, бестраншейные технологии, энергопотребление

INTRODUCTION

In recent years, Russia has seen an intensification of the digitalization process, as evidenced by the federal project "Digital Public Administration" proposed by the Ministry of Digital Development, Communications and Mass Media. This project includes the automation of

all stages of the real estate life cycle from design to operation of buildings and structures. The most important achievement of digitalization is the possibility of implementing multi-optional design in the field of water supply and sanitation [1]. At the same time, the practice of construction and reconstruction of underground pipelines using numerous operational and cost-effective trenchless methods can be considered as a particular very significant aspect [2].

Currently, more than 40% of underground steel pipeline networks of water supply systems on average in the Russian Federation require prompt repair due to aging, accompanied by the appearance of various kinds of defects (damage) in the form of through holes (fistulas), corrosion of internal walls of pipelines, divergence of welds, thinning of walls and thus violation of load-bearing capacity [3].

Restoration of pipelines consists of a set of technical measures to improve the functional properties of the existing pipeline with full or partial use of its structure [4]. Pipeline damage leads to water leakage and negative phenomena of groundwater level rise above the pipeline network, which leads to a decrease in the porosity of the soil mass and suffusion failures.

According to the standard service life, steel pipes should be used for 20 years. However, they fail much earlier due to the above-mentioned damages, exhausting their resource. Emergencies associated with the failure of dilapidated and obsolete engineering networks in Russian cities account for 31% of the total number of emergencies, which is second only to fires and explosions, which account for 34% [5].

If we talk about pipelines of domestic and drinking water supply, a big problem is the deterioration of organoleptic properties of water supplied to consumers. Despite the fulfillment of regulatory requirements for water treatment technology at water treatment plants, the consumer receives water with significantly inferior quality indicators due to numerous pipe defects [6]. In addition, the flow velocities in previously designed water supply networks decrease due to the increased roughness of their walls due to various deposits, which affects the deterioration of organoleptic indicators of water related to sanitary and hygienic parameters that characterize the optimal conditions of human activity [7, 8].

Reliable performance of pipeline networks under construction and reconstruction can be ensured if designers take into account the hydraulic performance of pipes and of new materials. There is a need for accurate data on their hydraulic characteristics, which can be found both in industry standards and technical documents and in business models [9].

There are also on the agenda the issues of effective management of electricity consumption in water transportation [10]. Electricity consumption in liquid transportation systems mainly depends on the power and efficiency of the pump units used, as well as on the optimal selection of the cross-section of pipeline networks, reduction of local resistance and head losses along the length of pipelines [11]. It follows that the key aspects in the design of new pipeline systems, as well as in the renovation (modernization) of dilapidated pressure pipelines is to ensure their appropriate energy performance, providing conditions for long-term and energy-efficient operation of pipeline communications [12].

Researchers repeatedly note not only the need to use pipelines with low roughness, but also to take into account the temperature factor, which affects the change in electricity consumption during water transportation. [13].

A number of investigators consider a promising and necessary measure for effective management of water supply networks (in particular, flow distribution at certain temperature ranges during the implementation of repair and rehabilitation works) a wide application of automated computer complexes with various subsystems [14].

The effects of resource and energy saving are achieved by applying trenchless pipeline repair technologies. In particular, it includes the technology of repair by preliminary thermomechanical compression of polymer pipes

and pulling them into old pipelines (Swagelining), as well as the quality indicators of transported drinking water are preserved by increasing its flow velocities [15].

Modern urban construction is impossible without utilization of the underground space of the city. Placement of all transporting routes of underground engineering systems is limited by residential buildings and transportation routes. Especially acute is the issue of accessibility of communications during repair works. To date, about 50% of engineering networks of various materials need to be replaced or restored. This only increases the urgency of solving this issue and the need to search for new methods of laying and reconstruction [16].

In some municipal districts of the Russian Federation, such as Podporozhsky and Volkhovsky in the Leningrad region, 62.8 and 84.2% of pipelines of water supply networks are in need of capital repair, respectively [17].

Lack of prompt measures to improve the efficiency, serviceability and renovation of underground water pipelines aggravates the situation with numerous negative consequences for the population and the natural environment. Water supply networks should provide a guaranteed physical barrier against contamination of the supplied water and maintain the required sanitary and hygienic indicators in it [18].

The application of traditional methods for reconstruction can be problematic under the modern urban development and traffic intensity, bring great inconvenience and financial costs.

METHODS AND MATERIALS

The study focuses on one of the numerous technologies for renovation of dilapidated pipelines using polymer pipes. These pipes are subjected to thermomechanical compression with subsequent straightening in the reconstructed pipeline after being pulled into the dilapidated existing pipeline (Swagelining).

The research method is the analysis of the results of automated calculation of electricity consumption during water transportation with different ambient temperature conditions, as well as identification of the most economical variant from among the alternatives for saving electricity costs during water transportation through reconstructed pipelines with different diameters and SDR values (Standard Dimensional Ratio, that is diameter to wall thickness ratio).

Two automated calculation programs were used to achieve the above objectives [19, 20].

Swagelining method is used for trenchless repair of all types of pipeline networks: pressure, gravity, underground, surface. The method is applicable for reconstruction of pipelines with diameter from 100 to 1200 mm with the length of the repaired section up to 1000 m.

The technology allows fast installation of polymer pipe of larger diameter into old pipelines of smaller diameter due to its preliminary thermomechanical compression. Thus, a new pipe, tightly pressed to the inner surface of the main pipe and superior to the latter in a number of characteristics, is formed inside worn-out pipelines during rehabilitation. In this way, the pipeline acquires a two-layer construction and is an independent structure. The tight fit of the new polymer pipe to the walls of the old pipeline creates conditions for a very slight reduction in its diameter with a simultaneous reduction in the coefficient of hydraulic friction, i.e., ensuring the energy-saving effect in water transportation.

Swagelining sanitized pipes have successfully passed tests for rapid crack localization during operation (a series of tests were conducted for more than 5000 hours) on fracture and temperature tests with a notch at +80 C.

The Swagelining method was applied for the reconstruction of 3.5 km of water supply networks in Moscow.

The advantages of the Swagelining method also include the possibility of providing such an internal diameter of the reconstructed pipeline system, at which through varying the value of SDR water flow velocities correspond to the design ones for drinking water supply systems (i.e. about 1 m/s). This measure leads to preservation of organoleptic characteristics of water.

The technology includes the process of compression of the pipeline, preheated to a temperature of 70-80 C (Figure 1). A conical matrix ensures that the pipeline is narrowed so that it can be pulled through the existing pipeline without obstruction. At the next stage, a new pipe with a reduced diameter is pulled into the old pipe by means of a cable and a winch installed in the next manhole along the course of the pipe. The pulling is carried out until the pipe is in the required position.

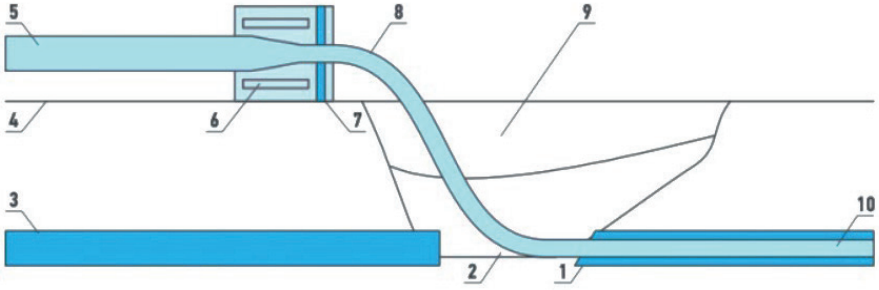


Figure 1. Pipeline rehabilitation scheme using the Swagelining method
1,3 - fragments of the dilapidated (restored) pipeline; 2, 9 - small-sized pit (or well); 4 - ground level; 5 - initial polymer pipeline, 6 - infrared heaters, 7 - conical matrix (narrowing device); 8 - pipeline after thermomechanical compression; 10 - double-layer pipeline

The reverse process of deformation of the polymer pipe inside the old pipeline occurs automatically due to the "memory" effect. The pipe expands until its outer diameter reaches the size of the inner diameter of the old pipeline and forms a tight joint with its wall. This eliminates the need for cement mortar or special hardeners. Figure 2 shows the result of rehabilitating an old pipeline to form a two-pipe construction.



Figure 2. View of the pipeline rehabilitation

In order to calculate power consumption ΔE while using polyethylene pipes during the period of Swagelining technology implementation for water transportation, including those depending on temperature conditions, equation (1) was applied:

$$\Delta E = 0{,}81 \cdot Q^3 \cdot l \cdot \lambda \cdot 24 \cdot 365 / (d^5 \cdot \eta_p) \qquad (1)$$

where ΔE is the value of consumed electricity, kWh/year; Q is the flow rate of water supplied by the pipeline, m^3/s; l s the length of the pipeline section, m; η_p is the efficiency factor of the pumping unit; 24 is the work hours of the pump per day, h; 365 is number of days per year; λ is the coefficient of hydraulic friction; d is the internal diameter of the pipeline, m.

RESULTS

To determine the level of deformation of pipelines (changes in the diameter and wall thickness of

polymer pipe after its thermomechanical compression and straightening operations) when using Swagelining technology, a special automated program was applied [20].

The initial parameters used in the automated calculations in both programs are as follows:

-internal diameter of the dilapidated steel pipeline 500 mm;

-length of the pipeline 600 m;

-internal diameter of polyethylene pipes 560 and 630 mm (SDR 21);

-Average temperature of the pipeline wall (soil around the pipe) 160 C;

- average temperature of water in the water supply source 160 C (summer period) and 80 C (winter period);

-flow rate of transported water 0.14 m3/s;

-internal diameters of the rehabilitated pipeline after renovation of the steel pipeline with polyethylene pipe with original diameters of 560 and 630 mm, respectively: 446.04 mm and 438.51 mm;

-coefficient of efficiency of the pumping unit 0.9.

Summary output information on the automated calculation of parameters in summer and winter periods is presented below (Tables 1 and 2) according to the data obtained from the results of the automated program [19].

Table 1. Summarized output information on the results of hydraulic and energy calculation of two-pipe construction in summer and winter periods at the internal diameter of the pipeline 446.04 mm

No	Estimated indicators	Indicator values	
		Summer period	Winter period
1	Water flow velocity in the pipeline, m/sec	0.896	0.896
2	Coefficient of dynamic viscosity related to the liquid flow, Pa-s.	0.001131151	0.001406528
3	Coefficient of dynamic viscosity related to the pipe wall temperature, Pa-s.	0.001131151	0.001131151
4	Dynamic viscosity ratio	1.0	1.243
5	Coefficient of kinematic viscosity of liquid, m2/sec.	0.000001096	0.000001380
6	Reynolds number	364758.11	289680.3
7	Calculated coefficient of hydraulic friction	0.013853	0.013885
8	Electricity consumption through the coefficient of hydraulic friction, kWh per year	10217.143	10224.114

Table 2. Summarized output information on the results of hydraulic and energy calculation of a two-pipe structure in summer and winter periods at the internal diameter of the pipeline 438.51 mm

No	Estimated indicators	Indicator values	
		Summer period	Winter period
1	Water flow velocity in the pipeline, m/sec	0.927	0.927
2	Coefficient of dynamic viscosity related to the liquid flow, Pa-s.	0.001131151	0.001406528
3	Coefficient of dynamic viscosity related to the pipe wall temperature, Pa-s.	0.001131151	0.001131151
4	Dynamic viscosity ratio	1.0	1.243
5	Coefficient of kinematic viscosity of liquid, m2/sec.	0.000001096	0.00000138
6	Reynolds number	371021.66	294654.63
7	Calculated coefficient of hydraulic friction	0.013897	0.013929
8	Electricity consumption through the coefficient of hydraulic friction, kWh per year	11089.143	11115.787

Comparing the values of electricity consumption in Tables 1 and 2 for points 8, i.e., with and without consideration of water and pipeline wall temperatures, there is a discrepancy. This indicates the influence of water temperature on electricity consumption: as the temperature in the water supply source increases, electricity consumption decreases. For example, for the winter period the difference in electricity consumption is as follows:

- for diameter 446.04 mm 10224.114 - 10217.143 = 6.971 kWh per year
- for diameter 438.51 mm 11115.787 - 11089.143 = 26.644 kWh per year.

In addition, it should be noted that even with a slight decrease in the diameter of polyethylene pipe (from 446.04 to 438.51 mm) there is an increase in energy costs. For example, for winter conditions it is 26.644 - 6.971 = 19.673 kWh per year or 26.16%.

It follows that the design and possible control of the water transportation process requires accounting for temperature factors to obtain the most probable values of electricity consumption. It is necessary to include data on the temperature parameters of the pipeline wall and transported water in the pipeline network construction projects and to calculate electricity consumption. This is facilitated by modeling, which allows to identify the optimal parameters of water transportation process control based on the search for minimum values of electricity consumption. Using the capabilities of the automated program, calculations of power consumption can be carried out in a wide range of temperatures of the pipe wall (corresponding material and diameter) and transported water for both northern and southern regions at different values of water flow rates and values of the efficiency factor of pumping units.

Below are presented summary calculation data (Tables 3-5), as well as graphical material regarding the most economical variant among the alternatives in terms of energy cost savings for water transportation through the Swagelining-rehabilitated pipelines with different diameters and SDR values. The tables clearly illustrate the dynamics of change in such indicators as wall thickness and the value of the new internal diameter of the repaired pipeline, as well as energy costs depending on the SDR of the pipe after the reconstruction of the steel pipeline by Swagelining.

The following initial data were adopted for the calculations: pipeline material is steel; internal diameter is 800 mm; length of the repaired section is 800 m; design water flow rate is 0.51 m^3/s, at which the head loss along the length in the steel pipeline is 1.12 m; efficiency factor of the pump and electric motor is 90%.

External diameters of the new polymer pipeline using Swagelining technology are: d_1=1000 mm, d_2=900 mm and d_3=800 mm.

Table 3. Indicators at outer diameter of a new pipeline d_1=1000 mm

Estimated values	*SDR*11	*SDR*17	*SDR*21	*SDR*26	*SDR*33	*SDR*41	*SDR*50
Inner diameter of the new pipeline after renovation, mm	608.84	677.78	702.43	722.04	737.84	748.89	759.62
Wall thickness after compression-straightening operations, mm	95.58	61.11	48.79	38.98	31.08	25.56	20.19
Head loss along the entire length of the pipeline after renovation, m	1.428	0.772	0.629	0.538	0.475	0.436	0.402
Average annual electricity savings							
Along the entire length of the pipeline thousand kWh/year	-16.549	18.906	26.637	31.606	34.996	37.093	38.403

Table 4. Indicators at outer diameter of a new pipeline d_2=900 mm

Estimated values	*SDR*11	*SDR*17	*SDR*21	*SDR*26	*SDR*33	*SDR*41	*SDR*50
Inner diameter of the new pipeline after renovation, mm	632.24	691.63	713.19	730.47	744.45	754.26	763.82
Wall thickness after compression-straightening operations, mm	83.88	54.19	43.40	34.77	27.78	22.87	18.09
Head loss along the entire length of the pipeline after renovation, m	1.15	0.688	0.577	0.503	0.451	0.419	0.389
Average annual electricity savings							
Along the entire length of the pipeline thousand kWh/year	-1.544	23.476	29.478	33.476	36.276	38.041	39.617

Table 5. Indicators at outer diameter of a new pipeline d_3=800 mm

Estimated values	*SDR*11	*SDR*17	*SDR*21	*SDR*26	*SDR*33	*SDR*41	*SDR*50
Inner diameter of the new pipeline after renovation, mm	654.8	705.2	723.8	738.8	751.0	759.6	768.
Wall thickness after compression-straightening operations, mm	72.6	47.4	38.1	30.6	24.5	20.2	16.0
Head loss along the entire length of the pipeline after renovation, m	0.941	0.615	0.53	0.471	0.429	0.402	0.377
Average annual electricity savings							
Along the entire length of the pipeline thousand kWh/year	9.779	27.396	32.008	35.188	37.471	38.937	40.265

According to the results of the modeling presented in Tables 3-5, the following conclusions can be drawn on the application of Swagelining technology for rehabilitation works:
- for the range of diameters considered (1000, 900 and 800 mm), the larger the SDR value (i.e., the smaller the wall thickness), the smaller the head losses along the length of the pipeline;
- the smaller the diameter of the pipeline, the lower the head losses and the greater the average annual energy savings, which is clearly illustrated by graphical relationships (Figure 3);
- at SDR 11 values for pipelines with diameter d_1=1000 mm and d_2=900 mm no energy saving is achieved (negative calculation result);
- at SDR 50 the values of average annual energy savings for three diameters of pipelines practically coincide.

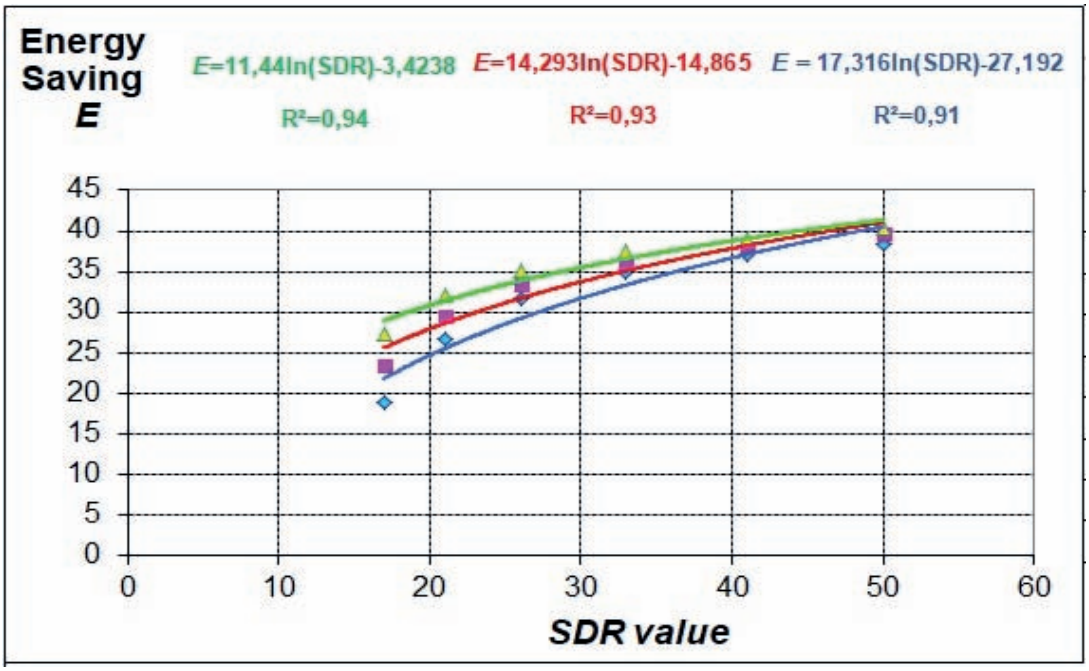


Figure 3. Graphs for average annual energy savings E, thousand kWh/year, depending on the value of SDR for the corresponding pipeline diameter:
1000 mm - blue (lower curve), 900 mm - red (middle curve); 800 mm - green (upper curve)

CONCLUSIONS

The analysis of the literature and practice of designing repair and restoration works on the underground pipeline network shows that the current state of pipelines of water supply and drainage systems in the countries of the world is unsatisfactory. There is a tendency of dynamic wear of pipelines with exceeding the normative service life of their service. This indicates the need for rapid replacement of individual sections of engineering networks.

The trenchless methods are promising approaches to the reconstruction of underground pipelines. They allow to significantly reduce the time and cost of construction works, ensure resource and energy efficiency of the reconstructed pipeline systems, as well as maintain organoleptic characteristics of transported water and reduce the risk of harm to the environment.

The performed research has established the advantages of trenchless reconstruction methods and recommended the wide use of Swagelining method. It allows to achieve a double effect at the same time: resource saving, as after the repair water leaks (exfiltration) and groundwater infiltration into pipelines (infiltration) will be eliminated, as well as energy saving, i.e., reduction of energy costs during water transportation, including at different ambient temperatures.

Hydraulic and energy calculations of a two-pipe underground structure of a certain diameter during various seasons of the year are presented on specific examples with the use of computer-aided programs, which showed the possibility of saving energy resources depending on temperature conditions.

REFERENCES

1. **Bazhenov V.I., Ermolchev A.M., Sobolevskaya E.A.** Digital development of water supply and wastewater disposal // The best available technologies of water supply and wastewater disposal. 2022. No. 4 Pp. 10-14

2. **Rybakov, A.P.** Fundamentals of trenchless technologies. -Moscow: Press Bureau No. 1. 2005. 304 p.
3. **Anikin Y.V., Tsarev N.P., Ushakova L.I., Naschetnikova O.B.** Technology of trenchless laying and repair of water supply and water disposal pipelines. // Ekaterinburg: Ural University Publishing House. 2022. 84 p.
4. SP 273.1325800.2016 "Water supply and water disposal. Rules of engineering and works at restoration of pipelines by flexible polymeric sleeves"
5. **Orlov V.A.** Trenchless technologies of construction and restoration of pipelines of water supply and water disposal systems. // Moscow; Vologda: Infra-Engineering. 2023. 228 p.
6. **Primin, O.G.** Water leaks. Moscow: Publishing house of NIU MGSU. 2022. 167 p.
7. **Aleksandrov V.I., Gvozdev O.B., Karelin A.E., Morozov A.A.** Assessment of the influence of the roughness of the inner surface of hydraulic transport pipelines on the value of specific head losses // Mining equipment and electromechanics. 2017. No 3 (130). Pp. 34-40.
8. **Prodous, O.A.; Yakubchik, P.P.** Hydraulic calculation of the pipelines made of polymeric materials taking into account the roughness parameters of the inner surface of the pipes // Water supply and sanitary engineering. 2020. № 11. Pp. 55-60.
9. **Osterwalder A., Pigneur Y., Tucci C.L.** Clarifying business models: Origins, present, and future of the concept. // Communications of the association for Information Systems. 2005. T. 16. No. 1. Pp. 1-40
10. **Leznov, B.P.** Energy saving and regulated drive-in pump and blower installations // Moscow: Energoatomizdat. 2006. 359 p.
11. **Glushkov, G.N.; Denisov, V.A.; Kraitsberg, M.I.** Electrical equipment and electrical supply of the construction. // M.: Stroyizdat. 1984. 311 c.
12. **Houghtalen R., Osman A., Akan A., Hwang N.** Fundamentals of Hydraulic Engineering Systems, 5th edition. // Pearson. 2016. 528 p.
13. **Gilda Gavrilaş, Mihai Gavrilas, Ovidiu Ivanov**. Electricity load prediction for water supply systems // Environmental Engineering and Management Journal, July/August 2008, Vol. 7, Nr. 4, ISSN: 1843 - 3707
14. **Bondarev, E.A.** Thermal and mechanical effect of engineering structures with frozen soils. // Novosibirsk: Nauka, 1977.- 140 P.
15. **Kuliczkowski A., Kuliczkowska E., Zwierzchowska A.** Technologie bezwykopowe w inżynierii środowiska. // Wydawnictwo Seidel-Przywecki. 2019. 735 p.
16. **Yudina A.F., Kobelev E.A**. Innovative technologies of trenchless laying of new and repair of old engineering networks. // Bulletin of Civil Engineers, 2017. no. 3 (62). p. p. 101-108
17. "Delovoy Peterburg", www.dp.ru, 17.07.2023, No. 75 (5847). 2 p.
18. **Khramenkov S.V.** Time to manage water. // Moscow: JSC Moscow textbooks and cartolithography. 2008. 280 p.
19. **Orlov, V.A.; Zotkin, P.; Inshakova, M.A.** Calculation of the electric power consumption at water transportation by the pressure pipelines. // Certificate of state registration of computer program No. 2021613107 from 02.03.2021.
20. **Orlov V.A., Zotkin S.P., Zotkina I.A., Khrenov K.E**. Calculation of the operation parameters of the pipelines restored by the pre-compressed polymer pipes. // Certificate of state registration of computer program No. 2014612753 dated 06.03.2014.

СПИСОК ЛИТЕРАТУРЫ

1. **Баженов В.И., Ермольчев А.М., Соболевская Е.А.** Цифровое развитие водоснабжения и водоотведения // Наилучшие доступные технологии водоснабжения и водоотведения. 2022. № 4 с. 10–14

2. **Рыбаков А.П.** Основы бестраншейных технологий.-М.: Пресс-Бюро № 1. 2005. 304 с.
3. **Аникин Ю.В., Царев Н.С., Ушакова Л.И., Насчетникова О.Б.** Технология бестраншейной прокладки и ремонта трубопроводов водоснабжения и водоотведения. // Екатеринбург: Издательство Уральского университета. 2022. 84 с.
4. СП 273.1325800.2016 «Водоснабжение и водоотведение. правила проектирования и производства работ при восстановлении трубопроводов гибкими полимерными рукавами»
5. **Орлов В.А.** Бестраншейные технологии строительства и восстановления трубопроводов систем водоснабжения и водоотведения. // Москва; Вологда: Инфра-Инженерия. 2023. 228 с.
6. **Примин О.Г.** Утечки воды. – М.: Издательство ФГБОУ ВО «НИУ МГСУ». 2022. 167 с.
7. **Александров В.И., Гвоздев О.Б., Карелин А.Э., Морозов А.А.** Оценка влияния шероховатости внутренней поверхности гидротранспортных трубопроводов на величину удельных потерь напора // Горное оборудование и электромеханика. 2017. № 3 (130). С. 34–40.
8. **Продоус О.А., Якубчик П.П.** Гидравлический расчет трубопроводов из полимерных материалов с учетом параметров шероховатости внутренней поверхности труб // Водоснабжение и санитарная техника. 2020. № 11. С. 55–60.
9. **Osterwalder A., Pigneur Y., Tucci C.L.** Clarifying business models: Origins, present, and future of the concept. // Communications of the association for Information Systems. 2005. Т. 16. №. 1. с. 1-40
10. **Лезнов Б.С.** Энергосбережение и регулируемый привод в насосных и воздуходувных установках // М.: Энергоатомиздат. 2006. 359 с.
11. **Глушков Г.Н., Денисов В.А., Крайцберг М.И.** Электрооборудование и электроснабжение строительства. // М.: Стройиздат. 1984. 311 с.
12. **Houghtalen R., Osman A., Akan A., Hwang N.** Fundamentals of Hydraulic Engineering Systems, 5th edition. // Pearson. 2016. 528 p.
13. **Gilda Gavrilaş, Mihai Gavrilas, Ovidiu Ivanov**. Electricity load prediction for water supply systems // Environmental Engineering and Management Journal, July/August 2008, Vol. 7, Nr. 4, ISSN: 1843 - 3707
14. **Бондарев Э.А.** Тепловое и механическое воздействие инженерных сооружений с мерзлыми грунтами. // Новосибирск: Наука, 1977.- 140 с.]
15. **Kuliczkowski A., Kuliczkowska E., Zwierzchowska A.** Technologie bezwykopowe w inżynierii środowiska. // Wydawnictwo Seidel-Przywecki. 2019. 735 p.
16. **Юдина А.Ф., Кобелев Е.А.** Инновационные технологии бестраншейной прокладки новых и ремонта старых инженерных сетей. // Вестник гражданских инженеров, 2017. № 3 (62). с. 101–108
17. «Деловой Петербург», www.dp.ru, 17.07.2023, № 75 (5847). 2 с.
18. **Храменков С.В**. Время управлять водой. // М.: ЗАО Московские учебники и картолитография. 2008. 280 с.
19. **Орлов В.А., Зоткин С.П., Иншакова М.А.** Расчет потребления электроэнергии при транспортировке воды по напорным трубопроводам. // Свидетельство о государственной регистрации программы для ЭВМ № 2021613107 от 02.03.2021
20. **Орлов В.А., Зоткин С.П., Зоткина И.А., Хренов К.Е.** Расчет параметров работы трубопроводов, восстанавливаемых предварительно сжатыми полимерными трубами. // Свидетельство о государственной регистрации программы на ЭВМ № 2014612753 от 06.03.2014

Orlov Vladimir A., Professor, Doctor of Technical Sciences; National Research Moscow State Construction University (NIU MSCU), Russia, 129337, Moscow, 26 Yaroslavskoe Shosse; E-mail: OrlovVA@mgsu.ru.

Орлов Владимир Александрович, профессор, доктор технических наук; Федеральное государственное бюджетное образовательное учреждение высшего образования «Национальный исследовательский Московский государственный строительный университет» (НИУ МГСУ), Россия, 129337, Москва, Ярославское шоссе, 26; E-mail: OrlovVA@mgsu.ru.

Zotkin Sergey P., Professor, Candidate of Technical Sciences; Russia, National Research Moscow State Construction University (NIU MSCU), Russia, 129337, Moscow, 26 Yaroslavskoe Shosse; E-mail: ZotkinSP@mgsu.ru.

Зоткин Сергей Петрович, профессор, кандидат технических наук; Россия, Федеральное государственное бюджетное образовательное учреждение высшего образования «Национальный исследовательский Московский государственный строительный университет» (НИУ МГСУ), 129337, Москва, Ярославское шоссе, 26; E-mail: ZotkinSP@mgsu.ru.

Podolyan Dmitry V., PhD student; National Research Moscow State Construction University (NIU MSCU), Russia, 129337, Moscow, 26 Yaroslavskoe Shosse; E-mail: dim.p-2010@yandex.ru.

Подолян Дмитрий Владимирович, аспирант; Федеральное государственное бюджетное образовательное учреждение высшего образования «Национальный исследовательский Московский государственный строительный университет» (НИУ МГСУ), Россия, 129337, Москва, Ярославское шоссе, 26; E-mail: dim.p-2010@yandex.ru

International Journal for Computational Civil and Structural Engineering, 19(4) 135–146 (2023)

DOI:10.22337/2587-9618-2023-19-4-135-146

DEPOSITION OF PARTICLES FROM A TURBULENT FLOW ON THE WALLS OF PIPES AND CHANNELS

Sergey V. Fedosov [1], Alexandr V. Markelov [2],

[1] National Research Moscow State University of Civil Engineering, Moskow, RUSSIA

[2] Yaroslavl State Technical University, Yaroslavl, RUSSIA

Abstract: The formation of sediment on the walls of pipes and channels has a significant impact on the efficiency and reliability of technological equipment. The article considers the effect of sediment formation on the process of ultrafiltration of wastewater from the plant of reinforced concrete structures, representing water-oil emulsions with a high content of suspended solids. On the basis of the theory of turbulent particle migration developed earlier by E.P. Mednikov in a shear turbulent gas flow, a solution of the problems of particle deposition on the walls of circular channels from a viscous fluid flow in a wide range of Schmidt numbers is obtained. The equations for determining the mass transfer coefficient from the core of the flow to the channel walls for a two–layer boundary layer according to the Prandtl theory, a three-layer Pocket and a modernized three-layer Landau-Levich were obtained. The results of calculations of the mass transfer coefficient of particles from the flow core to the channel surface according to the proposed upgraded model showed the highest intensity of deposition of particles with a diameter of 10 to 40 microns. The adequacy of the model was verified by comparing the calculated parameters with the results of well-known domestic and foreign researchers and showed good verification.

Keywords: Turbulent migration, circular channel, mass transfer coefficient

ОСАЖДЕНИЕ ЧАСТИЦ ИЗ ТУРБУЛЕНТНОГО ПОТОКА НА СТЕНКИ ТРУБ И КАНАЛОВ

С.В. Федосов [1], А.В. Маркелов [2]

[1] ФГБОУ ВО «Национальный исследовательский Московский государственный строительный университет», г. Москва, РОССИЯ

[2] ФГБОУ ВО «Ярославский государственный технический университет», г. Ярославль, РОССИЯ

Аннотация: Образование осадка на стенках труб и каналов оказывают существенное влияние на эффективность и надежность технологического оборудования. В статье рассмотрено влияние образование осадка на процесс ультрафильтрации сточных вод комбината железобетонных конструкций, представляющие водомасляные эмульсии с большим содержанием взвешенных веществ. На основе развитой ранее Е.П. Медниковым теории турбулентной миграции частиц в сдвиговом турбулентном потоке газа получено решение задач об осаждении частиц на стенки круглых каналов из потока вязких жидкостей в широком диапазоне числа Шмидта. Получены уравнения для определения коэффициента массоотдачи из ядра потока к стенкам канала для двухслойного пограничного слоя по теории Прандтля, трехслойного – Кармана и модернизированного трехслойного Ландау-Левича. Результаты расчетов коэффициента массоотдачи частиц от ядра потока к поверхности канала по предложенной модернизированной модели показали наибольшую интенсивность осаждения частиц диаметром от 10 до 40 мкм. Адекватность модели была проверена путем сравнения расчетных параметров с результатами известных отечественных и зарубежных исследователей и показала хорошую верификацию.

Ключевые слова: турбулентная миграция, круглый канал, коэффициент массоотдачи

INTRODUCTION

Turbulent particle migration is the process of moving particles inside a liquid or gas that occurs under the influence of flow turbulence. This process is characterized by chaotic and unpredictable particle movements caused by vortices and turbulent pulsations in the flow [1, 2].

Turbulent particle migration can occur both in liquid media (for example, water or oil) and in gases (for example, air), and is of great practical importance in various industrial sectors and municipal services. economy, including [2, 3]:
- formation of corrosion, wear of equipment and pipelines;
- reduced efficiency and reliability of equipment;
- uncontrolled pollution of water and air resources.

All these aspects make turbulent particle migration an important area of research with significant applied and theoretical significance.

In the construction industry, waste water containing suspended particles, petroleum products, surfactants, and other pollutants is formed in reusable forms during the production of reinforced concrete structures [4].

For wastewater treatment, the process of ultrafiltration can be used, i.e., the separation of particles and molecules by size using semipermeable membranes [5].

Sediment formation can have a significant impact on the ultrafiltration process, due to:
- reducing the permeability and efficiency of the process;
- damage to the active layer of the membrane, increasing its wear and reducing the service life of the membrane;
- changes in the chemical composition and concentration of the initial liquid in the boundary layer, which, in turn, can affect the filtration characteristics of the membrane.

Knowing the intensity of sediment formation will allow you to develop requirements for pretreatment, reasonable choice of the type of membrane, and timely monitoring and maintenance of such devices.

Research in the field of particle deposition under turbulent flow regimes has been carried out for more than 60 years, and there are a large number of scientific publications. However, even in the case of simplifying the formulation of the problem of precipitation of particles with a low concentration as a result of turbulent migration, complex analytical or numerical methods for solving it are required [2, 6-15]. Generalization of the theory and theoretical calculations in this area that are well consistent with experiments were obtained in the Russian scientific school founded by E. P. Mednikov [1].

In this paper, an attempt is made to adapt the theory of turbulent particle migration in aerosols to mass transfer in viscous liquids, taking into account phenomena in the boundary layers of circular channels.

1. Problem statement

Moving along the flow, particles at some stage of their movement reach the wall region and, when the distance to the wall becomes equal to their radius, touch it and settle on it, if the wall surface is "absorbing" [1].

The migration rate u_t characterizes the intensity of precipitation of particles from the turbulent flow onto the channel wall [1]

$$u_t = j / c\,, \tag{1}$$

where j - specific particle flow to the wall, kg/(m^2·s); c - concentration of particles in the solution, kg/m^3.

Then the specific flow of particles to the wall j is determined by the equation

$$j = u_t \cdot c\,. \tag{2}$$

Expression (2) is an analog of the well-known mass transfer equation [16]

$$j = \beta_d \cdot (c_R - c_w)\,, \tag{3}$$

where β_d - mass transfer coefficient, m/s; c_R - concentration of impurities in the flow core; c_w - concentration of impurities on the membrane surface.

Hence, it is possible to assume the identity of the deposition rate and the mass transfer coefficient of particles from the flow core to the membrane walls

$$u_t = \beta_d\,. \tag{4}$$

Theoretical methods for determining the mass transfer coefficient of the dispersed phase β_d will make it possible to perform calculations on the deposition of particles on the membrane walls with minimal use of experimental data.

We use a well-known approach, when the turbulent deposition of a finely dispersed phase is considered as a kind of diffusion process using the usual equations from the mass transfer theory [1].

The motion of very small particles practically does not differ from the motion of the carrier turbulent vortices of the medium, and then $D_P = D_S$, where D_P, D_S are the coefficients of turbulent diffusion of particles and the medium, m^2/s [1].

Consider a situation where the mass transfer resistance is concentrated in the boundary layer on the surface of a membrane element. Let *the y-axis* be directed normal to the surface of the membrane. In this case, using an analog of Fick's first law [1], the projection of the specific particle flux on *the y-axis* at any point of the boundary layer is written as

$$j(y) = (D_P + D_{Br})\frac{dc}{dy}, \qquad (5)$$

where D_{Br} - Brownian diffusion coefficient.

We introduce a new dimensionless quantity-the relative particle flux

$$j^* = \frac{j(y)}{j_w}. \qquad (6)$$

Then, using expression (6), we make a substitution in equation (5) to obtain

$$j^* \cdot j_w = (D_P + D_{Br})\frac{dc}{dy}. \qquad (7)$$

Then, separating the variables, we write the integral over the boundary layer thickness

$$\int_{c_w}^{c_R} \frac{dc}{j_w} = \int_0^{\delta} \frac{j^* \cdot dy}{D_P + D_{Br}}, \qquad (8)$$

where δ - turbulent boundary layer.

Using expression (3), we obtain

$$\frac{1}{\beta_d} = \int_0^{\delta} \frac{j^* \cdot dy}{D_P + D_{Br}}. \qquad (9)$$

Expression (9) is general and allows calculating the mass transfer coefficient based on the Brownian (molecular) and turbulent diffusion coefficients, as well as the relative specific particle flux in the boundary layer j^*.

In this model, the main resistance to mass transfer in the diffusion boundary layer is assumed, as well as the constancy of the flow across this layer $c_R = c_w$ hence $j^* = 1$.

2. Results and discussion

To obtain a universal solution of equation (9), we first reduce it to a dimensionless form by entering the following parameters:

- dimensionless distance along *the y-axis*

$$y^+ = y\frac{u^*}{\nu}, \qquad (10)$$

where u^* - dynamic flow velocity; ν - kinematic viscosity coefficient of the separated liquid.

In this case,

$$dy = \frac{\nu}{u^*} dy^+. \qquad (11)$$

Dimensionless mass transfer coefficient

$$\beta_d^+ = \frac{\beta_d}{u^*}. \qquad (12)$$

Dimensionless thickness of a viscous sublayer [2]

$$R_1^+ = \frac{u^* \cdot \delta_1}{\nu}, \qquad (13)$$

where δ_1 - value of the viscous sublayer.

For the Prandtl model R_1 =11.6 [2].

The dimensionless thickness of a turbulent boundary layer is determined by the expression

$$R_{\delta}^{+} = \frac{u^{*} \cdot \delta}{\nu}. \qquad (14)$$

The dimensionless thickness of a viscous sublayer on a rough surface will differ from $R_{1m}^{+} = 11.6$, that derived for a smooth plate [2].

For the boundary layer with various perturbations (roughness, two-phase, etc.), the expression [2] is obtained

$$R_{1m}^{+} = 11.6\sqrt{\frac{C_{f0}}{C_{fm}}}. \qquad (15)$$

After substituting the dimensionless quantities in equation (9), we obtain

$$\frac{1}{\beta_{d}^{+} \cdot u^{*}} = \int_{0}^{R_1} \frac{\nu \cdot dy}{(D_P + D_{Br}) \cdot u^{*}} \quad \text{or}$$

$$\frac{1}{\beta_{d}^{+}} = \int_{0}^{R_1} \frac{\nu \cdot dy}{(D_P + D_{Br})}. \qquad (16)$$

For particles subject to precipitation, the turbulent diffusion coefficient of particles can be determined by the expression [1]

$$D_P = \frac{D_S}{1 + \omega_E \cdot \tau_p}, \qquad (17)$$

where w_E - angular frequency of turbulent low-frequency pulsations of energy-intensive vortices; τ_p - relaxation time.

Usually, with a small error, they allow [1]

$$D_S \approx \nu_T, \qquad (18)$$

where ν_T - turbulent viscosity coefficient.

In expression (17), the angular frequency of turbulent low-frequency pulsations of energy-intensive vortices ω_E and the relaxation time τ_p are determined by expressions [1]

$$\omega_E = \frac{u^{*}}{0.1 \cdot r}, \quad \tau_p = \frac{\rho \cdot d_s^2}{18 \cdot \mu}, \qquad (19)$$

where d_s - diameter of impurity particles; μ - dynamic viscosity coefficient.

Various boundary layer models and functions for $\nu_T(y)$ are known in the literature, which can be classified according to the number of layers.

The Prandtl model. The two-layer Prandtl model suggests molecular transport in the viscous sublayer and turbulent transport beyond it [2].

In a viscous sublayer $\nu_T = 0$, and for $y > \delta_1$, $\nu_T = \chi \cdot u^{*} \cdot y$, where $\chi = 0.4$ is the Prandtl constant [2].

Then the transfer resistance of the fine phase in the boundary layer, using expression (9) and the model assumptions described above, is written as

$$\frac{1}{\beta_{d}^{+}} = \int_{0}^{R_1^{+}} \frac{\nu}{D_{Br}} \cdot dy^{+} + \int_{R_1^{+}}^{R_\delta^{+}} \frac{\nu}{D_P} \cdot dy^{+}. \qquad (20)$$

It is known that the ratio of the kinematic viscosity coefficient to the diffusion coefficient is determined by the Schmidt criterion [1]

$$Sc_{Br} = \nu / D_{Br}. \qquad (21)$$

In integral equation (20), we make substitutions using the expressions (10), (17), (18) and (21), we obtain

$$\frac{1}{\beta_{d}^{+}} = \int_{0}^{R_1^{+}} Sc_{Br} \cdot dy^{+} + \int_{R_1^{+}}^{R_\delta^{+}} \frac{(1 + \omega_E \cdot \tau_p) dy^{+}}{\nu_T} =$$

$$= \int_{0}^{R_1^{+}} Sc_{Br} \cdot dy^{+} + \int_{R_1^{+}}^{R_\delta^{+}} \frac{(1 + \omega_E \cdot \tau_p) \cdot u^{*} \cdot \nu \cdot dy^{+}}{\chi \cdot u^{*} \cdot y^{+} \cdot \nu}. \qquad (22)$$

We transform the expression (22) by taking the constant terms as the sign of the integral

$$\frac{1}{\beta_{d}^{+}} = Sc_{Br} \int_{0}^{R_1^{+}} dy^{+} + \frac{1 + \omega_E}{\chi} \int_{R_1^{+}}^{R_\delta^{+}} \frac{dy^{+}}{y^{+}} \cdot \qquad (23)$$

As a result of integrating (23), we obtain

$$\frac{1}{\beta_d^+} = Sc_{Br} \cdot R_1^+ + \frac{1+\omega_E}{\chi}\left[\ln(R_\delta^+ / R_1^+)\right]\cdot \quad (24)$$

Thus, the expression (24), after the corresponding transformation, can be represented as

$$\beta_d^+ = \frac{1}{Sc_{Br} \cdot R_1^+ + \frac{1}{\chi}\left(1+\omega_E\right)\ln(R_\delta^+ / R_1^+)}\cdot \quad (25)$$

In dimensions (25), it will look like

$$\beta_d = \frac{u^*}{Sc_{Br} \cdot \frac{u^* \cdot \delta_1}{\nu} + \frac{1}{\chi}\left(1+\omega_E\right)\ln(\delta / \delta_1)}\cdot \quad (26)$$

Karman Model. In the three-layer Karman model, the turbulent exchange functions have the form [2]:
– in a viscous sublayer at $y^+ < 5$, $\nu_T = 0$;
– in the transition region at $5 < y^+ < 30$,

$$\nu_T = u^* y / 5 - \nu; \quad (27)$$

– in the turbulent region at $y^+ > 30$,

$$\nu_T = \chi u^* y - \nu. \quad (28)$$

Assuming that for $y^+ > 5$ (outside the viscous sublayer) $D_{CP} >> \nu$, the particle transport resistance is written as

$$\frac{1}{\beta_d^+} = \int_0^{R_1^+} \frac{\nu \cdot dy^+}{D_{Br}} + \int_{R_1^+}^{R_2^+} \frac{\nu \cdot dy^+}{D_P} + \int_{R_2^+}^{R_\delta^+} \frac{\nu \cdot dy^+}{D_P}. \quad (29)$$

The value of the viscous sublayer δ_1 [1, 2]

$$\delta_1 = 5\nu / u^*; \quad (30)$$

Value of the transition sublayer [1, 2]

$$\delta_2 = 30\nu / u^*. \quad (31)$$

Then the dimensionless thickness of the viscous sublayer from equations (13) $R_1^+ = 5$, and the value of the transition sublayer from (14) $R_2^+ = 30$.

After integrating equation (28), taking into account the boundary conditions (27) by analogy with expression (20), we obtain the expression in the dimensionless form

$$\beta_d^+ = \frac{1}{5 \cdot Sc_{Br} + a \cdot \left[10,07 + 2,5 \cdot \ln\left(1 - \chi \cdot R_\delta^+\right)\right]},$$

where $a = 1 + \omega_E \tau_p$. (32)

When converting to dimensional values

$$\beta_d = \frac{u^*}{5 \cdot Sc_{Br} + a\left[10,07 + 2,5 \cdot \ln\left(1 - \frac{\chi \cdot u^* \cdot \delta}{\nu}\right)\right]}. \quad (33)$$

In the upgraded three-layer Landau-Levich model [17], it is assumed that the change in turbulent viscosity in a viscous sublayer is proportional *to* $\nu_T \sim y^4$, and in this case both Brownian and turbulent diffusion will act in it.
Then the expression (28) will take the form

$$\frac{1}{\beta_d^+} = \int_0^{R_1^+} \frac{\nu \cdot dy^+}{D_{Br} + D_P} + \int_{R_1^+}^{R_2^+} \frac{\nu \cdot dy^+}{D_P} + \int_{R_2^+}^{R_\delta^+} \frac{\nu \cdot dy^+}{D_P}. \quad (34)$$

Based on the Landau-Levitch theory, the following functions are used for each sublayer [17]:

$$\frac{\nu_T}{\nu} = 0,01\chi^4 \cdot (y^+)^4, \quad y^+ \le 5; \quad (35)$$

$$\frac{\nu_T}{\nu} = 0,2y^+ - 0,959, \quad 5 \le y^+ \le 30; \quad (36)$$

$$\frac{\nu_T}{\nu} = 0,4y^+ - 1, \quad y^+ \ge 30. \quad (37)$$

Consider the first integral of the right-hand side of equation (33)

$$\int_0^{R_1^+} \frac{\nu \cdot dy^+}{D_{Br} + D_P} = \int_0^{R_1^+} \frac{\nu \cdot dy^+}{(\frac{D_{Br}}{D_P} + 1) \cdot D_P} = \\ = \int_0^{R_1^+} \frac{(1 + \omega_E \cdot \tau_p) \cdot \nu \cdot dy^+}{(\frac{D_{Br}}{D_P} + 1) \cdot \nu_T} \quad . \quad . \quad (38)$$

Replace the ratio ν_T/ν with equation (35)

$$\int_0^{R_1^+} \frac{(1 + \omega_E \cdot \tau_p) \cdot \nu \cdot dy^+}{(\frac{D_{Br}}{D_P} + 1) \cdot \nu_T} = \\ = \int_0^{R_1^+} \frac{(1 + \omega_E \cdot \tau_p) \cdot dy^+}{(\frac{D_{Br}}{D_P} + 1) \cdot 0,01 \cdot \chi^4 \cdot (y^+)^4} = \\ = \int_0^{R_1^+} \frac{(1 + \omega_E \cdot \tau_p) \cdot dy^+}{(\frac{D_{Br}(1 + \omega_E \cdot \tau_p)}{\nu_T} + 1) \cdot 0,01 \cdot \chi^4 \cdot (y^+)^4} = \\ = \int_0^{R_1^+} \frac{(1 + \omega_E \cdot \tau_p) \cdot dy^+}{(\frac{D_{Br}(1 + \omega_E \cdot \tau_p)}{\nu \cdot 0,01 \cdot \chi^4 \cdot (y^+)^4} + 1) \cdot 0,01 \cdot \chi^4 \cdot (y^+)^4} = \\ = \int_0^{R_1^+} \frac{(1 + \omega_E \cdot \tau_p) \cdot dy^+}{Sc_{Br}(1 + \omega_E \cdot \tau_p) + 0,01 \cdot \chi^4 \cdot (y^+)^4}.$$

Introducing new variables

$$(1 + \omega_E \cdot \tau_p) = a; \;\; Sc_{Br}(1 + \omega_E \cdot \tau_p) = b; \\ 0,01 \cdot \chi = c \quad . \quad (39)$$

Let us transform equation (38) using (39) to the form

$$\int_0^5 \frac{a \cdot dy^+}{b + c \cdot (y^+)^4} \, . \quad (40)$$

As a result of integration, we get

$$\int_0^5 \frac{a \cdot dy^+}{b + c \cdot (y^+)^4} = 0,17 \cdot a \cdot \left(\frac{b}{c}\right)^{1/4} \times \\ \times \ln\left(\frac{\left(\sqrt{\frac{b}{c}} + 25 + 7,07\left(\frac{b}{c}\right)^{1/4}\right)}{\left(\sqrt{\frac{b}{c}} + 25 - 7,07\left(\frac{b}{c}\right)^{1/4}\right)}\right) + 0,35 \cdot a \cdot \left(\frac{b}{c}\right)^{1/4} \times \\ \times \left[arctg\left(\frac{\left(\frac{b}{c}\right)^{1/4} + 7,07}{\left(\frac{b}{c}\right)^{1/4}}\right) - arctg\left(\frac{\left(\frac{b}{c}\right)^{1/4} - 7,07}{\left(\frac{b}{c}\right)^{1/4}}\right)\right]. \quad (41)$$

Finally, for the first term of equation (33), we have

$$\int_0^{R_1^+} \frac{a \cdot dy^+}{Sc_{Br} \cdot a + 0,01 \cdot \chi^4 \cdot (y^+)^4} = \\ 0,17 \cdot a \cdot \left(\frac{Sc_{Br}(1 + \omega_E \cdot \tau_p)}{0,01\chi}\right)^{1/4} \times \\ \times \ln\left(\frac{\left(\sqrt{\frac{Sc_{Br} \cdot a}{0,01\chi}} + 25 + 7,07\left(\frac{Sc_{Br} \cdot a}{0,01\chi}\right)^{1/4}\right)}{\left(\sqrt{\frac{Sc_{Br} \cdot a}{0,01\chi}} + 25 - 7,07\left(\frac{Sc_{Br} \cdot a}{0,01\chi}\right)^{1/4}\right)}\right) + \\ + 0,35 \cdot a \cdot \left(\frac{Sc_{Br} \cdot a}{0,01\chi}\right)^{1/4} \times \\ \times \left[\begin{array}{l} arctg\left(\frac{\left(\frac{Sc_{Br} \cdot a}{0,01\chi}\right)^{1/4} + 7,07}{\left(\frac{Sc_{Br} \cdot a}{0,01\chi}\right)^{1/4}}\right) - \\ -arctg\left(\frac{\left(\frac{Sc_{Br} \cdot a}{0,01\chi}\right)^{1/4} - 7,07}{\left(\frac{Sc_{Br} \cdot a}{0,01\chi}\right)^{1/4}}\right) \end{array} \right] \quad (42)$$

Consider the second term of the right-hand side of equation (34)

$$\int_{R_1^+}^{R_2^+} \frac{\nu \cdot dy^+}{D_P} = \int_0^5 a \cdot \frac{\nu \cdot dy^+}{\nu_T} = a \int_5^{30} \frac{dy^+}{(0,2y^+ - 0,959)} =$$
$$= a \cdot \frac{1}{0,2} \cdot \ln \frac{30 \cdot 0,2 - 0,959}{5 \cdot 0,2 - 0,959} = 24 \cdot (1 + \omega_E \tau_p). \quad (43)$$

Consider the third term of the right-hand side of equation (34)

$$\int_{R_2^+}^{R_\delta^+} \frac{\nu \cdot dy^+}{D_P} = \int_{30}^{R_\delta^+} a \cdot \frac{\nu \cdot dy^+}{\nu_T} = a \int_{30}^{R_\delta^+} \frac{dy^+}{0,4y^+ - 1} =$$
$$= a \cdot \frac{1}{0,4} \cdot \ln \frac{R_\delta^+ \cdot 0,4 - 1}{30 \cdot 0,4 - 1} = 2,5 \cdot (1 + \omega_E \tau_p) \times \quad (44)$$
$$\times \ln \left(\frac{R_\delta^+ \cdot 0,4 - 1}{11} \right).$$

After integration, expression (34) takes the form

$$\frac{1}{\beta_d^+} = 0,17 \cdot a \cdot \left(\frac{Sc_{Br} \cdot a}{0,01\chi} \right)^{1/4} \times$$
$$\times \ln \left(\frac{\left(\sqrt{\frac{Sc_{Br} \cdot a}{0,01\chi}} + 25 + 7,07 \left(\frac{Sc_{Br} \cdot a}{0,01\chi} \right)^{1/4} \right)}{\left(\sqrt{\frac{Sc_{Br} \cdot a}{0,01\chi}} + 25 - 7,07 \left(\frac{Sc_{Br} \cdot a}{0,01\chi} \right)^{1/4} \right)} \right) +$$
$$+ 0,35 \cdot a \cdot \left(\frac{Sc_{Br} \cdot a}{0,01\chi} \right)^{1/4} \times$$
$$\times \left[arctg \left(\frac{\left(\frac{Sc_{Br} \cdot a}{0,01\chi} \right)^{1/4} + 7,07}{\left(\frac{Sc_{Br} \cdot a}{0,01\chi} \right)^{1/4}} \right) - \right.$$
$$\left. - arctg \left(\frac{\left(\frac{ScBr \cdot a}{0,01\chi} \right)^{1/4} - 7,07}{\left(\frac{ScBr \cdot a}{0,01\chi} \right)^{1/4}} \right) \right] + \quad (45)$$
$$+ a \cdot \left(24 + 2,5 \cdot \ln \left(\frac{R_\delta^+ \cdot 0,4 - 1}{11} \right) \right).$$

3. Model verification

To obtain the calculated values of the mass transfer coefficient, the following initial data were selected according to the proposed model:
- working fluid: water-oil emulsion in the form of waste water from a plant for the production of reinforced concrete structures;
- a tubular ceramic membrane element with an internal diameter of d =0.006 m, a length of L=0.8 m, and a membrane porosity of e = 0.6, manufactured by KeramikFilter LLC, Moscow;
- the average permeate flow rate W_p = 0.07-0.1 m/s;
- the concentration of suspended substances c = 0.01 kg/kg;
- sediment density ρ_s = 2100 kg/m^3;
- density and viscosity of the water-oil emulsion ρ = 900 kg/m^3 and m =0.0101 Pa·s;
- the flow rate of the emulsion in the membrane module u = 10 m/s.

An acoustic particle analyzer APS-100 was used to measure the contamination particles.

The results of calculating the mass transfer coefficient are presented in Table 1 and Figure 1.

Table 1. Results of calculating the mass transfer coefficient

Sc_{Br}	5	15	25	50	75	100	200	300	400
$d_s \cdot 10^6$, м	12	18	21	27	31,6	34,8	43,8	50,2	55,3
$\beta_d \cdot 10^3$									
(25)	91	41	27	14	9,7	7,6	3,7	2,5	1,9
(32)	63	28	18	9,4	6,4	4,8	2,45	1,6	1,2
(45)	44	21	15	9,5	7,2	5,9	3,8	2,9	2,4

From the calculated data obtained, it follows that the highest value of the mass transfer coefficient β_d and deposition intensity corresponds to the particle size ds from 10 to 35 microns.

The adequacy of the calculated values of the mass transfer coefficient was verified by the model validation method.

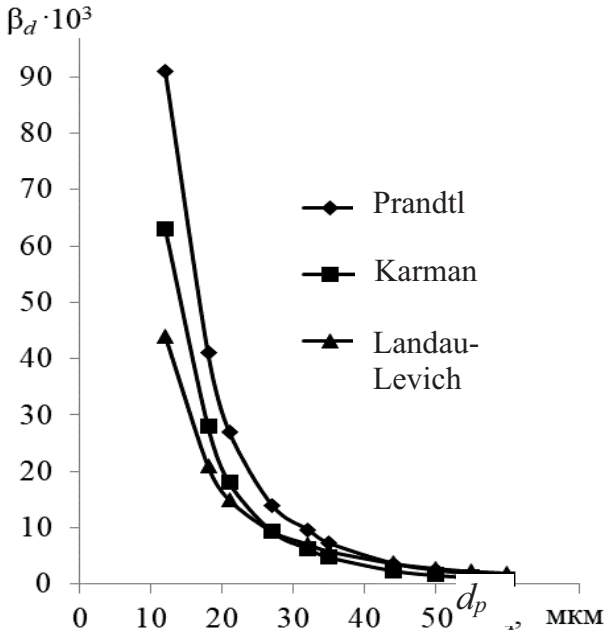


Figure 1. Changes in the mass transfer coefficient β_d an average flow rate u = 10 m/s

Since the known results on the deposition of particles on the walls of circular channels were obtained for various media with different physicochemical properties from the considered viscous heterogeneous systems, it is better to use dimensionless values for model validation.

In our case, it is convenient to consider the dependence (Fig. 2) of the dimensionless value of the mass transfer coefficient (deposition rate) β^+ on the inertia parameter τ^+ (dimensionless relaxation time).

The inertia parameter is determined taking into account the equation by the expression

$$\tau^+ = \frac{u^{*2} \cdot \tau_p}{\nu} = \frac{u^{*2} \cdot d_s^2}{18 \cdot \nu^2} \quad . \qquad (46)$$

To compare the data, the Reynolds criterion Re+ was used, based on the dynamic velocity and channel radius

$$\mathrm{Re}^+ = \frac{u^* \cdot r}{\nu}. \qquad (47)$$

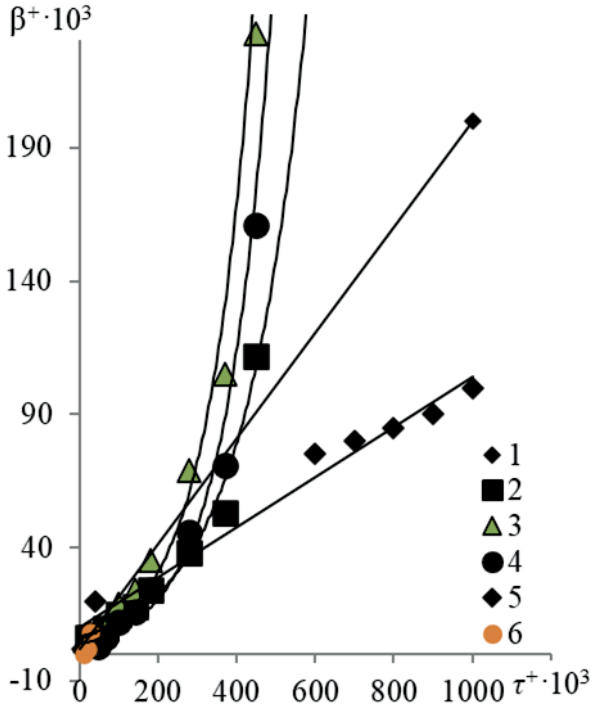


Figure 2. Dependence of the deposition rate on the inertia parameter:
1-empirical correlation (Sc_{Br} = 106, Re^+ = 150) [18]; 2, 3, 4 - data obtained from the developed models for the boundary layer according to the Landau-Levitch, Karman, and Prandtl theory, respectively (Sc_{Br} =5÷400, Re^+ = 100); 5 - direct numerical simulation data (Sc_{BR} = ∞, Re^+ = 150) [19]; 6 – data obtained in the paper (Sc_{Br} =1,310 106, Re^+ = 400÷1300) [20]

As well-known results, we used the data presented in the works of Koji Fukagata, Said Zaraya, and Fritz H. Bark, who obtained an empirical correlation of the deposition rate for the turbulent diffusion of copper particles with a size of 70 microns and glass particles with a size of 50 microns in a circular channel [18], Marchioli S., Picciotto M., Soldati A., who studied turbulent diffusion of copper particles with a size of in a vertical channel, based on the solution of the Navier-Stokes equation by direct Numerical Simulation [19], as well as data from Wells A. K. and Chamberlain A. K., which were used to study the deposition of radioactive particles in the form of polystyrene spheres with a diameter of 5 microns, containing 51Cr, drops

of tricresyl phosphate with a diameter of 2.1; 1.1 mm. and 0.65 microns with an activity of 32P and natural Aitken nuclei labeled ThB (212Pb) from air flows to vertical surfaces [20].

As can be seen from Figure 2, there is a satisfactory convergence of the results of calculating β^+ about ± 10%, calculated from expressions (25), (32) and (45) with the data known in the scientific literature within the inertia parameter τ^+ from 0 to $400 \cdot 10^{-3}$, which corresponds to a particle size from 12 to 40 microns at the flow velocity in the channel is 10 m/s, and allows us to recommend this method for calculating the mass transfer coefficient from the flow core to the channel walls for practical application.

CONCLUSIONS

The obtained expressions for determining the mass transfer coefficient have found practical application in the development of hardware design of the water-oil emulsion separation process. Before ultrafiltration of wastewater, they were pretreated on a centrifugal separator model SOG-913. The separator separation factor at maximum RPM was 10000. Figure 3 shows a fragment of quantitative analysis of dirt particles with sizes from 5 to 100 microns after centrifugal separation.

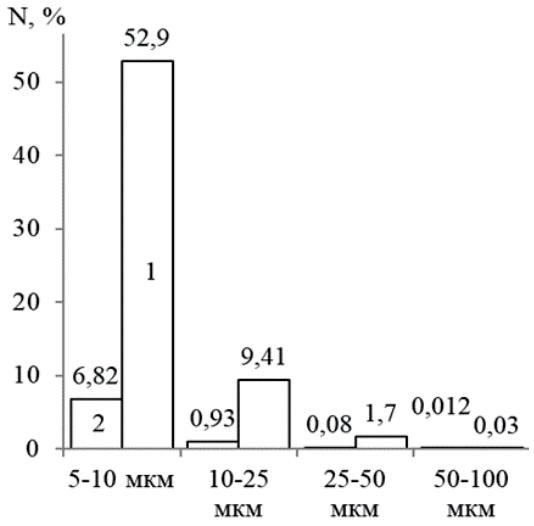


Figure 3. Proportion of dirt particles depending on their size: 1-before separation; 2-after separation

As can be seen from Figure 3, the proportion of particle sizes that meet the proposed mathematical model and are deposited on the channel walls is 50-60% before centrifugal separation, and 6-8% after separation. A large proportion of particles after pretreatment (80-90%) have a size of 1 to 3 microns.

These particles will not significantly affect the formation of sediment, as they completely follow the turbulent pulsations of the medium.

The results obtained indicate the adequacy of the upgraded model of turbulent migration of particles on the channel walls and give grounds to recommend it for practical use.

REFERENCES

1. **Mednikov E.P.** (1986) Turbulentny`j perenos i osazhdenie ae`rozolej [Turbulent transfer and deposition of aerosols]. Moskow: Nauka. (in Russian)
2. **Laptev A.G., Farakhov M.I.** (2008) Gidromehanicheskie processy` v neftehimii i e`nergetike [Hydromechanical processes in petrochemistry and power engineering]. Kazan: Publishing house of Kazan State University. (in Russian)
3. **Volgina L., Sergeev S.** (2023) Ocenka massy` otlozhenij, formiruyushhixsya v gorodskoj kollektornoj sisteme [Assessment of the mass of deposits formed in the urban collective system]. International Journal for Computational Civil and Structural Engineering, vol.19, no 1, pp. 23-31. (in Russian)
4. **Izmailova S.V., Vasiliev A.V.** (2016) Osnovny`e aspekty` razvitiya e`kologicheskoj nauki v XX - nachale XXI V. (na primere ochistki stochny`x vod) [Basic aspects of the development of environmental science in the XX - early XXI Century (on the example of wastewater treatment)]. Proceedings of the Samara Scientific Center of the Russian Academy of Sciences, vol. 18, no 4-5, pp. 974-977. (in Russian)

5. **Shaikhiev I.G., Andreev D.S., Fedotova A.V., Dryakhlov V.O.** (2017) Razdelenie vodoneftyanoj e`mul`sii polisul`fonamidny`mi membranami, obrabotanny`mi v potoke plazmy` v srede argona i vozduxa [Separation of water-oil emulsion by polysulfonamide membranes treated in a stream plasma in the argon and air environment]. Bulletin of the Kazan Technological University, vol. 20, no 1, pp. 139-142. (in Russian)
7. **Kjølaas J., Schümann H., Gonzalez D., Jo-hansen S.** (2022) Modelling of dispersed oil/water flow in a near-horizontal pipe. Chemical En-gineering Science, vol. 263, no 1:118074.
8. **Yao Y., Huan X., Capecelatro J.** (2022) Multi-fidelity uncertainty quantification of particle deposition in turbulent pipe flow. Journal of Aerosol Science vol. 166(44):106065
9. **Yan Zh., Li Z., Cheng Sh. Wang X., Zhang L., Zheng L. Saroj, Devendra.** (2022) Transport and deposition of solid phosphorus-based min-eral particles in urine diversion systems. Envi-ronmental technology, vol.44, pp. 1 – 34.
10. **Zaichik L.I., Alipchenkov V.M.** (2007) Statisticheskie modeli dvizheniya chasticz v turbulentnoj zhidkosti. [Statistical models of particle motion in a turbulent fluid]. Moskow: Fizmatlit. (in Russian)
11. **Shin M., Lee J.W.** (2001) Memory effect in the Eu-lerian particle deposition in a fully developed turbulent channel flow. J. Aerosol Sci., vol. 32, pp. 675−693.
12. **Derevich I.V.** (2000) Statistical modelling of mass transfer in turbulent two-phase dispersed flows. 1. Model development. Inter. J. Heat and Mass Transferl, vol. 43, no 19, pp. 3709−3723.
13. **Derevich I.V.** (2000) Statistical modelling of mass transfer in turbulent two-phase dispersed flows. 2. Calculation results. Inter. J. Heat and Mass Transfer, vol. 43, no 19, pp. 3725−3734.
14. **Soldati A., Marchioli S**. (2009) Physics and model-ling of turbulent particle deposition and en-trainment: Review of a systematic study. In-ter. J. Multiphase Flow, vol. 35, no 9, pp. 827−839.
15. **Sikovsky D.F.** (2010) Zakonomernosti osazhdeniya chasticz iz turbulentnogo gazodispersnogo potoka v kanalax [Regularities of particle deposition from turbulent gas-discharge flow in channels]. Izvestiya RAS. Fluid and gas mechanics, no 1, pp. 84-95. (in Russian)
16. **Kafarov V.V.** (1979) Osnovy` massoperedachi [Fundamentals of mass transfer]. Moskow: "Higher School". (in Russian)
17. **Fedosov S.V., Markelov A.V., Sokolov A.V., Osadchy Yu.P.** (2021) Matematicheskoe modelirovanie turbulentnoj migracii chasticz v pogranichnom sloe trubchatogo membrannogo e`lementa [Mathematical modeling of turbulent migration of particles in the boundary layer of a tubular membrane element]. Membranes and membrane technologies, vol. 11, no 6, pp. 435-446. (in Russian)
18. **Fukagata, K., Zahrai, S., Bark, F.H.** (1998) Force balance in a turbulent particulate channel flow. Inter. J. Multiphase Flow, vol.24, no 6, pp. 867−887
19. **Marchioli, C., Picciotto, M., Soldati A.** (2007) Influence of gravity and lift on particle velocity statistics and transfer rates in turbulent vertical channel flow. Inter. J. Multiphase Flow, vol. 33, no.3, pp. 227−251.
20. **Wells A.C., Chamberlain A.C.** (1967) T ransport of small particles to vertical surfaces. Brit. J. Appl. Phys, vol. 18, no. 12, pp. 1793−1799.

СПИСОК ЛИТЕРАТУРЫ

1. **Медников Е.П.** Турбулентный перенос и осаждение аэрозолей. – М.: Наука, 1986. – 176 с.

2. **Лаптев А.Г.,Фарахов М.И.** Гидромеханические процессы в нефтехимии и энергетике. – Казань: Изд-во Казанск. гос. ун-та, 2008. – 729 с.
3. **Волгина Л., Сергеев С.** Оценка массы отложений, формирующихся в городской коллекторной системе // International Journal for Computational Civil and Structural Engineering, 2023, №19(1). С. 23–31.
4. **Измайлова С.В., Васильев А.В.** Основные аспекты развития экологической науки в XX - начале XXI В. (на примере очистки сточных вод) // Известия Самарского научного центра Российской академии наук, 2016, № 18 (4-5). С. 974-977.
5. **Шайхиев И.Г., Андреев Д.С., Федотова А.В., Дряхлов В.О.** Разделение водонефтяной эмульсии полисульфонамидными мембранами, обработанными в потоке плазмы в среде аргона и воздуха // Вестник Казанского технологического университета, 2017, № 20 (1). С. 139-142.
6. **Guha A.** Transport and deposition of particles in turbulent and laminar flows // Ann. Rev. Fluid Mechanics, 2008, No. 40, pp. 311−341.
7. **Kjølaas J., Schümann H., Gonzalez D., Johansen S.** Modelling of dispersed oil/water flow in a near-horizontal pipe // Chemical Engineering Science September, 2022, No. 263(1):118074.
8. **Yao Y., Huan X., Capecelatro J.** Multifidelity uncertainty quantification of particle deposition in turbulent pipe flow // Journal of Aerosol Science, 2022, No. 166(44):106065
9. **Yan Zh., Li Z., Cheng Sh. Wang X., Zhang L., Zheng L. Saroj D**. Transport and deposition of solid phosphorus-based mineral particles in urine diversion systems // Environmental technology, 2022, No.44, pp. 1 – 34.
10. **Зайчик Л.И., Алипченков В.М.** Статистические модели движения частиц в турбулентной жидкости. – М.: Физматлит, 2007. - 308 с.
11. **Shin M., Lee J.W.** Memory effect in the Eulerian particle deposition in a fully developed turbulent channel flow // J. Aerosol Sci, 2001, No. 32. pp. 675−693.
12. **Derevich I.V.** Statistical modelling of mass transfer in turbulent two-phase dispersed flows. 1. Model development // Inter. J. Heat and Mass Transfer, 2000, Vol. 43, No. 19. pp. 3709−3723.
13. **Derevich I.V.** Statistical modelling of mass transfer in turbulent two-phase dispersed flows. 2. Calculation results // Inter. J. Heat and Mass Transfer, 2000, Vol. 43, No. 19. pp. 3725−3734.
14. **Soldati A., Marchioli S.** Physics and modelling of turbulent particle deposition and entrainment: Review of a systematic study // Inter. J. Multiphase Flow, 2009, Vol. 35, No. 9. pp. 827−839.
15. **Сиковский Д.Ф.** Закономерности осаждения частиц из турбулентного газодисперсного потока в каналах // Известия РАН. Механика жидкости и газа, 2010, № 1. С. 84−95.
16. **Кафаров В.В.** Основы массопередачи. — М.: "Высшая школа", 1979. - 439 с.
17. **Федосов С.В., Маркелов А.В., Соколов А.В., Осадчий Ю.П.** Математическое моделирование турбулентной миграции частиц в пограничном слое трубчатого мембранного элемента // Мембраны и мембранные технологии,2021, Т. 11, № 6, С. 435-446.
18. **Fukagata K., Zahrai S., Bark F.H.** Force balance in a turbulent particulate channel flow // Inter. J. Multiphase Flow, 1998, Vol.24, No. 6, pp. 867−887
19. **Marchioli C., Picciotto M., Soldati A.** Influence of gravity and lift on particle velocity statistics and transfer rates in turbulent vertical channel flow // Inter. J. Multiphase Flow, 2007, Vol. 33, No.3, pp. 227−251.
20. **Wells A.C., Chamberlain A.C.** Transport of small particles to vertical surfaces // Brit. J. Appl. Phys, 1967, Vol. 18, No. 12, pp. 1793−1799.

Sergey Viktorovich Fedosov – Academician of the RAACS, Doctor of Technical Sciences, Professor of the Department of Technology and Organization of Construction Production, National Research Moscow State University of Civil Engineering, 26, Yaroslavl Highway, Moscow, Russia, fedosov-academic53@mail.ru.

Alexander Vladimirovich Markelov – Candidate of Technical Sciences, Associate Professor of the Department of Infrastructure and Transport of the Yaroslavl State Technical University, 88, Moskovsky Prospekt, Yaroslavl, 150023, Russia, aleksandr203.37@mail.ru.

Сергей Викторович Федосов – академик РААСН, д.т.н., профессор кафедры технологии и организация строительного производства ФГБОУ ВО «Национальный исследовательский Московский государственный строительный университет» , ФГБОУ ВО «НИУ МГСУ», 26, Ярославское шоссе, г. Москва, Россия, fedosov-academic53@mail.ru.

Александр Владимирович Маркелов – к.т.н., доцент кафедры инфраструктуры и транспорта ФГБОУ ВО «Ярославский государственный технический университет» ФГБОУ ВО «ЯГТУ», 88, Московский проспект, г. Ярославль, 150023, Россия, aleksandr203.37@mail.ru.

International Journal for Computational Civil and Structural Engineering, 19(4) 147–154(2023)

DOI:10.22337/2587-9618-2023-19-4-147-154

DETERMINATION OF CONCRETE RHEOLOGICAL PARAMETERS USING NONLINEAR OPTIMIZATION METHODS

Anton S. Chepurnenko, Stepan V. Litvinov, Batyr M. Yazyev

Don State Technical University, Rostov-on-Don, RUSSIA

Abstract. The article proposes a method for processing concrete creep curves based on the nonlinear equation of V.M. Bondarenko. The experimental data of A.V. Yashin is used. The problem of finding rheological parameters and the nonlinearity function is posed as a nonlinear optimization problem. The objective function represents the sum of the squared deviations of the experimental values of the creep strain from the theoretical values for all creep curves for one concrete at different stress levels. The minimum of the objective function is found using the interior point method, the surrogate optimization method, the pattern search method, the genetic algorithm, and the particle swarm method. It has been established that the first of these methods has the greatest efficiency. The proposed approach provides high quality approximation of experimental curves at all stress levels. It is shown that for concrete the nonlinearity of creep deformations is more pronounced than the nonlinearity of instantaneous deformations, and the same function cannot be used to describe these two types of nonlinearity.

Keywords: concrete, creep, viscoelasticity, viscoplasticity, nonlinearity

ОПРЕДЕЛЕНИЕ РЕОЛОГИЧЕСКИХ ПАРАМЕТРОВ БЕТОНА ПРИ ПОМОЩИ МЕТОДОВ НЕЛИНЕЙНОЙ ОПТИМИЗАЦИИ

А.С. Чепурненко, С.В. Литвинов, Б.М. Язьев

Донской государственный технический университет, г. Ростов-на-Дону, РОССИЯ

Аннотация: В статье предлагается методика обработки кривых ползучести бетона на основе нелинейного уравнения В.М. Бондаренко. Используются экспериментальные данные А.В. Яшина. Задача поиска реологических параметров и функции нелинейности ставится как задача нелинейной оптимизации. Целевая функция представляет сумму квадратов отклонений экспериментальных значений деформации ползучести от теоретических по всем кривым ползучести для одного бетона при различных уровнях напряжений. Минимум целевой функции отыскивается при помощи метода внутренней точки, метода суррогатной оптимизации, метода шаблонного поиска, генетического алгоритма и метода роя частиц. Установлено, что наибольшей эффективностью обладает первый из указанных методов. Предлагаемый подход обеспечивает высокое качество аппроксимации экспериментальных кривых при всех уровнях напряжений. Показано, что для бетона нелинейность деформаций ползучести более выраженная, чем нелинейность мгновенных деформаций, и для описания этих двух видов нелинейности нельзя использовать одну и ту же функцию.

Ключевые слова: бетон, ползучесть, вязкоупругость, вязкопластичность, нелинейность

INTRODUCTION

There are a large number of different theories of nonlinear concrete creep in the literature, which differ in the set of hypotheses used and approaches to their construction [1-10].

One of the first variants of the nonlinear theory of concrete creep, which generalized the linear Harutyunyan-Maslov equation, was the theory of N.Kh. Harutyunyan and P.I. Vasiliev [11-13]:

$$\varepsilon(t)=\frac{\sigma(t)}{E(t)}-\int_{\tau_0}^{t}\frac{\partial}{\partial\tau}\left[\frac{1}{E(\tau)}\right]\sigma(\tau)d\tau- -\int_{\tau_0}^{t}\frac{\partial C(t,\tau)}{\partial\tau}F\left[\sigma(\tau)\right]d\tau, \quad (1)$$

where $C(t,\tau)$ is the measure of creep, $F\left[\sigma(\tau)\right]$ is the nonlinearity function, τ_0 the

initial moment of time at which the load is applied.

Equation (1) takes into account the nonlinear component of creep deformations, but does not take into account the instantaneous nonlinearity of deformation.

Another version of the Harutyunyan-Maslov equation generalization, which allows taking into account both nonlinear creep and instantaneous deformation nonlinearity, was proposed by Yu. N. Rabotnov [14]:

$$f\left[\varepsilon(t)\right]=\frac{\sigma(t)}{E(t)}-\int_{\tau_0}^{t}\frac{\partial}{\partial\tau}\left[\frac{1}{E(\tau)}\right]\sigma(\tau)d\tau- \\ -\int_{\tau_0}^{t}\frac{\partial C(t,\tau)}{\partial\tau}\sigma(\tau)d\tau, \quad (2)$$

where $f(\varepsilon)$ is the non-linear deformation function.

Close in essence to equation (2) is the viscoelastic-plastic model of hereditary aging of concrete, proposed by A.G. Tamrazyan [15]:

$$\varepsilon(t)=\frac{f[\sigma(t)]}{E(t)}-\int_{\tau_0}^{t}\frac{\partial C(t,\tau)}{\partial\tau}f[\sigma(\tau)]d\tau. \quad (3)$$

Equations (2) and (3) postulate the same nature of nonlinearity for instantaneous and long-term deformations, which does not correspond to the real rheological behavior of concrete.

More general is the equation of V.M. Bondarenko [16], having the form:

$$\varepsilon(t)=\frac{f_1\left[s(t)\right]}{E(t)}-\int_{\tau_0}^{t}\frac{\partial}{\partial\tau}\left(\frac{1}{E(\tau)}\right)f_1\left[s(\tau)\right]d\tau- \\ -\int_{\tau_0}^{t}\frac{\partial C(t,\tau)}{\partial\tau}f_2\left[s(\tau)\right]d\tau, \quad (4)$$

where $s(t)=\sigma(t)/R(t)$, $R(t)$ is the instant concrete strength, f_1 and f_2 are nonlinear functions corresponding to instantaneous and long-term deformation.

The instantaneous nonlinearity of concrete deformation is well studied, and the definition of the function f_1 does not cause great difficulties, which cannot be said about the function f_2.

The purpose of this work is to develop a methodology for finding the function f_2, as well as other rheological parameters that determine the measure of creep, from concrete creep curves at various stress levels.

METHODS

Let us consider the procedure for processing creep curves using the example of the curves presented in the work of A.V. Yashin [17]. In this paper, concrete with the compressive strength R_b = 30 MPa was tested at the age of $\tau_0=28$ days, with an initial modulus of elasticity $E_0=4\cdot10^4$ MPa at stress levels σ/R_b from 0.4 to 0.8 with a step of 0.1.

Thus, the total number of experimental curves for one class of concrete was 5.

As a measure of creep, the expression proposed by A.G. Tamrazyan was used [15]:

$$C(t,\tau)=C\frac{e^{\alpha t}-e^{\alpha\tau}}{e^{\alpha t}-1}+B\left(e^{-\gamma\tau}-e^{-\gamma t}\right). \quad (5)$$

This expression contains 4 rheological parameters C, B, α, γ to be determined. The advantage of the creep measure (5) is that its exponential form allows to pass from the integral creep law to the differential one and to calculate creep strains using the Euler or Runge-Kutta method. This transition is shown in [18].

Since the experimental data of A.V. Yashin do not contain information about the aging of concrete (change in time of its modulus of elasticity), then we will neglect this effect, i.e. we omit in equation (4) the term containing $\frac{\partial}{\partial\tau}\left(\frac{1}{E(\tau)}\right)$.

Then the dependence of the creep strain on time at a constant stress level $s = \sigma / R$ takes the form:

$$\varepsilon_{cr}(t) = f_2(s)\left(C\frac{e^{\alpha t} - e^{\alpha \tau_0}}{e^{\alpha t} - 1} + B\left(e^{-\gamma \tau_0} - e^{-\gamma t}\right)\right). \quad (5)$$

We pose the problem of determining the parameters C, B, α, γ, as well as the function $f_2(s)$, as a problem of nonlinear optimization. The objective function Z is built, the input parameters of which are C, B, α, γ, as well as 5 coefficients k_i according to the number of experimental curves, taking into account the nonlinear creep component depending on the stress level.

For the time points t_j at which the strains were measured, the objective function calculates the theoretical values of the creep strains using the formula:

$$\varepsilon_{cr,i}(t_j) = k_i\sigma_i\left(C\frac{e^{\alpha t_j} - e^{\alpha \tau_0}}{e^{\alpha t_j} - 1} + B\left(e^{-\gamma \tau_0} - e^{-\gamma t_j}\right)\right), \quad (6)$$

where σ_i is the stress in i-th experiment.

Next, the objective function Z calculates the sum of the squared deviations of the theoretical values of creep strains from the experimental values, multiplied by 1000, over all experimental curves:

$$Z = \sum_{i=1}^{5}\sum_{j=1}^{n}([\varepsilon_{cr,i,theor}(t_j) - \varepsilon_{cr,i,test}(t_j)]\cdot 1000)^2. \quad (7)$$

The objective function Z must reach a minimum.

The coefficients k_i must be greater than or equal to 1. We accept the range from 1 to 20 for them. The ranges for the parameters C, B, α, γ are presented in Table 1.

Table 1. Rheological parameters ranges

parameter	α, 1/day	γ, 1/day	C, MPa^{-1}	B, MPa^{-1}
min	10^{-4}	10^{-4}	10^{-5}	10^{-5}
max	0.1	0.1	10^{-4}	10^{-4}

The solution to the problem of creep curves processing was implemented in the MATLAB environment using the Optimization Toolbox and Global Optimization Toolbox packages. The following optimization methods were used to find the minimum of the objective function:

1. Interior point method [19]
2. Surrogate optimization method [20]
3. Pattern search method [21]
4. Genetic algorithm [22]
5. Particle swarm method [23-24].

The first of these methods allows to find a local minimum in the vicinity of the starting point of the search, the remaining methods are searching for a global minimum.

At the starting point of the search, the coefficients k_i were taken equal to 1. The values recommended in [15] were taken as the initial values for C, B, α, γ. They are given in Table. 2.

Table 2. Values of rheological parameters at the starting point of the search

α, 1/day	γ, 1/day	C, MPa^{-1}	B, MPa^{-1}
0.032	0.062	$3.77\cdot10^{-5}$	$5.68\cdot10^{-5}$

Note that the quality of the A.V. Yashin's experimental curves approximation with the indicated in the Table 2 values is unsatisfactory. They are probably defined for concrete of a different class or composition.

RESULTS AND DISCUSSION

Table 3 shows the values of the objective function obtained as a result of solving the problem of nonlinear optimization by the five methods indicated above.

Table 3. Minimal objective function values when using various optimization methods

Method	Z
Interior point	0.183
Surrogate optimization	2.26
Pattern search	2.25
Genetic algorithm	2.06
Particle swarm	1.42

It can be seen from Table 3 that the most effective of the methods used was the interior point method. The values of the constants C, B, α, γ, as well as the correction factors $k_1 \ldots k_5$, obtained by the internal point method, are given in Table 4.

Table 4. Rheological parameters of concrete obtained by the internal point method

α, 1/day	γ, 1/day	C, MPa^{-1}	B, MPa^{-1}
0.0014	0.0061	$1.02 \cdot 10^{-5}$	$1.78 \cdot 10^{-5}$

k_1	k_2	k_3	k_4	k_5
1.03	1.51	2.57	3.61	3.74

Fig. 1 shows the theoretical creep curves constructed using formula (6) and the parameters presented in Table. 4. Experimental points are marked with round markers.

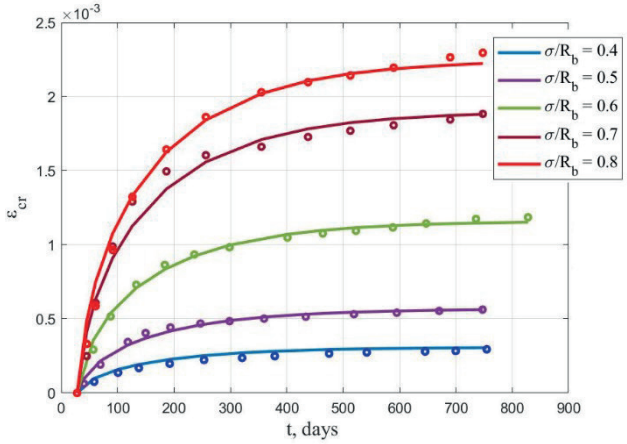


Figure 1. Comparison of theoretical creep curves with experimental results

The reliability of the approximation R^2 for each stress level is given in Table 5.

Table 5. Reliability of experimental curves approximation at different stress levels

$\frac{\sigma}{R_b}$	0.4	0.5	0.6	0.7	0.8
R^2	0.918	0.990	0.994	0.982	0.991

Fig. 2 shows the graph of the stress function $f_2(s)$, built on the basis of the calculated values of the coefficients $k_1 \ldots k_5$. For comparison, the graph of the function $f_1(s)$ is also shown, which corresponds to the Sargin formula [25] used in the Eurocodes to describe the instantaneous nonlinearity of concrete deformation:

$$f_1(s) = \frac{E_0 \varepsilon_R}{2}(k - (k-2)\cdot s - \sqrt{\left[(k-2)\cdot s - k\right]^2 - 4\cdot s}), \quad (8)$$

where E_0 is the concrete initial modulus of elasticity (at σ = 0), ε_R is the deformation at the top of the diagram $\sigma - \varepsilon$, $k = E_0 \varepsilon_R / R_b$ is the coefficient characterizing the curvature of the diagram $\sigma - \varepsilon$.

The deformation ε_R during plotting the $f_1(s)$ graph was determined by the empirical formula [26]:

$$\varepsilon_R = 0.058 \left(\frac{R_b}{E_0} \right)^{0.5}. \quad (9)$$

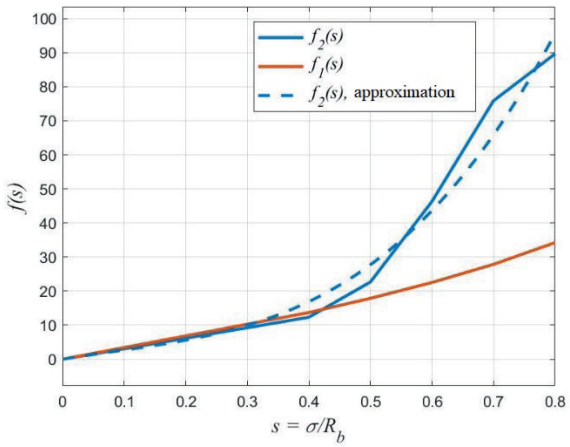


Figure 2. Comparison of the functions $f_1(s)$ and $f_2(s)$

It can be seen from Fig. 2 that for concrete, the nonlinearity of creep deformations is much more pronounced than the instantaneous nonlinearity of deformation, and these two types of nonlinearity cannot be described by one function, as is done in equations (2) and (3).

The dependence for $f_2(s)$ obtained by us is well approximated by the polynomial $f_2(s) = s \cdot (a \cdot s^2 + b \cdot s + c)$ at $a = 203.6$ MPa, $b = -51.25$ MPa, $c = 30.19$ MPa. This approximation is shown in Fig. 2 by dashed line. Reliability of approximation is $R^2 = 0.986$.

CONCLUSIONS

A technique for processing concrete creep curves based on the nonlinear theory of V.M. Bondarenko using nonlinear optimization methods is proposed. To solve the problem of nonlinear optimization, the interior point method, the surrogate optimization method, the pattern search method, the genetic algorithm, and the particle swarm method were applied. It has been established that the most effective method for the considered problem is the interior point method. On the basis of experimental concrete creep curves obtained by A.V. Yashin, its rheological parameters are determined. The use of the interior point method made it possible to achieve a high quality of approximation of the experimental curves.

It is shown that the nonlinearity of creep strains as a function of stress is more pronounced than the instantaneous nonlinearity of deformation, and these two types of nonlinearity cannot be described by a single function. On the basis of experimental data, the nonlinearity function for creep deformations was selected.

REFERENCES

1. **Zhang C., Zhu Z., Zhu S., He Z., Zhu D., Liu J., Meng S.** Nonlinear creep damage constitutive model of concrete based on fractional calculus theory //Materials. – 2019. – Vol. 12. – No. 9. – Article 1505.
2. **Li Y. et al.** Verification of concrete nonlinear creep mechanism based on meso-damage mechanics // Construction and Building Materials. – 2021. – Vol. 276. – Article 122205.
3. **Han B., Xie H.B., Zhu L., Jiang, P.** Nonlinear model for early age creep of concrete under compression strains //Construction and Building Materials. – 2017. – Vol. 147. – Pp. 203-211.
4. **Sanjarovskiy R., Ter-Emmanuilyan T., Manchenko M.** Creep of concrete and its instant nonlinear deformation in the calculation of structures //CONCREEP 10. – 2015. – Pp. 238-247.
5. **Sanjarovsky R., Manchenko M.** Creep of concrete and its instantaneous nonlinearity of deformation in the structural calculations //Scientific Israel-Technological Advantages. – 2015. – Vol. 17. – No. 1-2. – Pp. 180-187.
6. **Yu P., Li R.Q., Bie D.P., Yao X.M., Liu X. C., Duan Y.H.** A coupled creep and damage model of concrete considering rate effect // Journal of Building Engineering. – 2022. – Vol. 45. – Pp. 103621.
7. **Su L., Wang Y.F., Mei S.Q., Li P.F.** Experimental investigation on the fundamental behavior of concrete creep //Construction and Building Materials. – 2017. – Vol. 152. – Pp. 250-258.
8. **Bu P., Li Y., Wen L., Wang J., Zhang X.** Creep damage coupling model of concrete based on the statistical damage theory //Journal of Building Engineering. – 2023. – Vol. 63. – Article 105437.
9. **Mirzaahmedov A.T. et al.** Accounting For Non-Linear Work Of Reinforced Concrete In The Algorithms Of Calculation And Design Of Structures //The American Journal of Engineering and Technology. – 2020. – Vol. 2. – No. 11. – Pp. 54-66.
10. **Wang Q., Le J.L., Ren X.** Numerical modeling of delayed damage and failure of

concrete structures under sustained loading //Engineering Structures. – 2022. – Vol. 252. – Article 113568.
11. **Harutyunyan, N.Kh.** Some questions of the theory of creep. – M.: Gostekhteorizdat, 1952. – 323 p. (In Russian)
12. **Vasiliev P.I.** Connection between stresses and deformations in concrete under compression, taking into account the influence of time. Izv. VNIIG B.E. Vedeneeva. - 1951. - Vol. 45. - Pp. 76-93. (In Russian)
13. **Vasiliev P.I.** Some questions of plastic deformations of concrete // Izv. VNIIG B.E. Vedeneeva. - 1953. - Vol.49. – Pp. 17-102. (In Russian)
14. **Rabotnov Yu.N.** Creep of structural elements. – M.: Nauka, 1966. – 752 p. (In Russian)
15. **Tamrazyan A.G., Esayan S.G.** Concrete creep mechanics. – Moscow: MGSU. – 2012. – 524 p. (In Russian)
16. **Bondarenko V.M.** To the construction of a general theory of reinforced concrete (specifics, fundamentals, method) // Concrete and reinforced concrete. - 1978. - Pp. 20-22. (In Russian)
17. **Yashin A.V.** Deformations of concrete under prolonged exposure to high stresses and its long-term resistance in compression // Features of deformations of concrete and reinforced concrete and the use of computers to assess their influence on the behavior of structures / NIIZhB. - M.: Stroyizdat, 1969. - Pp. 38-76. (In Russian)
18. **Mailyan L., Chepurnenko A., Ivanov A.** Calculation of prestressed concrete cylinder considering creep of concrete // Procedia Engineering. – 2016. – Vol. 165. – Pp. 1853-1857.
19. **Byrd R.H., Hribar M.E., Nocedal J.** An interior point algorithm for large-scale nonlinear programming // SIAM Journal on Optimization. – 1999. – Vol. 9. – No. 4. – Pp. 877-900.
20. **Gutmann H.-M.** A radial basis function method for global optimization // Journal of Global Optimization. – 2001. – No. 19. Pp. 201–227.
21. **Kolda T.G., Lewis R. M., Torczon V.** A generating set direct search augmented Lagrangian algorithm for optimization with a combination of general and linear constraints // Technical Report SAND2006-5315. Sandia National Laboratories, 2006.
22. **Mirjalili, S.** Genetic algorithm // Evolutionary algorithms and neural networks. – Springer, Cham, 2019. – Pp. 43-55.
23. **Mezura-Montes E., Coello Coello C.A.** Constraint-handling in nature-inspired numerical optimization: Past, present and future. // Swarm and Evolutionary Computation, 2011. – Pp. 173–194.
24. **Pedersen M.E.** Good Parameters for Particle Swarm Optimization. – Luxembourg: Hvass Laboratories, 2010.
25. **Chepilko S.O.** Nonlinear creep in a steel-reinforced concrete beam // Vestnik grazhdanskikh inzhenerov. – 2020. – No. 5. - Pp. 108-116. (In Russian)
26. **Ishchenko A.V., Pogodin D.A.** Calculation of reinforced concrete arches on stability when creeping // IOP Conference Series: Materials Science and Engineering. – IOP Publishing, 2019. – Т. 698. – №. 2. – С. 022086.

СПИСОК ЛИТЕРАТУРЫ

1. **Zhang C., Zhu Z., Zhu S., He Z., Zhu D., Liu J., Meng S.** Nonlinear creep damage constitutive model of concrete based on fractional calculus theory //Materials. – 2019. – Vol. 12. – No. 9. – Article 1505.
2. **Li Y. et al.** Verification of concrete nonlinear creep mechanism based on meso-damage mechanics // Construction and Building Materials. – 2021. – Vol. 276. – Article 122205.
3. **Han B., Xie H.B., Zhu L., Jiang, P.** Nonlinear model for early age creep of concrete under compression strains

//Construction and Building Materials. – 2017. – Vol. 147. – Pp. 203-211.
4. **Sanjarovskiy R., Ter-Emmanuilyan T., Manchenko M.** Creep of concrete and its instant nonlinear deformation in the calculation of structures //CONCREEP 10. – 2015. – Pp. 238-247.
5. **Sanjarovsky R., Manchenko M.** Creep of concrete and its instantaneous nonlinearity of deformation in the structural calculations //Scientific Israel-Technological Advantages. – 2015. – Vol. 17. – No. 1-2. – Pp. 180-187.
6. **Yu P., Li R.Q., Bie D.P., Yao X.M., Liu X. C., Duan Y.H.** A coupled creep and damage model of concrete considering rate effect // Journal of Building Engineering. – 2022. – Vol. 45. – Pp. 103621.
7. **Su L., Wang Y.F., Mei S.Q., Li P.F.** Experimental investigation on the fundamental behavior of concrete creep //Construction and Building Materials. – 2017. – Vol. 152. – Pp. 250-258.
8. **Bu P., Li Y., Wen L., Wang J., Zhang X.** Creep damage coupling model of concrete based on the statistical damage theory //Journal of Building Engineering. – 2023. – Vol. 63. – Article 105437.
9. **Mirzaahmedov A.T. et al.** Accounting For Non-Linear Work Of Reinforced Concrete In The Algorithms Of Calculation And Design Of Structures //The American Journal of Engineering and Technology. – 2020. – Vol. 2. – No. 11. – Pp. 54-66.
10. **Wang Q., Le J.L., Ren X.** Numerical modeling of delayed damage and failure of concrete structures under sustained loading //Engineering Structures. – 2022. – Vol. 252. – Article 113568.
11. **Арутюнян, Н.Х.** Некоторые вопросы теории ползучести. – М.: Гостехтеориздат, 1952. – 323 с.
12. **Васильев П.И.** Связь между напряжениями и деформациями в бетоне при сжатии с учетом влияния времени // Изв. ВНИИГ им. Б.Е. Веденеева. – 1951. – Т. 45. – С. 76-93 .
13. **Васильев П.И.** Некоторые вопросы пластических деформаций бетона // Изв. ВНИИГ им. Б.Е. Веденеева. – 1953. – Т.49. – С. 17-102
14. **Работнов Ю.Н.** Ползучесть элементов конструкций. – М.: Наука, 1966. – 752 с.
15. **Тамразян А.Г., Есаян С.Г.** Механика ползучести бетона //М.: МГСУ. – 2012. – 524 с.
16. **Бондаренко В.М.** К построению общей теории железобетона (специфика, основы, метод) // Бетон и железобетон. – 1978. – С. 20-22.
17. **Яшин А.В.** Деформации бетона под длительным воздействием высоких напряжений и его длительное сопротивление при сжатии // Особенности деформаций бетона и железобетона и использование ЭВМ для оценки их влияния на поведение конструкций / НИИЖБ. – М.: Стройиздат, 1969. – С. 38-76.
18. **Mailyan L., Chepurnenko A., Ivanov A.** Calculation of prestressed concrete cylinder considering creep of concrete // Procedia Engineering. – 2016. – Vol. 165. – Pp. 1853-1857.
19. **Byrd R.H., Hribar M.E., Nocedal J.** An interior point algorithm for large-scale nonlinear programming // SIAM Journal on Optimization. – 1999. – Vol. 9. – No. 4. – Pp. 877-900.
20. **Gutmann H.-M.** A radial basis function method for global optimization // Journal of Global Optimization. – 2001. – No. 19. Pp. 201–227.
21. **Kolda T.G., Lewis R. M., Torczon V.** A generating set direct search augmented Lagrangian algorithm for optimization with a combination of general and linear constraints // Technical Report SAND2006-5315. Sandia National Laboratories, 2006.
22. **Mirjalili, S.** Genetic algorithm // Evolutionary algorithms and neural networks. – Springer, Cham, 2019. – Pp. 43-55.
23. **Mezura-Montes E., Coello Coello C.A.** Constraint-handling in nature-inspired

numerical optimization: Past, present and future. // Swarm and Evolutionary Computation, 2011. – Pp. 173–194.
24. **Pedersen M.E.** Good Parameters for Particle Swarm Optimization. – Luxembourg: Hvass Laboratories, 2010.
25. **Чепилко С.О.** Нелинейная ползучесть в сталежелезобетонной балке //Вестник гражданских инженеров. – 2020. – №. 5. – С. 108-116.
26. **Ishchenko A.V., Pogodin D.A.** Calculation of reinforced concrete arches on stability when creeping // IOP Conference Series: Materials Science and Engineering. – IOP Publishing, 2019. – Т. 698. – №. 2. – С. 022086.

Chepurnenko Anton Sergeevich, DSc, Professor of the Department of Strength of Materials, Don State Technical University, 344000, Russia, Rostov-on-Don, Gagarin sq., 1, tel. +7 (863) 201-91-36, e-mail: anton_chepurnenk@mail.ru

Litvinov Stepan Victorovich, PhD, Head of the Department of Strength of Materials, Don State Technical University, 344000, Russia, Rostov-on-Don, Gagarin sq., 1, tel. +7 (863) 201-91-02, e-mail: litvstep@yandex.ru

Yazyev Batyr Meretovich, DSc, Professor of the Department of Strength of Materials, Don State Technical University, 344000, Russia, Rostov-on-Don, Gagarin sq., 1, tel. +7 (863) 201-91-36, e-mail: ps62@yandex.ru

Чепурненко Антон Сергеевич, доктор технических наук, профессор кафедры «Сопротивление материалов» Донского государственного технического университета, 344000, г. Ростов-на-Дону, пл. Гагарина, 1, тел. +7 (863) 201-91-36 , e-mail: anton_chepurnenk@mail.ru

Литвинов Степан Викторович, кандидат технических наук, заведующий кафедрой «Сопротивление материалов» Донского государственного технического университета, 344000, г. Ростов-на-Дону, пл. Гагарина, 1, тел. +7 (863) 201-91-02 , e-mail: litvstep@yandex.ru

Язьев Батыр Меретович, доктор технических наук, профессор кафедры «Сопротивление материалов» Донского государственного технического университета, 344000, г. Ростов-на-Дону, пл. Гагарина, 1, тел. +7 (863) 201-91-36 , e-mail: ps62@yandex.ru

International Journal for Computational Civil and Structural Engineering, 19(4) 155–165(2023)

DOI:10.22337/2587-9618-2023-19-4-155-165

DEVELOPMENT OF COMPUTATIONAL SCHEMES OF GENERALIZED KINEMATIC DEVICES THAT PRECISELY REGULATE THE NATURAL FREQUENCY SPECTRUM OF ELASTIC SYSTEMS WITH A FINITE NUMBER OF DEGREES OF MASS FREEDOM, IN WHICH THE DIRECTIONS OF MOTION ARE PARALLEL, BUT DO NOT LIE IN THE SAME PLANE PART 2: SAMPLES OF ANALYSIS

Leonid S. Lyakhovich [1,2], Pavel A. Akimov [2], Zaur R. Galyautdinov [1], Andrey S. Plyaskin [1]

[1] Tomsk State University of Architecture and Civil Engineering, Tomsk, RUSSIA

[2] National Research Moscow State University of Civil Engineering, Moscow, RUSSIA

Abstract: To date, for some elastic systems with a finite number of degrees of mass freedom, in which the directions of mass movement are parallel and lie in the same plane, methods have been developed for creating additional generalized targeted constraints and generalized targeted kinematic devices. Each generalized targeted constraint increases, and each generalized targeted kinematic device reduces the value of only one selected natural frequency to a predetermined value, without changing the remaining natural frequencies and natural modes. Earlier, for elastic systems with a finite number of degrees of mass freedom, in which the directions of mass motion are parallel, but do not lie in the same plane (for example, plates), an approach for the computing of a matrix of additional stiffness and a method for the development of computational schemes of additional generalized targeted constraints were developed. Also earlier, for such systems, an approach was proposed for the computing of a special matrix with allowance for additional inertial forces that determine a generalized targeted kinematic device. At the same time, the method of development of computational schemes of kinematic devices was not proposed. The first part of the paper was devoted to approach, that made it possible to develop computational schemes of generalized targeted kinematic devices for such systems as well. A variant of the computational scheme of constraint for the rod system with one degree of activity was considered. Some special properties of such targeted kinematic devices were revealed. The distinctive second part of the paper is devoted to corresponding samples of analysis.

Keywords: localization, natural frequency, natural mode, additional generalized targeted constraint, stiffness coefficients, inertial forces, generalized targeted kinematic device, samples of analysis

ФОРМИРОВАНИЕ РАСЧЕТНЫХ СХЕМ ОБОБЩЕННЫХ КИНЕМАТИЧЕСКИХ УСТРОЙСТВ, ПРИЦЕЛЬНО РЕГУЛИРУЮЩИХ СПЕКТР ЧАСТОТ СОБСТВЕННЫХ КОЛЕБАНИЙ УПРУГИХ СИСТЕМ С КОНЕЧНЫМ ЧИСЛОМ СТЕПЕНЕЙ СВОБОДЫ МАСС, У КОТОРЫХ НАПРАВЛЕНИЯ ДВИЖЕНИЯ ПАРАЛЛЕЛЬНЫ, НО НЕ ЛЕЖАТ В ОДНОЙ ПЛОСКОСТИ ЧАСТЬ 2: ПРИМЕРЫ РАСЧЕТА

Л.С. Ляхович [1, 2], П.А. Акимов [2], З.Р. Галяутдинов [1], А.С. Пляскин [1]

[1] Томский государственный архитектурно-строительный университет, г. Томск, РОССИЯ

[2] Национальный исследовательский Московский государственный строительный университет, г. Москва, РОССИЯ

Аннотация: К настоящему времени для некоторых упругих систем с конечным числом степеней свободы масс, у которых направления движения масс параллельны и лежат в одной плоскости, разработаны методы создания дополнительных обобщенных прицельных связей и обобщенных прицельных кинематических устройств. Каждая обобщённая прицельная связь увеличивает, а каждое обобщенное прицельное кинематическое устройство уменьшает величину лишь одной выбранной собственной частоты до наперед заданного значения, не изменяя при этом остальные собственные частоты и формы собственных колебаний. Ранее для упругих систем с конечным числом степеней свободы масс, у которых направления движения масс параллельны, но не лежат в одной плоскости (например, пластины), разработан подход образования матрицы дополнительных жесткостей и метод формирования расчетных схем дополнительных обобщенных прицельных связей. Также ранее для таких систем предложен подход образования матрицы учета действия дополнительных инерционных сил, определяющих обобщенное прицельное кинематическое устройство. При этом способ формирования расчетных схем кинематических устройств, предложен не был. В первой части статьи был предложен подход, позволяющий формировать расчетные схемы обобщенных прицельных кинематических устройств и для таких систем. Был рассмотрен вариант расчетной схемы связи, представленный стержневой системой с одной степенью активности, выявлены некоторые особые свойства таких прицельных кинематических устройств. В настоящей второй части статьи рассматриваются соответствующие примеры расчетов.

Ключевые слова: частота собственных колебаний, форма собственных колебаний, дополнительная обобщенная прицельная связь, коэффициенты жесткости, инерционные силы, обобщенное прицельное кинематическое устройство, примеры расчетов

Let's consider a hingedly supported rectangular plate measuring 6 *m* by 6 *m*, carrying concentrated masses $m[1]=1000\,kg$, $m[2]=1100\,kg$, $m[3]=1150\,kg$, $m[4]=1200\,kg$ (Figure 1*a*). The thickness of the plate is equal to 0.12 *m*. The modulus of elasticity of the plate material is equal to $E=2.4\cdot10^{10}\ N/m^2$. Poisson's ratio is equal to $\nu_0=0.2$.

Let's select the main system of the displacement method (Figure 1*b*) and construct the corresponding system of equations (1) from [1] (matrices $A=\|r[i,k]\|$, $M=\|m[i]\|$ from [1]). From equation (2) from [1] we determine the natural frequencies and natural modes of the plate. The values of the frequencies of natural vibrations of the plate and the coordinates of the corresponding natural modes are presented in Table 1 (columns contain natural frequencies and coordinates of natural modes). Such a plate was also considered in [8, 11]. The results, presented here in Table 1 do not differ significantly from the corresponding results in [8, 11]. This difference is due to the different accuracy of computing the coefficients of matrix $A=\|r[i,k]\|$ (matrix (1) from [1]). In [8, 11] the coefficients were determined based on the plate analysis with the use of Ritz method with retention of about thirty terms of the approximating series. In this work, SCAD software was used to compute the coefficients.

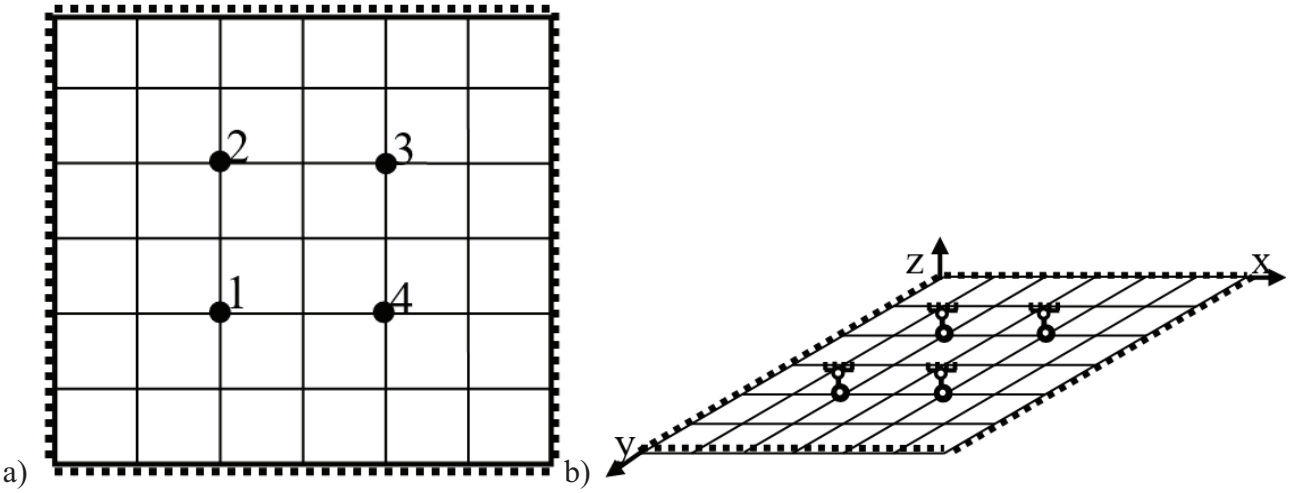
Let's assume that it is required to reduce the value of the first frequency of natural vibrations to 40 sec^{-1}.

To do this, in accordance with (4), (5), (8), (10) from [1], we can form a matrix of coefficients with allowance for the action of additional inertial forces (12). After forming this matrix, we can determine from equation (11) from [1] the modified spectrum of natural frequencies and the corresponding natural modes with allowance for the action of additional inertial forces (12) from [1].

The modified spectrum of natural frequencies and their corresponding natural modes are shown in Table 2.

The results, presented in Table 2, confirm that taking into account the matrix of additional inertial forces did not change any of the natural modes, but only reduced the value of only the first frequency of natural vibrations to a given value of 40 sec^{-1}.

The targeted kinematic device must correspond to the matrix of additional inertial forces (12). One of the variants of computational scheme of targeted kinematic device is shown in Figure 2*a* and Figure 2*b*. The accepted variant is represented by a statically determinate rod system.



a) b)

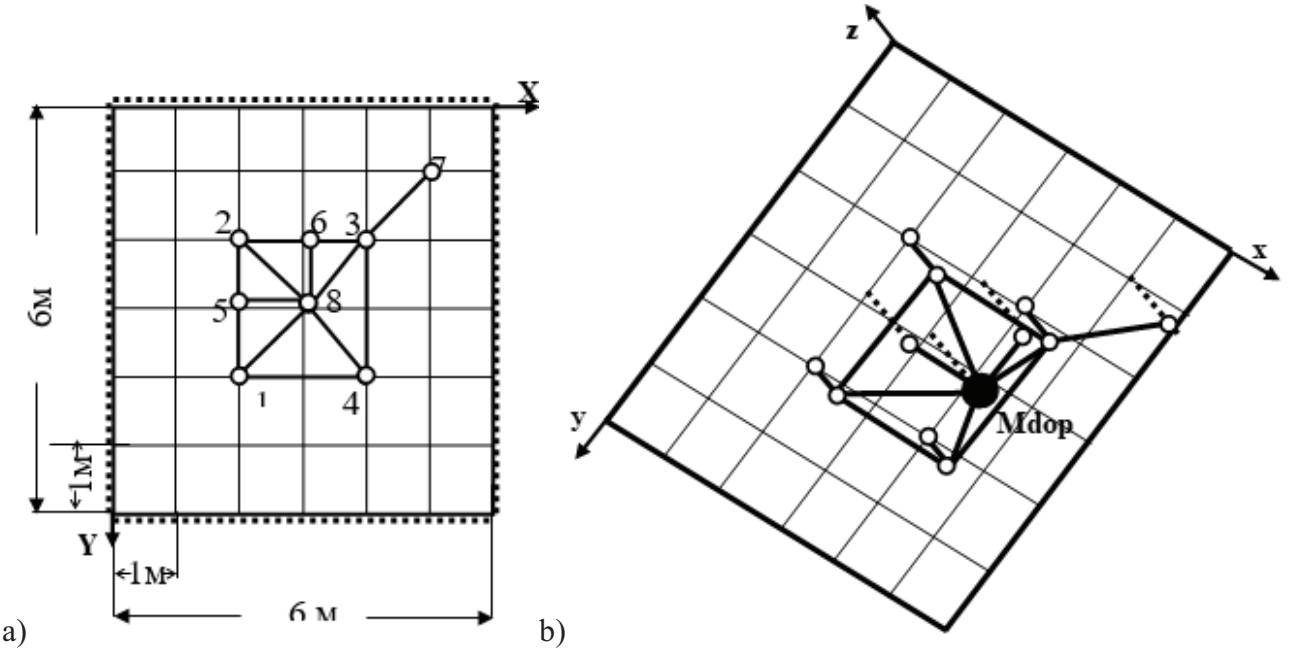
Figure 1. Considering system: a) initial problem; b) the main system of the displacement method.

Table 1. Results of analysis (natural frequencies and natural modes).

ω	60,932	138,865	143,624	196,414
1	0.4905	0.0001	0.7047	-0.5934
2	0.4966	-0.7075	0.0945	0.5167
3	0.5058	-0.0711	-0.7029	-0.4387
4	0.5069	0.7032	0.0190	0.4341

Table 2. Results of analysis (natural frequencies and natural modes).

ω	40.000	138.865	143.624	196.414
1	0.4905	0.0001	0.7047	-0.5934
2	0.4965	-0.7075	0.0945	0.5167
3	0.5058	-0.0711	-0.7029	-0.4387
4	0.5070	0.7032	0.0190	0.4341



a) b)

Figure 2. The first sample: a) device plan; b) general view of device.

Additional mass is applied at node 8. Rods 8-5 and 8-6 provide the additional mass with only one degree of freedom, namely the ability to move in parallel with the movements of the remaining masses during their natural vibrations.
The geometric parameters of the kinematic device are the lengths of the racks

$$l_{st}[i]\ (i=1,2,..,n)$$

and the coordinates of nodes 5, 6, 7, 8

$$X[i], Y[i], Z[i],\quad X_0, Y_0, Z_0 .$$

In the considering sample the length of the "base" rack $l_{st}[1]=-0.5\ m$ and the coordinates of some nodes are selected. Table 3 shows the accepted values of these coordinates in numbers.

Table 3. Coordinates of nodes.

Nodes	Coordinates		
	$X[i]$	$Y[i]$	$Z[i]$
1	2	4	-0.5
2	2	2	$l_{st}[2]$
3	4	2	$l_{st}[3]$
4	4	4	$l_{st}[4]$
5	2	Y_0	Z_0
6	X_0	2	Z_0
7	5	1	Z_0
8	X_0	Y_0	Z_0

The remaining cells show variable geometric parameters that form a space in which their values are found, giving the target function (15) from [1] a minimum. In order to define the target function, it is necessary to determine the inertial forces

$$\bar{R}_0[i]\ (i=1,\ 2,\ 3,\ 4).$$

After the formation of the matrix of additional inertial forces (12) from [1], the values $\bar{R}_0[i]\ (i=1,\ 2,\ 3,\ 4)$ are determined from dependence (14) from [1]. In the considering sample we have

$$\bar{R}_0[1]=-1036326.342;\quad \bar{R}_0[2]=-1153948.433;$$
$$\bar{R}_0[3]=-1228846.563;\quad \bar{R}_0[4]=-128231.533.$$

To assess proximity to the minimum, a small value OOO is assigned. In the considering sample we define $OOO=0.00001$. We have the following initial values of varied parameters:

$$l_{st}[2]=-0.52\ m;\quad l_{st}[3]=-0.4\ m;$$
$$l_{st}[4]=-0.42\ m;\quad X_0=3.15\ m;$$
$$Y_0=2.95\ m;\quad Z_0=-1\ m.$$

In order to search for the minimum of the target function (15) from [1] using the above algorithm in the space of variables, the random search method was used. Equilibrium equations were constructed for the nodes, located at the tops of the racks and node 8, to which additional mass will be applied. The found lengths of the rods of the kinematic device and forces in them are given in Table 4.

Table 4. Lengths of the rods of kinematic device and forces in them.

$l_{st}[1]=0.5000$	$N_{st}[1]=-1036326.34$
$l_{st}[2]=0.5137$	$N_{st}[2]=-1153948.44$
$l_{st}[3]=0.4026$	$N_{st}[3]=-1228846.56$
$l_{st}[4]=0.4172$	$N_{st}[4]=-1285231.53$
$l_p[8,5]=1.1549$	$N_p[8,5]=0.00$
$l_p[8,6]=0.9846$	$N_p[8,6]=0.00$
$l_p[7,3]=1.5360$	$N_p[7,3]=0.00$
$l_p[8,1]=1.6177$	$N_p[8,1]=-2871872.91$
$l_p[8,2]=1.5942$	$N_p[8,2]=-2918886.49$
$l_p[8,3]=1.4294$	$N_p[8,3]=-3576078.34$
$l_p[8,4]=1.4448$	$N_p[8,4]=-3504917.59$
$l_p[1,2]=1.0001$	$N_p[1,2]=1802838.58$
$l_p[2,3]=1.0062$	$N_p[2,3]=2127441.20$
$l_p[3,4]=1.0001$	$N_p[3,4]=2463557.45$
$l_p[1,4]=1.0034$	$N_p[1,4]=2057237.61$

From Table 4 it is clear that the forces in the racks in absolute values coincide quite accurately with the forces $\bar{R}_0[i]$. This circumstance confirms the minimum of the target function (12) and the fulfillment of the requirement that the relationships between forces $N_{st}[i]$ be proportional to the relationships between values $\bar{R}_0[i]$.

The values $\bar{R}_0[i]$ and forces in the rods of the kinematic device (14) from [1] depend on the coordinates of the natural modes $v_\omega[k, j]$. The coordinates $v_\omega[k, j]$ are the coordinates of the natural mode normalized to unity. In the process of real small vibrations, the coordinate values will be significantly less than in the normalized form, and therefore the forces in the rods of the kinematic device will also decrease. In the process of creation of kinematic device we defined following values of the remaining variable parameters:

$$X_0 = 3.15486; \quad Y_0 = 2.98459;$$
$$Z_0 = -1.002116.$$

After creation of computational scheme of the kinematic device, the value of additional mass M_{add} is determined. Before the creation of the kinematic device the considering system had four degrees of freedom. The kinematic device is formed in such a way that M_{add} is able to move only in parallel with the movements of other masses. Therefore, only one more degree of freedom is added in the considering system. Thus, now this system has five degrees of freedom. Now the system has an "additional" frequency. As noted above, the value of the "additional" natural frequency depends on the compliance parameters of the rods of the kinematic device. It can be either greater than the values of all "basic" frequencies or less than any of them.

Two variants of determining the value M_{add} are considered in the sample. Within the first variant, the amount of additional mass is determined without taking into account the influence of the compliance of the rods of the kinematic device. Within the second variant compliance is taken into account according to the method outlined above.

In the first variant the movement of additional mass v_m was determined under the condition that the kinematic device moves as an absolutely rigid body only due to the displacement of the nodes in which the masses of the original system are located. Within this variant the value

$$v_m = \sum_{i=1}^{4} v_\omega[i,(q)] N_{st,1}[i] = -0.500478$$

was determined in the sample by (21) from [1].

The forces in the racks from the action of a unit force applied to the node where the additional mass is located in the direction of its movement are determined from the equilibrium conditions of the nodes of the kinematic device. We have

$$N_{st}[1] = 0.220291; \quad N_{st}[2] = 0.245294;$$
$$N_{st}[3] = 0.261215; \quad N_{st}[4] = 0.273200.$$

The additional mass within this variant is determined by (20) from [1]:

$$M_{add} = 5874.825\ kg.$$

With this mass, three test analysis were performed with the use of SCAD software for different values of the parameters of rods of the kinematic device. All rods are assumed to have a round solid cross-section.

Modulus of elasticity of the rod material is equal to $E = 206000\ MPa$. Different diameters of rod sections were considered. The results are presented in tables 5, 6 and 7. As noted above, the targeting of the kinematic device is realized only in relation to the "basic" frequencies of natural vibrations. Therefore, after placing additional mass and increasing the number of degrees of freedom of the system by one, the normalization of the natural modes is carried out according to the "basic" four coordinates. This normalization allows researcher to compare the proper modes that arose before the creation of the kinematic device with the modes that arose after its introduction.

Table 5. Results of analysis for $D = 100$ mm (natural frequencies and natural modes).

ω	38,79	137,62	142,33	194,68	357,12
1	0.4906	-0.00011	0.7047	-0.5945	0.4908
2	0.4966	0.7074	0.0944	0.5178	0.4965
3	0.5058	0.0711	-0.7029	-0.4350	0.5058
4	0.5069	-0.7032	0.01898	0.4350	0.5067

Table 6. Results of analysis for $D = 60$ mm (natural frequencies and natural modes).

ω	38,21	137,62	142,33	194,68	217,54
1	0.4906	-0.00012	0.7047	-0.5945	0.4913
2	0.4966	0.7074	0.0944	0.5170	0.4961
3	0.5058	0.0711	-0.7029	-0.4384	0.5061
4	0.5069	-0.7032	0.01889	0.4344	0.5063

Table 7. Results of analysis for $D = 20$ mm (natural frequencies and natural modes).

ω	31,67	137,62	142,33	194,68	87,49
1	0.4906	-0.00058	0.7047	-0.5935	0.4905
2	0.4966	0.7075	0.0945	0.5166	0.4965
3	0.5058	0.0711	-0.7029	-0.4388	0.5058
4	0.5069	-0.7031	0.01897	0.4341	0.5070

Table 8. Summary of results.

D	100 mm	60 mm	20 mm
ω	38.79	38.21	31.67
Δ, %	3.025	4.475	20.875

The "additional" frequency and the corresponding natural mode, normalized by the "basic" coordinates, are shown in the rightmost column of the tables.

Analysis of the test results confirms the targeting of the kinematic device. In all three test calculations, the shapes of natural oscillations of the "basic" frequencies coincide with the accepted accuracy with those given in Tables 1 and 2. The values of the "basic" natural frequencies, except for the first, changed by fractions of a percent.

The first frequency differed from the intended value (40 sec^{-1}) depending on the compliance of rods of the kinematic device. With increasing compliance, the value of the first frequency found decreases (Table 8). In Table 8 we have

$$\Delta = ((40 - \omega_1) / 40) \cdot 100\% .$$

In the SCAD software, the compliance of rods of the kinematic device was taken into account. The additional mass at which the tests were performed in the considered variant was determined without taking into account the compliance of rods of the kinematic device. The test results confirm that the value of the "additional" natural frequency (ω_D) depends on the compliance parameters of rods of the kinematic device. At $D = 100\,mm$ and $D = 60\,mm$ the value does not fall into the "basic" part of the spectrum. At $D = 20\,mm$ for $\omega_D = 87.49$ sec^{-1} it turns out to be the second quantity in the full spectrum of natural frequencies.

In the sample additional test analysis was performed with the use of SCAD software for different values of the parameters of the rods of the kinematic device, but taking into account the influence of compliance according to the method outlined above. The parameters of rods of the kinematic device were taken to be the same as in previous tests. The results are presented in tables 9, 10 and 11.

Table 9. Results of analysis for $D = 100\ mm$, $M_{add} = 57.62044\ kN$ *(natural frequencies and natural modes (Z)).*

Nodes	39,5	137,52	142,14	194,64	375,93
1	0.4860	0.0379	0.7246	-0.5864	0.4523
2	0.4912	0.7270	0.0969	0.5247	0.4335
3	0.5117	0.0685	-0.6793	-0.4279	0.5720
4	0.5105	-0.6822	0.0641	0.4447	0.5294

Table 10. Results of analysis for $D = 60\ mm$, $M_{add} = 55.717807\ kN$ *(natural frequencies and natural modes (Z)).*

Nodes	39,37	137,49	142,08	194,59	230,37
1	0.4860	0.0494	0.7305	-0.5759	0.4859
2	0.4912	0.7326	0.0973	0.5359	0.3939
3	0.5117	0.0678	-0.6713	-0.4119	0.6060
4	0.5105	-0.6754	0.0788	0.4598	0.5170

Table 11. Results of analysis for $D = 20\ mm$, $M_{add} = 39.441538\ kN$ *(natural frequencies and natural modes (Z)).*

Nodes	38,08	137,66	142,42	194,69	93,97
1	0.4849	-0.0176	0.6955	-0.5944	0.5092
2	0.4912	0.6980	0.09282	0.5155	0.5179
3	0.5123	0.0725	-0.7126	-0.4403	0.4816
4	0.5110	-0.7121	-0.0001	0.4325	0.4905

Table 12. Summary of results.

D	100 *mm*	60 *mm*	20 *mm*
ω	39.5	39.37	38.08
Δ, %	1,225	1.575	4.80

Analysis of the results of these tests confirms the targeting of the kinematic device.

The values of the "basic" natural frequencies, except for the first one, changed by fractions of a percent. The first frequency differed from the intended value (40 sec^{-1}) depending on the compliance of rods of the kinematic device. With increasing compliance, the value of the first frequency found decreases (Table 12). A comparison of the data in Tables 8 and 12 shows that allowance for the compliance of rods of the kinematic device according to the method outlined above allows researcher to reduce the difference between the intended value (40 sec^{-1}) and the results obtained in the tests. Tests also showed that the method of taking into account the compliance of the rods of a kinematic device requires further analysis and improvement.

The results of tests carried out with allowance for the influence of the compliance of the rods of the kinematic device according to the method outlined above also confirm that the value of the "additional" natural frequency (ω_D) depends on the compliance parameters of the rods of the kinematic device. In cases of $D = 100\ mm$ and $D = 60\ mm$ the value of the "additional" frequency ω_D does not fall into the "basic" part of the spectrum of natural frequencies. In case of $D = 20\ mm$ and $\omega_D = 93.97\ sec^{-1}$ it turns out to be the second value in the full spectrum of natural oscillation frequencies.

The test results with allowance for compliance of the rods of the kinematic device show that the shapes of natural vibrations are close to those given in Tables 1 and 2.

Thus, [1] and the distinctive paper propose an approach that allows researcher to create computational schemes of targeted kinematic devices for elastic systems with a finite number of degrees of mass freedom, in which the directions of mass motion are parallel, but do not lie in the same plane. The necessity of taking into account the influence of the compliance of the rods of the kinematic device when determining the value of additional mass is shown. The need for further analysis and improvement of the corresponding methodology was also noted.

Some patterns of changes in the spectrum of frequencies of natural vibrations of the system have been identified after the formation of the targeted kinematic device.

REFERENCES

1. **Lyahovich L.S., Akimov P.A., Galyautdinov Z.R., Plyaskin A.S.** Development of Computational Schemes of Generalized Kinematic Devices that Precisely Regulate the Natural Frequency Spectrum of Elastic Systems with Finite Number of Degrees of Mass Freedom, in which the Directions of Motion are Parallel, but Do Not Lie in the Same Plane. Part 1: Theoretical Foundations. // International Journal for Computational Civil and Structural Engineering, 2023, Volume 19, Issue 3, pp. 173-183.
2. **Lyahovich L.S., Maletkin O.Ju.** O pricel'nom regulirovanii sobstvennyh chastot uprugih system [On targeted control of natural frequencies of elastic systems]. // Izvestija vuzov. Stroitel'stvo i arhitektura, 1990, No. 1, pp. 113-117 (In Russian).
3. **Lyahovich L.S.** Osobye svojstva optimal'nyh sistem i osnovnye napravlenija ih realizacii v metodah rascheta sooruzhenij [Special properties of optimal systems and the main directions of their implementation in the methods of structural analysis]. Tomsk, TGASU, 2009. – 372 pages (In Russian).
4. **Lyakhovich L.S., Akimov P.A.** Aimed control of the frequency spectrum of eigenvibrations of elastic plates with a finite number of degrees of freedom of masses by superimposing additional constraints. // International Journal for Computational Civil and Structural Engineering, 2021, Volume 17, Issue 2, pp. 76-82.
5. **Lyakhovich L.S., Akimov P.A.** Aimed control of the frequency spectrum of eigenvibrations of elastic plates with a finite number of degrees of freedom by introducing additional generalized kinematic devices. // International Journal for Computational Civil and Structural Engineering, 2021, Volume 17, Issue 3, pp. 14-20.
6. **Akimov P.A, Lyahovich L.S.** Pricel'noe regulirovanie spektra chastot sobstvennyh kolebanij uprugih plastin s konechnym chislom stepenej svobody mass putem vvedenija dopolnitel'nyh obobshhennyh svjazej i obobshhennyh kinematicheskih ustrojstv [Precision control for eigenfrequency of elastic plates with finite number of mass degrees of freedom by using additional generalized connections and kinematic devices]. // Vestnik Tomskogo gosudarstvennogo arkhitekturno-stroitel'nogo universiteta. Journal of Construction and Architecture, 2021, Vol. 23, No. 4, pp. 57-67 (In Russian).
7. **Lyakhovich L.S., Akimov P.A.** O formirovanii raschetnyh shem nekotoryh dopolnitel'nyh svjazej dlja uprugih sistem. Chast' 1: Teoreticheskie osnovy podhoda [About Development of Computational Schemes of Some Additional Constraints for Elastic Systems. Part 1: Theoretical Foundations]. // Promyshlennoe i Grazhdanskoe Stroitelstvo, 2022, No. 9, pp. 4-10 (in Russian).
8. **Lyakhovich L.S., Akimov P.A.** O formirovanii raschetnyh shem nekotoryh dopolnitel'nyh svjazej dlja uprugih sistem. Chast' 2: Primery raschetov [About Devel-

opment of Computational Schemes of Some Additional Constraints for Elastic Systems. Part 2: Samples of Analysis]. // Promyshlennoe i Grazhdanskoe Stroitelstvo, 2022, No. 9, pp. 4-10 (in Russian).

9. **Lyakhovich L.S., Akimov P.A.** Formation of Computational Schemes of Additional Targeted Constraints That Regulate The Frequency Spectrum of Natural Oscillations of Elastic Systems With a Finite Number of Degrees of Mass Freedom, the Directions of Movement of Which are Parallel, But Do Not Lie in the Same Plane. Part 1: Theoretical Foundations. // International Journal for Computational Civil and Structural Engineering, 2022, Volume 18, Issue 2, pp. 183-193.
10. **Teplyh A.V., Ozhogin R.B.** Novye vozmozhnosti SCAD Office 21.1.9.5 [New Features of SCAD Office 21.1.9.5]. // Promyshlennoe i Grazhdanskoe Stroitelstvo, 2020, No. 4, pp. 41-47 (in Russian).
11. **Lyakhovich L.S., Akimov P.A., Mescheulov N.V.** Formation of Computational Schemes of Additional Targeted Constraints That Regulate The Frequency Spectrum of Natural Oscillations of Elastic Systems With a Finite Number of Degrees of Mass Freedom, the Directions of Movement of Which are Parallel, But Do Not Lie in the Same Plane. Part 2: The First Sample of Analysis. // International Journal for Computational Civil and Structural Engineering, 2022, Volume 18, Issue 3, pp. 137-146.
12. **Bertola M.** Nonlinear steepest descent approach to orthogonality on elliptic curves. // Journal of Approximation Theory, 2022, Vol. 276, 105717.
13. **Chen Z., Fang Y., Kong X., Dehg L.** Identification of multi-axle vehicle loads on beam type bridge based on minimal residual norm steepest descent method. // Journal of Sound and Vibration, 2023, Vol. 563, 117866.
14. **Lapucci M., Mansueto P.** Improved front steepest descent for multi-objective optimization. // Operations Research Letters, 2023, Vol. 51, Issue 3, pp. 242-247.
15. **Mittal G., Gibi A.K.** A modified steepest descent method for solving non-smooth inverse problems. // Journal for Computational and Applied Mathematics, 2023, Vol. 424, 114997.
16. **Mittal G., Gibi A.K.** Convergence analysis of an optimally accurate frozen multi-level projected steepest descent iteration for solving inverse problems. // Journal of Complexity, 2023, Vol. 75, 101711.
17. **Ren Q.** Seismic acoustic full waveform inversion based on the steepest descent method and simple linear regression analysis. // Journal of Applied Geophysics, 2022, Vol. 203, 104686.
18. **Do B., Ohsaki M.** A random search for discrete robust design optimization of linear-elastic steel frames under interval parametric uncertainty. // Computers & Structures, 2021, Vol. 249, 106506.
19. **Oztas G.Z., Erdem S.** Random search with adaptive boundaries algorithm for obtaining better initial solutions. // Advances in Engineering Software, 2022, Vol. 169, 103141.
20. Wosniack M.E., Raposo E.P., Viswanathan G.M., da Luz M.G.E. A parallel algorithm for random searches. // Computer Physics Communications, 2015, Vol. 196, pp. 390-397.

СПИСОК ЛИТЕРАТУРЫ

1. **Lyahovich L.S., Akimov P.A., Galyautdinov Z.R., Plyaskin A.S.** Development of Computational Schemes of Generalized Kinematic Devices that Precisely Regulate the Natural Frequency Spectrum of Elastic Systems with Finite Number of Degrees of Mass Freedom, in which the Directions of Motion are Parallel, but Do Not Lie in the Same Plane. Part 1: Theoretical Foundations. // International Journal for Computational Civil and Structural Engi-

neering, 2023, Volume 19, Issue 3, pp. 173-183.

2. **Ляхович Л.С., Малеткин О.Ю.** О прицельном регулировании собственных частот упругих систем. // Известия вузов. Строительство и архитектура, 1990, № 1, с. 113-117.
3. **Ляхович Л.С.** Особые свойства оптимальных систем и основные направления их реализации в методах расчета сооружений. Монография. – Томск: Издательство ТГАСУ, 2009. - 372 с.
4. **Lyakhovich L.S., Akimov P.A.** Aimed control of the frequency spectrum of eigenvibrations of elastic plates with a finite number of degrees of freedom of masses by superimposing additional constraints. // International Journal for Computational Civil and Structural Engineering, 2021, Volume 17, Issue 2, pp. 76-82.
5. **Lyakhovich L.S., Akimov P.A.** Aimed control of the frequency spectrum of eigenvibrations of elastic plates with a finite number of degrees of freedom by introducing additional generalized kinematic devices. // International Journal for Computational Civil and Structural Engineering, 2021, Volume 17, Issue 3, pp. 14-20.
6. **Акимов П.А., Ляхович Л.С.** Прицельное регулирование спектра частот собственных колебаний упругих пластин с конечным числом степеней свободы масс путем введения дополнительных обобщенных связей и обобщенных кинематических устройств. // Вестник Томского государственного архитектурно-строительного университета, 2021, том 23, № 4, с. 57-67.
7. **Ляхович Л.С., Акимов П.А.** О формировании расчетных схем некоторых дополнительных связей для упругих систем. Часть 1. Теоретические основы подхода. // Промышленное и гражданское строительство, 202, №9, с. 4-10.
8. **Ляхович Л.С., Акимов П.А., Мешеулов Н.В.** О формировании расчетных схем некоторых дополнительных связей для упругих систем. Часть 2. Примеры расчёта. // Промышленное и гражданское строительство, 2022, №9, с. 11-19.
9. **Lyakhovich L.S., Akimov P.A.** Formation of Computational Schemes of Additional Targeted Constraints That Regulate The Frequency Spectrum of Natural Oscillations of Elastic Systems With a Finite Number of Degrees of Mass Freedom, the Directions of Movement of Which are Parallel, But Do Not Lie in the Same Plane. Part 1: Theoretical Foundations. // International Journal for Computational Civil and Structural Engineering, 2022, Volume 18, Issue 2, pp. 183-193.
10. **Теплых А.В., Ожогин Р.Б.** Новые возможности SCAD Office 21.1.9.5. // Промышленное и гражданское строительство, 2020, №4, с. 41-47.
11. **Lyakhovich L.S., Akimov P.A., Mescheulov N.V.** Formation of Computational Schemes of Additional Targeted Constraints That Regulate The Frequency Spectrum of Natural Oscillations of Elastic Systems With a Finite Number of Degrees of Mass Freedom, the Directions of Movement of Which are Parallel, But Do Not Lie in the Same Plane. Part 2: The First Sample of Analysis. // International Journal for Computational Civil and Structural Engineering, 2022, Volume 18, Issue 3, pp. 137-146.
12. **Bertola M.** Nonlinear steepest descent approach to orthogonality on elliptic curves. // Journal of Approximation Theory, 2022, Vol. 276, 105717.
13. **Chen Z., Fang Y., Kong X., Dehg L.** Identification of multi-axle vehicle loads on beam type bridge based on minimal residual norm steepest descent method. // Journal of Sound and Vibration, 2023, Vol. 563, 117866.
14. **Lapucci M., Mansueto P.** Improved front steepest descent for multi-objective optimization. // Operations Research Letters, 2023, Vol. 51, Issue 3, pp. 242-247.
15. **Mittal G., Gibi A.K.** A modified steepest descent method for solving non-smooth inverse problems. // Journal for Computational and Applied Mathematics, 2023, Vol. 424, 114997.

16. **Mittal G., Gibi A.K.** Convergence analysis of an optimally accurate frozen multi-level projected steepest descent iteration for solving inverse problems. // Journal of Complexity, 2023, Vol. 75, 101711.
17. **Ren Q.** Seismic acoustic full waveform inversion based on the steepest descent method and simple linear regression analysis. // Journal of Applied Geophysics, 2022, Vol. 203, 104686.
18. **Do B., Ohsaki M.** A random search for discrete robust design optimization of linear-elastic steel frames under interval parametric uncertainty. // Computers & Structures, 2021, Vol. 249, 106506.
19. **Oztas G.Z., Erdem S.** Random search with adaptive boundaries algorithm for obtaining better initial solutions. // Advances in Engineering Software, 2022, Vol. 169, 103141.
20. **Wosniack M.E., Raposo E.P., Viswanathan G.M., da Luz M.G.E.** A parallel algorithm for random searches. // Computer Physics Communications, 2015, Vol. 196, pp. 390-397.

Leonid S. Lyakhovich, Full Member of the Russian Academy of Architecture and Construction Sciences, Professor, DSc, Professor of Department of Structural Mechanics, Tomsk State University of Architecture and Building; 2, Solyanaya St., 2, Tomsk, 634003, Russia; Professor of Department of Applied Mathematics and Computer Sciences, National Research Moscow State University of Civil Engineering; 26, Yaroslavskoe Shosse, Moscow, 129337, Russia; E-mail: lls@tsuab.ru.

Pavel A. Akimov, Full Member of the Russian Academy of Architecture and Construction Sciences, Professor, Dr.Sc.; Rector of National Research Moscow State University of Civil Engineering; 26, Yaroslavskoe Shosse, Moscow, 129337, Russia; phone: +7(495) 651-81-85; Fax: +7(499) 183-44-38; E-mail: AkimovPA@mgsu.ru, rector@mgsu.ru, pavel.akimov@gmail.com.

Zaur R. Galyautdinov, Associate Professor, DSc, Professor of Department of Reinforced Concrete and Stone Structures, Tomsk State University of Architecture and Building; 2, Solyanaya St., 2, Tomsk, 634003, Russia; E-mail: gazr@yandex.ru.

Andrey S. Plyaskin, Associate Professor, Ph.D., Head of Department of Metal and Wooden Structures, Tomsk State University of Architecture and Building; 2, Solyanaya St., 2, Tomsk, 634003, Russia; E-mail: plyaskinandrei@mail.ru.

Ляхович Леонид Семенович, академик РААСН, профессор, доктор технических наук, профессор кафедры строительной механики, Томский государственный архитектурно-строительный университет; 634003, Россия, г. Томск, Соляная пл. 2; профессор кафедры информатики и прикладной математики Национального исследовательского Московского государственного строительного университета; 129337, Россия, г. Москва, Ярославское шоссе, дом 26; E-mail: lls@tsuab.ru

Акимов Павел Алексеевич, академик РААСН, профессор, доктор технических наук; ректор Национального исследовательского Московского государственного строительного университета; 129337, Россия, г. Москва, Ярославское шоссе, дом 26; телефон: +7(495) 651-81-85; факс: +7(499) 183-44-38; Email: AkimovPA@mgsu.ru, rector@mgsu.ru, pavel.akimov@gmail.com.

Галяутдинов Заур Рашидович, доцент, доктор технических наук, доцент кафедры железобетонных и каменных конструкций, Томский государственный архитектурно-строительный университет; 634003, Россия, г. Томск, Соляная пл. 2; E-mail: gazr@yandex.ru.

Пляскин Андрей Сергеевич, доцент, кандидат технических наук, заведующий кафедрой металлических и деревянных конструкций, Томский государственный архитектурно-строительный университет; 634003, Россия, г. Томск, Соляная пл. 2; E-mail: plyaskinandrei@mail.ru.

International Journal for Computational Civil and Structural Engineering, 19(4) 166–181(2023)

DOI:10.22337/2587-9618-2023-19-4-166-181

STATIC BEARING CAPACITY OF STEEL-PLATE COMPOSITE WALLS

Vladimir I. Travush [1], Petr D. Arleninov [2,3], Mikhail A. Desyatkin [4], Andrey N. Ivaschenko [4], Semen S. Kaprielov [2], Denis V. Konin [5], Alexey S. Krylov [5], Sergey B. Krylov [2], Igor A. Chilin [2], Andrey V. Sheinfeld [2]

[1] Gorproject, Moscow, RUSSIA
[2] JSC Research Center of Construction NIIZHB named after A.A. Gvozdev, Moscow, RUSSIA
[3] National Research Moscow State University of Civil Engineering, Moscow, RUSSIA
[4] Inforsproekt, Moscow, RUSSIA
[5] JSC Research Center of Construction TSNIISK named after V.A. Koucherenko, Moscow, RUSSIA

Abstract: The features of the behavior of steel-plate composite walls for static loads are considered. Based on the analysis of modern technical and regulatory documentation, the rationale for the chosen research topic is given. A review of the literature is performed, and the features of development are noted. A detailed description and features of the experimental structures under study and the materials used are presented. The features of the test are considered, and the test equipment is described. Analytical and numerical calculations of structures for eccentric compression have been performed. The description of the calculation complex and the used models of materials is presented; the description of numerical models, the features of their construction and calculation are given, the results of calculations are presented – stress distributions, deformations, features of cracking. The general types of experimental eccentric compression wall models are presented, the nature of the loss of bearing capacity of experimental structures is described, and a picture of destruction is presented. The analysis of the experimental data obtained and their comparison with analytical and numerical calculations are performed.

Keywords: concrete, steel, reinforced concrete, composite steel and concrete structure, steel-plate reinforcement, steel-plate composite (SC) walls, adhesion, stud

НЕСУЩАЯ СПОСОБНОСТЬ СТАЛЕЖЕЛЕЗОБЕТОННЫХ СТЕН С ЛИСТОВЫМ АРМИРОВАНИЕМ НА СТАТИЧЕСКИЕ НАГРУЗКИ

В.И. Травуш [1], П.Д. Арленинов [2,3], М.А. Десяткин [4], А.Н. Иващенко [4], С.С. Каприелов [2], Д.В. Конин [5], А.С. Крылов [5], С.Б. Крылов [2], И.А. Чилин [2], А.В. Шейнфельд [2]

[1] ЗАО «ГОРПРОЕКТ», г. Москва, РОССИЯ
[2] Научно-исследовательский, проектно-конструкторский и технологический институт бетона и железобетона (НИИЖБ) им. А.А. Гвоздева АО «НИЦ «Строительство», г. Москва, РОССИЯ
[3] ФГБОУ ВО «Национальный исследовательский Московский государственный строительный университет» (НИУ МГСУ), г. Москва, РОССИЯ
[4] ООО «Инфорспроект», г. Москва, РОССИЯ
[5] Центральный научно-исследовательский институт строительных конструкций (ЦНИИСК) имени В.А. Кучеренко АО «НИЦ «Строительство», г. Москва, РОССИЯ

Аннотация: Рассмотрены особенности работы сталежелезобетонных стен с листовым армированием при воздействии статических сжимающих нагрузок. Дано обоснование выбранной темы исследования на основе анализа современной технической и нормативной документации. Выполнен обзор литературы, отмечены особенности развития вопроса. Представлено подробное описание и особенности исследуемых экспериментальных конструкций, использованные материалы. Рассмотрены особенности испытания

образцов, описано испытательное оборудование. Выполнены аналитические и численные расчеты конструкций на внецентренное сжатие. Представлено описание расчетного комплекса и использованных моделей материалов; дано описание численных моделей, особенности их построения и расчета, приведены результаты расчетов – характер распределения напряжения, деформации, особенности трещинообразования. Представлены общие виды экспериментальных моделей стен, испытанных на внецентренное сжатие, описан характер потери несущей способности экспериментальных конструкций, приведена картина разрушения. Выполнен анализ полученных экспериментальных данных, их сравнение с аналитическими и численными расчетами.

Ключевые слова: бетон, сталь, железобетон, сталежелезобетонная конструкция, листовое армирование, композитные стены с листовым армированием, сцепление, анкерное устройство

INTRODUCTION

The start of the use of composite steel and concrete structures in high-rise buildings in Russia is recorded in the 50s of the 20th century. The history of composite steel and concrete structures in Russia started with the construction of «Stalin's skyscrapers». The Eurasia skyscraper in Moscow City and the Lakhta Center in St. Petersburg are the latest examples of composite steel and concrete structures in Russia. The use of composite structures in Europe, Asia and the USA has long been known, and also popular in high-rise buildings and bridge construction.

The listed buildings are examples of «classic» composite steel and concrete structures. At the end of the 20th century, another type of composite steel and concrete structure was developed. These are steel-plate composite (SC) structures. They are used in the construction of nuclear power plants in Japan, China, South Korea, the USA and Russia. Initially, the steel-plates were used only as an external formwork, which is not involved in structural strength calculations.

Significant research on the behavior of SC walls for various loading conditions has been performed in Japan [1, 2], China [3…5], and South Korea [6…11]. The research in Japan and South Korea has been the basis for design standards for steel-plate composite construction in Japan (JEAG (2005), Technical Guidelines for Seismic Design of Nuclear Power Plants, JEA (Japan Electric Association)) and South Korea (KSSC (2010), Specification for Safety-Related Steel Plate Concrete Structures for Nuclear Facilities, KEPIC-SNG, Board of KEPIC Policy, Structural Committee, Korea Electric Association).

In the United States, extensive research has been conducted over the past decade to evaluate the behavior of steel-plate composite walls and connections and to develop design standards, such as the AISC Specification for Safety-Related Steel Structures for Nuclear Facilities (AISC, 2015). Some scientific research is given below [33].

The out-of-plane shear behavior of steel-plate composite walls was evaluated by Varma et al. [12], Sener and Varma [13], and Sener et al. [14]. The out-of-plane flexure behavior of SC walls was analyzed by Sener et al. [15]. The in-plane behavior and design of SC walls was evaluated by Varma et al. [16], Seo et al. [17], and Kurt et al. [18]. The local buckling behavior of steel face plates in steel-plate composite walls and the composite action between steel plates and concrete infill was evaluated by Varma et al. [19], Zhang [20], Zhang et al. [21], and Bhardwaj and Varma [22]. The behavior of steel-plate composite walls subjected to combined in-plane forces and out-of-plane flexure was presented by Varma et al. [23, 24]. The behavior, design and shear strength of SC wall-towall T-joints and L-joints were evaluated by Seo et al. [25], Seo [26], and Seo and Varma [27]. The design and detailing of faceplates, steel anchors and ties of SC walls to prevent local buckling, interfacial shear failure, and section delamination failure were presented in Bhardwaj et al. [28]. This paper also presented the design of steel anchors and ties to account for the effect of combined

shear forces [33]. The lateral load capacity of SC walls with boundary elements was evaluated by Booth et al. [29]. The lateral load capacity of SC walls without boundary elements was evaluated by Epackachi et al. [30], Kurt et al. [31], and Bhardwaj et al. [32, 33].

SC construction has numerous advantages over reinforced concrete construction:

- increased resistance to radiation, explosions and flying debris;
- increased resistance to loads from the plane - bending and shear;
- transferring most of the work to factory conditions;
- reduction of work on the construction site (no formwork, no reinforcing frame and no maintenance of concrete);
- no need to apply waterproofing due to the tightness of the structure;
- modular assembly and, consequently, a reduction in the time of work on the construction site;
- improving the quality of construction work.

In Russia, steel-plate composite structures were used in the construction of nuclear power plants. For the development of the construction industry in Russia, including high-rise construction, with the use of modern technologies, a series of experiments of steel-plate composite walls was planned. The results of this experiment will be used as the basis for numerical studies of composite steel and concrete constructions in a nonlinear setting contact interaction simulation. The obtained experimental data are the necessary stage of work for further verification of calculation methods.

The purpose of the work is to test models of steel-plate composite walls for experimental and theoretical justification of their use in high-rise building structures.

Tasks of the work:

• analysis of the available literature on the research topic;

• make work programs for experimental research;

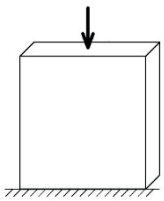
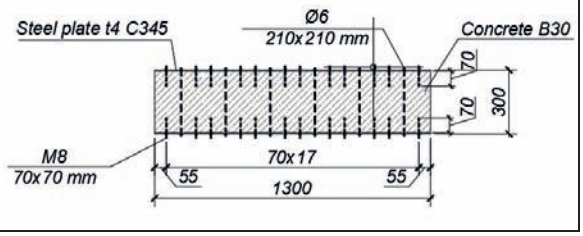
• experimental research;

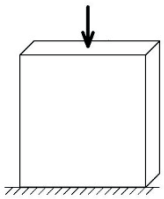
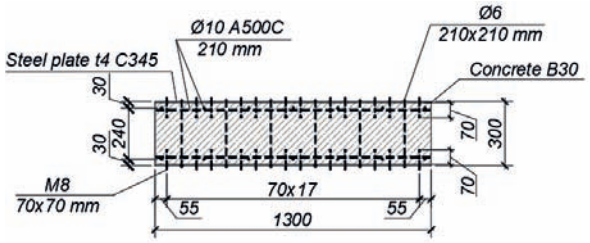
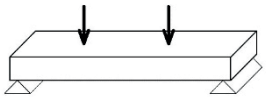
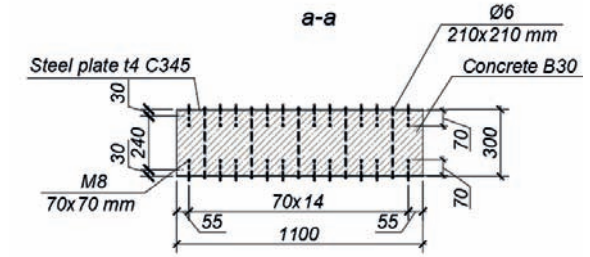
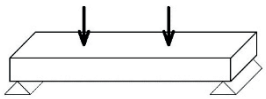
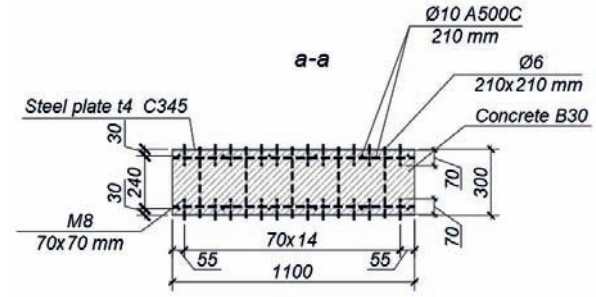
• numerical modeling of structures in specialized research software systems, comparison with test results.

METHODS

Within the research 12 models of steel-plate composite walls with rectangular cross-section 1300 (1100) x 300mm and a length 3000 mm have been tested. Six models have been tested for eccentric compression, and six models have been tested for bending. The models characteristics (cross-section type, construction materials) are stated in Table 1.

Table 1. The Models Characteristics

Group of models	Number of models in the group	Concrete compression breaking strength class	Diagram of load application to the models	Cross-section
1.1	3	B30		

1.2	3	B30		
2.1	3	B30		
2.2	3	B30		

Steel headed stud anchors (was modeled by bolts) were installed on the inside of all the steel plates (Figure 1). The steel plates were connected by tie bars. Models 1.1, 2.1 did not have bar reinforcement of concrete, models 2.1, 2.2 were reinforced with bars.

Preparation of the models for the experiment has been carried out in the following sequence: steel plates have been manufactured and frame reinforcement has been tied (Figure 1); resistive-strain sensors have been installed on the pretreated steel surface and protected (Figure 2); concrete has been poured and resistive-strain sensors have been attached to the steel-plates. The sensors location schemes are shown in Figure 3.



Figure 1. Steel plates and frame reinforcement

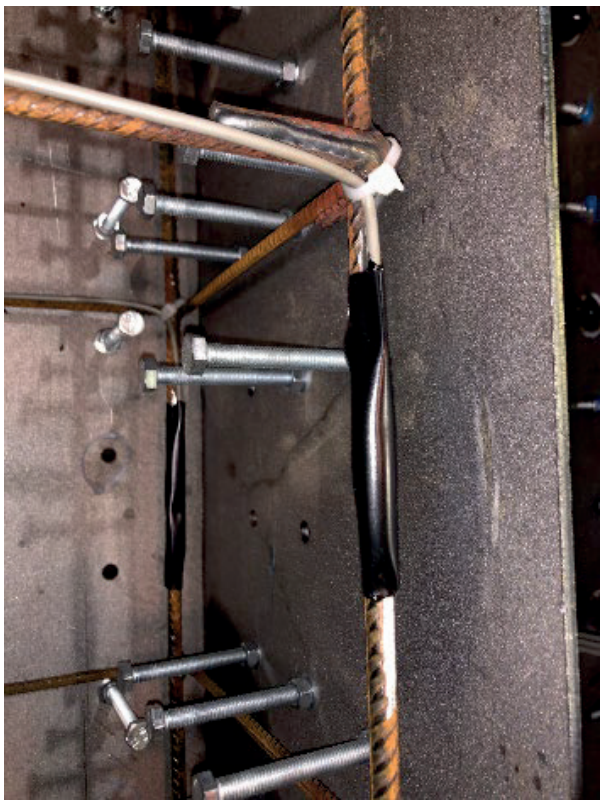


Figure 2. Resistive-strain sensors. Installation and protection

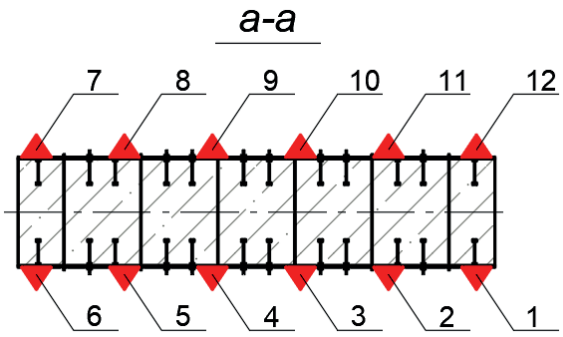


Figure 3a. The sensors location schemes for models 1.1, 2.1 (the section in the center of the height)

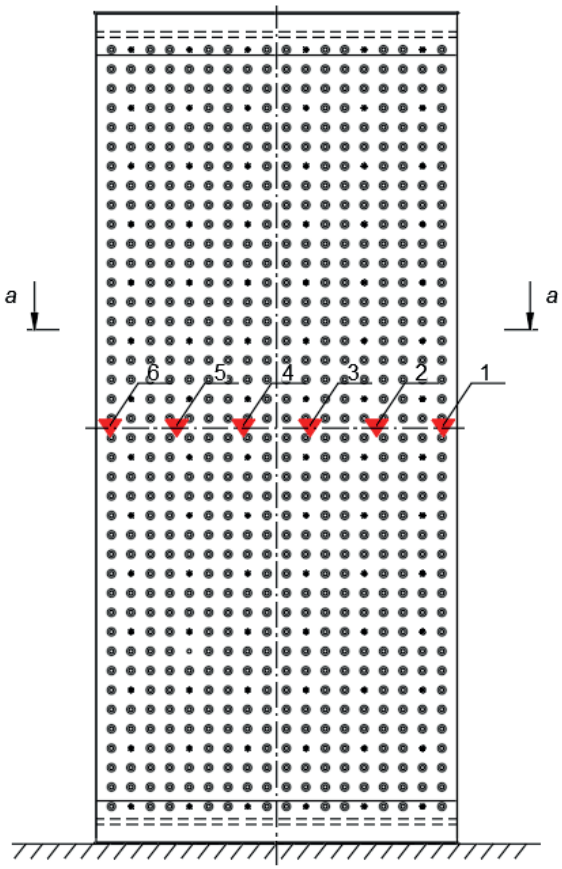


Figure 3b. The sensors location schemes for models 1.1, 2.1 (side view)

Models supports were hinge. A typical view of models tested for bending is shown in Figure 4. A typical view of models tested for eccentric compression is shown in Figure 5.

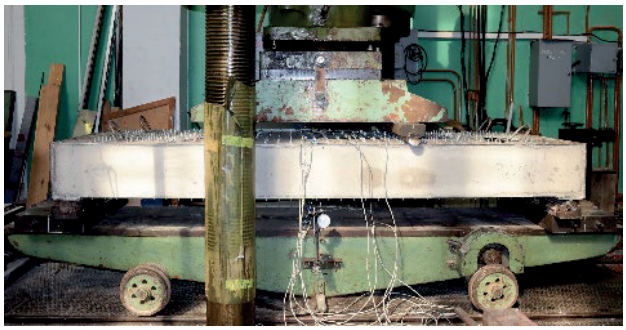


Figure 4. Typical view of models tested for bending

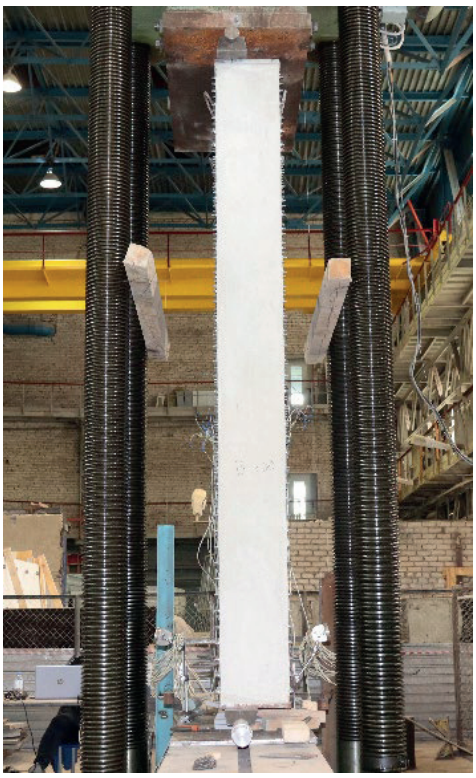


Figure 5. Typical view of models tested for eccentric compression

Very important characteristic of steel-plate composite walls is rigidity, also long-term rigidity. Elastic and plastic deformations due to creep and shrinkage depend on long-term rigidity. The standard formulas of structural mechanics make it possible to determine the elastic stiffness characteristics of a composite steel and concrete element. Determining the long-term modulus of elasticity remains an incompletely solved problem. Based on the best practices in terms of model compliance, during the transition from actual structural elements to small samples, special steel-reinforced concrete samples were prepared for testing to determine the shrinkage and creep of concrete. An article on these tests is being prepared by the authors and will be published soon.

RESULTS AND DISCUSSION

According to the test results, the types of destruction of the models were obtained and the maximum bearing capacity was determined.

The destruction of eccentrically compressed models (models 1.1, 1.2) was on compressed concrete, characterized by limit stress followed by concrete chipping and steel sheet crumpling. The destroyed model is shown in Figure 6. The destruction of the bent models (models 2.1, 2.2) was due to the shear force, characterized by the formation and opening of an inclined crack - from the load transfer zone to the support. The destroyed model is shown in Figure 7.

The results of the experiment showed the combined work of steel plates with concrete at all stages of loading up to the destruction of models.



Figure 6. Typical view of destruction of models tested for eccentric compression



Figure 7a. Typical view of destruction of models tested for bending



Figure 7b. Typical view of destruction of models tested for bending

Diagrams of vertical deformations from the load are obtained. Diagrams for models 1.1, 1.2 are shown in Figure 8, for models 2.1, 2.2 are shown in Figure 9.

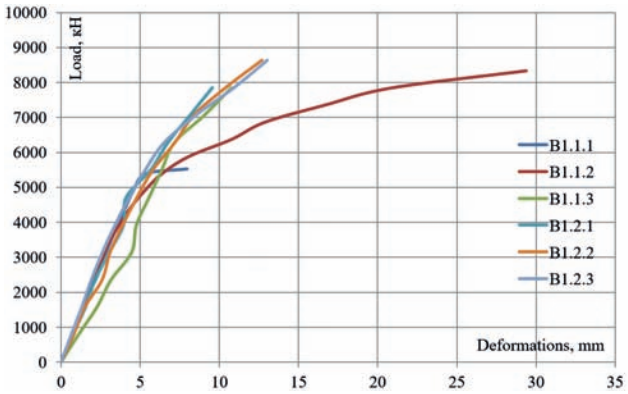


Figure 8. Load-deformation diagrams for models 1.1, 1.2

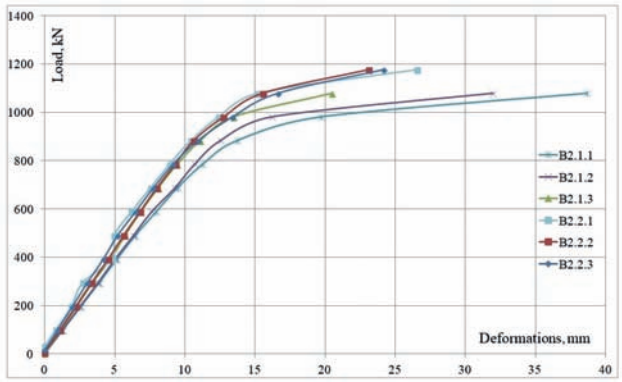


Figure 9. Load-deformation diagrams for models 2.1, 2.2

Diagrams for stress in faceplates are shown in the Figures 10, 11 for models 1.1, 1.2 and 2.1, 2.2 respectively.

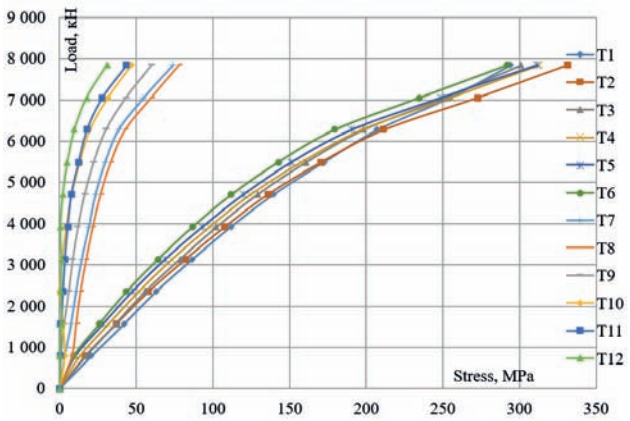


Figure 10. Stress-load diagrams for model faceplates (for model 1.2.1 for example)

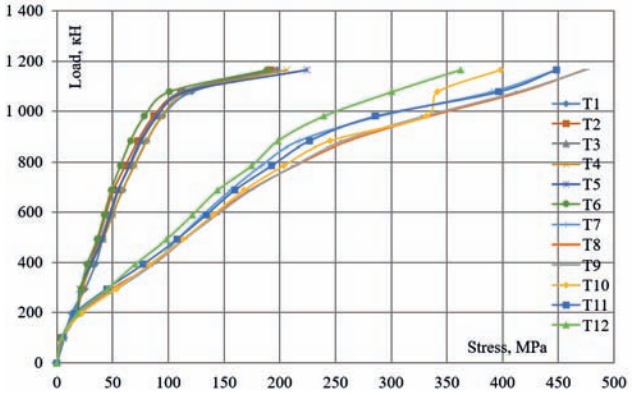


Figure 11. Stress-load diagrams for modes faceplates (for model 2.1.2 for example)

Diagrams of stress distribution according to models are obtained. Diagrams for models 2.1, 2.2 (bending tests) are shown in Figure 12.

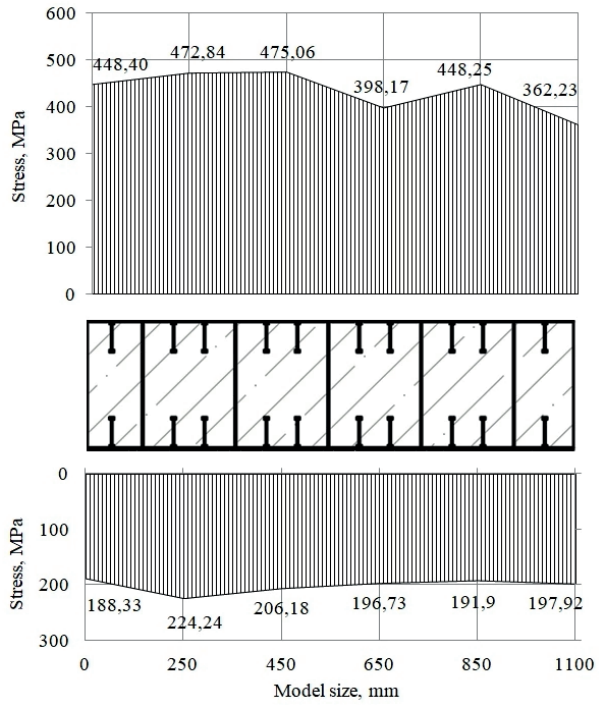


Figure 12. Diagrams of stress distribution for model faceplates (bending tests, models 2.1, 2.2)

For a detailed study of the features of the structures, numerical modeling was performed in the ATENA software package (developed by Červenka Consulting).

The calculations of the models are performed by the finite element method. The software package has an extensive database of various types of finite elements and material models. Numerical models are developed taking into account the recommendations of the software using 1D (bar reinforcement) and volume 3D Solid Elements (concrete and steel plate) finite elements. The dimensions of the finite element grid, the calculation parameters were selected and set based on the solution of test problems, in the necessary places the grid had a smaller size of the FE. The number of load application steps was taken 20...50. The conditions of support and loading of the models are set in accordance with similar parameters in the experiments. The parameters of reinforcement and concrete are described by actual diagrams of deformation of materials.

The calculation models are shown in Figures 13, 14.

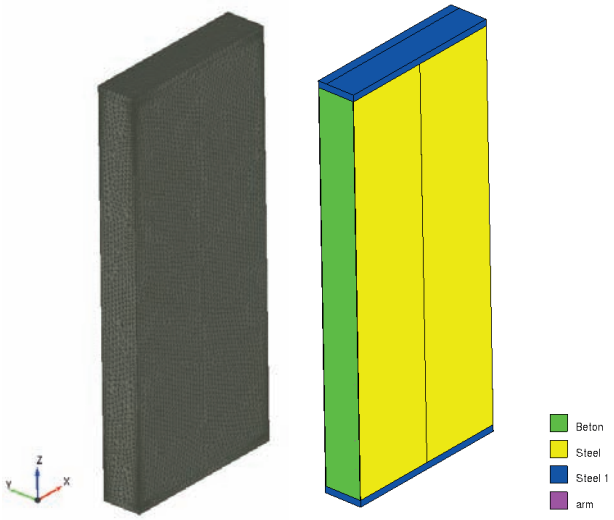


Figure 13. Calculation models 1.1, 1.2 (eccentric compression tests)

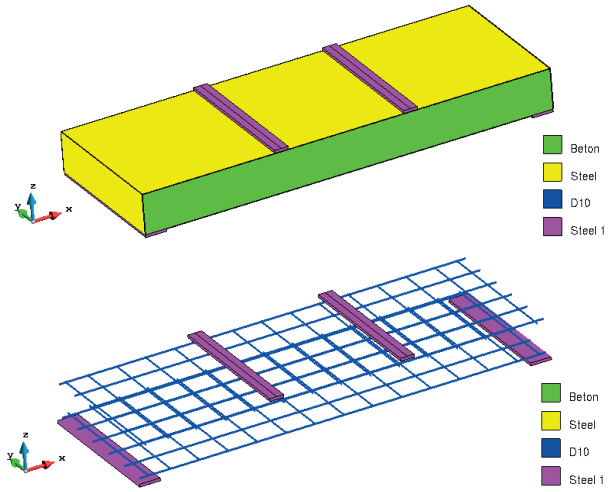


Figure 14. Calculation models 1.1, 1.2 (bending tests)

The calculation results are shown in the Figures 15…18. The width of the opening and the location of cracks in the structure are in good agreement with the experimental results (Figure 15). The analysis of the results of numerical calculations showed that the stresses in steel plates and concrete have limiting values, which corresponds to experimental data (Figure 16, 17).

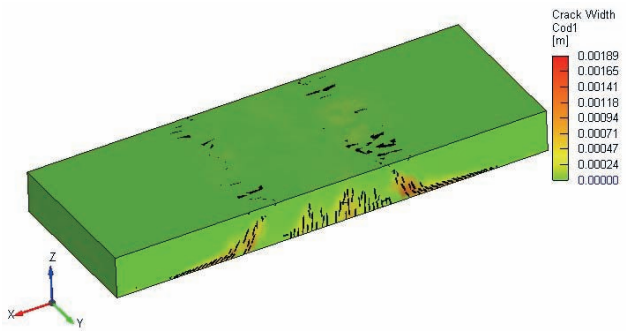


Figure 15. Calculation results. Crack opening width

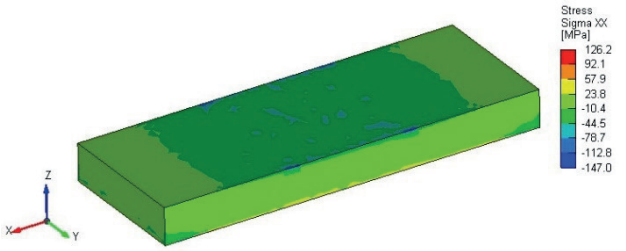


Figure 16. Calculation results. Stress in concrete

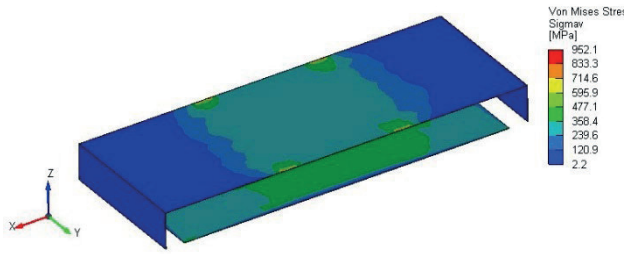


Figure 17. Calculation results. Stress in faceplates

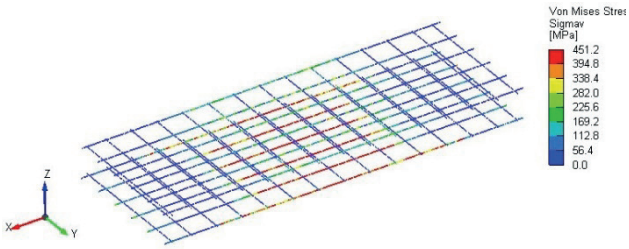


Figure 18. Calculation results. Stress in bar reinforcement

CONCLUSION

1. In this paper the issues of the development of composite steel and concrete structures have been considered. The review of experimental and theoretical studies of steel-plate composite structures is carried out.
2. According to the experimental research program, 12 models of steel-plate composite structures were tested for eccentric compression and bending. The analysis and processing of experimental data has been performed.
3. Numerical models have been constructed to study the features of the stress-strain state of steel-plate composite structures. Based on the calculations performed, the values of the bearing capacity of structures were obtained; the nature of cracking and deformation of steel-plate composite structures under eccentric compression and bending was assessed. The results of numerical studies allow for a more detailed assessment of the stress-strain state of structures.
4. The data of experimental, numerical and theoretical studies are analyzed. The data obtained indicate that the numerical and experimental models correspond. This allows us to extend the results of numerical calculations to a large list of models with different sizes and made of different classes of concrete. Based on the tests, it is planned to develop an analytical methodology for calculating steel-plate composite walls, taking into account possible various design solutions.
5. According to the results of this work, it was noted that the type of structures under study is technologically advanced and has great potential. It is necessary to continue research to form a complete picture of the actual behavior of structures for the development of calculation methods.
6. The data in this article are a small part of a large experiment. A large series of experimental work on the study of steel-plate composite structures is planned. Various parameters were studied on a large group of models under various conditions of support and loading. Studies of elastic and plastic deformations due to creep and shrinkage are also carried out. At the moment, most of the experimental studies have been completed,

and data processing is in progress. An article on these tests with detailed results is being prepared by the authors and will be published soon.

ACKNOWLEDGEMENT

The authors of the article thank their colleagues for their help in experimental work:

- Daria Morozova, Ksenia Morozova, Dmitry Gavrilov, Anastasia Zhdanova, Maria Voropaeva (Research Institute of Building Constructions (TSNIISK) Named After V. A. Koucherenko JSC "Research center of Construction") – preparation of experimental models (installation of strain gauges), analysis and processing of experimental results;
- Artur Dottuev, Zaur Abrekov, Nurik Aliyev (Research Institute of Building Constructions (TSNIISK) Named After V. A. Koucherenko JSC "Research center of Construction") – experimental research, preparation of strain measurements, strain gauge processing

REFERENCES

1. **Takeuchi M., Narikawa M., Matsuo I., Hara, K. and Usami S**. (1998) Study on a Concrete Filled Structure for Nuclear Power Plants. *Nuclear Engineering and Design*, vol. 179, no 2, pp. 209–223.
2. **Takeuchi M., Fujita F., Funakoshi A., Shohara R., Akira S. and Matsumoto R.** (1999) Experimental Study on Steel Plate Reinforced Concrete Structure, Part 2: Response of SC Members Subjected to Out-of-Plane Load (Outline of the Experimental Program and the Results). *Proceedings of the Annual Conference of Architectural Institute of Japan, (in Japanese)*, pp. 1.037–1.038.
3. **Song X., Chu M., Ge H. and Wang H.** (2014) A Failure Criterion for Steel-Concrete Composite Walls. *Sustainable Development of Critical Infrastructure, ASCE*, pp. 324–331.
4. **Leng Y.-B., Song X.-B., Chu M. and Ge H.-H.** (2015) Experimental Study and Theoretical Analysis of Resistance of Steel-Concrete-Steel Sandwich Beams. *Journal of Structural Engineering, ASCE,* vol. 141, no. 2.
5. **Leng Y.-B., Song X.-B. and Wang H.-L.** (2015) Failure Mechanism and Shear Strength of Steel-Concrete-Steel Sandwich Deep Beams*, Journal of Constructional Steel Research*, vol. 106, pp. 89–98.
6. **Moon I.H., Kim S.M., Kim W.B. and Kim W.K.** (2007) The Use of Steel Plate Concrete for Structural Module of NPP Structures, *Journal of the Korean Society of Steel Construction (in Korean)*, vol. 19, no. 2, pp 740–745.
7. **Moon I.H., Kim T.Y. and You S.T.** (2008) Nuclear Power Plant Structure and SC Structure Design, *Journal of the Korean Society of Steel Construction (in Korean)*, vol. 20, no. 2, pp. 14–23.
8. **Kim W.B. and Kim W.K.** (2008) Status and Background in Developing SC Structure Specifications for Nuclear Power Plants, *Journal of the Korean Society of Steel Construction (in Korean)*, vol. 20, no. 2, pp. 9–13.
9. **Lee U.W., Kim K.K., Mun T.Y. and Sun W.S.** (2008) Nuclear Power Plant Construction and SC Structures, *Journal of the Korean Society of Steel Construction (in Korean)*, vol. 20, no. 2.
10. **Lee S.J., Choi B.J. and Kim T.K.** (2009) An Experimental Study on the Behavior of Steel Plate Concrete Wall with Vertical Ribs, *Journal of the Korean Society of Steel Construction (in Korean)*, vol. 21, no. 3, pp. 277–287.
11. **Hong S., Kim W., Lee K., Hong N.K. and Lee D.** (2009) Out-of-Plane Shear Strength of Steel Plate Concrete Walls Dependent on Bond Behavior, *Transactions of the 20th International Conference on Structural Mechanics in Reactor Technology*, SMiRT-20, Div-6: Paper 1,855, Espoo, Finland,

IASMIRT, North Carolina State University, Raleigh, NC, pp. 1–10.

12. **Varma A.H., Sener K.C., Zhang K., Coogler K. and Malushte S.R.** (2011) *Out-of-Plane Shear Behavior of SC Composite Structures*, Transactions of the 21st International Association for Structural Mechanics in Reactor Technology Conference, SMiRT-21, New Delhi, India, IASMART, North Carolina State University, Raleigh, NC.
13. **Sener K.C. and Varma A.H.** (2014) Steel-Plate Composite Walls: Experimental Database and Design for Out-of-Plane Shear, *Journal of Constructional Steel Research*, vol. 100, pp. 197–210.
14. **Sener K.C., Varma A.H. and Seo J.** (2016) Experimental and Numerical Investigation of the Shear Behavior of Steel-Plate Composite (SC) Beams without Shear Reinforcement, *Engineering Structures*, vol. 127, pp. 495–509.
15. **Sener K.C., Varma A.H., Booth P.N. and Fujimoto R.** (2015) Seismic Behavior of a Containment Internal Structure Consisting of Composite SC Walls, *Nuclear Engineering and Design*, vol. 295, pp. 804–816.
16. **Varma A.H., Zhang K., Chi H., Booth P.N. and Baker T.** (2011) *In-Plane Shear Behavior of SC Walls: Theory vs. Experiment*, Transactions of the 21st International Association for Structural Mechanics in Reactor Technology Conference, SMiRT-21, Div. X, Paper 761, New Delhi, India, IASMART, North Carolina State University, Raleigh, NC.
17. **Seo J., Varma A.H., Sener K. and Ayhan D.** (2016) Steel-Plate Composite (SC) Walls: In-Plane Shear Behavior, Database, and Design, *Journal of Constructional Steel Research*, vol. 119, pp. 202–215.
18. **Kurt E.G., Varma A.H., Booth P.N. and Whittaker A.** (2016) In-plane Behavior and Design of Rectangular SC Wall Piers Without Boundary Elements, *Journal of Structural Engineering, ASCE*, vol. 142, no. 6.
19. **Varma A.H., Zhang K. and Malushte S.R.** (2013), *Local Buckling of SC Composite Walls at Ambient and Elevated Temperatures*, Transactions of the 22nd International Conference on Structural Mechanics in Reactor Technology, SMiRT-22, San Francisco, CA, IASMART, North Carolina State University, Raleigh, NC.
20. **Zhang K.** (2014) Axial Compression Behavior and Partial Composite Action of SC Walls in Safety-Related Nuclear Facilities, Ph.D. Dissertation, Purdue University, West Lafayette, IN.
21. **Zhang K., Varma A.H., Malushte S.R. and Gallocher S.** (2014) Effect of Shear Connectors on Local Buckling and Composite Action in Steel Concrete Composite Walls, *Journal of Nuclear Engineering and Design, Special Issue on SmiRT-21 Conference*, vol. 269, pp. 231–239.
22. **Bhardwaj S.R. and Varma A.H.** (2016) Effect of Imperfections on the Compression Behavior of SC Walls, *Proceedings of the Annual Stability Conference, Structural Stability Research Council*, Orlando, FL, April 12–15.
23. **Varma A.H., Malushte S.R., Sener K. and Lai Z.** (2011), *Steel-Plate Composite Walls for Safety Related Nuclear Facilities: Design for Combined In-Plane and Out-of-Plane Demands*, Transactions of the 21st International Association for Structural Mechanics in Reactor Technology Conference, SMiRT-21, Paper ID 760, New Delhi, India, IASMART, North Carolina State University, Raleigh, NC.
24. **Varma A.H., Malushte S.R., Sener K.C. and Lai Z.** (2014) Steel-Plate Composite (SC) Walls for Safety Related Nuclear Facilities: Design for In-Plane Forces and Out-of-Plane Moments, *Nuclear Engineering and Design, Special Issue on SMiRT-21 Conference*, vol. 269, pp. 240–249.
25. **Seo J., Varma A.H. and Winkler D.** (2013) *Preliminary Investigations of the Joint Shear Strength of SC Wallto-Wall T-Joints*, Transactions of the 22nd International

Association for Structural Mechanics in Reactor Technology Conference, SMiRT-22, San Francisco, CA, IASMART, North Carolina State University, Raleigh, NC, pp. 1–10.
26. **Seo J.** (2014) Design of Steel Concrete Composite Wallto-Wall Joints for Safety-Related Nuclear Facilities, Ph.D. Dissertation, Purdue University, West Lafayette, IN.
27. **Seo J. and Varma A.H.** (2015) *Behaviour and Design of Corner or L-Joints in SC Walls*, Transactions of the 23rd International Association for Structural Mechanics in Reactor Technology Conference, SMiRT-23, Paper ID 695, Manchester, UK, IASMIRT, North Carolina State University, Raleigh, NC.
28. **Bhardwaj S.R., Varma, A.H. and Malushte S.R.** (2017) Minimum Requirements and Section Detailing Provisions for Steel-Plate Composite (SC) Walls in Nuclear Power Plants, *Engineering Journal*, *AISC*, vol. 54, no. 2.
29. **Booth P., Varma A.H. and Seo J.** (2015), *Lateral Load Capacity of Steel Plate Composite Wall Structures*, Transactions of the 23rd International Conference on Structural Mechanics in Reactor Technology, SMiRT-23, Paper ID 791, Manchester, UK, IASMIRT, North Carolina State University, Raleigh, NC, pp. 1–10.
30. **Epackachi S., Nguyen N., Kurt E., Whittaker A. and Varma, A.** (2015) In-Plane Seismic Behavior of Rectangular Steel-Plate Composite Wall Piers, *Journal of Structural Engineering, ASCE*, vol. 141, no. 7.
31. **Kurt E.G., Varma A.H., Booth P.N. and Whittaker A.** (2016) In-plane Behavior and Design of Rectangular SC Wall Piers Without Boundary Elements, Journal of Structural Engineering, ASCE, vol. 142, no. 6.
32. **Bhardwaj S.R., Kurt E.G., Terranova B., Varma A.H., Whittaker A.S. and Orbovic, N.** (2015) Preliminary Investigation of the Effects of Out-of-Plane Loading on the In-Plane Behavior of SC Walls, *Transactions of the 23rd Structural Mechanics in Reactor Technology*, SMiRT-23, Paper ID 712, Manchester, UK, IASMIRT, North Carolina State University, Raleigh, NC, pp. 1–10.
33. AISC Design Guide 32: Modular Steel-Plate Composite Walls for Safety-Related Nuclear Facilities. American Institute of Steel Construction.

СПИСОК ЛИТЕРАТУРЫ

1. **Takeuchi M., Narikawa M., Matsuo I., Hara, K. and Usami S**. // Study on a Concrete Filled Structure for Nuclear Power Plants. Nuclear Engineering and Design, 1998, Vol. 179, no 2, pp. 209–223.
2. **Takeuchi M., Fujita F., Funakoshi A., Shohara R., Akira S. and Matsumoto R.** Experimental Study on Steel Plate Reinforced Concrete Structure, Part 2: Response of SC Members Subjected to Out-of-Plane Load (Outline of the Experimental Program and the Results) // Proceedings of the Annual Conference of Architectural Institute of Japan, Japan, 1999, pp. 1.037–1.038.
3. **Song X., Chu M., Ge H. and Wang H. A**. Failure Criterion for Steel-Concrete Composite Walls // Sustainable Development of Critical Infrastructure, ASCE, 2014, pp. 324–331.
4. **Leng Y.-B., Song X.-B., Chu M. and Ge H.-H.** Experimental Study and Theoretical Analysis of Resistance of Steel-Concrete-Steel Sandwich Beams // Journal of Structural Engineering, ASCE, 2015, Vol. 141, No. 2.
5. **Leng Y.-B., Song X.-B. and Wang H.-L.** Failure Mechanism and Shear Strength of Steel-Concrete-Steel Sandwich Deep Beams // Journal of Constructional Steel Research, 2015, Vol. 106, pp. 89–98.
6. **Moon I.H., Kim S.M., Kim W.B. and Kim W.K.** The Use of Steel Plate Concrete for Structural Module of NPP Structures, // Journal of the Korean Society of Steel

Construction (in Korean), 2007, Vol. 19, No. 2, pp 740–745.

7. **Moon I.H., Kim T.Y. and You S.T.** Nuclear Power Plant Structure and SC Structure Design // Journal of the Korean Society of Steel Construction (in Korean), 2008, Vol. 20, No. 2, pp. 14–23.
8. **Kim W.B. and Kim W.K.** Status and Background in Developing SC Structure Specifications for Nuclear Power Plants // Journal of the Korean Society of Steel Construction (in Korean), 2008, Vol. 20, No. 2, pp. 9–13.
9. **Lee U.W., Kim K.K., Mun T.Y. and Sun W.S.** Nuclear Power Plant Construction and SC Structures // Journal of the Korean Society of Steel Construction (in Korean), 2008, Vol. 20, No. 2.
10. **Lee S.J., Choi B.J. and Kim T.K.** An Experimental Study on the Behavior of Steel Plate Concrete Wall with Vertical Ribs // Journal of the Korean Society of Steel Construction (in Korean), 2009, Vol. 21, No. 3, pp. 277–287.
11. **Hong S., Kim W., Lee K., Hong N.K. and Lee D.** Out-of-Plane Shear Strength of Steel Plate Concrete Walls Dependent on Bond Behavior // Transactions of the 20th International Conference on Structural Mechanics in Reactor Technology, SMiRT-20, Div-6: Paper 1,855, Espoo, Finland, IASMIRT, North Carolina State University, Raleigh, NC, 2009, pp. 1–10.
12. **Varma A.H., Sener K.C., Zhang K., Coogler K. and Malushte S.R.** Out-of-Plane Shear Behavior of SC Composite Structures // Transactions of the 21st International Association for Structural Mechanics in Reactor Technology Conference, SMiRT-21, New Delhi, India, IASMART, North Carolina State University, Raleigh, NC, 2009.
13. **Sener K.C. and Varma A.H.** Steel-Plate Composite Walls: Experimental Database and Design for Out-of-Plane Shear // Journal of Constructional Steel Research, 2014, Vol. 100, pp. 197–210.
14. **Sener K.C., Varma A.H. and Seo J.** Experimental and Numerical Investigation of the Shear Behavior of Steel-Plate Composite (SC) Beams without Shear Reinforcement // Engineering Structures, 2016, Vol. 127, pp. 495–509.
15. **Sener K.C., Varma A.H., Booth P.N. and Fujimoto R.** Seismic Behavior of a Containment Internal Structure Consisting of Composite SC Walls // Nuclear Engineering and Design, 2015, Vol. 295, pp. 804–816.
16. **Varma A.H., Zhang K., Chi H., Booth P.N. and Baker T.** In-Plane Shear Behavior of SC Walls: Theory vs. Experiment, Transactions of the 21st International Association for Structural Mechanics in Reactor Technology Conference, SMiRT-21, Div. X, Paper 761, New Delhi, India, IASMART, North Carolina State University, Raleigh, NC, 2011.
17. **Seo J., Varma A.H., Sener K. and Ayhan D.** Steel-Plate Composite (SC) Walls: In-Plane Shear Behavior, Database, and Design // Journal of Constructional Steel Research, 2016, Vol. 119, pp. 202–215.
18. **Kurt E.G., Varma A.H., Booth P.N. and Whittaker A.** In-plane Behavior and Design of Rectangular SC Wall Piers Without Boundary Elements // Journal of Structural Engineering, ASCE, 2016, Vol. 142, No. 6.
19. **Varma A.H., Zhang K. and Malushte S.R.** Local Buckling of SC Composite Walls at Ambient and Elevated Temperatures, Transactions of the 22nd International Conference on Structural Mechanics in Reactor Technology, SMiRT-22, San Francisco, CA, IASMART, North Carolina State University, Raleigh, NC, 2013.
20. **Zhang K.** Axial Compression Behavior and Partial Composite Action of SC Walls in Safety-Related Nuclear Facilities, Ph.D. Dissertation, Purdue University, West Lafayette, IN, 2014.
21. **Zhang K., Varma A.H., Malushte S.R. and Gallocher S.** Effect of Shear Connectors on Local Buckling and

Composite Action in Steel Concrete Composite Walls // Journal of Nuclear Engineering and Design, Special Issue on SmiRT-21 Conference, 2014, Vol. 269, pp. 231–239.

22. **Bhardwaj S.R. and Varma A.H.** Effect of Imperfections on the Compression Behavior of SC Walls, Proceedings of the Annual Stability Conference, Structural Stability Research Council, Orlando, FL, April 12–15, 2016.
23. **Varma A.H., Malushte S.R., Sener K. and Lai Z.** Steel-Plate Composite Walls for Safety Related Nuclear Facilities: Design for Combined In-Plane and Out-of-Plane Demands, Transactions of the 21st International Association for Structural Mechanics in Reactor Technology Conference, SMiRT-21, Paper ID 760, New Delhi, India, IASMART, North Carolina State University, Raleigh, NC, 2011.
24. **Varma A.H., Malushte S.R., Sener K.C. and Lai Z.** Steel-Plate Composite (SC) Walls for Safety Related Nuclear Facilities: Design for In-Plane Forces and Out-of-Plane Moments // Nuclear Engineering and Design, Special Issue on SMiRT-21 Conference, 2014, Vol. 269, pp. 240–249.
25. **Seo J., Varma A.H. and Winkler D.** Preliminary Investigations of the Joint Shear Strength of SC Wallto-Wall T-Joints, Transactions of the 22nd International Association for Structural Mechanics in Reactor Technology Conference, SMiRT-22, San Francisco, CA, IASMART, North Carolina State University, Raleigh, NC, 2013, pp. 1–10.
26. **Seo J.** Design of Steel Concrete Composite Wallto-Wall Joints for Safety-Related Nuclear Facilities, Ph.D. Dissertation, Purdue University, West Lafayette, IN, 2014.
27. **Seo J. and Varma A.H.** Behaviour and Design of Corner or L-Joints in SC Walls, Transactions of the 23rd International Association for Structural Mechanics in Reactor Technology Conference, SMiRT-23, Paper ID 695, Manchester, UK, IASMIRT, North Carolina State University, Raleigh, NC, 2015.
28. **Bhardwaj S.R., Varma, A.H. and Malushte S.R.** Minimum Requirements and Section Detailing Provisions for Steel-Plate Composite (SC) Walls in Nuclear Power Plants // Engineering Journal, AISC, 2017, Vol. 54, No. 2.
29. **Booth P., Varma A.H. and Seo J.** Lateral Load Capacity of Steel Plate Composite Wall Structures, Transactions of the 23rd International Conference on Structural Mechanics in Reactor Technology, SMiRT-23, Paper ID 791, Manchester, UK, IASMIRT, North Carolina State University, Raleigh, NC, 2015, pp. 1–10.
30. **Epackachi S., Nguyen N., Kurt E., Whittaker A. and Varma, A.** In-Plane Seismic Behavior of Rectangular Steel-Plate Composite Wall Piers, Journal of Structural Engineering, ASCE, 2015, Vol. 141, No. 7.
31. **Kurt E.G., Varma A.H., Booth P.N. and Whittaker A.** In-plane Behavior and Design of Rectangular SC Wall Piers Without Boundary Elements, Journal of Structural Engineering, ASCE, 2016, Vol. 142, No. 6.
32. **Bhardwaj S.R., Kurt E.G., Terranova B., Varma A.H., Whittaker A.S. and Orbovic, N.** Preliminary Investigation of the Effects of Out-of-Plane Loading on the In-Plane Behavior of SC Walls, Transactions of the 23rd Structural Mechanics in Reactor Technology, SMiRT-23, Paper ID 712, Manchester, UK, IASMIRT, North Carolina State University, Raleigh, NC, 2016, pp. 1–10.
33. **AISC Design Guide 32**: Modular Steel-Plate Composite Walls for Safety-Related Nuclear Facilities. American Institute of Steel Construction.

Travush V.I., GORPROJECT, Moscow. Doctor of technical Sciences, Professor. Chief designer, Deputy General Director on scientific work. Vice-President of Russian Academy of Architecture and Construction Sciences, 105064, Nizhnyi Susal'nyi lane 5/5A, Moscow, Russia, e-mail: travush@mail.ru.

Arleninov P.D., Department of Reinforced Concrete and Masonry Structures, National Research Moscow State University of Civil Engineering, 129337, Yaroslavskoye shosse, 26, Moscow, Russia; JSC Research Center of Construction NIIZHB named after A.A. Gvozdev, laboratory of reinforced concrete mechanics, 109428, 6, building 5., 2nd Institutskaya str., Moscow, Russia, e-mail: arleninoff@gmail.com.

Desyatkin M.A, Chief Structural Engineer LLC "Inforsproekt", 115280, 19, Leninskaya Sloboda str., Moscow, Russia, e-mail: mdesyatkin@mail.ru,

Ivashchenko A.N, Chief Structural Engineer LLC "Inforsproekt", 115280, 19, Leninskaya Sloboda str., Moscow, Russia, e-mail: a.ivaschenko@inforceproject.ru,

Kaprielov S.S., Doctor of Technical Sciences, Academician of the Russian Academy Architecture and Construction of Sciences, head of Laboratory №16 «Research Institute for Concrete and Reinforced Concrete» named after A. A. Gvozdev, JSC Research Center of Construction, 109428, 6, building 5., 2nd Institutskaya str., Moscow, Russia, e-mail: kaprielov@masterbeton-mb.ru.

Konin D.V., Candidate of Technical Sciences, Deputy Director for Scientific Work, Chief manager of Laboratory of High-rise Buildings and Structures of the Department of Metal Structures, Research Institute of Building Constructions (TSNIISK) Named After V. A. Koucherenko JSC Research center of Construction,109428, 6, 2nd Institutskaya str., Moscow, Russia, e-mail: konden@inbox.ru.

Krylov A.S., Candidate of Technical Sciences, Leading Researcher of Laboratory of High-rise Buildings and Structures, Research Institute of Building Constructions (TSNIISK) Named After V. A. Koucherenko JSC Research center of Construction, 109428, 6, 2nd Institutskaya str., Moscow, Russia, e-mail: kryl07@mail.ru.

Krylov S.B, Doctor of Engineering Sciences. JSC Research Center of Construction NIIZHB named after A.A. Gvozdev, Head of Laboratory of Reinforced Concrete Mechanics, 109428, 6, building 5., 2nd Institutskaya str., Moscow, Russia, e-mail: Krylov_s_b@mail.ru.

Травуш Владимир Ильич, ЗАО «ГОРПРОЕКТ», г. Москва, Доктор технических наук, профессор. Главный конструктор, заместитель генерального директора по научной работе. Вице-президент РААСН, 105064, Москва, Нижний Сусальный переулок, д. 5, стр. 5А, e-mail: travush@mail.ru

Арленинов Петр Дмитриевич, кандидат технических наук, ФГБ0У ВО «Национальный исследовательский Московский государственный строительный университет» Минобрнауки России (НИУ МГСУ), 129337, Москва, Ярославское шоссе, д. 26; заместитель заведующего лаборатории Механики железобетона, Научно-исследовательский, проектно-конструкторский и технологический институт бетона и железобетона (НИИЖБ) им. А. А. Гвоздева АО «НИЦ «Строительство», 109428, Москва, 2-я Институтская ул., д.6, корп. 5, e-mail: arleninoff@gmail.com

Десяткин Михаил Александрович, главный конструктор ООО "Инфорспроект", 115280, Москва,ул. Ленинская Слобода, д. 19, e-mail: mdesyatkin@mail.ru

Андрей Николаевич Иващенко, технический директор ООО "Инфорспроект", 115280, Москва,ул. Ленинская Слобода, д. 19, e-mail: a.ivaschenko@inforceproject.ru

Каприелов Семен Суренович, доктор технических наук, академик РААСН, заведующий лабораторией № 16 НИИЖБ им. А. А. Гвоздева АО «НИЦ «Строительство», 109428, Москва, 2-я Институтская ул., д.6, корп. 5, e-mail: kaprielov@masterbeton-mb.ru

Денис Владимирович Конин, кандидат технических наук, заместитель Директора по научной работе, заведующий лабораторией Высотных зданий и сооружений отдела металлических конструкций, ЦНИИСК им. В.А. Кучеренко АО "НИЦ "Строительство", Москва, 2-я Институтская улица, д.6, e-mail: konden@inbox.ru

Крылов Алексей Сергеевич, кандидат технических наук, ведущий научный сотрудник лаборатории Высотных зданий и сооружений, ЦНИИСК им. В.А. Кучеренко АО "НИЦ "Строительство", Москва, 2-я Институтская улица, д.6, e-mail: kryl07@mail.ru

Крылов Сергей Борисович, доктор технических наук, заведующий лабораторией Механики железобетона, Научно-исследовательский, проектно-конструкторский и технологический институт бетона и железобетона (НИИЖБ) им. А. А. Гвоздева АО «НИЦ «Строительство», 109428, Москва, 2-я Институтская ул., д.6, корп. 5, e-mail: Krylov_s_b@mail.ru

Chilin I.A., Engineer, Researcher of Laboratory №16 «Research Institute for Concrete and Reinforced Concrete» named after A. A. Gvozdev, JSC Research Center of Construction, 109428, 6, building 5., 2nd Institutskaya str., Moscow, Russia, e-mail: chilin@masterbeton-mb.ru.

Sheynfeld A.V., Doctor of Technical Sciences, Advisor of the Russian Academy Architecture and Construction of Sciences. Deputy Head of Laboratory №16 «Research Institute for Concrete and Reinforced Concrete» named after A. A. Gvozdev, JSC Research Center of Construction, 109428, 6, building 5., 2nd Institutskaya str., Moscow, Russia, e-mail: sheynfeld@masterbeton-mb.ru.

Чилин Игорь Анатольевич, инженер, научный сотрудник лаборатории № 16 НИИЖБ им. А. А. Гвоздева АО «НИЦ «Строительство», 109428, Москва, 2-я Институтская ул., д.6, корп. 5, e-mail: chilin@masterbeton-mb.ru

Шейнфельд Андрей Владимирович, доктор технических наук, советник РААСН, заместитель заведующего лабораторией № 16 НИИЖБ им. А. А. Гвоздева АО «НИЦ «Строительство», 109428, Москва, 2-я Институтская ул., д.6, корп. 5, e-mail: sheynfeld@masterbeton-mb.ru.

International Journal for Computational Civil and Structural Engineering, 19(4) 182–195(2023)

DOI:10.22337/2587-9618-2023-19-4-182-195

PERFORMANCE OF A BASE-ISOLATED RC BUILDING SUPPORTED ON SQUARE UN-BONDED FIBER REINFORCED ELASTOMERIC ISOLATOR UNDER EARTHQUAKES

Van-Thuyet Ngo

Civil Engineering Department, Thuyloi University, Hanoi, VIETNAM

Abstract: Un-bonded fiber reinforced elastomeric isolator (U-FREI) is a relatively new type of multi-layer elastomeric isolator in which fiber layers are used as reinforcement to replace steel sheets in conventional steel reinforced elastomeric isolators. It is installed directly between the substructure and superstructure without any connection at the interfaces. Most of the previous studies on the U-FREIs supported to the base-isolated buildings are masonry or stone structures. In this study, the dynamic responses of a reinforced concrete (RC) building supported on square U-FREIs under the action of recorded real time-history ground motions of earthquakes are investigated by finite element analysis using SAP2000 software. A hypothetical 4-storey reinforced concrete building constructed in Vietnam is selected for the study. Comparison of the dynamic responses of the base-isolated building and corresponding fixed-base building is carried out to evaluate the seismic vulnerability of the base-isolated building under earthquakes. Finite element analysis results show that peak values of floor acceleration and inter-storey drifts at different floor levels, and peak value of base shear of the base-isolated building are lower than those of the corresponding fixed-base building. The U-FREIs are found to be very effective in reducing seismic vulnerability of low and mid-rise RC buildings.

Keywords: Base isolation, un-bonded fiber reinforced elastomeric isolator, effective horizontal stiffness, effectiveness of base-isolated building, earthquake

ЭФФЕКТИВНОСТЬ КВАДРАТНОГО АРМИРОВАННОГО ВОЛОКНОМ ЭЛАСТОМЕРНОГО ИЗОЛЯТОРА ДЛЯ ЖЕЛЕЗОБЕТОННОГО ЗДАНИЯ ПРИ ЗЕМЛЯТРЕСЕНИЯХ

Ван-Тхует Нго

Факультет гражданского строительства, Университет Туйлоя, г. Ханой, ВЬЕТНАМ

Аннотация: Эластомерные изоляторы, армированные фибровым волокном без сцепления (U-FREI), являются относительно новым типом многослойной изоляции, в которой в качестве армирующего используются вместо стальных листов используется слои волокна. Такой слой устраивается непосредственно между верхней и нижней опорными пластинами без какого-либо соединения по поверхности контакта. Большинство ранее выполненных исследований, посвященных U-FREI, были связаны с каменными конструкциями. В данной работе динамические характеристики железобетонного здания, опирающегося на квадратные изоляторы U-FREI, исследуются методом конечных элементов с использованием программного обеспечения SAP2000 при зарегистрированных в реальном времени колебаниях грунта, вызванных землетрясением. Для исследования выбрано 4-этажное железобетонное здание, построенное во Вьетнаме. Сравнение динамических откликов здания с изоляцией основания и соответствующего здания с фиксированным основанием проводится для оценки сейсмостойкости. Результаты расчета методом конечных элементов показывают, что пиковые значения ускорения перекрытий, межэтажные смещения, а также пиковое значение смещения основания здания с изоляцией ниже, чем у соответствующего здания с фиксированным основанием. Выявлено, что U-FREI эффективны для повышения сейсмостойкости малоэтажных и средне этажных зданий.

Ключевые слова: изоляция основания, эластомерный изолятор, армированный волокном, эффективная горизонтальная жесткость, эффективность здания с изоляцией основания, землетрясение

1. INTRODUCTION

Base isolation is an effective solution to reduce the vulnerability of a structure when earthquakes occur [1,2]. Normally base isolators are usually placed above the substructure and below the superstructure of the building. Base isolation can undergo large horizontal displacement from earthquakes due to the low horizontal stiffness of the isolators. Moreover, the large equivalent viscous damping of the isolators is dissipated the energy of earthquakes transmitted to the superstructure. Meanwhile, the vertical stiffness of the isolators has a large value to ensure that the isolators can undergo the weight of the construction and the vertical loads acting on the superstructure.

Most of the buildings used the base isolators in the world are often of high importance and high cost [3]. They often use conventional multi-layer elastomeric isolator such as natural rubber bearing (NRB), high-damping rubber bearing (HDRB), and lead rubber bearing (LRB). Over the past two decades, a new type of multi-layer elastomeric isolator as un-bonded fiber reinforced elastomeric isolator (U-FREI) is studied and developed. The U-FREI consists of alternating layers of rubber and fiber fabric as reinforcement. It is installed directly between the substructure and superstructure without any connection at the interfaces. Therefore, when the isolator is subjected to horizontal displacement, elastomer layers at top and bottom of the U-FREI will lose contact with the supports lead to “rollover deformation” [4]. The U-FREI is lighter, easier in manufacturing and installation than the conventional multi-layer elastomeric isolator. It is expected to replace the conventional multi-layer elastomeric isolator for seismic response control of low and mid-rise lifeline buildings in developing countries like Vietnam, Indonesia, India, etc.

Some studies for the U-FREI have been conducted in recent times. The vertical and horizontal behavior of the U-FREI under cyclic loading was investigated by both finite element (FE) analysis and experimental tests [5-15]. These studies were determined the mechanical properties of the U-FREIs with different sizes, including horizontal stiffness, vertical stiffness and damping factor. Analytical approaches were proposed to calculate the effective plan area in contact with the support surfaces and the effective horizontal stiffness of the U-FREI [16,17]. Some shake table tests of the base-isolated buildings supported on U-FREIs were carried out to ascertain its effectiveness in controlling seismic response [18-20]. A little effort to apply the U-FREIs for the residential buildings in developing countries was presented [2,21-25]. Most of these studies investigated the seismic effectiveness of the base-isolated masonry buildings supported on U-FREIs. Thus, the seismic performance of the U-FREIs supported to the base-isolated reinforced concrete (RC) buildings should be further studied.

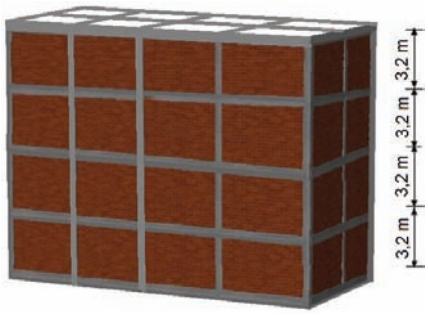
In this study, the seismic performance of a base-isolated RC building supported on square U-FREIs is investigated by FE analysis using SAP2000 software. A hypothetical base-isolated building constructed in Vietnam is selected for the study. The mechanical characteristics of the U-FREIs are determined with an analytical approach as proposed by the previous study. Dynamic response of the building under the action of various recorded real time history ground motions of earthquakes in two cases: fixed-base and base-isolated conditions are investigated. From results of FE analysis, comparison of the floor acceleration, inter-storey drift responses and base shear of the base-isolated building with those of the corresponding fixed-base building is carried out to evaluate the seismic vulnerability of the base-isolated building under earthquakes.

2. DESCRIPTION OF A BASE-ISOLATED RC BUILDING

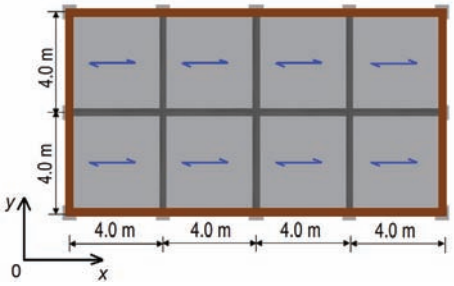
As mentioned above, U-FREI is a relatively new type of seismic isolator, which is expected to be used for low and mid-rise civil buildings.

There have not been many base-isolated buildings supported on the isolators. There is an actual base-isolated two-storey masonry building supported on square U-FREIs which was successfully constructed in October 2016 at Tawang, Arunachal Pradesh State, India. This is the first U-FREIs supported prototype low-rise building to be constructed anywhere in the world [2]. In this study, a hypothetical RC building supported on square U-FREIs is selected as the research object.

A base-isolated 4-storey RC building with hypothetical constructed location, hypothetical dimensions and hypothetical material properties is considered for this study. It is constructed in Muong Lay town, Dien Bien province, Vietnam. Dien Bien is a province in the north-western region, where has the largest seismic activity in Vietnam. Materials used in the building are concrete of B15 grade (weight per unit volume of 25 kN/m^3, modulus of elasticity of 2.3x10^7 kN/m^2 and poisson's ratio of 0.2) and reinforcement of CIII group grade (f_y = 400 N/mm^2) according to Vietnam design standard TCVN 5574 [26]. Cross-sectional dimensions of all beams and columns are 0.30m x 0.45m and 0.30m x 0.30m respectively. Thickness of all slabs is 0.12m. There are 5 bays of 4.0m in X-direction, 3 bays of 4.0m in Y-direction, i.e. plan dimensions are 16.0m x 8.0m. Each floor height is 3.2m. Brick masonry walls with thickness of 0.11m are built around the perimeter of the building. Three-dimensional view and typical floor plan of the base-isolated building are shown in Fig. 1.



(a) View of the superstructure



(b) Typical floor plan

Figure 1. The base-isolated 4-storey RC building

The superstructure is placed on an isolation system consisting of fifteen square U-FREIs placed under fifteen columns (Fig. 2). There exists a rigid slab at the base level that connects all isolation elements. It is considered that the weight of the superstructure is equally transferred to each isolator under the column. The maximum possible vertical load on an isolator as computed considering all possible load combinations as per Vietnam standard TCVN 9386 (Design of structures for earthquake resistances) [27] is W = 580 kN. The fixed-base period of the superstructure is estimated to be about 0.42 seconds (from simulated model in SAP2000 v.15.2.1 software [28]). The project site is located in Muong Lay town on a site with soil class B as per Vietnam standard [27].



Figure 2. View showing locations of base isolators in the building

3. SELECTING THE SIZE AND MECHANICAL CHARACTERISTICS OF SQUARE U-FREIS

3.1. Methodology

3.1.1. Shape factor

One of the most important parameters in the design of multi-layer elastomeric isolator is shape factor (S) defined as the ratio of the

loaded area to load free area of a rubber layer [3]. For a square isolator with the width of a and a single rubber layer thickness of t_e, the shape factor is computed by

$$S = \frac{a}{4t_e} \tag{1}$$

Generally, for better seismic performance, the prototype isolators should have the value of shape factor more than 10 [3].

3.1.2. Horizontal stiffness of a square U-FREI

According to [3], the horizontal stiffness of a conventional multi-layer elastomeric isolator is given by

$$K_h^b = \frac{GA}{t_r} \tag{2}$$

where G is the initial shear modulus, A is the full cross-sectional area of the isolator (for a square isolator with the width of a, the full cross-sectional area is $A = a^2$), and t_r is the total thickness of rubber layers in the isolator.

The horizontal stiffness of a U-FREI is calculated according to an analytical approach which is proposed by Ngo et al. [17] as

$$K_h^{ub} = \frac{G_{eff} A_{eff}}{t_r} \tag{3}$$

where G_{eff} is the effective shear modulus of isolator and A_{eff} is the effective plan area in contact with the support surfaces of the U-FREI at the horizontal displacement (u).

The effective shear modulus (G_{eff}) is affected by many factors such as the magnitude of the horizontal displacement (u) and the value of the vertical load acting on the isolator. For a square isolator with the width of a, the effective shear modulus (G_{eff}) is given as:

For $0 < u \leq 1.0t_r$:

$$G_{eff} = G\left[1-\left(\frac{p_z}{p_{crit,0}\left(1-\left(\frac{u}{a}\right)^2\right)}\right)^2\right]\left(1-\frac{u}{a}\right) \tag{4}$$

For $1.0t_r < u \leq 1.5t_r$:

$$G_{eff} = G\left[1-\left(\frac{p_z}{p_{crit,0}\left(1-\left(\frac{t_r}{a}\right)^2\right)}\right)^2\right]\left(1-\frac{t_r}{a}\right) \tag{5}$$

where $p_{crit,0}$ is the critical stress state according to Kelly [29] and is given by

$$p_{crit,0} = \frac{P_{crit}}{a^2} \tag{6}$$

$$P_{crit} = \frac{\sqrt{2}\pi GASr}{t_r} \tag{7}$$

$$r = \frac{a}{2\sqrt{3}} \tag{8}$$

r is the radius of gyration; p_z is the vertical pressure on the isolator and is calculated as

$$p_z = \frac{W}{A} \tag{9}$$

W is the vertical load on the isolator.

According to [16], the effective plan area (A_{eff}) of a square isolator with the width of a is calculated as

$$A_{eff} = a(a-d) \tag{10}$$

where, d is the projected length of the curved part of the rollover region along the horizontal plane as shown in Fig. 3, and is given as

$$d = \frac{25}{16}\alpha h \tag{11}$$

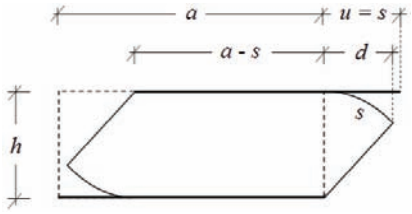


Figure 3. Deformed configuration of an U-FREI

where, h is the total height of the isolator, α is a geometrical parameter which relates d and curved length (s) at a given horizontal displacement (u). The relation between u, s and α as proposed by Toopchi-Nezhad [16] is expressed as

$$u = s = \frac{25}{64} h \left[2\alpha\sqrt{1+4\alpha^2} + \ln\left(2\alpha + \sqrt{1+4\alpha^2}\right) \right] \quad (12)$$

Thus, for a known value of u and h, α is found from Eq. (12), which is used for the evaluation of A_{eff} using Eq. (10).

3.1.3. Vertical stiffness of a square U-FREI

Vertical stiffness (K_v) of a multi-layer elastomeric isolator is given by [3]

$$K_v = \frac{E_c A}{t_r} \quad (13)$$

where E_c is the compression modulus of the isolator, for a square isolator is $E_c = 6.73GS^2$.

3.2. Selecting the size of square U-FREIs supported to the base-isolated building

A design procedure for determing the size of the conventional multi-layer elastomeric isolators (including NRBs, HDRBs, LRBs) supported to base-isolated structures was presented by Mayes and Naeim [30]. There are few documents giving detailed design procedure for determing the size of the U-FREIs. Ngo [31] was proposed a design procedure following the design provisions of ASCE 7 [32] for selecting the size of U-FREIs supported to a base-isolated building. In this study, the step-by-step selecting size of square U-FREIs is presented according to the design procedure proposed by Ngo [31].

Step 1: Evaluation of spectral response acceleration parameter at a period of 1 second, S_1 ($S_1 \leq 0.60$):

According to Vietnam standard TCVN 9386 [27], the peak value of reference ground acceleration in Muong Lay town is $a_{gR} = 0.1516g$. Note that the spectral acceleration (S_1) in ASCE 7 [32] is calculated according to the repetition period of $T_{ASCE} = 2500$ years, while it, in the Vietnam standards, is calculated according to the repetition period of $T_{VN} = 500$ years [27]. Therefore, it is necessary to convert the peak value of reference ground acceleration in Vietnam standards from the 500-year repetition period to the 2500-year repetition period. According to [27], the conversion formula is as follows:

$$S_1 = \left(T_{VN} / T_{ASCE}\right)^{(-1/3)} \left(a_{gR}/g\right) \quad (14)$$

$$S_1 = \left(500/2500\right)^{(-1/3)} \left(0.1516g/g\right)$$
$$S_1 = 1.71 \times 0.1516 = 0.2592$$

Step 2: Determine the site coefficient, F_v:

The building is located on a site with soil class B as per Vietnam standard [27]. The site soil class B in TCVN 9386 [27] corresponds to the site soil class C in ASCE 7 [32]. Thus, the value of $F_v = 1.50$ is obtained from Table 11.4-2 in ASCE 7 [32] for site class C and $S_1 = 0.2592$.

Step 3: Determine the seismic coefficient, S_{M1}:

The spectral coefficient needed for calculation of minimum displacements is obtained from Eq. (15):

$$S_{M1} = F_v S_1 \quad (15)$$
$$S_{M1} = 1.50 \times 0.2592 = 0.389$$

Step 4: Select the damping coefficient, B_M:

The equivalent viscous damping of the U-FREIs is usually in the range of 6% to 15% [1-5]. For preliminary design purpose, 10% damping is assumed for isolator type of U-FREI. From Table Table 17.5-1 in ASCE 7 [32], $B_M = 1.20$.

Step 5: Select a desired period of the isolated structure at the design displacement, T_M:

The effective period of the base-isolated structure at the design displacement is calculated from Eq. (16):

$$T_M \geq 3T_{fixed-base} \tag{16}$$

where $T_{fixed\text{-}base}$ is the fixed-base period of the building. T_M is often selected in range from 1.5 to 2.5 seconds for low and mid-rise civil buildings. Thus,

$$T_M \geq 3 \times 0.42 = 1.26(\sec)$$

Take T_M = 1.60 (sec) for preliminary design.

Step 6: Estimate the effective horizontal of the isolator, K_h:

The effective horizontal stiffness of the isolator is obtained from Eq. (17) as

$$T_M = 2\pi\sqrt{\frac{W}{K_{\mathrm{M,min}}g}} \quad \rightarrow \quad K_h = \frac{W}{g}\left(\frac{2\pi}{T_M}\right)^2 \tag{17}$$

where $K_{M,min}$ is the minimum effective horizontal stiffness of the isolator at the design displacement (T_M), W is the maximum possible vertical load on an isolator (W = 580 kN) and g is the acceleration of gravity (g = 9.81 m/s^2). Thus,

$$K_h = \frac{580}{9.81} \times \left(\frac{2\pi}{1.60}\right)^2 = 911.8(kN/m)$$

Step 7: Estimate the design horizontal displacement, D_M:

The design displacement is obtained from Eq. (18) as

$$D_M = \left(\frac{g}{4\pi^2}\right)\frac{S_{M1}T_M}{B_M} \tag{18}$$

$$D_M = \left(\frac{9.81}{4\pi^2}\right) \times \frac{0.389 \times 1.60}{1.20} = 0.129(m)$$

Step 8: Estimate the total rubber thickness required, t_r:

$$\gamma = \frac{D_M}{t_r} = 150\% \quad \rightarrow \quad t_r = \frac{D_M}{1.5} \tag{19}$$

$$t_r = \frac{0.129}{1.50} = 0.086(m) = 86(mm)$$

Step 9: Choose the full cross-sectional area of the U-FREI:

$$A > \frac{K_h t_r}{G} \tag{20}$$

The initial shear modulus (G) depends on the type or rubber used in the isolator. Generally, the value of G is selected in range from 0.5 to 1.35 MPa. To take a typical rubber with G = 0.90 MPa. From Eq. (20):

$$A > \frac{911.8 \times 0.086}{0.9 \times 10^3} = 0.0871(m^2)$$

$$a > \sqrt{A} = \sqrt{0.0871} = 0.295(m)$$

In fact, the horizontal stiffness of a U-FREI is calculated by Eq. (3) relates to the reduction in shear modulus with increasing displacement and the effective plan area in contact with the support surfaces [17]. Thus, it is chosen a = 0.32 (m) = 320 (mm) for the square U-FREIs supported to the base-isolated building.

Step 10: Choose the number of rubber layers, n_e, thickness of a rubber and fiber layer, t_e and t_f, and total thickness of U-FREI, h:

According to [3], the shape factor typical for seismic isolation is in range of 10 to 20. Selecting a shape factor of S = 16 for the isolators of seismic isolation, from Eq. (1) we can calculate the thickness of an individual rubber layer, t_e, as

$$t_e = \frac{a}{4S} = \frac{320}{4 \times 16} = 5(mm)$$

Choose t_e = 5 (mm). Thus, the number of rubber layers is n = 86/5 = 17.2. Choose n = 18.

The total thickness of rubber layers in the isolator is

$$t_r = n \times t_e = 18 \times 5 = 90(mm)$$

Using t_f = 0.55 (mm) thick of a carbon fiber reinforcement layer. The total height of the isolator is

$$h = 90 + 0.55 \times (18 - 1) = 99.35 \approx 100\,(mm)$$

Thus, the sizes of the isolators are **320x320x100** (mm). Three-dimensional view of the U-FREI is shown in Fig. 4.



Figure 4. View showing sizes of the U-FREIs

3.3. Determination of mechanical characteristics of the square U-FREIs

3.3.1. The shape factor

The actual shape factor of the U-FREIs is:

$$S = \frac{a}{4t_e} = \frac{320}{4 \times 5} = 16$$

3.3.2. The effective horizontal stiffness (K_h^{ub})

According to [32], the limit horizontal displacement amplitude of an isolation system is $1.50t_r$ (135 mm). Therefore, values of the effective horizontal stiffness of the U-FREIs at the increasing horizontal displacement amplitude up to $1.50t_r$ are determined with the analytical approach above, and are given results in Table 1.

According to [32], the effective horizontal stiffness of an isolator relates the shear force and the horizontal displacement amplitude by

$$K_h = \frac{F}{u} \tag{21}$$

From Eq. (21), the shear force of the isolator is obtained by

$$F = K_h u \tag{22}$$

Table 1. Effective horizontal stiffness of the U-FREIs

u (mm)	u/t_r	G_{eff} (N/mm^2)	α	d (mm)	A_{eff} (mm^2)	K_h^{ub} (kN/m)
20.0	0.22	0.8374	0.1267	19.80	96065.00	838.86
40.0	0.44	0.7815	0.2464	38.50	90080.00	734.03
60.0	0.67	0.7254	0.3559	55.61	84605.00	639.97
80.0	0.89	0.6721	0.4505	70.39	79875.00	559.79
90.0	1.00	0.6412	0.5015	78.36	77325.00	517.00
112.5	1.25	0.6412	0.5983	93.48	72485.00	484.64
135.0	1.50	0.6412	0.6867	107.30	68065.00	455.09

The shear force-horizontal displacement amplitude relationships of these isolators with increasing horizontal displacement amplitude up to $1.50t_r$ as obtained from the analytical approach and idealized lines as given by bi-linear behaviour are shown in Fig. 5. The bi-linear behaviour is selected because this model can be effectively used for all isolation systems used in practice.

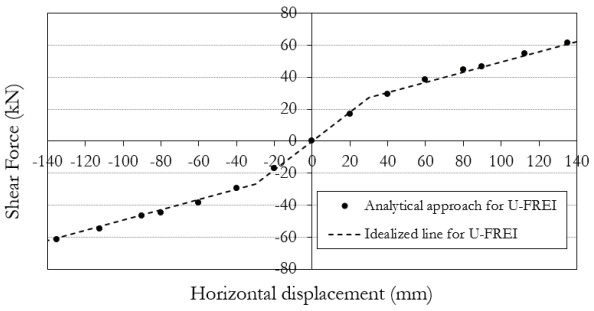


Figure 5. Shear force – horizontal displacement amplitude relationships of the isolators

3.3.3. The Vertical Stiffness of U-FREIs

The compression modulus and vertical stiffness of the U-FREIs are calculated as

$$E_c = 6.73 \times 0.90 \times 16^2 = 1550.59 \left(N / mm^2 \right);$$

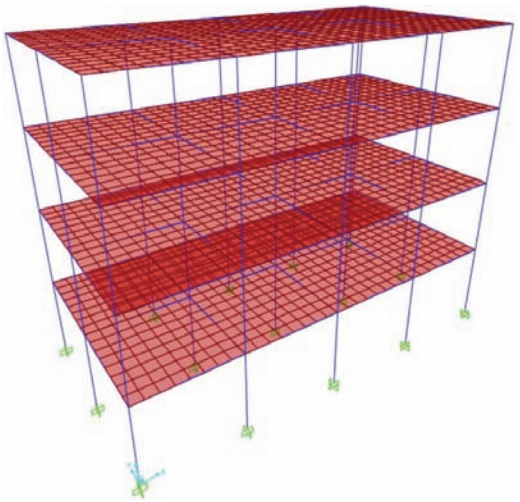
$$K_V = \frac{1550.59 \times 320^2}{90} = 1764229.12 \left(kN / m \right).$$

4. INVESTIGATION OF THE EFFECTIVENESS OF THE BASE-ISOLATED BUILDING UNDER EARTHQUAKES

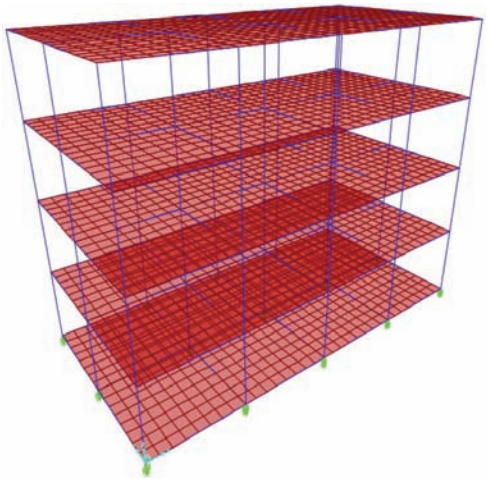
The response of the base-isolated building supported on the U-FREIs and the corresponding fixed-base building under the action of various recorded real time-history ground motions of earthquakes are investigated by FE analysis using SAP2000 v.15.2.1 software [28]. Comparison of the floor acceleration, inter-storey drift responses and base shear of the base-isolated building with those of the corresponding fixed-base building is carried out to evaluate the seismic vulnerability of the base-isolated building under earthquakes.

The fixed-base and base-isolated buildings are simulated in 3D finite element model by SAP2000 (Fig. 6). The beams and columns are modelled using frame elements. All floors are modelled using shell elements, in which each floor is assigned by a diaphragm constraint. For the base-isolated building, U-FREIs are modelled by rubber isolator element defined under link type of elements (rubber isolator). The nonlinear force-horizontal displacement behaviour (bi-linear curve) of the isolators as shown in Fig. 5 is used to represent the mechanical properties of the isolators along X and Y-axis. The vertical stiffness of the isolators above is used to present the mechanical properties of the isolators along Z-axis. For the fixed-base building, all nodes at ground level are fixed in all the directions.

The dynamic responses of the fixed-base and base-isolated buildings under the action of various recorded real earthquake time-history ground motions of earthquakes are investigated by time history analysis. Two time-history ground motions from real earthquake records as El-Centro earthquake (USA, 18/05/1940, Comp – 180, peak acceleration value of 0.32*g*) and Kobe earthquake (Japan, 16/01/1995, Comp – FUK000, peak acceleration value of 0.33*g*) as shown in Fig. 7, are selected to investigate the seismic performance of the base-isolated building. Time history analysis is carried out along the weaker axis of the building, i.e. Y-axis (Fig. 1b).

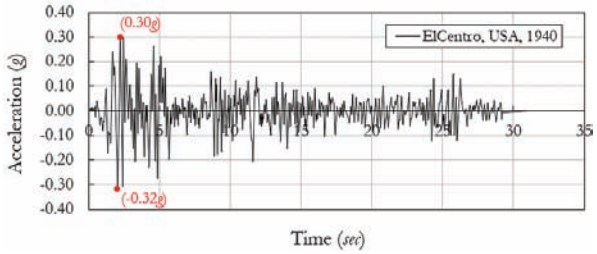


(a) Fixed-base building

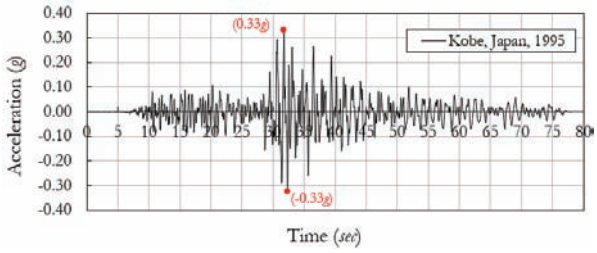


(b) Base-isolated building

Figure 6. Three-dimensional FE model of the building



(a) El-Centro earthquake



(b) Kobe earthquake

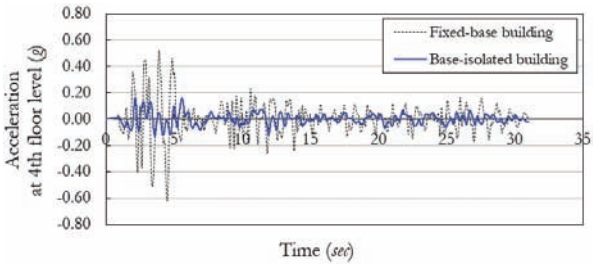
Figure 7. Real time-history record of selected earthquake motions

Comparison of the peak absolute values of floor accelerations, inter-storey drifts and base shear of the base-isolated building with those of the fixed-base building are presented in Table 2. Comparison of the detailed time-history of floor acceleration at roof level (the level has the maximum magnitude of peak floor acceleration), inter-storey drifts at the 2nd storey (the level has the maximum magnitude of peak inter-storey drift) and base shear of the base-isolated and fixed-base buildings under each earthquake excitation are shown in Figs. 8-10 respectively.

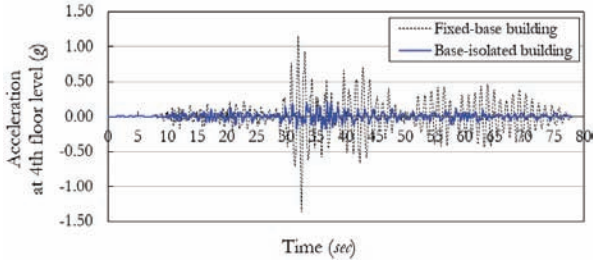
It may be observed from Table 2 that the magnitudes of peak floor acceleration and inter-storey drifts at different floor levels, and the magnitude of peak base shear of base-isolated building are lower than those of fixed-base building. For example, the peak floor acceleration value at roof level, the peak inter-storey drift value at 2nd storey and peak value of base shear of the base-isolated building are reduced by (74.2%, 72.6% and 69.9% respectively), (84.7%, 88.0% and 84.4% respectively) as compared to the corresponding values in the fixed-base building under ElCentro, Kobe earthquakes respectively. Further, the magnitudes of peak floor acceleration at different floor levels of the base-isolated building are almost the same under each excitation, while the magnitude of peak floor acceleration of the fixed-base building is amplified along the height of the building model. This finding is in agreement with the observation made by Das et al. [19] based on the shake table testing results of a scaled model of base-isolated un-reinforced brick masonry building supported on U-FREIs. It indicates that the possibility of any damage in the superstructure of the base-isolated building is clearly lower than that of fixed-base building. Thus, the mitigation of seismic vulnerability of the base-isolated building supported on the U-FREIs is better than that of the fixed-base building under the same earthquakes.

Table 2. Comparison of the peak values of dynamic responses of the fixed-base and base-isolated buildings under earthquakes

Parameter	Fixed-base building		Base-isolated building	
	El-Centro	Kobe	El-Centro	Kobe
Peak floor acceleration value at 1st floor level (*g*)	0.35	0.55	0.12	0.14
Peak floor acceleration value at 2nd floor level (*g*)	0.42	0.84	0.09	0.13
Peak floor acceleration value at 3rd floor level (*g*)	0.46	1.11	0.13	0.14
Peak floor acceleration value at roof level (*g*)	0.62	1.37	0.16	0.21
Peak inter-storey drift value at 1st storey (mm)	42.2	100.1	12.9	14.1
Peak inter-storey drift value at 2nd storey (mm)	46.4	112.2	12.7	13.5
Peak inter-storey drift value at 3rd storey (mm)	38.2	86.6	9.8	11.4
Peak inter-storey drift value at 4th storey (mm)	20.8	45.9	5.2	6.5
Peak value of base shear (kN)	2788.9	6566.7	838.9	1023.1

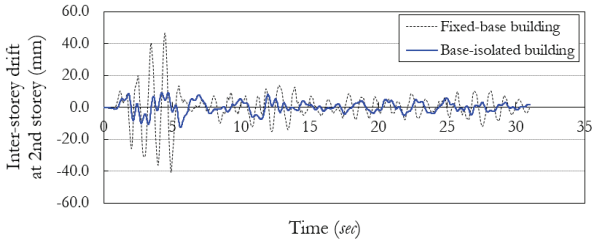


(a) El-Centro earthquake

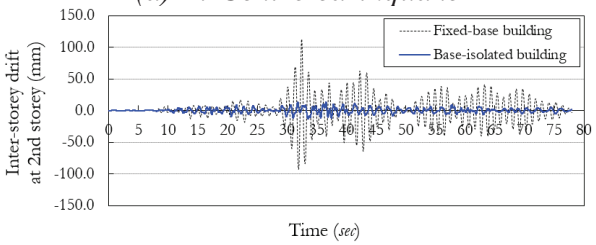


(b) Kobe earthquake

Figure 8. Floor acceleration responses at the roof level of the building under various earthquakes

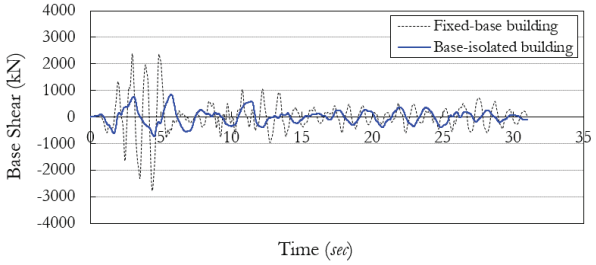


(a) El-Centro earthquake

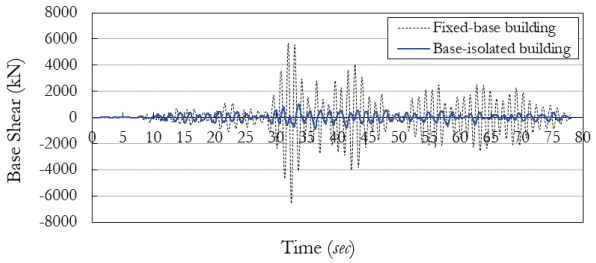


(b) Kobe earthquake

Figure 9. Inter-storey drift responses at the 2nd storey of the building under various earthquakes



(a) El-Centro earthquake



(b) Kobe earthquake

Figure 10. Base shear responses of the building under various earthquakes

5. CONCLUSION

This study presents the seismic performance of a base-isolated reinforced concrete building supported on square un-bonded fiber reinforced elastomeric isolators. A hypothetical base-isolated 4-storey RC building constructed in Muong Lay town, Dien Bien province, Vietnam is considered for the study. The size of the square U-FREIs is selected following the design provisions of ASCE 7. The mechanical properties of the square U-FREIs with the selected size, including horizontal and vertical stiffnesses, are calculated with an analytical approach as proposed by previous study. Investigation the time-history responses of both fixed-base and base-isolated buildings under the action of various recorded real earthquake time-history ground motions of earthquakes are carried out by FE analysis using SAP2000 software. From results of FE analysis, comparison of the dynamic responses of the fixed-base and base-isolated buildings is presented to evaluate the seismic vulnerability of the base-isolated building under earthquakes. The concluding remarks are as follows:

- Magnitudes of peak floor acceleration and inter-storey drifts at different floor levels of the base-isolated building are lower than those of the fixed-base building. Thus, the possibility of any damage in the superstructure of the base-isolated building is clearly lower than that of the corresponding fixed-base building.

- Magnitude of peak base shear of the base-isolated building is lower than that of the fixed-base building. The seismic vulnerability of the base-isolated building is mitigated in comparison with that of the corresponding fixed-base building under the same earthquakes.
- U-FREIs are found to be very effective in reducing seismic vulnerability of low and mid-rise RC buildings. Thus, U-FREIs are recommended for seismic isolation of low and mid-rise RC buildings.

REFERENCES

1. **Kumar P., Petwal S.** (2019). Seismic performance of secondary systems housed in isolated and non-isolated building. *Earthquakes and Structures, an international journal*, 16(4), 401-413.
2. **Ngo V.T., Deb S.K., Dutta A.** (2018). Mitigation of seismic vulnerability of a prototype low-rise masonry building using U-FREIs. *Journal of Performance of Constructed Facilities, ASCE*, 32(2), 04017136.
3. **Naeim F., Kelly J.M.** (1999). Design of seismic isolated structures: From theory to practice. *John Wiley & Sons Inc.*, New York, USA.
4. **Toopchi-Nezhad H., Tait M.J., Drysdale R.G.** (2008). Lateral response evaluation of fiber-reinforced neoprene seismic isolator utilized in an unbonded application. *Journal of Structural Engineering, ASCE*, 134(10), 1627-1637.
5. **Moon B.Y., Kang G.J., Kang B.S., Kelly J.M.** (2002). Design and manufacturing of fiber reinforced elastomeric isolation. *Journal of Material Processing Technology*, 130-131, 145-150.
6. **Ashkezari G.D., Aghakouchak A.A., Kokabi M.** (2008). Design, manufacturing and evaluation of the performance of steel like fiber reinforced elastomeric seismic isolators. *Journal of Material Processing Technology*, 197, 140-150.
7. **Toopchi-Nezhad H., Tait M.J., Drysdale R.G.** (2009). Simplified analysis of a low-rise building seismically isolated with stable un-bonded fiber reinforced elastomeric isolators. *Canadian Journal of Civil Engineering*, 36(7), 1182-1194.
8. **Russo G., Pauletta M.** (2013). Sliding instability of fiber-reinforced elastomeric isolators in un-bonded applications. *Engineering Structures*, 48, 70-80.
9. **Spizzuoco M., Calabrese A., Serino G.** (2014). Innovative low-cost recycled rubber-fiber reinforced isolator: Experimental test and finite element analyses. *Engineering Structures*, 76, 99-111.
10. **Naghshineh A.K., Akyuz U., Caner A.** (2014). Comparison of fundamental properties of new types of fiber-mesh-reinforced seismic isolators with conventional isolators. *Earthquake Engineering and Structural Dynamics*, 43(2), 301-316.
11. **Dezfuli F.H., Alam M.S.** (2014). Performance of carbon fiber-reinforced elastomeric isolators manufactured in a simplified process: Experimental investigations. *Structural Control and Health Monitoring*, 21(11), 1347-1359.
12. **Osgooei P.M., Tait M.J., Konstantinidis D.** (2014). Finite element analysis of unbonded square fiber-reinforced elastomeric isolators (FREIs) under lateral loading in different directions. *Composite Structures*, 113, 164-173.
13. **Van Engelen N.C., Osgooei P.M., Tait M.J., Konstantinidis D.** (2014). Experimental and finite element study on the compression properties of modified rectangular fiber-reinforced elastomeric isolators (MR-FREIs). *Engineering Structures*, 74, 52-64.
14. **Ngo V.T.** (2020). Effect of shape factor on the horizontal response of prototype un-bonded fiber reinforced elastomeric

isolators under cyclic loading. *Structural Integrity and Life*, 20(3), 303-312.

15. **Ngo V.T.** (2021). Influence of vertical load on the horizontal response of prototype unbonded fiber reinforced elastomeric isolator. *Structural Integrity and Life*, 21(3), 229-237.
16. **Toopchi-Nezhad H.** (2014). Horizontal stiffness solutions for unbonded fiber reinforced elastomeric bearings. *Structural Engineering and Mechanics, an international journal*, 49(3), 395-410.
17. **Ngo V.T., Dutta A., Deb S.K.** (2017). Evaluation of horizontal stiffness of fibre reinforced elastomeric isolators. *Earthquake Engineering and Structural Dynamics*, 46(11), 1747-1767.
18. **Toopchi-Nezhad H., Tait M.J., Drysdale R.G.** (2009). Shake table study on an ordinary low-rise building seismically isolated with SU-FREIs (stable unbonded-fiber reinforced elastomeric isolators). *Earthquake Engineering and Structural Dynamics*, 38(11), 1335-1357.
19. **Das A., Deb S.K., Dutta A.** (2016). Shake table testing of un-reinforced brick masonry building test model isolated by U-FREI. *Earthquake Engineering and Structural Dynamics*, 45(2), 253-272.
20. **Losanno D., Spizzuoco M., A. Calabrese A.** (2019). Bidirectional shaking table tests of unbonded recycled rubber fiber-reinforced bearings (RR-FRBs). *Structural Control and Health Monitoring*, 26(9), e2386.
21. **Calabrese A., Losanno D., Spizzuoco M., Strano S., Terzo M.** (2019). Recycled rubber fiber-reinforced bearings (RR-FRBs) as base isolators for residential buildings in developing countries: The demonstration building of Pasir Badak, Indonesia. *Engineering Structures*, 192, 126-144.
22. **Habieb A.B., Valente M., Milani G.** (2019). Base seismic isolation of a historical masonry church using fiber reinforced elastomeric isolators. *Soil Dynamics and Earthquake Engineering*, 120, 127-145.
23. **Ngo V.T.** (2021). Effectiveness of base-isolated low-rise masonry building under excitation from earthquakes. *Magazine of Civil Engineering*, 108(8), 10803.
24. **Habieb A.B., Formisano A., Milani G., Pianese G.** (2022). Seismic performance of Unbonded Fiber-Reinforced Elastomeric Isolators (UFREI) made by recycled rubber. Influence of suboptimal crosslinking. *Engineering Structures*, 256, 114038.
25. **Losanno D., Ravichandran N., Parisi F.** (2023). Seismic fragility models for base-isolated unreinforced masonry buildings with fibre-reinforced elastomeric isolators. *Earthquake Engineering and Structural Dynamics*, 52(2), 308-334.
26. **TCVN 5574.** (2018). Concrete and reinforced concrete structures. *Vietnam Design standard*, Hanoi, Vietnam.
27. **TCVN 9386.** (2012). Design of structures for earthquake resistances. *Vietnam standard*, Hanoi, Vietnam.
28. **SAP2000 v.15.2.1.** (2014). CSI Analysis Reference Manual. *Computers and structures Inc.*, Berkeley, California, USA.
29. **Kelly J.M.** (2003). Tension buckling multilayer elastomeric bearings. *Journal of Engineering Mechanics, ASCE*, 129(12), 1363-1368.
30. **Mayes R.L., Naeim F.** (2001). Design of Structures with Seismic Isolation. in *The Seismic Design Handbook, Springer*, Boston, Massachusetts, USA, Ch. 14, 723-756.
31. **Ngo V.T.** (2017). Seismic performance evaluation of prototype unbonded fibre-reinforced elastomeric isolators. PhD thesis, Department of Civil Engineering, Indian Institute of Technology Guwahati-781039, Assam, India.
32. **ASCE 7.** (2016). Minimum design load for buildings and other structure. *American Society of Civil Engineers (ASCE)*, Reston, Virginia, USA.

СПИСОК ЛИТЕРАТУРЫ

1. **Kumar P., Petwal S.** (2019). Seismic performance of secondary systems housed in isolated and non-isolated building. *Earthquakes and Structures, an international journal*, 16(4), 401-413.
2. **Ngo V.T., Deb S.K., Dutta A.** (2018). Mitigation of seismic vulnerability of a prototype low-rise masonry building using U-FREIs. *Journal of Performance of Constructed Facilities, ASCE*, 32(2), 04017136.
3. **Naeim F., Kelly J.M.** (1999). Design of seismic isolated structures: From theory to practice. *John Wiley & Sons Inc.*, New York, USA.
4. **Toopchi-Nezhad H., Tait M.J., Drysdale R.G.** (2008). Lateral response evaluation of fiber-reinforced neoprene seismic isolator utilized in an unbonded application. *Journal of Structural Engineering, ASCE*, 134(10), 1627-1637.
5. **Moon B.Y., Kang G.J., Kang B.S., Kelly J.M.** (2002). Design and manufacturing of fiber reinforced elastomeric isolation. *Journal of Material Processing Technology*, 130-131, 145-150.
6. **Ashkezari G.D., Aghakouchak A.A., Kokabi M.** (2008). Design, manufacturing and evaluation of the performance of steel like fiber reinforced elastomeric seismic isolators. *Journal of Material Processing Technology*, 197, 140-150.
7. **Toopchi-Nezhad H., Tait M.J., Drysdale R.G.** (2009). Simplified analysis of a low-rise building seismically isolated with stable un-bonded fiber reinforced elastomeric isolators. *Canadian Journal of Civil Engineering*, 36(7), 1182-1194.
8. **Russo G., Pauletta M.** (2013). Sliding instability of fiber-reinforced elastomeric isolators in un-bonded applications. *Engineering Structures*, 48, 70-80.
9. **Spizzuoco M., Calabrese A., Serino G.** (2014). Innovative low-cost recycled rubber-fiber reinforced isolator: Experimental test and finite element analyses. *Engineering Structures*, 76, 99-111.
10. **Naghshineh A.K., Akyuz U., Caner A.** (2014). Comparison of fundamental properties of new types of fiber-mesh-reinforced seismic isolators with conventional isolators. *Earthquake Engineering and Structural Dynamics*, 43(2), 301-316.
11. **Dezfuli F.H., Alam M.S.** (2014). Performance of carbon fiber-reinforced elastomeric isolators manufactured in a simplified process: Experimental investigations. *Structural Control and Health Monitoring*, 21(11), 1347-1359.
12. **Osgooei P.M., Tait M.J., Konstantinidis D.** (2014). Finite element analysis of unbonded square fiber-reinforced elastomeric isolators (FREIs) under lateral loading in different directions. *Composite Structures*, 113, 164-173.
13. **Van Engelen N.C., Osgooei P.M., Tait M.J., Konstantinidis D.** (2014). Experimental and finite element study on the compression properties of modified rectangular fiber-reinforced elastomeric isolators (MR-FREIs). *Engineering Structures*, 74, 52-64.
14. **Ngo V.T.** (2020). Effect of shape factor on the horizontal response of prototype un-bonded fiber reinforced elastomeric isolators under cyclic loading. *Structural Integrity and Life*, 20(3), 303-312.
15. **Ngo V.T.** (2021). Influence of vertical load on the horizontal response of prototype un-bonded fiber reinforced elastomeric isolator. *Structural Integrity and Life*, 21(3), 229-237.
16. **Toopchi-Nezhad H.** (2014). Horizontal stiffness solutions for unbonded fiber reinforced elastomeric bearings. *Structural Engineering and Mechanics, an international journal*, 49(3), 395-410.
17. **Ngo V.T., Dutta A., Deb S.K.** (2017). Evaluation of horizontal stiffness of fibre reinforced elastomeric isolators.

Earthquake Engineering and Structural Dynamics, 46(11), 1747-1767.

18. **Toopchi-Nezhad H., Tait M.J., Drysdale R.G.** (2009). Shake table study on an ordinary low-rise building seismically isolated with SU-FREIs (stable unbonded-fiber reinforced elastomeric isolators). *Earthquake Engineering and Structural Dynamics*, 38(11), 1335-1357.
19. **Das A., Deb S.K., Dutta A.** (2016). Shake table testing of un-reinforced brick masonry building test model isolated by U-FREI. *Earthquake Engineering and Structural Dynamics*, 45(2), 253-272.
20. **Losanno D., Spizzuoco M., A. Calabrese A.** (2019). Bidirectional shaking table tests of unbonded recycled rubber fiber-reinforced bearings (RR-FRBs). *Structural Control and Health Monitoring*, 26(9), e2386.
21. **Calabrese A., Losanno D., Spizzuoco M., Strano S., Terzo M.** (2019). Recycled rubber fiber-reinforced bearings (RR-FRBs) as base isolators for residential buildings in developing countries: The demonstration building of Pasir Badak, Indonesia. *Engineering Structures*, 192, 126-144.
22. **Habieb A.B., Valente M., Milani G.** (2019). Base seismic isolation of a historical masonry church using fiber reinforced elastomeric isolators. *Soil Dynamics and Earthquake Engineering*, 120, 127-145.
23. **Ngo V.T.** (2021). Effectiveness of base-isolated low-rise masonry building under excitation from earthquakes. *Magazine of Civil Engineering*, 108(8), 10803.
24. **Habieb A.B., Formisano A., Milani G., Pianese G.** (2022). Seismic performance of Unbonded Fiber-Reinforced Elastomeric Isolators (UFREI) made by recycled rubber. Influence of suboptimal crosslinking. *Engineering Structures*, 256, 114038.
25. **Losanno D., Ravichandran N., Parisi F.** (2023). Seismic fragility models for base-isolated unreinforced masonry buildings with fibre-reinforced elastomeric isolators. *Earthquake Engineering and Structural Dynamics*, 52(2), 308-334.
26. **TCVN 5574.** (2018). Concrete and reinforced concrete structures. *Vietnam Design standard*, Hanoi, Vietnam.
27. **TCVN 9386.** (2012). Design of structures for earthquake resistances. *Vietnam standard*, Hanoi, Vietnam.
28. **SAP2000 v.15.2.1.** (2014). CSI Analysis Reference Manual. *Computers and structures Inc.*, Berkeley, California, USA.
29. **Kelly J.M.** (2003). Tension buckling multilayer elastomeric bearings. *Journal of Engineering Mechanics, ASCE*, 129(12), 1363-1368.
30. **Mayes R.L., Naeim F.** (2001). Design of Structures with Seismic Isolation. in *The Seismic Design Handbook, Springer*, Boston, Massachusetts, USA, Ch. 14, 723-756.
31. **Ngo V.T.** (2017). Seismic performance evaluation of prototype unbonded fibre-reinforced elastomeric isolators. PhD thesis, Department of Civil Engineering, Indian Institute of Technology Guwahati-781039, Assam, India.
32. **ASCE 7.** (2016). Minimum design load for buildings and other structure. *American Society of Civil Engineers (ASCE)*, Reston, Virginia, USA.

Van-Thuyet Ngo, Civil Engineering Department, Thuyloi University, Hanoi, Vietnam. E-mail: thuyet.kcct@tlu.edu.vn

Ван-Тхует Нго, Факультет гражданского строительства, Университет Туйлоя, Ханой, Вьетнам. E-mail: thuyet.kcct@tlu.edu.vn

International Journal for Computational Civil and Structural Engineering, 19(4) 196–207(2023)

DOI:10.22337/2587-9618-2023-19-4-196-207

COMPARATIVE STUDY OF AXIAL BEARING CAPACITY FOR PILE FOUNDATION BASED ON EMPIRICAL, NUMERICAL METHOD AND PILE DRIVING ANALYZER TEST

Tsaana Khoirunisaa, Bambang Setiawan, Yusep M. Purwana

Civil Engineering Department, Sebelas Maret University, Surakarta City, INDONESIA

Abstract: Axial bearing capacity is an important factor in designing of foundation. It must be able to carry the load of upper structure without any significant deformation due to important role in pile design. A part from empirical and numerical methods, axial pile bearing capacity can be predicted by pile driving analyzer test that use wave equation analysis during the test. Prediction of the axial bearing capacity and its distribution can be achieved by combining wave equation analysis with dynamic pile monitoring. This paper compares the axial capacity of pile obtained from PDA records with predicted axial capacities obtained using empirical, numerical, and interpretation of static load test method. The empirical method used NSPT data from bore testing that conduct in site, finite element method that uses in this study is Plaxis 8.6. Both of them was compared with PDA test result of axial bearing capacity. There is a difference value of the calculation results of axial pile bearing capacity and foundation settlement. Comparing with PDA, from empirical method has smallest deviation for axial bearing capacity which equal to -268.45 kN with percentage -6.05%, smallest settlement equal to 0,0044 m. Plaxis result shows that distinction between Qult result equal to -11.00 kN with percentage -0.24% and settlement of foundation equal to 0,005 m. From interpretation of static loading test method smallest deviation for Qult which equal to -40,00 kN, with percentage -0,90%, and smallest settlement equal to 0,0055 m. So, from all method the smallest deviation for Qult and PDA result is used finite element method. This is due to many data parameters has been inputted and analyzed in the Plaxis program, so the results of calculation analysis are more detailed and closer to the situation in the research site. Differences in axial bearing capacity can be caused by the test was carried out which depends on the accuracy of operator and parameters that used in the calculations.

Keywords: Axial bearing capacity, empirical method, static load testing method, finite element method, PDA

ИССЛЕДОВАНИЕ НЕСУЩЕЙ СПОСОБНОСТИ СВАЙ НА ОСНОВЕ ЭМПИРИЧЕСКИХ ДАННЫХ, ДИНАМИЧЕСКИХ ИСПЫТАНИЙ И ЧИСЛЕННОГО МОДЕЛИРОВАНИЯ

Тсаана Хойрунисаа, Бамбанг Сетиаван, Юсеп М. Пурвана

Факультет гражданского строительства, Университет Себелас Марет, г. Суракарта, ИНДОНЕЗИЯ

Аннотация: Несущая способность на вдавливание является важным фактором при проектировании фундамента. Он должен нести нагрузку от сооружения без значительных деформаций. Помимо эмпирических и численных методов, несущая способность сваи на вдавливание может быть предсказана с помощью анализатора забивки свай PDA, принцип работы которого основан на оценке параметров волнового уравнения во время испытаний. Прогнозирование несущей способности на вдавливание и ее распределения может быть выполнено путем оценки параметров волнового уравнения при динамическом мониторинге забивки свай. В данной работе сравнивается несущая способность сваи на вдавливание, полученная по данным PDA, с эмпирическими данными, результатами численного моделирования и испытаний статической нагрузкой. Эмпирические данные о несущей способности NSPT были получены по результатам испытаний в скважинах. Численное моделирование выполнено по методу конечных элементов в программном комплексе Plaxis 8.6. Полученные результаты сравнивались с результатами испытаний PDA несущей способности на вдавливание. Выявлено, что результаты расчетов несущей способности свай на вдавливание и осадки фундамента по различным методам оценки различаются. По сравнению с PDA, эмпирический метод имеет наименьшее отклонение, которое составило -268.45 кН или -6.05%. Наименьшая осадка равна 0,0044 м. Результат моделирования в Plaxis показывают, что различие между результатом Qult составило -11.00 кН или -0.24%. Осадка фундамента при этом равна 0,005 м. Для метода статического нагружения наименьшее отклонение Qult было -40,00 кН или -0,90%. А наименьшая

осадка составила 0,0055 м. Таким образом, из всех методов наименьшее отклонение для Qult по сравнению с данными динамических испытаний, выполненных с использованием PDA, имеет метод конечных элементов. Это связано с тем, что использовалось большое число исходных параметров, которые были введены в программе Plaxis. Поэтому результаты расчетного анализа более детальны и приближены к ситуации на объекте исследования. Различия в несущей способности на продавливание могут быть вызваны тем, какие именно испытания проводились. Это зависит от квалификации оператора и параметров, которые используются в расчетах.

Ключевые слова: несущая способность на вдавливание, эмпирический метод, метод статических испытаний, метод конечных элементов, Pile driving analyzer (PDA)

INTRODUCTION

Foundation is the main structure that very important in every building construction, and has function to transmitting load of upper structure to the soil layer below. In some cases, foundations are insufficient to support the structural load, and deep foundations are required [1]. Various type of deep foundations is classified into categorized according to geologic condition, installation method, structural material, ground effect, function, cross-section, loading, isolation, inclination, and other characteristics [2]. Axial pile bearing capacity is a maximum vertical axial load on foundation that can support before it reaches the ultimate capacity. To determine axial pile bearing capacity it can be use empirical and numerical method. The use of different design methods, resulting in various estimates of axial bearing capacity, selection of appropriate and accurate design schemes to minimize errors due to axial bearing capacity predictions are required [3]. Estimation of the axial bearing capacity has an important role in pile design. Part of semi-empirical and numerical methods, the axial bearing capacity of piles can be predicted through static loading tests and dynamic load test [4]. Several studies compared pile bearing capacity of analytical and field test [5], [6], [7].

One of common method used to measure and analyze the dynamic response of piles is PDA. The results show that PDA data can provide the best prediction of axial pile bearing capacity. Subsequent research discussed the pile bearing capacity using PDA and CAPWAP, which is standard practice for testing offshore piles [8]. Testing of piles under axial loads has been carried out on in-situ piles. Simulation has carried out for a single pile with axial load at the top of pile, so it can be evaluate the settlement of the pile [9].

Various analytical, numerical and software approaches using Plaxis 2D software, with design results of more than 30 heaps, for the piles analyzed the largest relative error between theoretical and numerical method in this study was around 14%, these errors can be reduced significantly by modifying the meshing and making it smoother [10]. Analysis in plaxis software use several model parameters such as Mohr-Coulomb, soft soil, hard soil, and many more [11].

The problem of predicting and assessing pile bearing capacity is complex. The most important thing is to determine the method used to predict and evaluate pile bearing capacity based on the level of accuracy and consistency values required [12]. Knowing the characteristics of the axial bearing capacity of concrete piles embedded in soil layer is important before carrying out tests [13].

This study was conducted to compare the axial pile bearing capacity of foundation with several methods. Empirical method formulated of geotechnical expert, numerical method of finite element method (FEM) and interpretation of static load testing method. All of them were compared and validated with PDA test result in research location.

METHODS

This study is located in Cirebon, West Java, Indonesia. The method of studies is divided into

several stages. First stage is the analysis and data processing based on Standard Penetration Test (SPT) using empirical methods and soil parameters through laboratory tests. At this stage it calculates axial pile bearing capacity using empirical formula developed by, Luciano Decourt, Meyerhoff, Briaud et al and Shioi & Fukui. Two problems arise when determining soil qualities through laboratory testing: (1) Difficulties in obtaining an "undisturbed" soil sample, and (2) sample size limitations. Data from in-situ test such as Standard Penetration Test (SPT) indicate a significant amount of soil. The test is relatively simple and data information is easy to obtain during the site investigation. The crossection of soil layers in this study can be shown in the Figure 1.

Second stage is the modeling stage using numerical method. At this stage Finite Emelent Method (FEM) modeling with Plaxis software using Mohr-Coloumb. Soil parameters that used in this program are young's modulus (E.), Poisson ratio (v), unit weight of saturated soil (γsat), unit weight of unsaturated soil (γunsat), Cohesion (c.), friction angle (φ), and dilatation angle (ψ). Result from this modeling is axial bearing capacity, soil settlement, and safety factor.

Third stage is interpretation of static load test method using Mazurkiewicz (1972) and Davisson (1973). The final stage is to compare both analytical, numerical, and static load test method by Pile Driving Analyzer that conducted in this research location.

RESULTS AND DISCUSSION

The soil test data for this study were collected from a project that located in Cirebon, West Java, Indonesia. Prestressed concrete pile type spun pile with diameter 600 mm and 35 m length. Site investigation data includes laboratory tests data, material properties from SPT within 70.45 m depth.

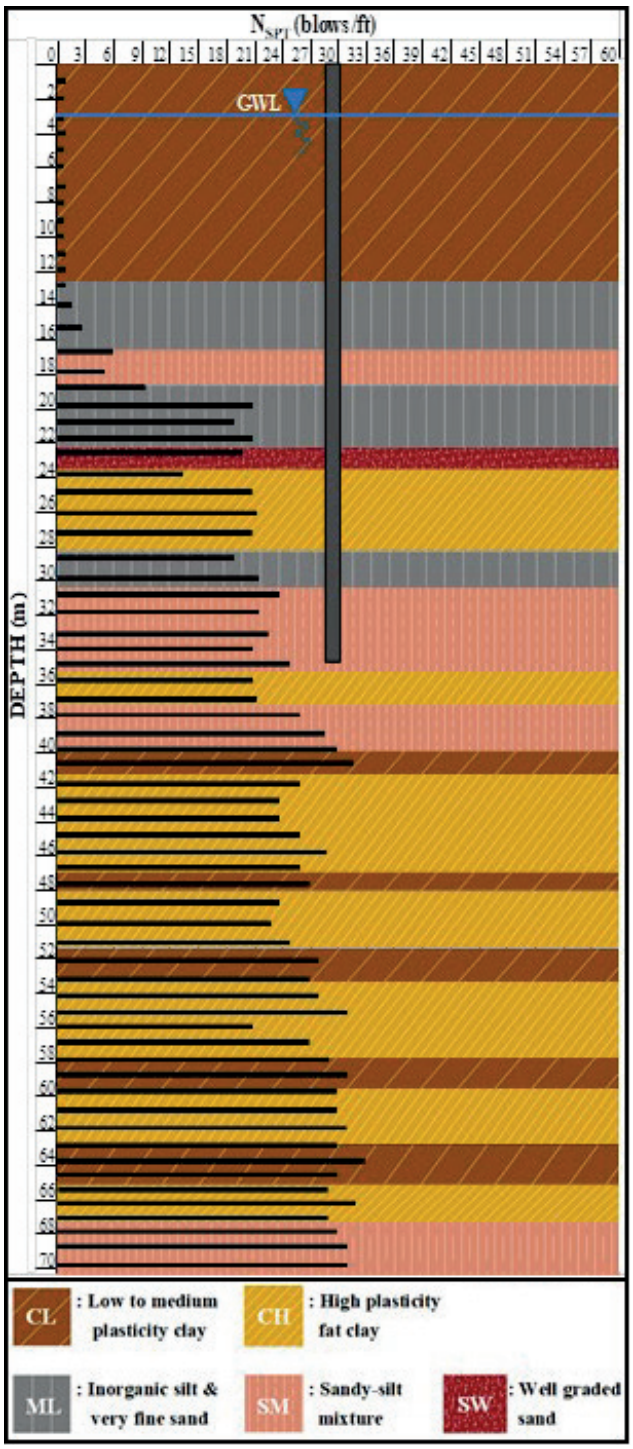


Figure 1. Cross-section profile of soil layer

Empirical Method

Empirical method of Luciano Decourt (1982), Meyerhoff (1956), Briaud et al (1985), and Shioi & Fukui (1982) are utilized in this study can be shown in Table 1 and Figure 2.

Table 1. Axial pile bearing capacity based on empirical method

Empirical Method	Axial Pile Bearing Capacity				Deviation	
	End Bearing	Skin Resistance	Total Axial Capacity	PDA Test	Q_{ult}	Q_{ult}
	Q_p (kN)	Q_s (kN)	Q_{ult} (kN)	RMX (kN)	(kN)	(%)
L. Decourt (1982)	1.696,46	3.653,91	5.350,37	4.440	910,37	20,50
Meyerhoff (1956)	2.375,04	1.796,51	4.171,55		-268,45	-6,05
Briaud et al (1985)	1.722,19	3.151,27	4.873,46		433,46	9,76
Shioi & Fukui (1982)	195,09	1.796,51	1.991,60		-2.448,40	-55,14

The ultimate axial pile bearing capacity (Qult) based on the planning design is 4,500 kN. PDA testing was carried out three times. This because during first PDA test, the axial bearing capacity result had a high difference from the design plan, so a re-test was carried out. From the results of PDA test, the Qult value of 4,440 kN is used as a reference for compare the bearing capacity of empirical and numerical methods. From the result above Luciano Decourt method has Qult equal to 5,350.37 kN, is the highest value compared to other methods, because soil coefficient is used as a multiplier.

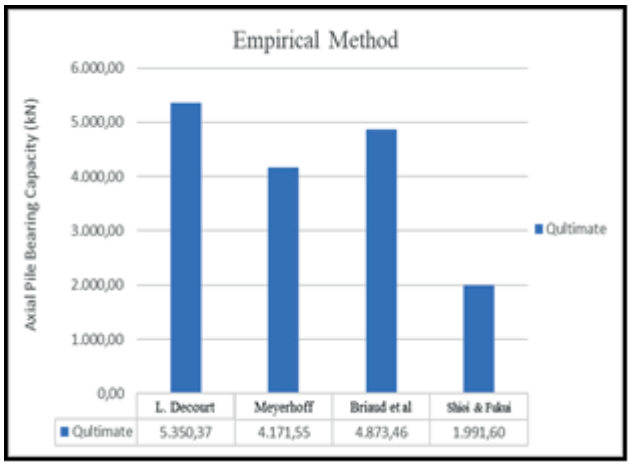


Figure 2. Graph of Axial Pile Bearing Capacity Calculation Based on NSPT Data (Empirical Method)

Compared with PDA test result, based on the calculation analysis of the axial bearing capacity of the empirical method above, the Meyerhoff method has the smallest deviation, with value -268.45 kN and percentage of 6.05%, Briaud et al method has a deviation 433.46 kN with a percentage of 9.76%, followed by the L. Decourt method with a deviation 910.37 kN and a percentage of 20.50%. The biggest deviation is using the Shioi & Fukuni method with a value of -2,298.40 kN and a deviation percentage of -55.14%.

Meyerhoff method is usually used on non-cohesive soils or sandy soils, based on the results of borelog testing of the soil layers at the research study, which are classified as soft soils. The borelog test was carried out to a depth of 70.45 m, the composition ratio of soft soil and sandy soil layers was 68% for soft soil and 32% for sandy soil. The pile foundation used in this study has a length of 35 m. The composition of the layers of soft soil and sandy soil along the foundation is 50% for soft soil and 50% for clay, this affects the analysis of the empirical method used. Pile was embedded in a layer of sandy soil at 35 m depth, so Meyerhof method can be used in this research study, and has the smallest difference compare with other empirical formula validated by Pile Driving Analyzer test result.

Finite Element Method (FEM)

FEM is numerical method that divides a problem into a finite number of elements to represent a problem that actually has an infinite number of elements (continuum). The interactions between these small parts are determined based on the physical phenomena to be resolved. Material of soil that used in Plaxis is Mohr-Coulomb model. Parameter data for this method comes from secondary data and correlation calculations, it can be shown in Table 2.

To calculate Young's Modulus (E.) using Schmermann (1970) formula:

Correlation of sand soil

$E = 766.\ NSPT$ (1)

$E = 2\ qc$ (2)

Correlation of clay soil

Clay soil *normally consolidated* (NC)

$$E = 250\ Cu - 500\ Cu \quad (3)$$

Clay Soil *over consolidated* (OC)

$$E = 750\ Cu - 1000\ Cu \quad (4)$$

Another parameter was found from laboratory testing. Parameter profile of the pile foundation must be included during Plaxis analysis, it can be shown in Table 3.

Table 2. Mohr-Coloumb Parameter of Soil layer

Parameter	Value		Source
	1st Soil Layer (0.00 m – 3.00 m)	4th Soil Layer (13.00 m –17.00 m)	
USCS Chart	CL	ML	Secondary data
Material Model	Mohr-Coulomb	Mohr-Coulomb	-
Material Behavior	Undrained	Drained	-
Unit weight of unsaturated soil (γ_{unsat})	6,68 kN/m^3	9,06 kN/m^3	Calculation
Unit weight of saturated soil (γ_{sat})	14,90 kN/m^3	15,00 kN/m^3	Secondary data
Young's Modulus (E)	3125 kN/m^2	2298 kN/m^2	Correlation and calculation
Poison Ratio (v)	0,2	0,3	Secondary data
Cohesion (c)	6,25 kN/m^2	0,35 kN/m^2	Secondary data
Friction ratio (φ)	18,87°	21,71°	Secondary data
Dilatation angle (ψ)	0°	0°	

Table 3. Pile foundation specification

Parameter	DP6	Unit
Pile Test No	**DP6-7**	
Foundation Type	Spun PC-Pile	mm
Diameter	600	mm
Thickness	100	mm
Length	35	m
Area	0,28	m^2
Modulus Elasticity	33.892.182	kN/ m^2
Fc' of Pile	52	Mpa
Allowable stress	15,49	Mpa
Allowable compressive stress	38	Mpa
E	33892182	kN
I	5,2 x 10^{-4}	m^4
EI	17457,46	kNm^2/m
EA	9582789	kNm^2/m
W	3,768	kN/m
V	0.2	

Based on the results of the Plaxis analysis, the allowable pile bearing capacity (Qall), settlement, safety factor (MSF), load-deformation curves are obtained. The results of the analysis can be seen in Figure 3.

Based on the results of the plaxis analysis, the Qall value equal to 3.720 kN and the MSF equal to 1.1906. So to get the value of the axial bearing capacity (Qult) using the formula :

$$Qu = Qall \times \Sigma MSF$$
$$= 3.720 \times 1.1906$$
$$= 4.429\ kN.$$

Compared with the axial bearing capacity (Qult) from the PDA test results of 4,440 kN, the Qult deviation is very small, equal to -11.00 kN with a percentage of -0.24%.

By using plaxis, deformation occurs on the soil layer can be determined. Figures 4 and 5 shows the typical deformation that occurs in soil due to loading on continuous foundation. On the left and right side of the foundation there is heaving, i.e, ballooning. This is due to the soil under the foundation pushed in all directions, which is eventually it will also push the ground above it.

Pile foundation with a diameter of 0.6 m and a length of 35 m, deformation of 0.005 m will occur in the soil layer around pile. Effective stress from plaxis can be shown in Figure 6.

Plaxis analysis can be used as a modeling pile load test at the study site. The relationship curve between the total multiplier load (Sum-Mload) and settlement can be seen in Figure 7. Based on the curve, the ultimate Sum-Mload is 66.419.

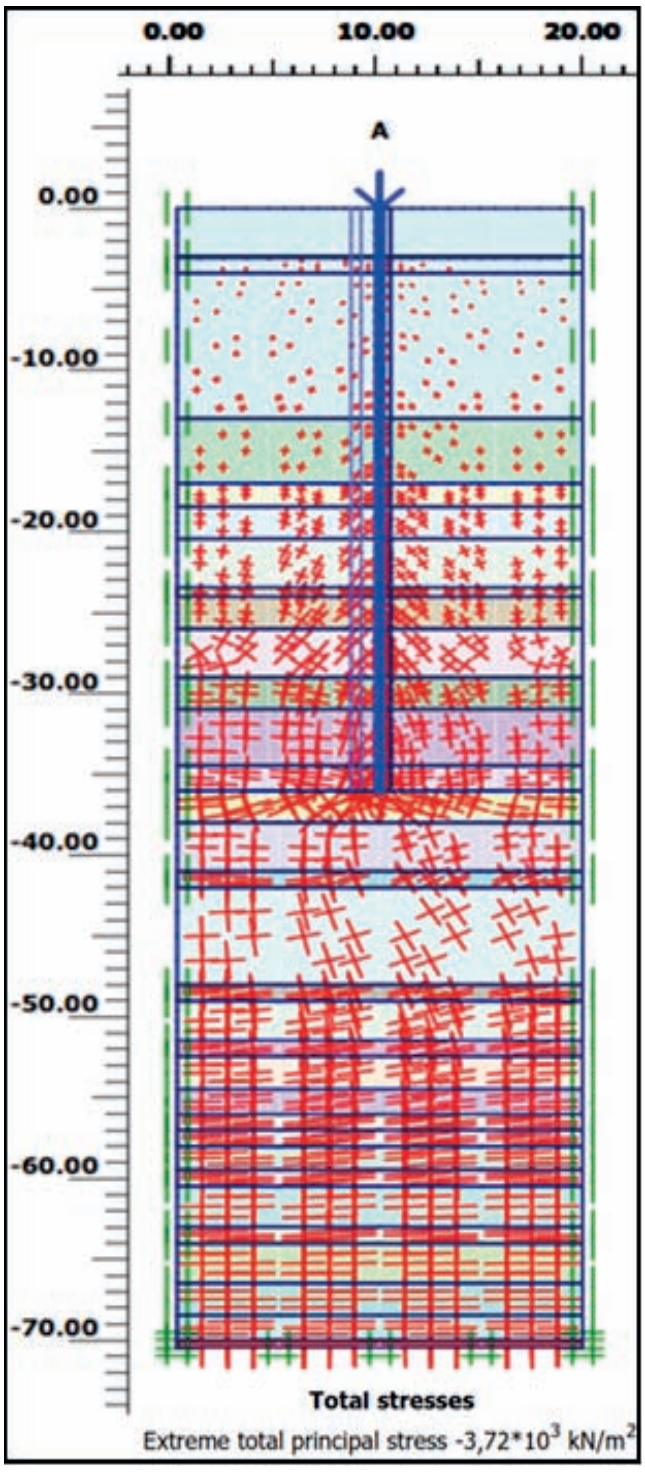


Figure 3. Allowable pile bearing capacity (Qall)

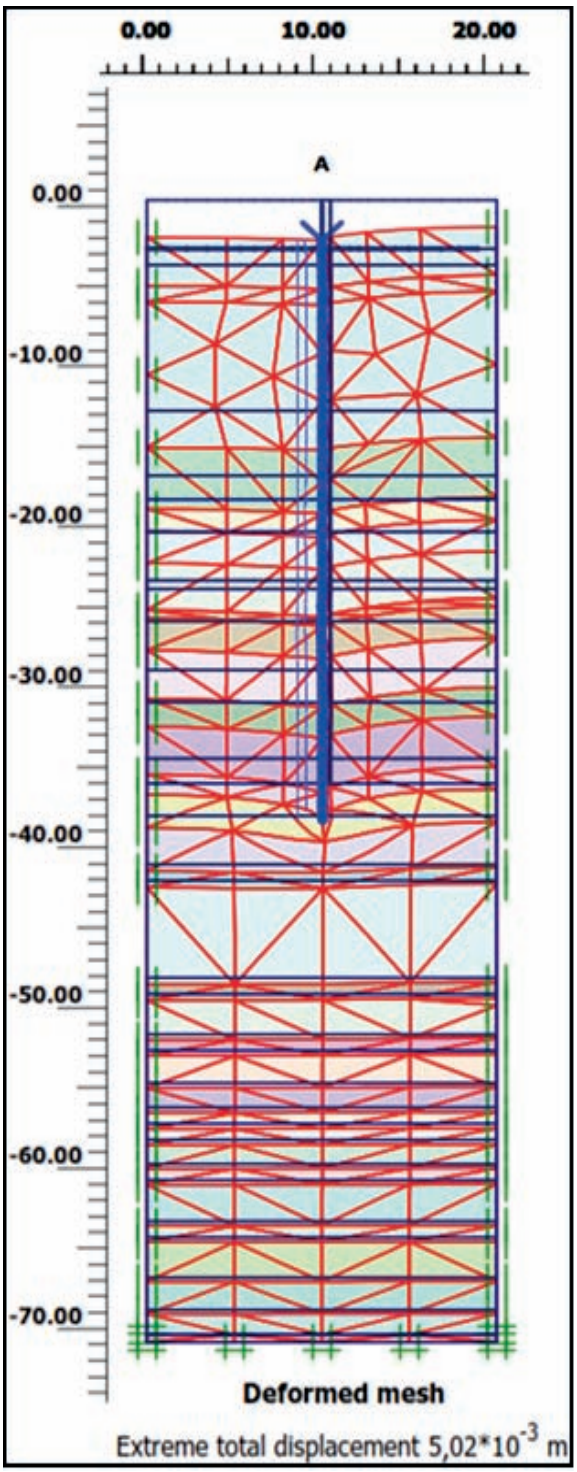


Figure 4. Soil deformation due to pile foundation loads

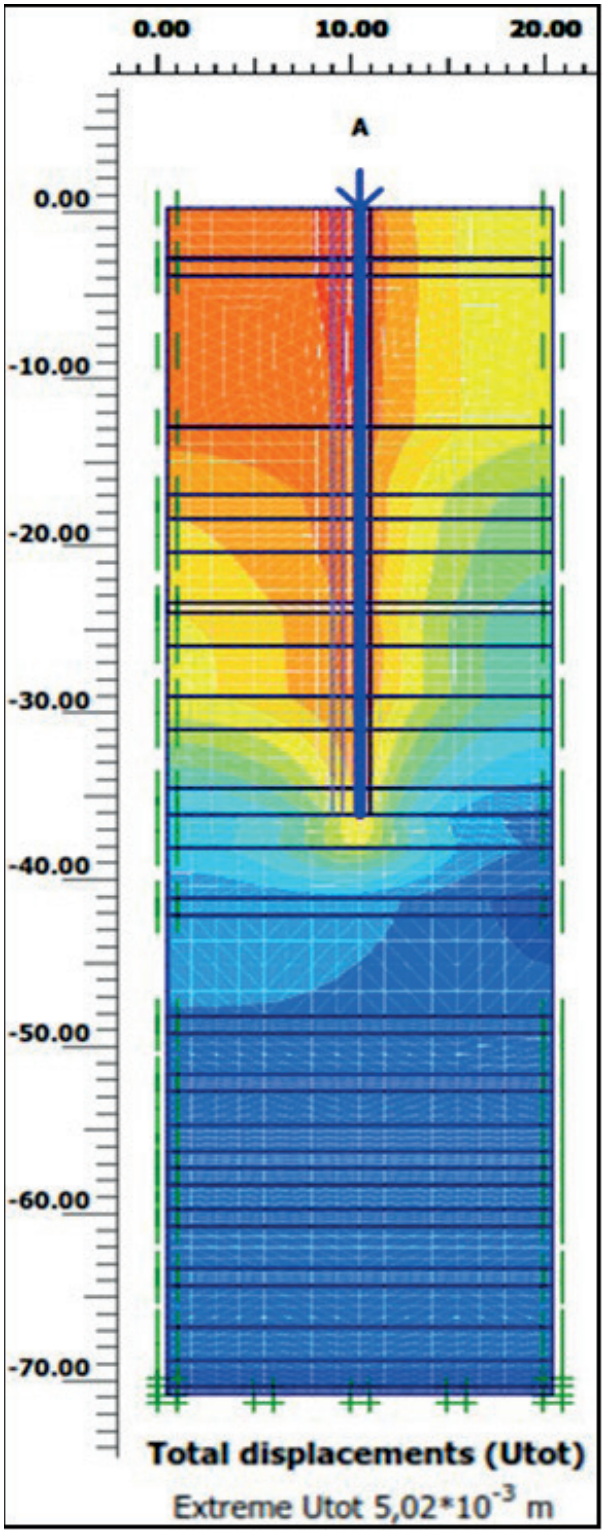


Figure 5. Soil deformation

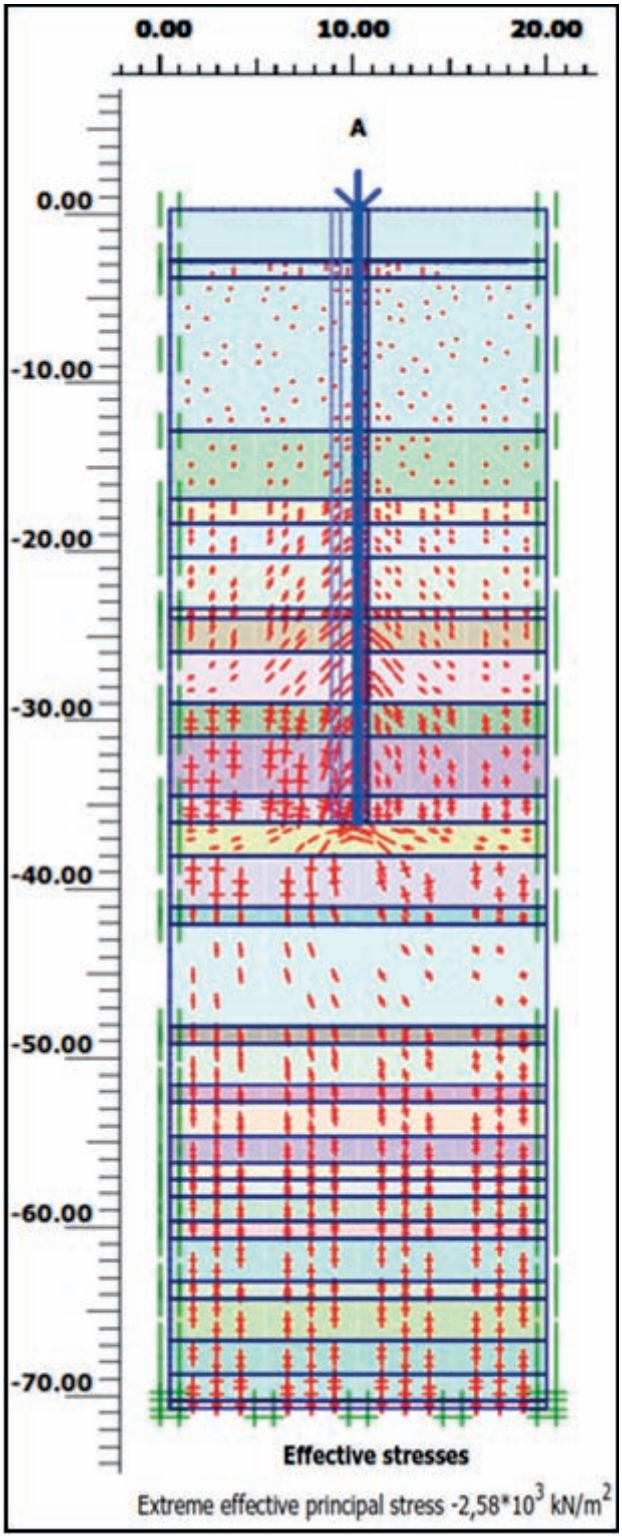


Figure 6. Effective stress from Plaxis analysis

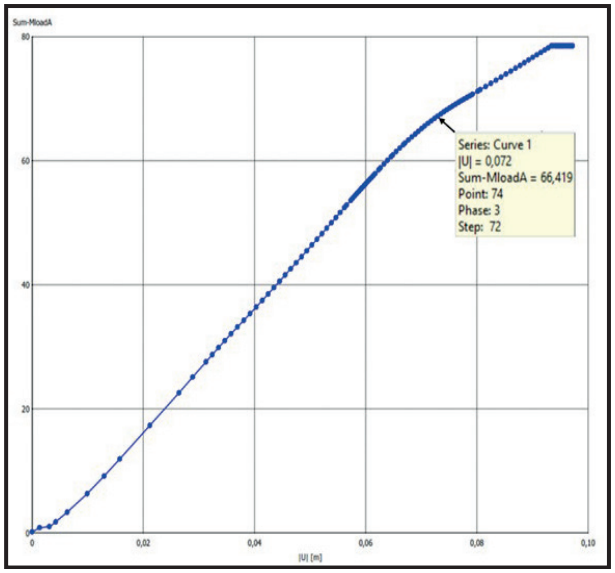


Figure 7. Curve of load-settlement of soil

Static Load Test Interpretation Method

Interpretation of loading test data using the Mazurkiewicz (1972) and Davisson (1973) can be shown in Figures 8 and 9.

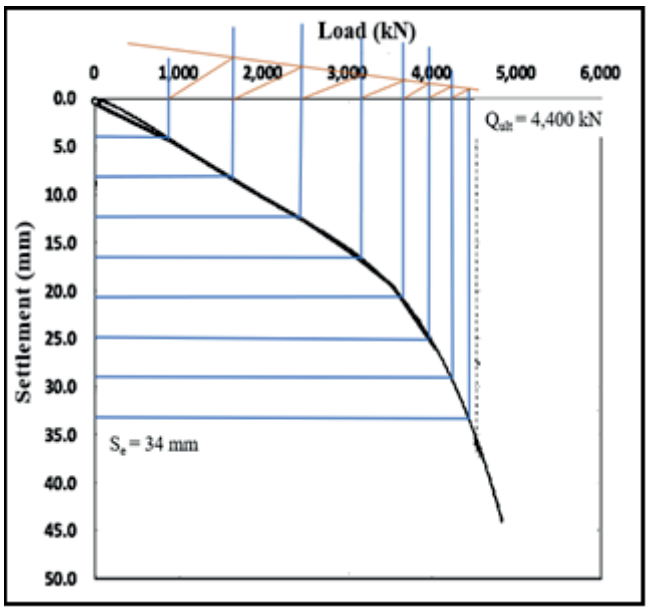


Figure 8. Load and settlement curve with the interpretation of Mazurkiewicz method (1972)

Result from Mazurkiewicz method for piles with a diameter of 0.6 m with a concrete quality (f'c) of 52 MPa after plotting the relationship curve between load and settlement of the pile load test obtains an ultimate load value of 4,400 kN with a decrease of 0.034 m.

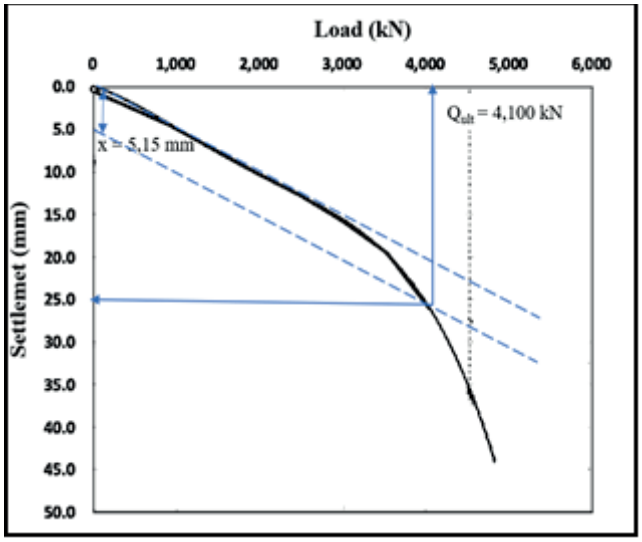


Figure 9. Load and settlement curve with the interpretation of Davisson. method (1973)

Result from Davisson method, obtains an elastic settlement value (Se) of 0.00548 m. To determine the ultimate load, the value of X based on the pile diameter is 5.15 mm. After plotting the relationship curve between load and settlement, an ultimate load of 4,100 kN is obtained with a settlement of 0.025 m.

Pile Foundation Settlement

Pile foundation settlement based on empirical, and numerical method can be shown in Table 4 and Figure 10.

Table 4. Soil Settlement of Pile Foundation

Method		Settlement (m)
Empirical	L. Decourt (1982)	0,0129
	Meyerhoff (1956)	0,0121
	Briaud et al (1985)	0,0121
	Shioi & Fukui (1982)	0,0044
FEM	Mohr-Coulomb Parameter	0,0050
Static load test	Mazurkiewicz (1972)	0,0340
	Davisson (1973)	0,0055

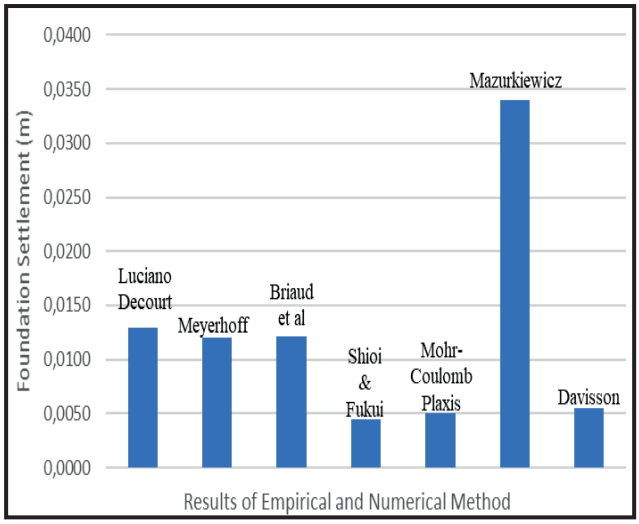


Figure 10. Pile foundation settlement graph uses three interpretation methods

Allowable foundation settlement (Sall) is 10% of the diameter of the foundation used, then Sall equal to 0.06 m. Based on pile foundation settlement calculation using empirical methods, Shioi & Fukui (1982) has the smallest settlement with value 0.0044 m, while the largest settlement of pile foundations using static load test interpretation method of Mazurkiewicz (1972) with a value 0.034 m. The results pile foundation settlement analysis by Shioi & Fukui method, this due to end bearing capacity of the soil under tip point of pile foundation (Qp) and skin friction bearing capacity from shear force or adhesion between pile and soil (Qs) in this method has a small result, because it affects the results of foundation settlement. The greater the value of Qp and Qs directly proportional to pile foundation settlement.

Both empirical and numerical methods show that pile foundation settlement is declared safe to use because the Stotal < Sall. Based on the finite element method using plaxis software with the parameters of the Mohr-Coulomb model, the pile foundation settlement is 0.005 m. The results of this decrease are still within safe limits because Stotal < Sall.

Comparation of Axial Pile Bearing Capacity

Comparation between axial pile bearing capacity of empirical and numerical method with PDA test result can be shown in Table 5 and Figure 11.

Table 5. Comparation of Axial Pile Bearing Capacity Using three interpretation methods and PDA testing

Methods		Q_{ult} (kN)	PDA Test RMX (kN)	Q_{ult} Deviation	
				(kN)	(%)
Empirical	L. Decourt (1982)	5.350,37	4.440,00	910,37	20,50
	Meyerhoff (1956)	4.171,55		-268,45	-6,05
	Briaud et al (1985)	4.873,46		433,46	9,76
	Shioi & Fukui (1982)	1.991,60		-2.448,40	-55,14
Finite Element	Mohr-Coulomb Parameter	4.429,00		-11,00	-0,25
Static Load Test	Mazurkiewicz (1972)	4.400,00		-40,00	-0,90
	Davisson M.T. (1973)	4.100,00		-340,00	-7,66

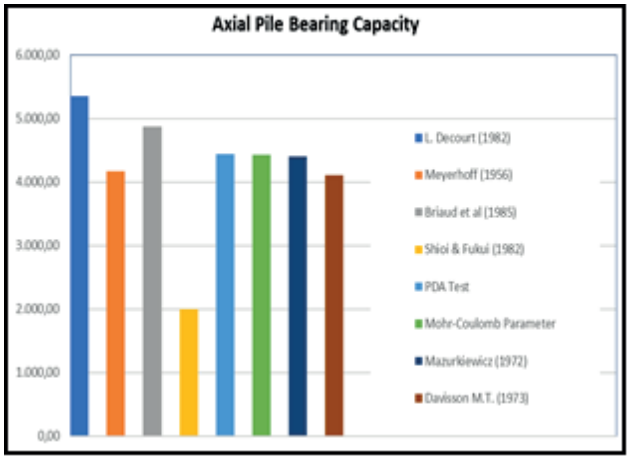


Figure 11. Graph of axial pile bearing capacity

Axial pile bearing capacity (Qult) based on empirical and numerical method, compared with PDA test results shows that, the smallest difference is using the finite element method with Mohr-Coulomb parameter model. The resulting Qult difference is -11.00 kN with percentage of -0.25%. This is due to many data parameters has been inputted and analyzed in the Plaxis program, so the results of calculation analysis are more detailed and closer to the situation in the research site.

The next closest Qult was generated using the static load testing interpretation method by Mazurkiewicz (1972) with deviation of Qult equal to -40.00 kN and a percentage -0.90%. Next closest Qult was generated through empirical methods by Meyerhoff (1956)

deviation of Qult equal to -268.45 kN and percentage of -6.05%. Level of results the comparison of Qult with the PDA test is the Davisson. (1973) method with a Qult difference of -340.00 kN and a percentage of -7.66%, Briaud et al. (1985) method has deviation of Qult equal to of 433.46 kN and a percentage of 9.76%, the L. Decourt method. (1982) with a Qult difference 910.37 kN and percentage of 20.50%, and the largest difference was obtained by calculating the Shioi & Fukui method. (1982) with deviation of Qult value -2,448.40 kN and a percentage of -55.14%.

CONCLUSION

Based on the results of comparison between axial pile bearing capacity on soil with PDA test result, it can be concluded that:

1. The result of finite element analysis shows that the ultimate axial pile bearing capacity is in good agreement with the axial capacities obtained using pile driving analyzer (PDA) test result.
2. From the results of empirical and numerical methods, it's observed that axial pile bearing capacity obtained by those method is quite variable hence they must be validated with other reliable methods such as PDA and static load test.
3. Differences in axial bearing capacity can be caused by the test was carried out which depends on the accuracy of operator and parameters that used in the calculations.

REFERENCES

1. **M. Budhu,** Soil Mechanics and Foundations Engineering, 3rd ed. Hoboken: John Wiley & Sons, Inc, 2011.
2. **W.F. Chen and L. Duan,** Bridge Engineering Handbook Substructure Design, 2nd Editio. CRC Press, 1999.
3. **G.H. Sara, C.J. Reza, and E. Abolfazl**, "Reliability based assessment of axial pile bearing capacity: static analysis, SPT and CPT-based methods", Georisk: Assessment and Management of Risk for Engineered Systems and Geohazards, vol. 14, issue 3, 2020.
4. **E. Momeni, H. Maizir, N. Gofar, and R. Nazir**, "Comparative study on prediction of axial bearing capacity of driven piles in granular materials", Jurnal Teknologi (Sciences and Engineering), 61(3) 15-20, 2013.
5. **R.A. Mangushev,** "Analytical and Field Evaluation Methods of The Bearing Capacity of Deep Piles and Barrettes in Soft Soil at St. Peterburg," Architecture and Engineering, vol. 1, no. 1, pp. 54–59, 2016, doi: 10.23968/2500-0055-2016-1-1-54-59.
6. **S. Henrina, E. Bahsan, and T. Ilyas,** "Comparison of direct SPT method for calculating axial capacity of piles in Jakarta Area Comparison of direct SPT method for calculating axial capacity of piles in Jakarta Area," 2019, doi: 10.1088/1757-899X/673/1/012027.
7. **E. Anamali, N. Shkodrani, and L. Dhimitri**, "Axial Load Capacity of Cast in Place Piles from SPT and CPTU Data," no. May, pp. 100–108, 2014.
8. **R. Gohil, and C. Parthasarathy**, "Intelligent Assessment of Axial Capacity of Pipe Piles Using High Strain Dynamic Pile Load Tests in Offshore Environment", Lecture Notes in in Civil Engineering, 2023, 296 271-287.
9. **S. Thounaojam, and ParbinSultana,** "Prediction of bearing capacity of bored cast- in situ pile", IOSR Journal of Mechanical and Civil Engineering (IOSR-JMCE), vol.1, no.6, 2015.
10. **V. Ghiasi, and S. Eskandari**, "Comparing a single pile's axial bearing capacity using numerical modeling and analytical techniques", Results in Engineering, 17, March, 100893, 2023.

11. **A. Al-Dawoodi, F. Rahil, and M. Waheed,** "Numerical Simulation of Shallow Foundation Behavior Rested on Sandy Soil", IOP Conference Series: Earth and Environmental Science, 2021, 856(1).
12. **H. Maizir, and R. Suryanita**, "Evaluation of axial pile bearing capacity based on pile driving analyzer (PDA) test using Neural Network", IOP Conference Series: Earth and Environmental Science, 2018, 106(1).
13. **W. Deng, X. Ding, and Y. Peng,** "A study of vertical bearing capacity of expansive concrete pile in coral sand foundation", Yantu Lixue/Rock and Soil Mechanics, 41(8), 2814-2820, 2020.

СПИСОК ЛИТЕРАТУРЫ

1. **M. Budhu,** Soil Mechanics and Foundations Engineering, 3rd ed. Hoboken: John Wiley & Sons, Inc, 2011.
2. **W.F. Chen and L. Duan,** Bridge Engineering Handbook Substructure Design, 2nd Editio. CRC Press, 1999.
3. **G.H. Sara, C.J. Reza, and E. Abolfazl**, "Reliability based assessment of axial pile bearing capacity: static analysis, SPT and CPT-based methods", Georisk: Assessment and Management of Risk for Engineered Systems and Geohazards, vol. 14, issue 3, 2020.
4. **E. Momeni, H. Maizir, N. Gofar, and R. Nazir**, "Comparative study on prediction of axial bearing capacity of driven piles in granular materials", Jurnal Teknologi (Sciences and Engineering), 61(3) 15-20, 2013.
5. **R.A. Mangushev,** "Analytical and Field Evaluation Methods of The Bearing Capacity of Deep Piles and Barrettes in Soft Soil at St. Peterburg," Architecture and Engineering, vol. 1, no. 1, pp. 54–59, 2016, doi: 10.23968/2500-0055-2016-1-1-54-59.
6. **S. Henrina, E. Bahsan, and T. Ilyas,** "Comparison of direct SPT method for calculating axial capacity of piles in Jakarta Area Comparison of direct SPT method for calculating axial capacity of piles in Jakarta Area," 2019, doi: 10.1088/1757-899X/673/1/012027.
7. **E. Anamali, N. Shkodrani, and L. Dhimitri**, "Axial Load Capacity of Cast in Place Piles from SPT and CPTU Data," no. May, pp. 100–108, 2014.
8. **R. Gohil, and C. Parthasarathy**, "Intelligent Assessment of Axial Capacity of Pipe Piles Using High Strain Dynamic Pile Load Tests in Offshore Environment", Lecture Notes in in Civil Engineering, 2023, 296 271-287.
9. **S. Thounaojam, and ParbinSultana,** "Prediction of bearing capacity of bored cast- in situ pile", IOSR Journal of Mechanical and Civil Engineering (IOSR-JMCE), vol.1, no.6, 2015.
10. **V. Ghiasi, and S. Eskandari**, "Comparing a single pile's axial bearing capacity using numerical modeling and analytical techniques", Results in Engineering, 17, March, 100893, 2023.
11. **A. Al-Dawoodi, F. Rahil, and M. Waheed,** "Numerical Simulation of Shallow Foundation Behavior Rested on Sandy Soil", IOP Conference Series: Earth and Environmental Science, 2021, 856(1).
12. **H. Maizir, and R. Suryanita**, "Evaluation of axial pile bearing capacity based on pile driving analyzer (PDA) test using Neural Network", IOP Conference Series: Earth and Environmental Science, 2018, 106(1).
13. **W. Deng, X. Ding, and Y. Peng,** "A study of vertical bearing capacity of expansive concrete pile in coral sand foundation", Yantu Lixue/Rock and Soil Mechanics, 41(8), 2814-2820, 2020.

Tsaana Khoirunisaa, Student of Civil Engineering Department, Sebelas Maret University, Surakarta, Indonesia; email: tsaanakh@student.uns.ac.id

Bambang Setiawan, Lecturer of Civil Engineering Department, Sebelas Maret University, Surakarta, Indonesia; email: bambangsetiawan@staff.uns.ac.id

Yusep M. Purwana, Lecturer of Civil Engineering Department, Sebelas Maret University, Surakarta, Indonesia; email: ymuslih@staff.uns.ac.id

Тсаана Хойрунисаа, Студент факультета гражданского строительства, Университет Себелас Марет, город Суракарта, Индонезия, Indonesia; email: tsaanakh@student.uns.ac.id

Бамбанг Сетиаван, Преподаватель факультета гражданского строительства, Университет Себелас Марет, город Суракарта, Индонезия; email: bambangsetiawan@staff.uns.ac.id

Юсеп М. Пурвана, Преподаватель факультета гражданского строительства, Университет Себелас Марет, город Суракарта, Индонезия; email: ymuslih@staff.uns.ac.id

DOI:10.22337/2587-9618-2023-19-4-208-221

STRENGTH ANALYSIS OF FORMWORK USING FALSEWORK FLYING SYSTEM ON SLAB-ON PILE STRUCTURE

Fendi Hary Yanto
Disaster Research Center, Sebelas Maret University, Jebres, Surakarta, INDONESIA
Faculty of Vocational School Sebelas Maret University, Surakarta, INDONESIA

Abstract: The Semarang-Demak Toll Road was planned with detailed procedures to address disorganized road networks, increased traffic volumes, congestion, land subsidence, and tidal floods. It has toll entrances in Semarang, Genuk, and Sayung sub-districts and ends in Demak City. Its purpose is to minimize traffic jams, provide access to tourist cities, and serve as a tidal barrier sea embankment. The formwork support system's proper design is crucial to ensure the safe construction of the main structure. A unique disk lock and steel tubular scaffold are utilized for a slab-on-pile structure employing a flying falsework system. This approach results in a structurally sound and secure construction that is not susceptible to twisting, providing quick erection and disassembly, significantly improving construction efficiency. The system was employed in a portion of the Semarang-Demak toll road project, and its efficacy was evaluated using finite element analysis software. The software provides security and convenience in analyzing structures, paying attention to the nominal strength of each steel profile and the internal forces at work. All components are safe as their actual deflection falls within the maximum limit.

Keywords: finite element, analysis, formwork

ИССЛЕДОВАНИЕ ПРОЧНОСТИ ОПАЛУБКИ С ПРИМЕНЕНИЕМ ПОДВЕСНОЙ СИСТЕМЫ ДЛЯ ПЛИТНО-СВАЙНОЙ КОНСТРУКЦИИ

Фенди Гарри Янто
Центр исследования катастроф, Университет Себелас Марет, Джебрес, Суракарта, Индонезия

Аннотация: Платная дорога Семаранг – Демак была запроектирована с учетом подробных процедур, имея целью решение проблем хаотичной дорожной сети, увеличения интенсивности движения, дорожных заторов, просадок грунта и приливных водных потоков. Он имеет платные въезды в подрайоны Семаранг, Генук и Саюнг и заканчивается в городе Демак. Его цель — минимизировать дорожные пробки, обеспечить доступ к туристическим городам и служить приливно-отливным барьером для морской набережной. Правильная конструкция системы опирания опалубки имеет решающее значение для обеспечения безопасного строительства основной конструкции. Для конструкции «плита-на-сваях» с использованием системы подвесных опалубок используются уникальный дисковый замок и стальные трубчатые леса. Такой подход позволяет получить конструктивно прочную и надежную систему, не подверженную скручиванию, обеспечивающую быстрый монтаж и демонтаж, значительно повышая эффективность строительства. Система использовалась в рамках проекта платной дороги Семаранг – Демак, ее эффективность оценивалась с помощью программного обеспечения для анализа методом конечных элементов. Программное обеспечение обеспечивает безопасность и удобство анализа конструкций с учетом номинальной прочности каждого стального профиля и действующих внутренних сил. Все компоненты безопасны, поскольку их фактическое отклонение находится в пределах максимального предела.

Ключевые слова: конечный элемент, анализ, опалубка

INTRODUCTION

The development of toll roads in Indonesia has experienced significant progress and quality improvement [1]. The construction of toll roads itself is a form of effort by the government to help the Indonesian people carry out activities that require the mobilization of goods or

services, in economic or economic terms, well and short.

Semarang is the capital of Central Java, with high economic growth. This growth can be seen in new industrial buildings, residential areas, and the expansion of city areas. This development also results in problems such as disorganized road networks and increasing traffic volumes, which cause congestion. Changes in land use result in the absorption area being reduced, causing land subsidence and tidal floods [2].

It was planned to build a toll road under detailed and thorough planning procedures, namely the Semarang-Demak Toll Road, which is integrated with the Semarang City Sea Embankment. With this plan, it is hoped to overcome the congestion problem due to the increase in vehicle volume on the Semarang-Demak highway and the sea embankment, which is expected to overcome tidal floods in the Semarang coastal area [3]. The Semarang-Demak Toll Road Project, which stretches from West to East, is part of the Toll Road system connecting the city of Semarang and the city of Demak. This toll road has a length of 27 km, which is divided into two packages. Package 1 is planned to start from Semarang to Sayung, which has a length of 10.69 km. Package 2 is planned to start from Sayung to Demak, which has a length of 16.31 km. The toll entrance is located in the Semarang, Genuk, and Sayung sub-districts, which end in Demak City [4].

The function of the Semarang-Demak toll road is to minimize traffic jams on the Semarang-Demak-Surabaya north coast route and also to get to tourist cities in Demak, namely the Kadilangu/Sunan Kalijaga Tomb and the Great Mosque of Demak, as well as to overcome existing tidal floods along the north coast as a tidal barrier sea embankment [5].

PROJECT CONDITIONS

The condition in the area Project Development Road Toll Semarang Demak STA 10+394 up to STA 27+000, Which length is around 16.31 km, dominated by rice fields and swamps. Land base from project This Also has characteristics that are very soft to a depth of about 30 m below the existing surface. Due to the depth of the soil, the heap's limitation is from the H-Critical factor. An Embankment with PVD Preloading soil improvement treatment cannot accommodate a finish grade that is too high. Thus, a Slab-on Pile structure is needed to meet the need for road Finish Grade [6].

A slab on a pile is a slab structure that stretches between piles. This structure is suitable for roads with high Finish Grade designs and cannot accommodated by heap land customary. Structure This consists of Pile, Pile Heads, and Decks Slabs.

The following is a typical slab-on-pile design and work map:

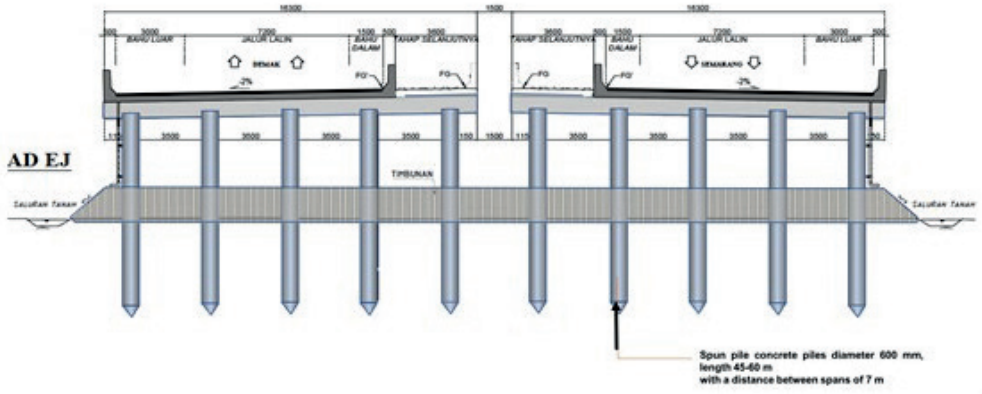


Figure 1. Slab On Pile Structure

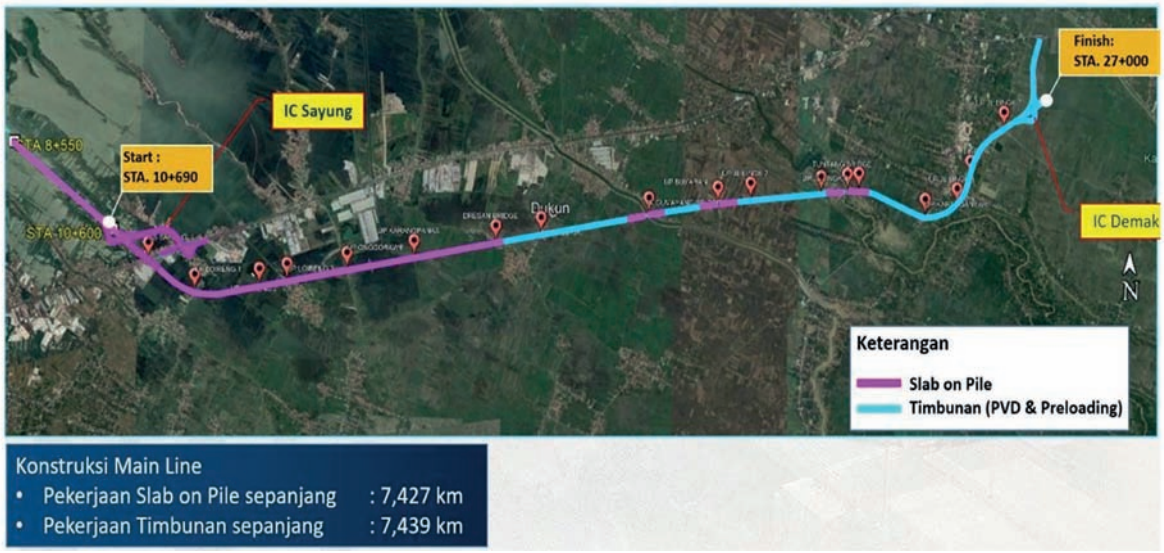


Figure 2. Scope of work for Slab On Pile

FLYING FALSEWORK SYSTEM FORMWORK

Shoring System (Scaffolding)

In making a building element using reinforced concrete as the primary material, a mold is needed so that the reinforced concrete takes the same shape desired element. The mold in question is formwork [7]. Slabs on roads, toll roads, or bridges usually use formwork supported by scaffolding because this work is done at a height. Scaffolding will withhold heavy Alone from formwork, And concrete bony ones that will cast.

The shoring system is a slab formwork system that uses a series of scaffolding, which is used to support the deck slab formwork [8] when casting concrete. The scaffolding needed to support the formwork is usually quite a lot. Apart from that, the support of this scaffolding is the subgrade.

Flying Falsework System

Based on geotechnical investigations in the Semarang-Demak 2 STA 10+690 – 27+000. The soil conditions are in the dominant line of clay soil, so the soil's carrying capacity is relatively low. In making formwork supported by scaffolding, it is necessary to prepare firm scaffolding ground to accommodate the load from the formwork and concrete, which will set a land base [9]. It needs time A relatively long. Apart from that, much scaffolding material is needed to make formwork matter. It usually Can overcome with processing slab per segment, so there is work on dismantling and re-installing scaffolding and formwork. However, the problem is that disassembly and installation take a long time. Therefore PT. PP made an innovation, namely Flying Falsework (Formwork Flying).

Flying Falsework is formwork for slab casting. This formwork uses steel material, which is arranged in such a way. This formwork hangs between the pile heads. Load from casting and weight from formwork will detained by the pile head. So that place Which needed will less And need setup land base For tool heavy Which Also.

The following is a 3D design of formwork [10] with a flying falsework system :

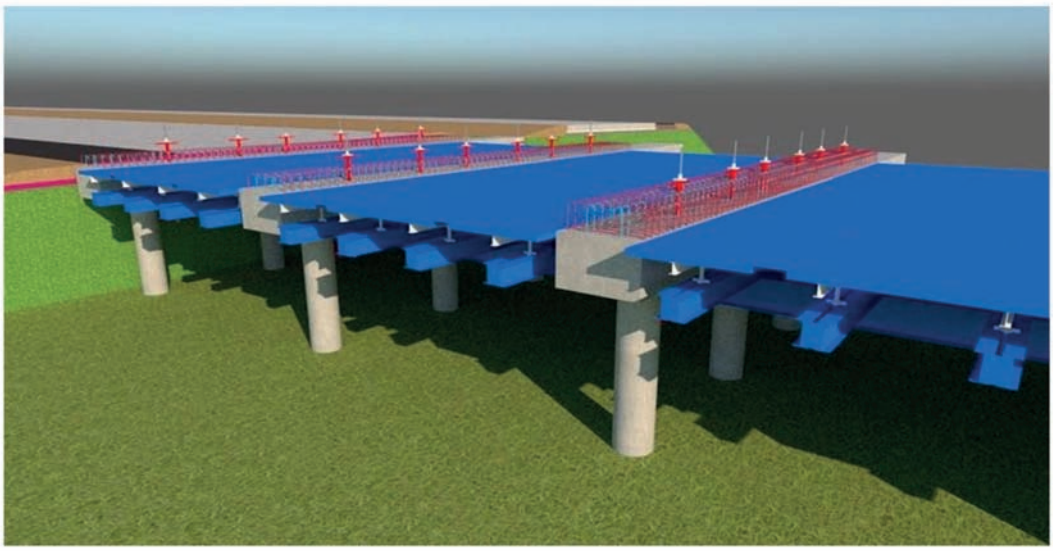


Figure 3. Flying Falsework 3D Rendering

Advantages of Flying System Formwork Falsework

In making a slab, scaffolding is needed to support the formwork from the slab (shoring method), which rests on the subgrade. The subgrade soil in constructing the Semarang Demak toll road has characteristics that are not strong enough to be used as a footing. Therefore, slab formwork using a flying falsework system is used. The following are the advantages of the flying falsework formwork system in terms of cost, quality, and time [11].

Flying Falsework Formwork System has advantages in terms of cost, namely that it is expensive at the start but cheap during implementation [12]. Due to high costs, elicitation material steel For structure flying falsework. However, because the structure slab on the pile Is very long, so far, 9.56 km, the use of costs will be more efficient when compared to using scaffolding.

The use of the shoring method requires a firm base soil. In case subsidence occurs, land consequence burden from implementation work deck slabs, so results from the deck slab will be deflection. So the quality provided could be better [13].

Concrete deck slabs on flying falsework structures will have minimal deflection if using a flying falsework system because the support is directly dependent on the pile head. Therefore, the work will be more precise with maximum results.

Using flying falsework formwork has the advantage that the formwork series can reach 3-5 spans on a slab or pile. Compared to the shoring method, which can only have a maximum of one formwork span due to the large amount of scaffolding required for one span [14]. So, the time used for slab casting will be faster than the shoring method.

The proper design of the formwork support system is paramount to ensure the safe construction of the main structure. A unique disk lock and steel tubular scaffold are utilized for a slab-on-pile structure utilizing a flying falsework system to establish a stable connection between members in multiple directions. This approach results in a structurally sound and secure construction that is not susceptible to twisting. Furthermore, the formwork support system provides quick erection and disassembly, significantly improving construction efficiency. Given these benefits, this system is widely employed in formwork support. The formwork support system was leveraged in a portion of the Semarang-Demak toll road project, and its efficacy was evaluated using finite element analysis [15] software SAP2000.

MATERIAL & MODEL

Material

The materials used for flying falsework work are as follows:
Steel Grade A36
Material Properties of Steel Grade A 36 are as follows:
E = 200000 MPa
$F\,y$ = 240 MPa
$F\,u$ = 400 MPa
The steel used for flying falsework formwork has the following dimensions:
a. WF 300.150.6,5.9 Double
The WF 300.150.6,5.9 Double steel profile is used as a support that depends on the PT Bar.



Figure 4. WF 300.150.6,5.9 Double

b. WF 150.75.5.7
WF 150.75.5.7 steel profile directly supports 6mm plates for slab formwork.



Figure 5. WF 150.75.5.7 (before installation)



Figure 6. WF 150.75.5.7 (After installation)

c. HB 350.350.12.19
HB 350.350.12.19 Steel Profile is used as a longitudinal connector placed on a WF 300.150.6,5.9 Double support.



Figure 7. HB 350.350.12.19

d. 6 mm plate and UNP 80
Steel plates are used to support the slab to be cast directly, with a plate steel thickness of 6mm And supported with a configuration.
UNP 80 steel to increase the stiffness of the steel plate. This steel plate has an area per segment of 3.5 m x 1.5 m.



Figure 8. 6mm Steel Plate

e. Jack U Head

The U Head Jack is used to adjust the slope and elevation of the steel plate. So, the slab shape can be adjusted using the U-Head Jack.



Figure 9. U Head Jack 50mm

PT BAR Grade 830/1030

Material Properties of PT BAR Grade 830/1030 are as follows:

E = 200000 MPa

$F\,y$ = 830 MPa

$F\,u$ = 1030 MPa

PT Bar D32 is used as a support hung on the pile head. This jack is inserted into the pile head via a sparing pipe and then locked on the pile head.



Figure 10. PT Bar D32



Figure 11. Sparing Pipe



Figure 12. PT Bar Washing at Pile Head

Modeling Material SAP 2000 Software

The following is the material modeling of the FalseWork Flying Formwork:

a. Steel Grade A36

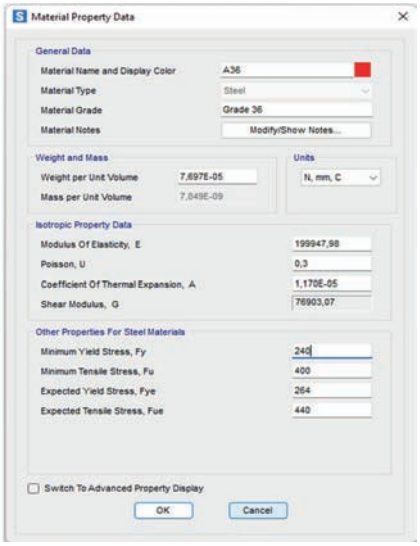


Figure 13 A36 Steel Modeling

b. PT BAR

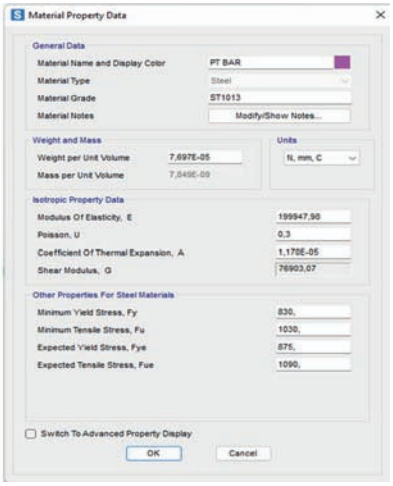


Figure 14. PT BAR 830/1030 Steel Modeling

Section Modeling Properties

The following is the modeling of the steel structure used in the formwork:

a. HB 350.350.12.19



Figure 15. Modeling HB 350.350.12.19

b. HB 350.350.12.19 Double

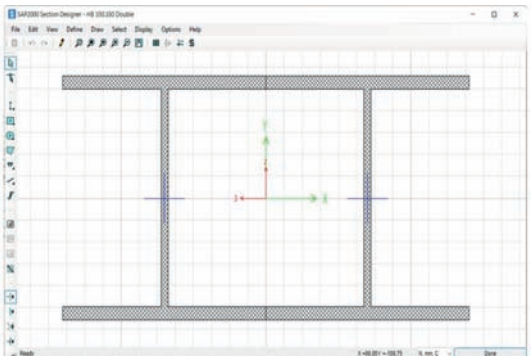


Figure 16. Modeling HB 350.350.12.19 Double

c. WF 300.150.6,5.9 Double

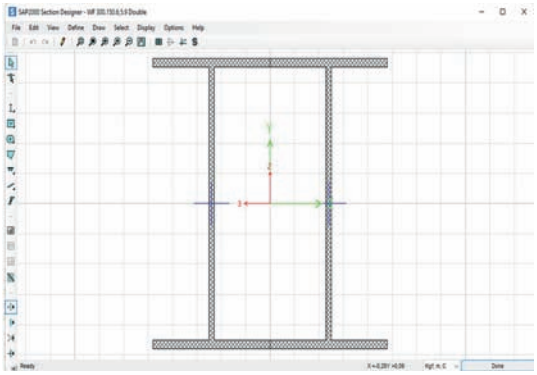


Figure 17. Modeling WF 300.150.6,5.9 Double

d. WF 150.75.5.7

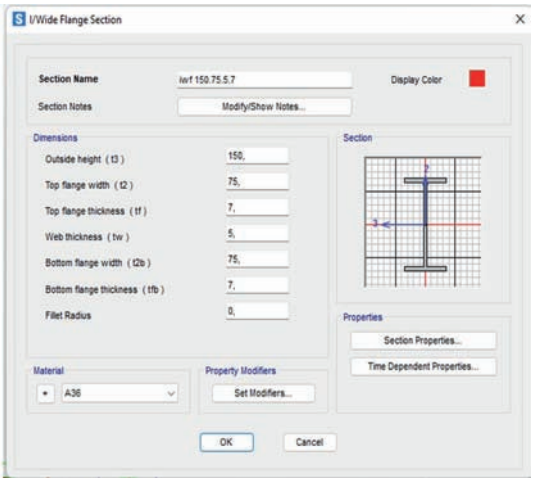


Figure 18. WF Modeling 150.75.5.7

e. UNP 80



Figure 19. UNP 80 Modeling

f. UNP 80 Double

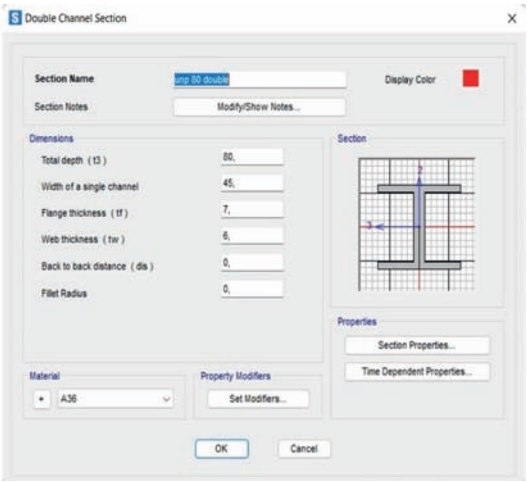


Figure 20. Modeling UNP 80 Double

g. Jack U Head 50 mmm

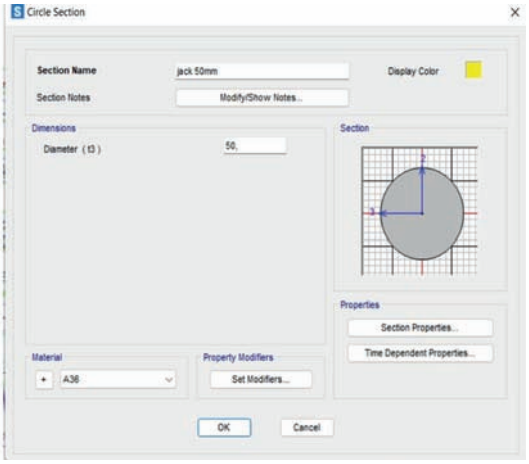


Figure 21. 50 mm U Head Jack Modeling

h. Steel Plate 6 mmm

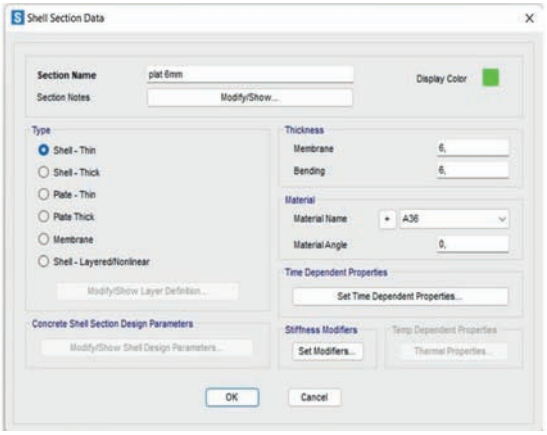


Figure 22. Modeling of 6 mm steel plate

i. PT BAR 32

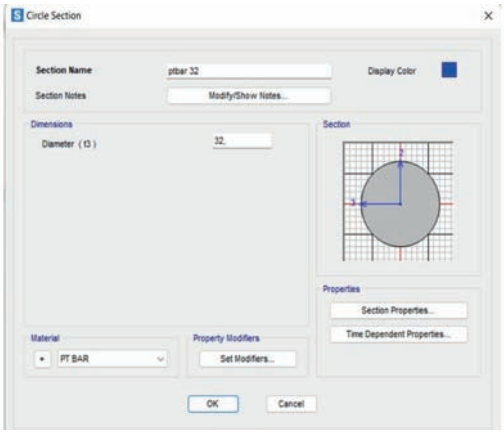


Figure 23. Modeling PT BAR 32 mm

Load Pattern and Load Combination

a. Input Load Patterns

In the SAP2000 program, several load patterns are included in the table below:

Table1. Definition of load pattern

Load Pattern	Definition
D.L	Dead load that has been modeled in SAP2000 (ex: IWF Beam, Steel Plate)
SIDL	Additional dead load (example: Fresh concrete, Reinforcing Steel)
LL	Living Expenses (ex: Worker Expenses)

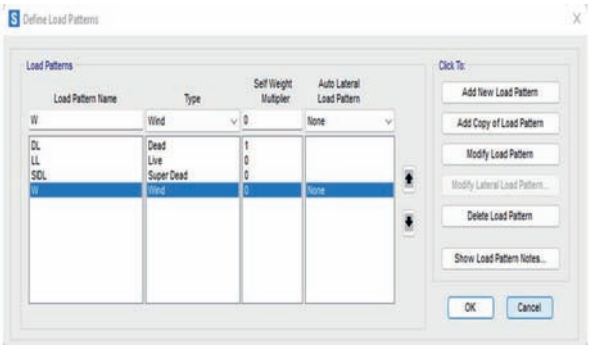


Figure 24. Define load pattern

b. Input Load Combination

On modeling structure slats system flying falsework used Loading combinations are as follows :
1. 1.4 D
2. 1.2 D + 1.6 LL
This combination is based on SNI 1727:2020 concerning Minimum Loads on Buildings[16]. The following is the load combination input in the SAP2000 program:
a. 1.4 D

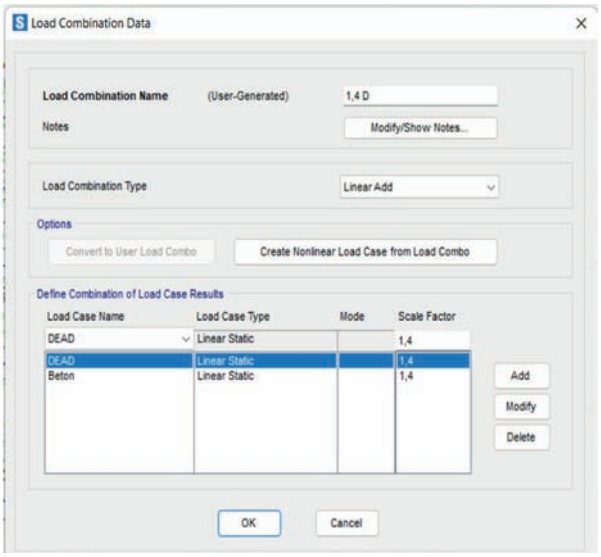


Figure 25. 1.4 D combination

b. 1.2 D + 1.6 LL

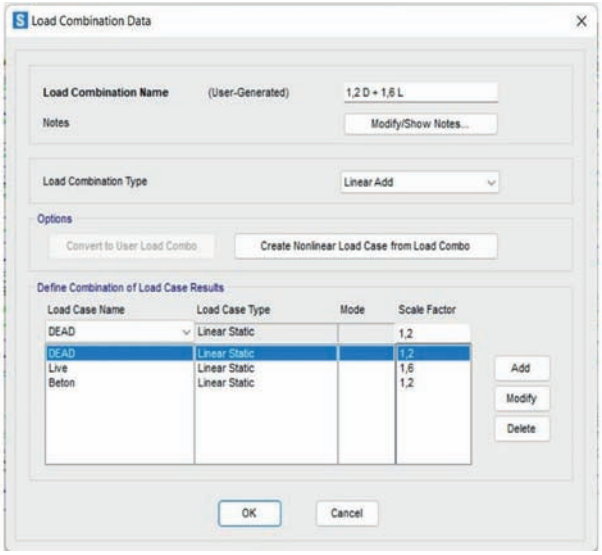


Figure 26. Combination 1.2 D + 1.6 LL

c. Envelopes
The envelope is used to find the most significant force on each element in SAP2000 based on the load combination that has been entered.

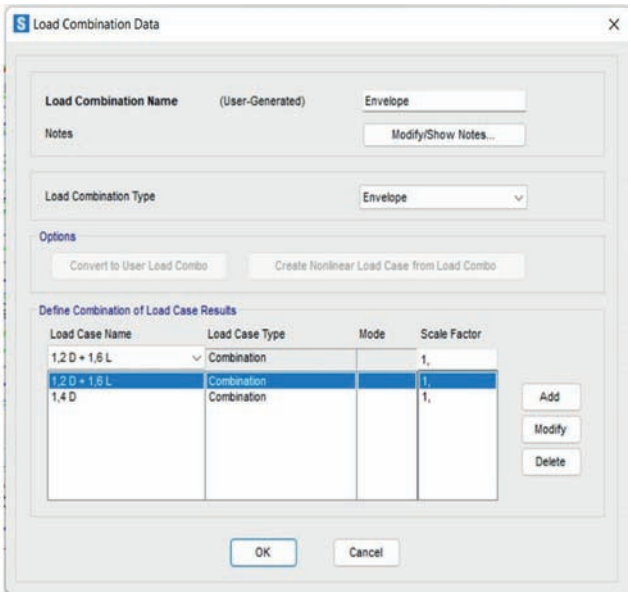


Figure 27. Envelope combination

The formwork frame is modeled according to the approved shop drawing. Modeled from PT Bar Hanger, WF 300 Hanger Beam Double, Beam Transverse HB 350,350, Beam Elongated WF 300 double, Beam support WF 150.75 to Jack U Head and Floor Plate steel.
The UNP frame modeling is more superficial than that in the shop drawing because the UNP function in this modeling only distributes the construction load to the mainframes. The modeling is made into 5 Slab on Pile spans (5 x 7m) to represent the analysis of internal forces in the middle and edge spans.
Modeling formwork flying falsework need to give a linear link on a number of the meeting point between the rods so that the load distribution works correctly and as expected. Below is the linear link modeling and formwork structure modeling with the entire flying falsework system in the SAP 2000 program :

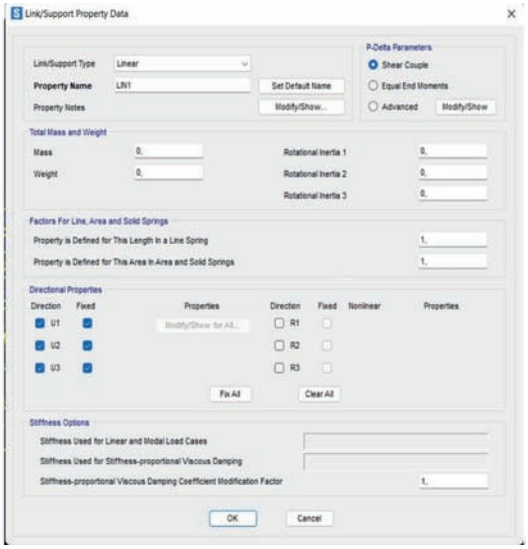


Figure 28. Linear link modeling

Loading

Load, Which happens in structure formwork systems flying falsework, consists of additional dead loads from fresh concrete and loads from workers and tools. The value of the imported load can be seen from the calculation below.

a. Dead Load

$q\ SIDL$ = Thick × **γ** concrete
= 0.35 × 2690
= 941.5 kg/m 2

b. Life

$q\ LL$ = 250 kg/m 2

The load above is input to the steel plate as a load evenly distributed over the area.

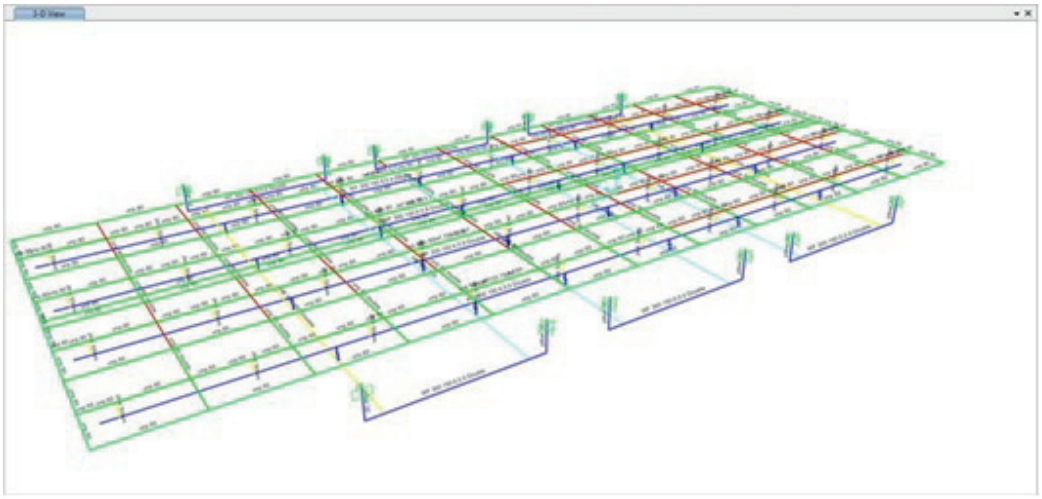


Figure 29. Overall modeling

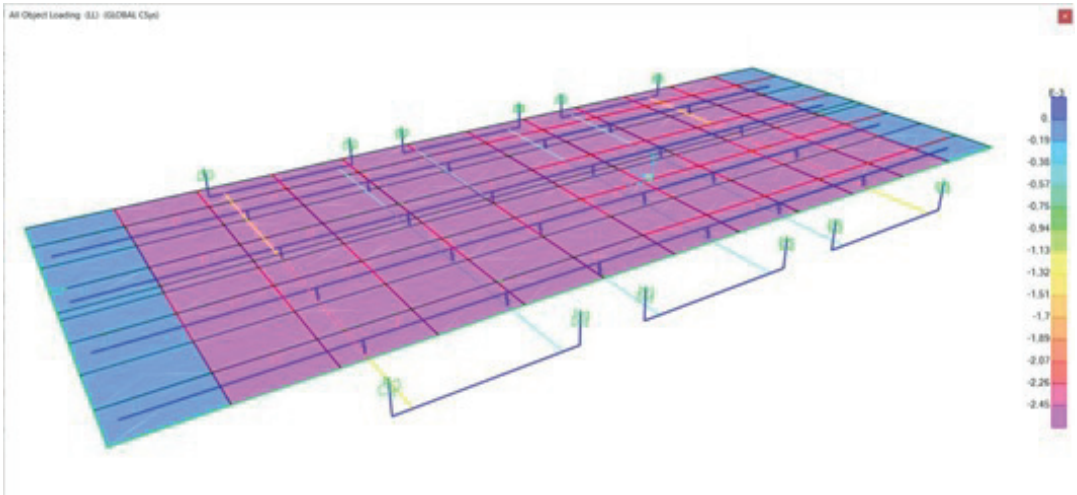


Figure 30. Loading are

RESULTS AND DISCUSSION

The analysis provides security and convenience output from modeling with SAP 2000 software.

a. Security Controls Structure

The structure modeled in SAP2000 software is analyzed by paying attention to the nominal strength of each steel profile with the internal forces that will work. If the ratio between these two things is below the value 1, the structure is strong enough to withstand the working load. In the results of the analysis Figure 31, it can be seen that all profiles have a capacity ratio below 1. Therefore, the structure is safe and robust enough to withstand the existing load.

b. Deflection Control Structur

The deflection limits that pertain to steel structures utilized in building construction are in accordance with SNI 1729:2020 [16]. As per the prevailing standards of the industry, the deflection limit that applies to standard beam components is set at L/240 (see Table 2).

The software SAP 2000 provides both security and convenience in analyzing structures. Analyzing the structure modeled in SAP2000 software involves paying attention to the nominal strength of each steel profile and the internal forces at work. If the capacity ratio of a profile is below 1, it means the structure is strong enough to withstand the existing load. Figure 31 shows the capacity ratio of each profile, and it is evident that all profiles have a capacity ratio below 1, meaning the structure is safe and robust.

Table 2. Deflection limit controls

No	Structural Components	Location	L (mm)	Max Deflection (mm)	Actual deflection (mm)	Status
1	Longitudinal Beam	Middle of Span	3000 (edge)	12.5	8.73 (edge)	Safe
2	Longitudinal Beam	Span Edge	7000 (mid) 3000 (edge)	29.1 12.5	5.6 (mid) 7.8 (edge)	Safe
3	Transverse Beam	Middle of Span	3500	14.5	2.8	Safe
4	Transverse Beam	Span Edge	3500	14.5	8.6	Safe

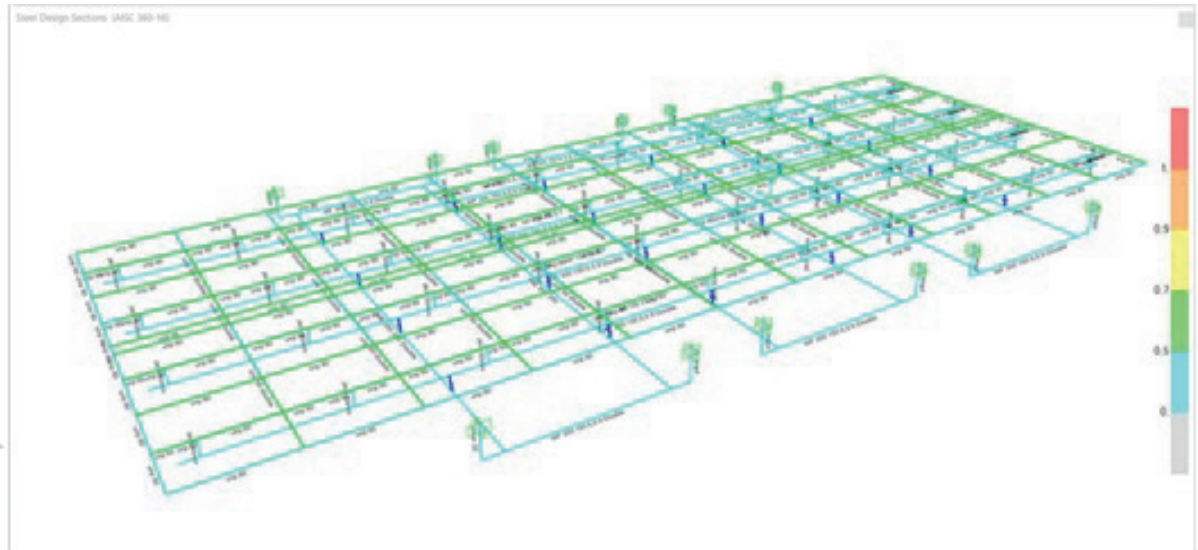


Figure 31. Structure capacity ratio

CONCLUSION

The software for analyzing structures with the SAP 2000 is an excellent tool that provides security and convenience. To ensure proper analysis of the structure modeled in SAP2000 software, it is essential to consider the nominal strength of each steel profile and the internal forces at work. If the capacity ratio of a profile is less than 1, it indicates that the structure can withstand the existing load. Fortunately, all profiles have a capacity ratio below 1, meaning the structure is safe and robust.

As per SNI 1729:2020 Steel Structure Planning for Buildings, for regular beam structural components, the deflection limit is L/240. This limit controls different structural components, including longitudinal beams, transverse beams, and their locations, maximum deflection, actual deflection, and status. Fortunately, all components are safe, as their actual deflection falls within the maximum limit. This implies that the structure is strong, and all its components can withstand all the internal and external forces.

REFERENCES

1. **L.B. Sihombing,** "A new financial model of toll road infrastructure," *2014 Int. Symp. Bus. ...*, vol. i, 2014.
2. **Z. Mahroini,** "Local Government Managament And Local Communty Mitigation Of Tidal Flooding In Sayung Sub-District Demak Regency, Central Java Province, Indonesia," Jul. 2021.
3. **R. Mudiyono and G. Asfari,** "Kajian Pengaruh Pembangunan Jalan Tol Semarang - Demak Terhadap Kinerja Jalan Raya Kaligawe," *J. Planol.*, vol. 18, p. 132, Apr. 2021, doi: 10.30659/jpsa.v18i1.13316.
4. **U. Sari, S. P. Wardani, A. Muntohar, W. Partono, and K. Sadono**, "Consolidation settlement prediction and monitoring of toll road embankment at STA 23+650 Semarang–Demak Toll Road section," *E3S Web Conf.*, vol. 429, Sep. 2023, doi: 10.1051/e3sconf/202342904026.
5. **E. Biruni and W. Kurniawati**, "Tingkat Kesiapan Masyarakat Kecamatan Sayung Terhadap Rencana Pengintegrasian Pembangunan Tanggul Laut Dengan Jalan Tol Semarang-Demak," *Tek. PWK (Perencanaan Wil. Kota)*, vol. 10, pp. 117–126, May 2021, doi: 10.14710/tpwk.2021.30798.
6. **I. Aini, E. Maulana, and H.T. Santoso,** "Evaluasi Metode Perbaikan Tanah Lunak dengan Preloading Kombinasi PVD-PHD pada Proyek Pembangunan Jalan Tol Semarang-Demak Paket II," *Bentang J. Teor. dan Terap. Bid. Rekayasa Sipil*, vol. 11, pp. 21–36, Jan. 2023, doi: 10.33558/bentang.v11i1.4622.
7. **H. Jin and P. Goodrum**, "Integrated Decision Support Framework of Optimal Scaffolding System for Construction Projects," *Algorithms*, vol. 16, p. 348, Jul. 2023, doi: 10.3390/a16070348.
8. **D. Kot**, "Study Of Samples Of Permanent Post-Tension Reinforced Concrete Formwork Slabs For Bridges Deck," *Automob. ROADS ROAD Constr.*, pp. 174–183, Jun. 2022, doi: 10.33744/0365-8171-2022-111-174-183.
9. **T. Siwowski,** *Bridge Engineering - Selected Issues*. 2018.
10. **M. Szóstak and M. Napiórkowski,** "Formwork designing in BIM technology," vol. 94, pp. 39–41, Feb. 2023, doi: 10.5604/01.3001.0016.2696.
11. **R. Kotwal, N. Pawar, R. Funde, M. Chidre, and V. Bhusare**, "Modified Formwork System for Slab Element," *Int. J. Res. Appl. Sci. Eng. Technol.*, vol. 10, pp. 210–212, May 2022, doi: 10.22214/ijraset.2022.42098.
12. **S. Muhammad,** *Building Formwork*. 2020. doi: 10.13140/RG.2.2.29749.29923.
13. **J. André, R. Besle, and A. Baptista,** "Risk Analysis of Bridge Falsework Structures," 2017, pp. 409–426. doi: 10.1007/978-3-319-47886-9_28.

14. **A. Elsayed, M. Darwish, and K. Nassar,** "Design and Constructability of Novel Extendable Arched Steel Truss Falsework," *J. Constr. Eng. Manag.*, vol. 147, Dec. 2020, doi: 10.1061/(ASCE)CO.1943-7862.0001989.
15. **M. Abbu, D. Talib Hashim, H.M.A. Albegmprli, and ahmed S.Naje**, "Fe Modelling For Capacities Of Headed Stud Shear Connectors In Composite Steel Beams With Slabs Concrete," *Int. J. Comput. Civ. Struct. Eng.*, vol. 19, no. 3 SE-Материалы выпуска, pp. 83–91, Sep. 2023, doi: 10.22337/2587-9618-2023-19-3-83-91.
16. **J. Aloysius, J. Sumito, D. Prayogo, and H. Santoso,** "Optimization of concentrically braced steel frame structures based on SNI 1726:2019, SNI 1727:2020, SNI 1729:2020, and AISC 341-16," *IOP Conf. Ser. Earth Environ. Sci.*, vol. 907, p. 12010, Nov. 2021, doi: 10.1088/1755-1315/907/1/012010.

СПИСОК ЛИТЕРАТУРЫ

1. **L.B. Sihombing,** "A new financial model of toll road infrastructure," *2014 Int. Symp. Bus. ...*, vol. i, 2014.
2. **Z. Mahroini,** "Local Government Managament And Local Communty Mitigation Of Tidal Flooding In Sayung Sub-District Demak Regency, Central Java Province, Indonesia," Jul. 2021.
3. **R. Mudiyono and G. Asfari,** "Kajian Pengaruh Pembangunan Jalan Tol Semarang - Demak Terhadap Kinerja Jalan Raya Kaligawe," *J. Planol.*, vol. 18, p. 132, Apr. 2021, doi: 10.30659/jpsa.v18i1.13316.
4. **U. Sari, S. P. Wardani, A. Muntohar, W. Partono, and K. Sadono**, "Consolidation settlement prediction and monitoring of toll road embankment at STA 23+650 Semarang–Demak Toll Road section," *E3S Web Conf.*, vol. 429, Sep. 2023, doi: 10.1051/e3sconf/202342904026.
5. **E. Biruni and W. Kurniawati**, "Tingkat Kesiapan Masyarakat Kecamatan Sayung Terhadap Rencana Pengintegrasian Pembangunan Tanggul Laut Dengan Jalan Tol Semarang-Demak," *Tek. PWK (Perencanaan Wil. Kota)*, vol. 10, pp. 117–126, May 2021, doi: 10.14710/tpwk.2021.30798.
6. **I. Aini, E. Maulana, and H.T. Santoso,** "Evaluasi Metode Perbaikan Tanah Lunak dengan Preloading Kombinasi PVD-PHD pada Proyek Pembangunan Jalan Tol Semarang-Demak Paket II," *Bentang J. Teor. dan Terap. Bid. Rekayasa Sipil*, vol. 11, pp. 21–36, Jan. 2023, doi: 10.33558/bentang.v11i1.4622.
7. **H. Jin and P. Goodrum**, "Integrated Decision Support Framework of Optimal Scaffolding System for Construction Projects," *Algorithms*, vol. 16, p. 348, Jul. 2023, doi: 10.3390/a16070348.
8. **D. Kot**, "Study Of Samples Of Permanent Post-Tension Reinforced Concrete Formwork Slabs For Bridges Deck," *Automob. ROADS ROAD Constr.*, pp. 174–183, Jun. 2022, doi: 10.33744/0365-8171-2022-111-174-183.
9. **T. Siwowski,** *Bridge Engineering - Selected Issues*. 2018.
10. **M. Szóstak and M. Napiórkowski,** "Formwork designing in BIM technology," vol. 94, pp. 39–41, Feb. 2023, doi: 10.5604/01.3001.0016.2696.
11. **R. Kotwal, N. Pawar, R. Funde, M. Chidre, and V. Bhusare**, "Modified Formwork System for Slab Element," *Int. J. Res. Appl. Sci. Eng. Technol.*, vol. 10, pp. 210–212, May 2022, doi: 10.22214/ijraset.2022.42098.
12. **S. Muhammad,** *Building Formwork*. 2020. doi: 10.13140/RG.2.2.29749.29923.
13. **J. André, R. Besle, and A. Baptista,** "Risk Analysis of Bridge Falsework Structures," 2017, pp. 409–426. doi: 10.1007/978-3-319-47886-9_28.
14. **A. Elsayed, M. Darwish, and K. Nassar,** "Design and Constructability of Novel

Extendable Arched Steel Truss Falsework," *J. Constr. Eng. Manag.*, vol. 147, Dec. 2020, doi: 10.1061/(ASCE)CO.1943-7862.0001989.

15. **M. Abbu, D. Talib Hashim, H.M.A. Albegmprli, and ahmed S.Naje**, "Fe Modelling For Capacities Of Headed Stud Shear Connectors In Composite Steel Beams With Slabs Concrete," *Int. J. Comput. Civ. Struct. Eng.*, vol. 19, no. 3 SE-Материалы выпуска, pp. 83–91, Sep. 2023, doi: 10.22337/2587-9618-2023-19-3-83-91.
16. **J. Aloysius, J. Sumito, D. Prayogo, and H. Santoso,** "Optimization of concentrically braced steel frame structures based on SNI 1726:2019, SNI 1727:2020, SNI 1729:2020, and AISC 341-16," *IOP Conf. Ser. Earth Environ. Sci.*, vol. 907, p. 12010, Nov. 2021, doi: 10.1088/1755-1315/907/1/012010.

Fendi Hary Yanto, Disaster Research Center, Sebelas Maret University, Jebres, Surakarta, 57126, Indonesia. Faculty of Vocational School Sebelas Maret University, Jalan Kolonel Sutarto Nomor 150K, Jebres, Surakarta City, Central Java 57126, Indonesia. fendi@staff.uns.ac.id

Фенди Гарри Янто, Центр исследования катастроф, Университет Себелас Марет, Джебрес, Суракарта, 57126, Индонезия, fendi@staff.uns.ac.id